Jingfu Liu · Guibin Jiang *Editors*

Silver Nanoparticles in the Environment

Springer

Silver Nanoparticles in the Environment

Jingfu Liu • Guibin Jiang
Editors

Silver Nanoparticles in the Environment

Springer

Editors
Jingfu Liu
State Key Laboratory of Environmental Chemistry and Ecotoxicology
Research Center for Eco-Environmental Sciences
Chinese Academy of Sciences
Beijing
China

Guibin Jiang
State Key Laboratory of Environmental Chemistry and Ecotoxicology
Research Center for Eco-Environmental Sciences
Chinese Academy of Sciences
Beijing
China

ISBN 978-3-662-46069-6 ISBN 978-3-662-46070-2 (eBook)
DOI 10.1007/978-3-662-46070-2

Library of Congress Control Number: 2015931546

Springer Heidelberg New York Dordrecht London

Printed on acid-free paper

Springer is part of Springer Science+Business Media (www.springer.com)

Preface

Due to their unique physical and chemical properties, silver nanoparticles (AgNPs) are extensively used in antibacterial and medical products, electronics, catalysts, and biosensors. The increasing production and use of AgNPs in industrial and commercial products would increase their release into the environment, which arosed the growing public and regulatory concerns to the potential risks they may pose to humans and the environmental organisms in recent years. To evaluate the environmental and biological safety, data on the occurrence, transport, transformation, distribution, fate, effects, and toxicity of AgNPs in the environments are needed. Owning to the distinguished chemical properties of Ag, AgNPs are highly dynamic in physical and chemical species in the environment, giving rise to characteristics that are different from other nanoparticles, such as dissolution and re-reduction, sulfidation, and chlorination. Although great achievements have been made during the past years, large knowledge gaps exist in the areas of characterization and determination, environmental processes and effects, and biological toxicity of AgNPs. It is for the purpose of promoting in-depth study on the environmental issues of AgNPs, we edit the book *Silver Nanoparticles in the Environment*.

This book is designed to bring the state of the art of knowledge on environmental aspects of AgNPs. We believe it will be a valuable resource to students and researchers in environmental science and technology, chemistry, toxicology and health sciences, to scientists in material science and nanotechnology for designing environmentally benign AgNPs, as well as to producers and consumers involved in the production and consumption of AgNPs in various areas including catalysis, consumer products, food technology, textiles/fabrics, and medical products and devices.

As a comprehensive book, the chapters in this book cover the main environmental issues of AgNPs. The first chapter describes briefly the history, properties, applications, and environmental concerns of AgNPs. Then, the methods for separation, characterization, and determination of AgNPs in environmental and biological matrices were addressed in Chap. 2. The following three chapters focus on the environmental processes and effects of AgNPs, with emphasis on the pathway to environment, transformation and fate, as well as toxicological effects and mechanisms. In the last chapter, the environmental bioeffects and safety assessment of AgNPs in environment are discussed.

We are very grateful to the authors, our colleagues, to undertake the absorbing task of writing chapters, and the support from Springer in the production of this book.

Beijing, China Jingfu Liu and Guibin Jiang

Contents

Contributors

Guibin Jiang State Key Laboratory of Environmental Chemistry and Ecotoxicology, Research Center for Eco-Environmental Sciences, Chinese Academy of Sciences, Beijing, China

Lingxiangyu Li State Key Laboratory of Environmental Chemistry and Ecotoxicology, Research Center for Eco-Environmental Sciences, Chinese Academy of Sciences, Beijing, China

Jingfu Liu State Key Laboratory of Environmental Chemistry and Ecotoxicology, Research Center for Eco-Environmental Sciences, Chinese Academy of Sciences, Beijing, China

Wei Liu Institute of Chemical Safety, Chinese Academy of Inspection and Quarantine, Beijing, China

Yanmin Long State Key Laboratory of Environmental Chemistry and Ecotoxicology, Research Center for Eco-Environmental Sciences, Chinese Academy of Sciences, Beijing, China

Mohai Shen State Key Laboratory of Environmental Chemistry and Ecotoxicology, Research Center for Eco-Environmental Sciences, Chinese Academy of Sciences, Beijing, China

Cheng Sun State Key Laboratory of Environmental Chemistry and Ecotoxicology, Research Center for Eco-Environmental Sciences, Chinese Academy of Sciences, Beijing, China

Xiaoya Yang State Key Laboratory of Environmental Chemistry and Ecotoxicology, Research Center for Eco-Environmental Sciences, Chinese Academy of Sciences, Beijing, China

Yongguang Yin State Key Laboratory of Environmental Chemistry and Ecotoxicology, Research Center for Eco-Environmental Sciences, Chinese Academy of Sciences, Beijing, China

Sujuan Yu State Key Laboratory of Environmental Chemistry and Ecotoxicology, Research Center for Eco-Environmental Sciences, Chinese Academy of Sciences, Beijing, China

Qunfang Zhou State Key Laboratory of Environmental Chemistry and Ecotoxicology, Research Center for Eco-Environmental Sciences, Chinese Academy of Sciences, Beijing, China

Xiaoxia Zhou State Key Laboratory of Environmental Chemistry and Ecotoxicology, Research Center for Eco-Environmental Sciences, Chinese Academy of Sciences, Beijing, China

Chapter 1
Introduction

Sujuan Yu and Jingfu Liu

Abstract Due to their unique physical and chemical properties, silver nanoparticles (AgNPs) are extensively used in electronics, catalysts, biosensors, medical areas, and large commercial antibacterial products, which has paralleled growing public and regulatory concerns as to the potential risks they may pose to humans and the environmental organisms. Aiming to give a brief introduction of AgNPs, this chapter describes the history, general physical and chemical properties, main applications, as well as environmental concerns of AgNPs.

1.1 History

Metal silver (Ag) is a naturally occurring and rare element, with the 67th in abundance among the elements and located 47th in the periodic table. As a precious metal and with the white metallic luster appearance, silver has long been used as currency, jewelry, and high-quality cutlery. As early as the ancient times, silverware was believed to prevent decay of foodstuffs and used to store water and wine. The use of silver in medicine also has a long history. The first recorded medical use of silver could date back to the eighth century. In 980 AD, Avicenna used silver filings as a blood purifier to treat offensive breath and palpitations of the heart [1]. Silver nitrate was used to treat chronic wounds or ulcers in the seventeenth and eighteenth centuries. And in the nineteenth century, J.N. Rust first reported the use of diluted silver nitrate solution (0.2%) for fresh burns [2]. Silver nitrate rod or pencils also formed as part of the standard surgical equipment at that time. Around 1884, a German obstetrician C. S. F. Crede introduced 1% silver nitrate eyedrop solution to prevent infection for new born babies [3]. In 1967, silver sulfadiazine (a combined formulation made from silver nitrate and sodium sulfadiazine) for topical treatment

J. Liu (✉) · S. Yu
State Key Laboratory of Environmental Chemistry and Ecotoxicology,
Research Center for Eco-Environmental Sciences, Chinese Academy of Sciences,
P.O. Box 2871, 100085 Beijing, China
e-mail: jfliu@rcees.ac.cn

S. Yu
e-mail: sjyu@ rcees.ac.cn

J. Liu, G. Jiang (eds.), *Silver Nanoparticles in the Environment,*
DOI 10.1007/978-3-662-46070-2_1

of burns was first introduced by Fox [4], and even today it is still the gold standard in serous burn wounds.

Chronic exposure to silver or silver compounds may cause the permanent grey or blue grey discoloration of skin or eyes, i.e., argyris or argyrosis [1, 5]. Because of this problem and with the advent of more effective antibiotics like penicillin and cephalosporin, the golden period of silver as a disinfectant passed round about the time of the second world war. Unfortunately, the abuse of antibiotics has produced a lot of superbugs. Thanks to the development of the modern nanotechnology, it does not take many years for silver to renew its lost lustre. Silver nanoparticles (AgNPs) also exhibit superior antimicrobial properties. It is believed that AgNPs showed the biocidal action by the slow release of Ag^+ and by multiple mechanisms such as interaction with thiol groups in proteins and enzymes, inhibition of DNA replication, and induction of oxidative stress [6], making it more difficult for bacteria to create resistant strains. Moreover, the large surface area, which promotes the reactivity and sorption with pathogens, makes AgNPs ideal candidates for antibacterial applications.

Actually, nanosilver is not new and has been used for more than 100 years, though not under the name of "nano" [7]. As early as 1889, Lea had first reported the synthesis of a citrate-stablized silver colloid with an average diameter between 7 and 9 nm [8]. The stabilization of nanosilver by proteins was also reported in 1902 [9]. Other different synthetic methods of nanosilver with diverse coating agents and diameters were also developed in the next decades. Nanosilver has been commercially used for therapeutic purposes since 1897 with the name of "collargol." The first registered biocidal silver product in the USA was "Algaedyn," which was still used today as an algicide [7]. During the past decades, nanosilver has been a blossoming field of research. Their remarkable biological activities and unusual physicochemical properties have drawn extensive interests for the development of new applications.

1.2 General Physical and Chemical Properties

1.2.1 Antimicrobial Ability

Nanosilver represents a broad spectrum of antimicrobial activity, and can kill both Gram-positive and Gram-negative bacteria (including *Escherichia coli*, *Staphylococcus aureus*, *Pseudomonas aeruginosa*, *Staphylococcus aureus*, and *Streptococcus mutans*) [10, 11]. The antibacterial activity on different drug-resistant pathogens of clinical importance, such as multidrug-resistant *Pseudomonas aeruginosa*, ampicillin-resistant *E. coli O157:H7* and erythromycin-resistant *Streptococcus pyogenes*, was also reported [12]. Nanosilver could inhibit bacteria growth rate from the initial contact of the pathogens, and played their antibacterial activity by killing bacteria rather than bacteriostatic mechanism [13].

Nanosilver also has antifungal activity. They could inhibit a large number of ordinary fungal strains, including *Aspergillus fumigatus*, *Mucor*, *Candida albicans*, *Candida glabrata*, *Candida tropicalis*, *Saccharomyces cerevisiae*, and *Aspergillus fumigatus* [14].

The antiviral properties of AgNPs are also reported in the literature. AgNPs prepared in Hepes buffer could inhabit HIV-1 replication, and the anti-HIV activity (98%) was much higher than gold nanoparticles (6–20%) [15]. The inhibition of hepatitis B virus [16] and herpes simplex virus [17] were also valued.

1.2.2 Size and Shape

With the nanofever, much effort has been devoted to the synthesis of nanosilver with various sizes and shapes. The size distribution of AgNPs may not stay constant and is dependent on the surrounding chemical and physical environment. In real aquatic systems with high salinity or harsh pH values, AgNPs tend to aggregate to form large clusters and their physicochemical properties and mobility may change as well.

AgNPs with different sizes and shapes exhibit distinct antimicrobial activity. Smaller particles are more efficient to kill bacteria than the larger ones, probably due to the higher surface areas, which make it easier for them to attach to cell membranes and enter the cells. The antibacterial effects of nanosilver with different shapes including nanoparticles, nanorods, and truncated triangular silver nanoplates were also tested [18]. Truncated triangular silver nanoplates, which contained more $\{111\}$ facets, displayed the strongest antibacterial activity. The high atom to density facet $\{111\}$ may directly interact with the bacteria surface to kill the pathogens.

1.2.3 Surface Area and Chemistry

Being in the nanoscale dimension, AgNPs have greater specific surface areas compared to the same mass of the bulk ones, which provides them more reactive sites and higher surface energy. It means that smaller AgNPs are more sensitive to the oxygen and easier to receive electrons, which could represent increased antimicrobial ability.

AgNPs are thermodynamically unstable, so adjacent particles are prone to coalesce to form large clusters. As a consequence, capping agents are always added to stabilize AgNPs by steric repulsion, electrostatic repulsion or both, making AgNPs modified with various functional groups and charges, thus influencing their reactivity. Surface charge-dependent toxicity of nanosilver was examined by Badawy and the coworkers [19]. They showed that AgNPs with various surface charges (ranging from highly negative to highly positive) exhibit distinct inhibition effects toward *bacillus* species, probably because cellular membranes of bacteria contain carboxyl, phosphate, and amino groups, providing them with diverse charges. Different charged AgNPs may attract or repulse the pathogens to undergo distinct antibacterial activities.

1.2.4 Conductive and Optical Properties

Pure silver has high thermal and electrical conductivity and relatively low contact resistance, which makes it an ideal candidate in electronics. Moreover, the electrons on the surface of AgNPs are highly interactive with electromagnetic fields, resulting in a high surface plasmon resonance (SPR) in the UV-visible spectroscopy (UV-vis) wavelength range. The width and position of the SPR peaks are affected by the size, shape, and dispersion state of nanoparticles [20]. These properties facilitate the use of AgNPs in biomolecular detection and labeling and in other electronic sensor areas.

1.3 Main Applications

1.3.1 As Antimicrobial Agents

Due to the excellent antibacterial properties, applications of AgNPs especially in healthcare fields have been extensively explored. Nanosilver is becoming one of the fastest growing product categories in the nanotechnology industry, and has the highest degree of commercialization [21]. Data showed that, of the 1628 consumer products containing nanomaterials on the market (October, 2013), 383 are claimed to contain AgNPs [22], including food packaging materials, food storage containers, cosmetics, odor-resistant socks and underwear, room sprays, laundry detergents, lotions, and soaps. Silver-impregnated water filters which were used to kill harmful bacteria in drinking water and swimming pools are also safely used for decades [7].

Nanosilver is also encouraged to use in medicinal areas because of the useful anti-inflammatory effects and the ability to promote wound healing. AgNPs are incorporated into wound dressings, scaffolds, medical textiles, catheters, and contraceptive devices [23]. AgNPs are also used in orthopedics and dentistry such as additives in bone cements, coatings of implants for joint replacement and intramedullary nails for bone fractures, and additives in polymerizable dental materials [24]. The potential medical applications of AgNPs in the treatment of cancer and in the field of pharmaceutics and drug delivery are also promising.

1.3.2 As Catalysts

The large surface area of AgNPs provides them more possible reactive sites and high surface energy, making them the ideal candidate catalysts. AgNPs and nanocomposites are capable of catalyzing a large amount of reactions, such as CO and benzene oxidation [25], reduction of Rhodamine B (RhB) [26], and reduction of 4-nitrophenol to 4-aminophenol [27, 28]. Properties of AgNPs can be controlled and tailored in a predictable manner and imparting them with functional groups or supporting materials can result in catalysts with high activities and a long lifetime.

1.3.3 Electronic and Optical Applications

The high thermal and electrical conductivity and relatively low contact resistance qualify AgNPs one of the most promising materials in electronics. Nanosilver could find applications in electronic equipment, mainly in solder for circuit connections and as nanoconnectors or nanoelectrodes to manufacture nanoelectronic devices [20]. AgNPs are also applied to fabricate active waveguides in optical devices [29], as pastes and inks for printed circuit boards [30] and data storage devices.

AgNPs are widely used for surface enhance Raman scattering (SERS). The enhancement factors could be as much as 10^{14}–10^{15} fold, which allows the single molecule detection [31]. AgNPs also exhibit high SPR peaks in the visible spectrum upon irradiation of light. Because of these optical properties, AgNPs are promoted to be used in sensing applications, such as the detection of DNA and RNA [32], colorimetric chiral recognition of enantiomers [33], the antioxidant capacity measurement of polyphenols [34], as well as selective colorimetric sensing of mercury [35], enzyme [36], H_2O_2, and glucose [37].

1.4 Environmental Concerns

By eating, breathing, or skin contact, humans are easily exposed to AgNPs. Moreover, during the production, transport, erosion, washing, and disposal of AgNPs containing products, AgNPs would be inevitably released into the environment. As a result, the vast applications of AgNPs arouse an intense concern in parallel. Though the use of silver has a long history, and it is traditionally believed that silver is relatively nontoxic to mammalian cells, more and more results showed that AgNPs can cause adverse effects to both aquatic and terrestrial organisms.

AgNPs were demonstrated to affect the early growth of zebrafish embryos. Single nanoparticles could be transported into and out of embryos through chorion pore canals, and trigger the developmental abnormality or death at a critical concentration of 0.19 nM [38]. AgNPs also disrupted seed growth of plants such as wheat [39], ryegrass [40], phaseolus radiates [41], and onion [42], causing silver accumulation in the shoots. The bioaccumulation of AgNPs in green algae [43], ragworm [44] and gastropod [45] were reported as well. The predator-prey interactions may also influenced by a low concentration of AgNPs [46], which may elicit important environmental risks.

To accurately predict the potential hazard of AgNPs, information of the fate, transport, and bioavaibility of AgNPs in the natural system is urgently needed. In this book, we focus on the the environmental and toxicological chemistry of AgNPs, starting with the analysis and sources of AgNPs, which is followed by the possible fate, mobility, and toxicity in the environment, and their potential bioeffects and safety risks are also discussed.

References

1. Wadhera A, Fung M (2005) Systemic argyria associated with ingestion of colloidal silver. Dermatol Online J 11(1):12.
2. Klasen HJ (2000) Historical review of the use of silver in the treatment of burns. I. Early uses. Burns 26(2):117–130. doi:10.1016/s0305-4179(99)00108-4
3. Russell AD, Hugo WB (1994) Antimicrobial activity and action of silver. Prog Med Chem 31:351–370. doi:10.1016/S0079-6468(08)70024-9
4. Klasen HJ (2000) A historical review of the use of silver in the treatment of burns. II. Renewed interest for silver. Burns 26(2):131–138. doi:10.1016/s0305-4179(99)00116-3
5. Drake PL, Hazelwood KJ (2005) Exposure-related health effects of silver and silver compounds: a review. Ann Occup Hyg 49(7):575–585. doi:10.1093/annhyg/mei019
6. Luoma SN (2008) Silver nanotechnologies and the environment: old problems or new challenges? Woodrow Wilson International Center for Scholars, Washington, DC
7. Nowack B, Krug H, Height M (2011) 120 years of nanosilver history: implications for policy makers. Environ Sci Technol 45(7):3189–3189. doi:10.1021/es103316q
8. Lea MC (1889) On allotropic forms of silver. Am J Sci 37:476–491
9. Paal C (1902) On colloidal silver. Berichte Der Deutschen Chemischen Gesellschaft 35:2224–2236. doi:10.1002/cber.190203502182
10. Birla SS, Tiwari VV, Gade AK, Ingle AP, Yadav AP, Rai MK (2009) Fabrication of silver nanoparticles by Phoma glomerata and its combined effect against *Escherichia coli*, *Pseudomonas aeruginosa* and *Staphylococcus aureus*. Lett Appl Microbiol 48(2):173–179. doi:10.1111/j.1472-765X.2008.02510.x
11. Li WR, Xie XB, Shi QS, Duan SS, Ouyang YS, Chen YB (2011) Antibacterial effect of silver nanoparticles on *Staphylococcus aureus*. Biometals 24(1):135–141. doi:10.1007/s10534-010-9381-6
12. Shahverdi AR, Fakhimi A, Shahverdi HR, Minaian S (2007) Synthesis and effect of silver nanoparticles on the antibacterial activity of different antibiotics against *Staphylococcus aureus* and *Escherichia coli*. Nanomedicine 3(2):168–171. doi:10.1016/j.nano.2007.02.001
13. Lara HH, Ayala-Nunez NV, Turrent LDI, Padilla CR (2010) Bactericidal effect of silver nanoparticles against multidrug-resistant bacteria. World J Microbiol Biotechnol 26(4):615–621. doi:10.1007/s11274-009-0211-3
14. Wright JB, Lam K, Hansen D, Burrell RE (1999) Efficacy of topical silver against fungal burn wound pathogens. Am J Infect Control 27(4):344–350. doi:10.1016/S0196-6553(99)70055-6
15. Sun RWY, Chen R, Chung NPY, Ho CM, Lin CLS, Che CM (2005) Silver nanoparticles fabricated in Hepes buffer exhibit cytoprotective activities toward HIV-1 infected cells. Chem Commun (40):5059–5061. doi:10.1039/b510984a
16. Lu L, Sun RWY, Chen R, Hui CK, Ho CM, Luk JM, Lau GKK, Che CM (2008) Silver nanoparticles inhibit hepatitis B virus replication. Antivir Ther 13(2):253–262
17. Baram-Pinto D, Shukla S, Perkas N, Gedanken A, Sarid R (2009) Inhibition of herpes simplex virus type 1 infection by silver nanoparticles capped with mercaptoethane sulfonate. Bioconjug Chem 20(8):1497–1502. doi:10.1021/bc900215b
18. Pal S, Tak YK, Song JM (2007) Does the antibacterial activity of silver nanoparticles depend on the shape of the nanoparticle? A study of the gram-negative bacterium *Escherichia coli*. Appl Environ Microbiol 73(6):1712–1720. doi:10.1128/aem.02218-06
19. El Badawy AM Silva RG Morris B Scheckel KG Suidan MT Tolaymat TM (2011) Surface charge-dependent toxicity of silver nanoparticles. Environ Sci Technol 45(1):283–287. doi:10.1021/es1034188
20. Tolaymat TM, El Badawy AM, Genaidy A, Scheckel KG, Luxton TP, Suidan M (2010) An evidence-based environmental perspective of manufactured silver nanoparticle in syntheses and applications: a systematic review and critical appraisal of peer-reviewed scientific papers. Sci Total Environ 408(5):999–1006. doi:10.1016/j.scitotenv.2009.11.003
21. Chen X, Schluesener HJ (2008) Nanosilver: a nanoproduct in medical application. Toxicol Lett 176(1):1–12. doi:10.1016/j.toxlet.2007.10.004
22. http://www.nanotechproject.org/cpi/about/analysis/. Accessed 10 Dec 2014

23. Chaloupka K, Malam Y, Seifalian AM (2010) Nanosilver as a new generation of nanoproduct in biomedical applications. Trends Biotechnol 28(11):580–588. doi:10.1016/j.tibtech.2010.07.006
24. Wijnhoven SWP, Peijnenburg W, Herberts CA, Hagens WI, Oomen AG, Heugens EHW, Roszek B, Bisschops J, Gosens I, Van de Meent D, Dekkers S, De Jong WH, Van Zijverden M, Sips A, Geertsma RE (2009) Nano-silver—a review of available data and knowledge gaps in human and environmental risk assessment. Nanotoxicology 3(2):109–138. doi:10.1080/17435390902725914
25. Ye Q, Zhao JS, Huo FF, Wang J, Cheng SY, Kang TF, Dai HX (2011) Nanosized Ag/alpha-MnO(2) catalysts highly active for the low-temperature oxidation of carbon monoxide and benzene. Catal Today 175(1):603–609. doi:10.1016/j.cattod.2011.04.008
26. Ai LH, Zeng CM, Wang QM (2011) One-step solvothermal synthesis of Ag-Fe(3)O(4) composite as a magnetically recyclable catalyst for reduction of Rhodamine B. Catal Commun 14(1):68–73. doi:10.1016/j.catcom.2011.07.014
27. Naik B, Hazra S, Prasad VS, Ghosh NN (2011) Synthesis of Ag nanoparticles within the pores of SBA-15: an efficient catalyst for reduction of 4-nitrophenol. Catal Commun 12(12):1104–1108. doi:10.1016/j.catcom.2011.03.028
28. Manesh KM, Gopalan AI, Lee KP, Komathi S (2010) Silver nanoparticles distributed into polyaniline bridged silica network: a functional nanocatalyst having synergistic influence for catalysis. Catal Commun 11(10):913–918. doi:10.1016/j.catcom.2010.03.013
29. Tate J, Rogers JA, Jones CDW, Vyas B, Murphy DW, Li WJ, Bao ZA, Slusher RE, Dodabalapur A, Katz HE (2000) Anodization and microcontact printing on electroless silver: solution-based fabrication procedures for low-voltage electronic systems with organic active components. Langmuir 16(14):6054–6060. doi:10.1021/la991646b
30. Li YN, Wu YL, Ong BS (2005) Facile synthesis of silver nanoparticles useful for fabrication of high-conductivity elements for printed electronics. J Am Chem Soc 127(10):3266–3267. doi:10.1021/ja043425k
31. Qian XM, Nie SM (2008) Single-molecule and single-nanoparticle SERS: from fundamental mechanisms to biomedical applications. Chem Soc Rev 37(5):912–920. doi:10.1039/b708839f
32. Cao YWC, Jin RC, Mirkin CA (2002) Nanoparticles with Raman spectroscopic fingerprints for DNA and RNA detection. Science 297(5586):1536–1540. doi:10.1126/science.297.5586.1536
33. Zhang M, Ye B-C (2011) Colorimetric chiral recognition of enantiomers using the nucleotide-capped silver nanoparticles. Anal Chem 83(5):1504–1509. doi:10.1021/ac102922f
34. Ozyurek M, Gungor N, Baki S, Guclu K, Apak R (2012) Development of a silver nanoparticle-based method for the antioxidant capacity measurement of polyphenols. Anal Chem 84(18):8052–8059. doi:10.1021/ac301925b
35. Roy B, Bairi P, Nandi AK (2011) Selective colorimetric sensing of mercury(II) using turn off-turn on mechanism from riboflavin stabilized silver nanoparticles in aqueous medium. Analyst 136(18):3605–3607. doi:10.1039/c1an15459a
36. Wei H, Chen C, Han B, Wang E (2008) Enzyme colorimetric assay using unmodified silver nanoparticles. Anal Chem 80(18):7051–7055. doi:10.1021/ac801144t
37. Chen S, Hai X, Chen XW, Wang JH (2014) In situ growth of silver nanoparticles on graphene quantum dots for ultrasensitive colorimetric detection of H_2O_2 and glucose. Anal Chem 86(13):6689–6694. doi:10.1021/ac501497d
38. Lee KJ, Nallathamby PD, Browning LM, Osgood CJ, Xu XHN (2007) In vivo imaging of transport and biocompatibility of single silver nanoparticles in early development of zebrafish embryos. ACS Nano 1(2):133–143. doi:10.1021/nn700048y
39. Dimkpa CO, McLean JE, Martineau N, Britt DW, Haverkamp R, Anderson AJ (2013) Silver nanoparticles disrupt wheat (Triticum aestivum L.) growth in a sand matrix. Environ Sci Technol 47(2):1082–1090. doi:10.1021/es302973y
40. Yin LY, Cheng YW, Espinasse B, Colman BP, Auffan M, Wiesner M, Rose J, Liu J, Bernhardt ES (2011) More than the ions: the effects of silver nanoparticles on Lolium multiflorum. Environ Sci Technol 45(6):2360–2367. doi:10.1021/es103995x

41. Lee W-M, Kwak JI, An Y-J (2012) Effect of silver nanoparticles in crop plants Phaseolus radiatus and Sorghum bicolor: media effect on phytotoxicity. Chemosphere 86(5):491–499. doi:10.1016/j.chemosphere.2011.10.013
42. Kumari M, Mukherjee A, Chandrasekaran N (2009) Genotoxicity of silver nanoparticles in Allium cepa. Sci Total Environ 407(19):5243–5246. doi:10.1016/j.scitotenv.2009.06.024
43. Piccapietra F, Allue CG, Sigg L, Behra R (2012) Intracellular silver accumulation in Chlamydomonas reinhardtii upon exposure to carbonate coated silver nanoparticles and silver nitrate. Environ Sci Technol 46(13):7390–7397. doi:10.1021/es300734m
44. Garcia-Aonso J, Khan FR, Misra SK, Turmaine M, Smith BD, Rainbow PS, Luoma SN, Valsami-Jones E (2011) Cellular internalization of silver nanoparticles in gut epithelia of the estuarine polychaete Nereis diversicolor. Environ Sci Technol 45(10):4630–4636. doi:10.1021/es2005122
45. Croteau MN, Misra SK, Luoma SN, Valsami-Jones E (2011) Silver bioaccumulation dynamics in a freshwater invertebrate after aqueous and dietary exposures to nanosized and ionic Ag. Environ Sci Technol 45(15):6600–6607. doi:10.1021/es200880c
46. Pokhrel LR, Dubey B (2012) Potential impact of low-concentration silver nanoparticles on predator-prey interactions between predatory dragonfly nymphs and Daphnia magna as a prey. Environ Sci Technol 46(14):7755–7762. doi:10.1021/es204055c

Chapter 2
Separation and Determination of Silver Nanoparticles

Sujuan Yu, Xiaoxia Zhou and Jingfu Liu

Abstract The accurate analysis of silver nanoparticles (AgNPs) in complicated environmental and biological matrix is the premise for the assessment of AgNP risks. In the past few decades, a myriad of methods have been developed for the concentration and determination of AgNPs. In this chapter, methodologies for the separation, characterization, and quantification of AgNPs are introduced, and the advantages and shortcomings of each technique are also discussed. In most cases, multiple schemes are often needed to get comprehensive information of the analytes. To meet the ultra-trace detection of AgNPs in the environment, techniques with higher resolution and sensitivity are required.

2.1 Separation

Once released into the environment, silver nanoparticles (AgNPs) would interact with complex environmental matrices, making it a big challenge to trace the fate and transport of AgNPs in natural systems. For the ultra-trace analysis of AgNPs in real samples, proper preconcentration and separation methods are required. The traditionally used methods are centrifugation, membrane filtration, dialysis, and centrifugal ultrafiltration. Irreversible agglomeration or aggregation may occur during centrifugation and filtration, making it difficult to track the original morphology of nanoparticles (NPs). Moreover, the separation efficiency varies in according to the nature of NPs and small sized NPs may suffer from significant mass loss. The dialysis method is time-consuming and frequently changing the dialysis fluid is rather annoying. Centrifugal ultrafiltration can avoid the particle aggregation to some extent, and shows to be a powerful tool to concentrate NPs. Membranes are designed to guarantee that no particle larger than the pore size penetrates the mem-

J. Liu (✉) · S. Yu · X. Zhou
State Key Laboratory of Environmental Chemistry and Ecotoxicology, Research Center for Eco-Environmental Sciences, Chinese Academy of Sciences,
P. O. Box 2871, 100085 Beijing, China
e-mail: jfliu@rcees.ac.cn

S. Yu
e-mail: sjyu@rcees.ac.cn

J. Liu, G. Jiang (eds.), *Silver Nanoparticles in the Environment,*
DOI 10.1007/978-3-662-46070-2_2

brane. However, it does not mean that particles smaller than the pore size could pass through the membrane quantitatively. It is always suffered from the low recovery. To date, a number of techniques are developed to isolate AgNPs, including extraction methods like cloud point extraction (CPE), chromatographic techniques like size-exclusion chromatography (SEC) and high performance liquid chromatography (HPLC), electrophoresis methods like capillary electrophoresis (CE), and other methods like field-flow fractionation (FFF) and density-gradient centrifugation.

2.1.1 Cloud Point Extraction

Cloud point extraction was first described by Watanabe and co-workers in 1987 [1, 2], and since then this method has received enormous attention and is rapidly developed. Based on the solubilization ability and the cloud points of nonionic surfactants, CPE can be easily done. Typically, there are three simple steps in the extraction: (i) adding sufficient nonionic surfactant into the sample solution to solubilize the analytes; (ii) changing external conditions such as the temperature, pressure, pH, or ion strength to attain cloud points, i.e., incomplete solubilization; (iii) facilitating phase separation by centrifugation or long-term placing. In the end, analytes are concentrated into the surfactant-rich phase due to the analyte-micelle interaction. Because of the high extraction efficiency, easily handling, low costs, and environmental benign of CPE, it is popular in the determination of metal ions (e.g., Cr, Cu, Cd), organic pollutions and other biopolymers [3].

Liu et al. for the first time reported the thermoreversible separation of nanomaterials (NMs) by CPE [4]. Based on a commercially available nonionic surfactant Triton X-114 (TX-114), several NMs with various coatings and shapes, including PVP-coated AgNPs, citrate stabilized gold nanoparticles (AuNPs), C_{60}, TiO_2, and single-walled carbon nanotubes, can be concentrated.

The CPE method was proved to be an efficient approach to extract AgNPs from environmental waters [5]. The extraction efficiency was influenced by several parameters such as pH, salinity, surfactant concentrations, incubation time and temperature. Generally, the highest extraction efficiency is achieved at about the zero point charge pH of AgNPs, under which conditions the electrostatic repulsion is relatively low and particles tend to present in the nonionic surfactant phase. The presence of salts also reduces the Coulomb repulsion between charged NPs and promotes the phase separation [4]. However, high concentration of salts may induce the aggregation of AgNPs. The extraction efficiency typically increases with the surfactant concentration up to a maximum value, and then levels off. As a relative high surfactant concentration means an increase in the surfactant-rich phase volume and thus reduces the enrichment factor, choosing a proper surfactant concentration is important. It is reported that the analyte recovery and preconcentration factor increase when the equilibration temperature used for phase separation is progressively increased above the cloud point temperature of the system [6]. However, high temperature may reduce the association of NPs to the surfactant micelles, causing

the reduction of AgNP recoveries [5]. Under the optimized conditions, 57–116% of AgNPs could be effectively recovered from different environmental waters at the spiking level of 0.1–146 μg/L, with an enrichment factor of 100. Most of all, the extraction did not disturb the pristine size and shape of AgNPs, and the analytes can be subsequently characterized by other techniques, such as transmission electron microscopy (TEM), scanning electron microscopy (SEM), and ultraviolet-visible spectroscopy (UV-vis) (Fig. 2.1). After microwave digestion and quantified by inductively coupled plasma mass spectrometry (ICP-MS), the detection limit is 0.006 μg/L (34.3 fmol/L particles of AgNPs), allowing the ultratrace detection of AgNPs in aquatic systems.

Speciation analysis of AgNPs and Ag^+ in complex matrices is highly demanded because of their distinct difference in environmental behavior and toxicity. The CPE method also offers great potential to selectively separate AgNPs and Ag^+ by adding an efficient chelating agent like $Na_2S_2O_3$ [7] and EDTA [8]. During the extraction, Ag^+ could form hydrophilic complexes with the chelating agent to be preserved in the upper aqueous phase, while AgNPs are transferred into the nether TX-114-rich phase. The interference of Ag^+ was negligible when the concentration of Ag^+ was lower than two times that of AgNPs [5]. It was successfully applied to determine AgNPs and Ag^+ in environmental samples such as commercial available products [7], HepG2 cells [9] and municipal wastewater [10, 11]. Previous study reported the speciation analysis of AgNPs and Ag^+ in six antibacterial products based on CPE [7]. AgNPs were quantified by analyzing Ag contents in the TX-114-rich phase by ICP-MS after microwave digestion, while the concentration of Ag^+ was determined by subtracting AgNP contents from the total amount of silver in the products (Fig. 2.2). The limits of quantification (S/N = 10) for antibacterial products were 0.4 μg/kg and 0.2 μg/kg for AgNPs and total silver, respectively.

Recently, Schuster et al. also reported the determination of AgNPs in environmental waters and wastewater samples by means of CPE [8]. The extracted AgNPs could be directly analyzed by electrothermal atomic absorption spectrometry without any additional sample digestion process, thus a limit of detection as low as 0.7 ng/L was obtained, which enables us to track the fate and transport of AgNPs in the environment. Based on the developed method, they further quantified nanoscale silver particles in the influents and effluents collected from nine municipal wastewater treatment plants in Germany [10]. It was found that the total silver concentration in the unfiltered influent was in the range of 0.32–3.05 μg/L, while about 0.18–1.30 μg/L silver was remained in the filtered influent, revealing a great number of silver was associated with the suspended organic matters with sizes larger than 0.45 μm. The mechanical treatment was demonstrated to efficiently reduce the concentration of nanoscale silver particles in wasterwater samples with an average removal efficiency of 35%, and the subsequent biological treatment can further eliminate more than 72% of the remaining particles in the semitreated wasterwater. As a result, nanoscale silver particles in the effluent was relatively low (< 12 ng/L), indicating that wastewater treatment plants were not the pollution source of nanoscale silver particles to the aquatic system.

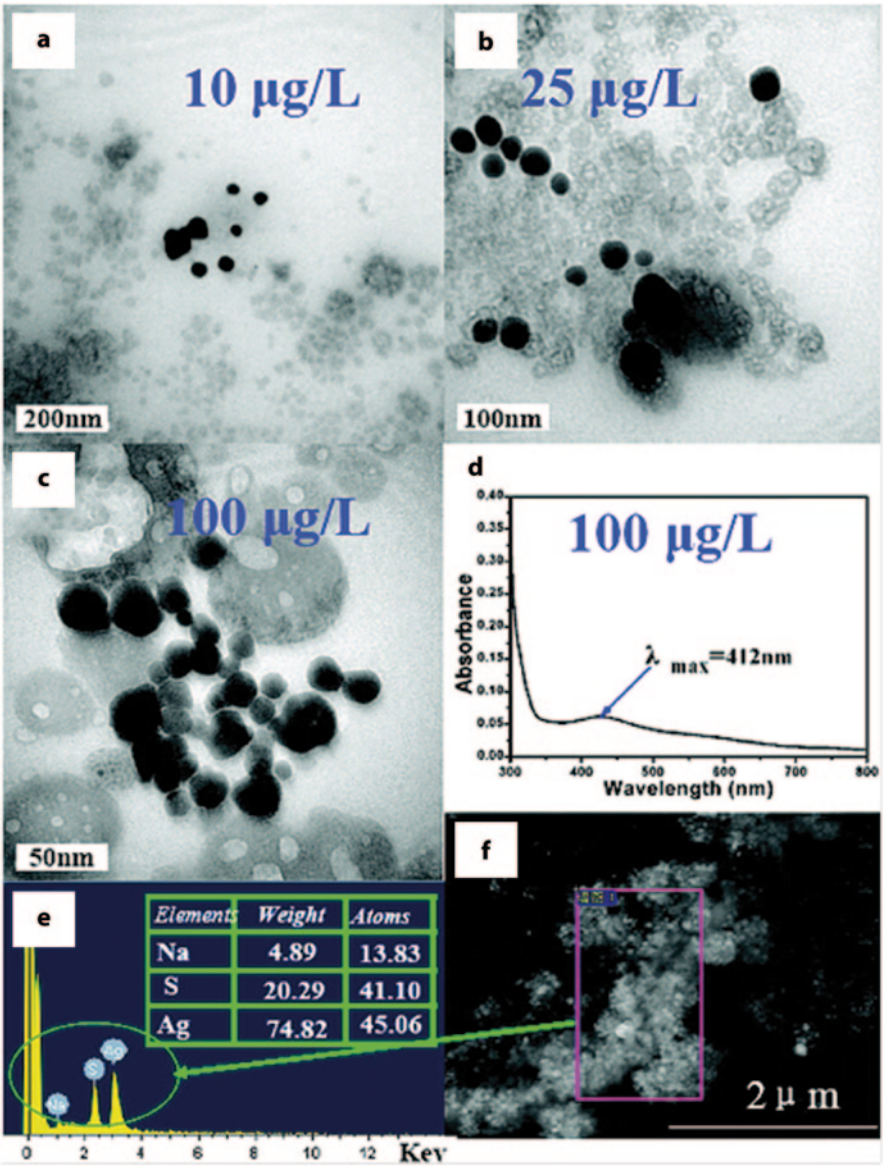

Fig. 2.1 Identification of AgNPs enriched in the TX-114-rich phase. TEM images of the TX-114-rich phase separated from the extraction of samples containing 10 µg/L (**a**) and 25 µg/L (**b**) AgNPs. TEM image (**c**) and UV-vis spectrum (**d**) of the TX-114-rich phase separated from extraction of a sample containing 100 µg/L AgNPs. EDS (**e**) and SEM image (**f**) of the TX-114-rich phase separated from the extraction a sample containing 1 mg/L AgNPs. Reprinted with the permission from ref. [5], Copyright 2009 American Chemical Society

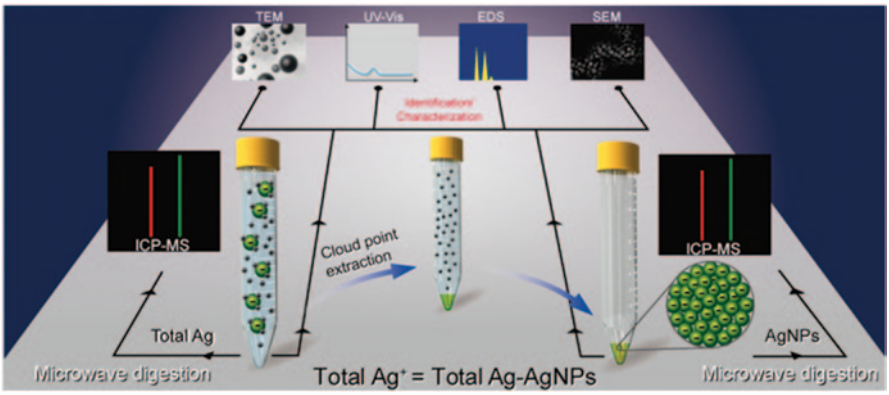

Fig. 2.2 Speciation analysis of AgNPs and Ag^+ in antibacterial products and environmental waters via cloud point extraction-based separation. Reprinted with the permission from ref. [7], Copyright 2011 American Chemical Society

The CPE method allows us to quantify the uptake of AgNPs and Ag^+ to cells as well [9]. Under the optimized conditions, AgNPs and Ag^+ can be readily separated and quantified in HepG2 cells. It was found that about 67.8 ng Ag was assimilated per 10^4 cells after cells were exposed to 10 mg/L AgNPs for 24 h, in which about 10.3 % silver existed as Ag^+ (Fig. 2.3). The substantial amount of Ag^+ in exposed cells indicated that the contribution of Ag^+ cannot be ignored in assessing the toxicity of AgNPs to organisms.

2.1.2 Field-Flow Fractionation

FFF is a flow-assisted hydrodynamic separation technique that was designed to separate and size the macromolecular, colloidal, and particulate materials [12–14]. The separation process is very similar to chromatography except that the isolation relies on physical forces and without the need of a stationary phase. All separation is performed in a thin channel, and samples are separated according to their diverse diffusion coefficients. An axial flow of carrier liquid transports analytes in the direction of the outlet of the channel, while an externally generated field is applied perpendicular to the carrier-driven flow. The external field drives the particles toward the so-called accumulation wall from where they diffuse back into the channel, resulting in the retention of the particles. The basic principle of FFF has been described in previous studies [12, 13]. Depending on the "fields" utilized, FFF can be divided into different types, such as thermal FFF (ThFFF), sedimentation FFF (SdFFF), crossflow FFF (FlFFF), dielectrophoretic FFF (DEP-FFF), and magnetic FFF (MgFFF).

The high resolution and capability to isolate particles with a wide range of sizes makes FFF popular to separate NPs, such as metals, metal oxides, and SiO_2 [15].

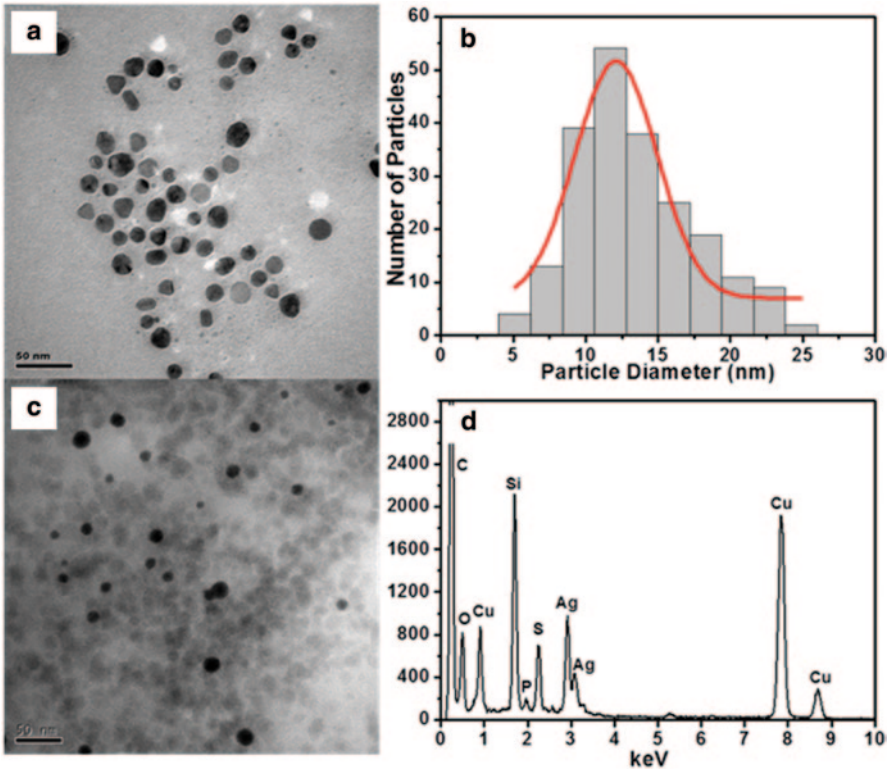

Fig. 2.3 Characterization of pristine AgNPs and identification of AgNPs enriched in TX-114 rich phase after CPE. Up, TEM image (**a**) and particle size distribution (**b**) of the stock AgNP solution; down, TEM image (**c**) and EDS image (**d**) of AgNPs in the TX-114 rich phase after CPE of the exposed cells. The scalar bar is 50 nm. Reprinted with the permission from ref. [9], Copyright 2013 American Chemical Society

Moreover, the absence of a stationary phase avoids the irreversible interaction with the particles, which prevents the low recovery and undesirable morphology change during separation. FFF enables fractionation of ENPs with diverse sizes and different fractions can be further characterized by a variety of detectors. On-line detectors include UV-vis, fluorescence, dynamic light scattering (DLS), inductively-coupled plasma atomic emission spectroscopy (ICP-AES), and ICP-MS, while off-line detectors include TEM, SEM, atomic force microscopy (AFM), and atomic absorption spectrophotometry.

SdFFF was employed to separate and determine AgNPs with about 100 nm in diameter [16]. Using 0.1 % FL-70 as the carrier and on-line UV-vis as the detector, bimodal mixtures of AgNPs can be isolated and characterized [17]. ThFFF also shows promises to retain metal nanoparticles (e.g., Ag, Au, Pd, Pt) suspended in either aqueous or organic carrier solutions [18]. Among the different types of FFF, flow FFF is the most popular technique. Figure 2.4 shows the set-up of a typical FFF system.

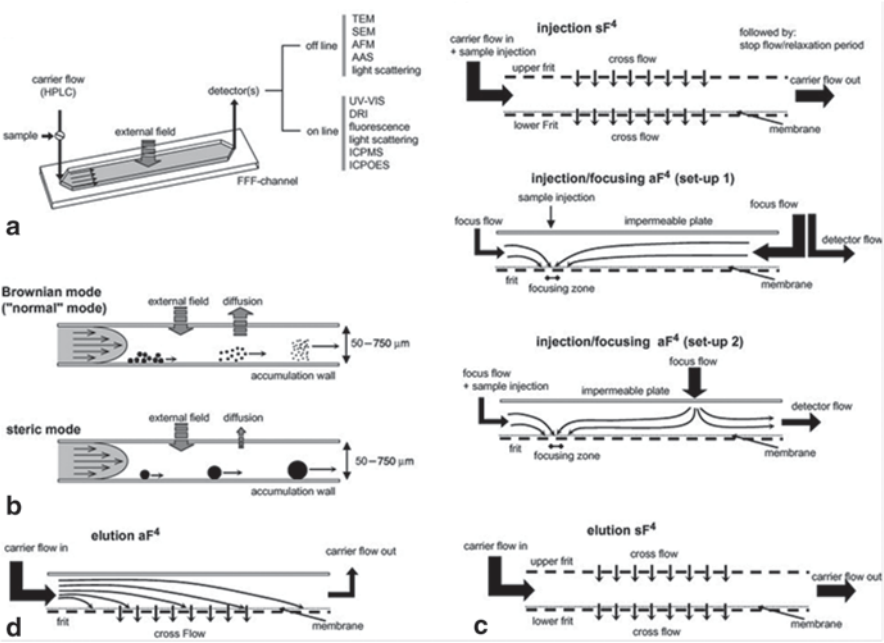

Fig. 2.4 **a** Typical field-flow fractionation (*FFF*) lay-out with examples of different detectors, **b** lateral cross sections through the FFF channel, presenting the principle of particle-size fractionation for the "normal" Brownian and the steric elution modes, **c** lateral cross section through the FFF channel, describing the injection and focusing procedure for symmetric flow-FFF (sF^4) (*top*) and symmetric flow-FFF (aF^4) (*middle and bottom*), and **d** lateral cross section through the FFF channel, showing the elution procedure for sF^4 and aF^4. Reprinted from ref. [13], Copyright 2011 with the permission from Elsevier

Asymmetric flow FFF (AF4) can act as a membrane-filtration unit, which enables the on-line pre-concentration of analytes. It allows up to 50 mL samples to be injected, thus the signal response can be largely improved [15]. To get reasonable results regarding especially the NP size distribution and a good recovery of the analyte, a number of parameters have to be optimized, including the carrier liquid composition, field force, types of membranes, sample injection and relaxation, cross flow rates, and injected mass [19–21]. The carrier solution (i.e. pH, ion strength, and composition) affect the electrostatic properties of the NPs and membranes, and thus influence the retention or adsorption of NPs in the channel. Typically, the carrier provides particles and membranes with the same electrical polarity (both negative or both positive), and sufficient electrostatic repulsion could not only hinder the attachment or loss of the particles to the membrane, but also control the thickness of the repulsive electrostatic double layers to make the particles approach the membrane as closely as possible, and to avoid a repulsion-cushion effect which can induce the particles to elute earlier than would be expected based on their diffusion coefficient [13]. To avoid the undesirable aggregation or dissolution of AgNPs,

the chosen carrier solution should have similar properties with the matrix in which the NPs are suspended. Moreover, a bactericide (e.g., sodium azide) is always added into the carrier solution to prevent the growth of bacteria [22].

In AF4, the membrane is designed to hinder the macromolecules and particles from escaping the channel. The most commonly used membranes are regenerated cellulose and polyether sulphone (PES) with a molecular weight cut-off in range of 300–10,000 Da. In general, losses through the membrane permeation and sorption on the membrane surface are the most common causes of low recoveries [20]. Thus, choosing a proper membrane is of great importance. For highly-charged AgNPs, a lower charged membrane is recommended, as enough repulsion is gained. And for lower-charged ones, membranes with higher charged such as regenerated cellulose are better choices.

The cross flow, which generates the field force and determines the resolution and quality of fractionation, is a key parameter that should be considered. As a general rule, low cross flows are used to sort particles with larger sizes, while a high cross flow can be applied to separate smaller particles, though prolonged retention times are required with higher cross flows [22]. For polydisperse AgNPs or AgNPs with a size larger than 100 nm, constant cross flows may not work well, and a gradient elution is preferred [21].

Under the optimized conditions, AF4 can obtain the size distribution of AgNPs in different matrices to further monitor their stability and transformation in the environment. AF4 results showed that the size of citrate-stabilized AgNPs increased as pH increased from 5 to 8 at low ionic strengths, and higher concentration of Ca^{2+} induced the aggregation and precipitation of AgNPs even with the characteristic FFF peak missing in the fractogram [23]. Pectin and alginate coated-AgNPs were much more stabile than citrate-AgNPs, and humic acid could enhance the stability of AgNPs in real environmental waters [24]. By using 0.01 % (m/v) sodium dodecyl sulfate (SDS) solution at pH 8.0 as the carrier and PES with a cutoff of 1 kDa as the ultrafiltration membrane, casein stabilized AgNPs can be easily separated in the culture medium by AF4-UV-vis. The AF4 fractogram revealed that the size of AgNPs increased from 17 nm to 32 nm after AgNPs were incubated in the culture medium for 24 h. UV-vis spectra showed no differences at the absorbance maximum wavelength before and after the incubation, indicating no obvious aggregation occurred. The increment in the size distribution probably due to the“protein corona” effect [25]. Compare with other techniques like TEM, AF4 can get similar results but is much faster and simpler [21, 23].

For successful separation by AF4, NPs have to be in liquid suspensions [19]. Thus, to analyze complex samples such as food, meat, and sediments, proper decomposition methods are necessary to liberate AgNPs into the liquid suspension. Traditional digestion methods are based on sonication, strong acids, bases, or enzymes. Low pH may lead to the dissolution of AgNPs, which limites the application of strong acid digestion. AgNPs were extracted from tissues of freshwater worms by continuous sonication, and followed by centrifugation and isolated by AF4 coupled with ICP-MS. It was observed that the size of AgNPs increased from approximately 31 nm to 46 nm, which was in good agreement with data derived from DLS, imply-

ing the possible characteristic change of AgNPs during exposure [26]. After enzymolysis by Proteinase K at 37 °C for 40 min, AgNPs spiked in chicken meat samples can be liberated and further separated by AF4-ICP-MS with a recovery of around 80 % [27]. The size distribution of AgNPs in the meat digestate did not change much with that in aqueous solutions, revealing no detectable aggregation or dissolution of AgNPs took place during the sample preparation stage. Alkaline digestion mainly focus on potassium hydroxide (KOH), sodium hydroxide (NaOH), and tetramethylammonium hydroxide (TMAH). However, KOH and NaOH may induce the aggregation of AgNPs [28], and TMAH, which does not change the integrity of AgNPs in short times, appears more suitable for digesting complex samples. AgNPs associated with the cultured HepG2 cells were readily identified by AF4-ICP-MS after a digestion process based on TMAH and Triton X-100 [25]. FFF can also find their way in analyzing AgNPs in consumer products [20], dietary supplements [20], and untreated wastewater [29], showing promises to study the environmental fate of AgNPs in the complex systems.

Hollow-fiber flow FFF system (HF FlFFF) was regarded as the third type of flow FFF, in which fractionation was conducted in a cylindrical hollow fiber instead of the rectangular channel [30]. HF FlFFF was spearheaded by Lee and Jönsson's groups, and has been extensively applied in the analysis of synthetic polymers, cells, bacteria, and biological macromolecules [31]. The main merits of the system included cheapness, miniaturization, simple installation and operation, and comparable separation ability with AF4/F4. In separation, the target was first driven toward the HF wall under the radial flow and located at the equilibrating position, and then moved along HF channels under the axis flow to the detector at different speeds according to the size [32]. As the theoretical basis of HF FlFFF was evolved from the traditional FFF, the diameter of AgNPs in the colloidal could be measured based on their retention parameters. HF FlFFF is expected to play an important role in separation of AgNPs.

2.1.3 Chromatographic Methods

SEC is one of the most commonly used techniques to separate submicron particles. With the porous packing materials filled in the column, particles with the size smaller or equal to the pores of packing materials can permeate deep inside the column packing materials and cause a longer pathway, while larger particles would be rejected by the pores and eluted first. The separation efficiency depends on the average diameter and pore size of packing materials, the column length and mobile phase flow rate. The SEC analysis is fast, simple, repeatable, and rather economical. However, it also faced the problem of limited separation selectivity [33]. For samples with a wide range of size distribution, several columns (usually three or four) are needed to get a satisfying separation result [34]. Moreover, there is a risk that large particles may block pores of the column, so a pre-treatment step is always required.

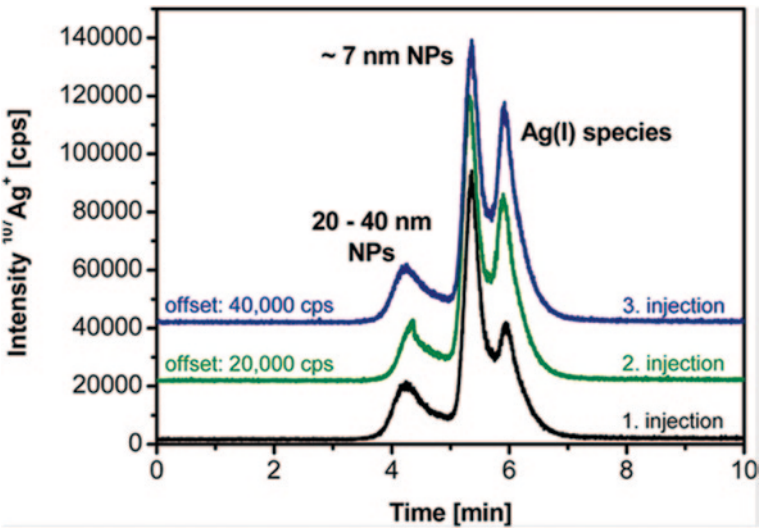

Fig. 2.5 Chromatograms of a solution extracted from sport socks by reversed-phase liquid chromatography coupled to ICP-MS. Reprinted with the permission from ref. [35], Copyright 2013 American Chemical Society

Reversed-phase HPLC was also used to separate different sized AgNPs, and coupled with ICP-MS for the speciation analysis of AgNPs and Ag^+ [35]. The separation of NPs followed a size-exclusion mechanism, so that larger ones eluted first. With the addition of thiosulfate to the mobile phase, Ag^+ can be successfully eluted from the C18 column, and well separated from AgNPs in a single run, with recoveries >80% for both of AgNPs and Ag^+. The limits of detection were in the medium range of ng/L, which allowed the analysis of trace silver in the environment. When separating complex samples, such as fetal bovine serum solutions, the retention time of AgNPs might be altered due to the attachment of proteins to the surface of NPs, which can be readily calibrated by the use of AuNPs as internal size standards. The proposed method is also capable of analyzing real samples, such as extracts from sports socks (Fig. 2.5), showing reproducible analytical results and low detection limits.

Very recently, Liu et al. reported the speciation analysis of dissoluble Ag(I) and silver-containing nanoparticles of 1–100 nm using HPLC coupled with ICP-MS [36]. In that work, the separation was conducted by using an amino column with a pore size of 500 Å, and 0.1% (v/v) FL-70 (a surfactant) and 2 mM $Na_2S_2O_3$ were added into the aqueous mobile phase to facilitate the elution of dissoluble Ag(I) and nanoparticulate Ag from the column. Under the optimized conditions, nanoparticulate Ag with various sizes (ranging from 1 to 100 nm), coating agents (including citrate, PVP and PVA) and species (such as Ag^0 and Ag_2S) can be baseline separated from the dissoluble Ag(I) (Fig. 2.6). The concentration of dissoluble Ag(I) can be directly analyzed by the on-line coupled ICP-MS with a detection limit of

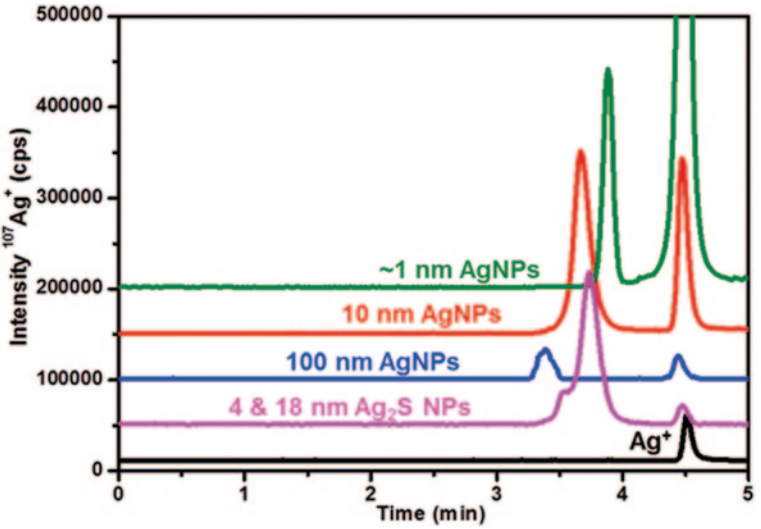

Fig. 2.6 Separation of Ag(I) from different nanoparticulate Ag. Reprinted with the permission from ref. [36], Copyright 2014 American Chemical Society

0.019 μg/L, while nanoparticulate Ag was quantified by subtracting the amount of dissoluble Ag(I) from the total Ag content which was determined by ICP-MS after microwave digestion. The superior separation efficiency and high sensitivity also enable this method to be applied to analyze nanoparticulate Ag in commercially available antibacterial products and environmental waters. Data demonstrated that the developed method performed satisfying chromatography repeatedly, with the relative standard deviation for peak area less than 2% and for retention time less than 0.6%. The spiking recoveries in environmental waters were in the range of 86.6–102% for Ag(I) and 81.3–106% for nanoparticulate Ag. The HPLC-ICP-MS method could be a powerful tool for identifying NPs and their correspondingly released ions from a variety of environmental samples.

Although HPLC is a simple, rapid, and efficient method for the separation of Ag(I) and nanoparticulate Ag, there are also some drawbacks. For example, since the column is packed with porous stationary phase, a small part of nanoparticulate Ag and Ag(I) might be retained in the column, causing the blockage of the column and therefore limiting the usage of times. Additionally, the baseline separation of different sized nanoparticulate Ag, especially for the ones with close size, would be a big challenge. The main reason is that even the most monodisperse particles show a certain size distribution and not with a single size, so for different NPs with close average sizes, some NPs may overlap during separation, resulting in the incomplete resolution. Given the effective size of particles in SEC includes the core size and the electrical double layer thickness of particles [37], increasing salt contents in the eluent would change the electrical double layer and increase retention times of nanoparticulate Ag and Ag(I), thus improving the separation efficiency.

Meanwhile, it was found that when coupling HPLC with ICP-MS, the sensitivities of different sized nanoparticulate Ag are size-dependent in the ICP-MS determination, making it difficult to directly quantify nanoparticulate Ag [35]. Although previous studies ascribed this phenomenon to the size-dependent vaporization and diffusion effects in the ICP-MS determination [38], the exact reason for the size-dependent signal response of nanoparticulate Ag is not very clear yet and needs further investigation.

Hydrodynamic chromatography (HDC) is another size-based separation method, and appears to be an improvement technique of SEC. The column is packed with nonporous microparticles, and separation is achieved by flow velocity and the velocity gradient across them [39]. Larger particles, which cannot fully access slow-flow regions near the conduit walls, are transported faster than small ones, resulting in shorter retention time. In one application for the analysis of AgNPs, HDC coupled with ICP-MS was used to separate AgNPs from sewage sludge supernatant. The size against retention times of the HDC column was calibrated by six AuNP standards with different sizes and a 20 nm gold internal standard was also utilized to compensate drifts of the instrument. After mixing with sewage for 6 h, more than 90 % of AgNPs were adsorbed to sludge. AgNPs survived in the supernatant can be directly isolated and subsequently quantified by HDC-ICP-MS without even the need for filtration, revealing the potential for studying the occurrence and fate of AgNPs in real samples [40, 41]. However, for NPs with a broad size distribution, HDC faces the problem of poor chromatographic resolution.

Counter-current chromatography (CCC), which is known as a support-free liquid–liquid chromatography, is also applied to the size discrimination of AgNPs. A step-gradient extraction-based CCC to separate carboxylate-anion-modified AgNPs was developed by Yu and coworkers [42]. Hydrophilic AgNPs can be readily transferred to the organic phase (toluene/hexane = 1:1, v/v) by forming ion-pair adducts with a surfactant tetraoctylammonium bromide (TOAB). Smaller particles were easier to transfer during this dynamic extraction. The size distribution of collected fractions can be controlled by the concentration of TOAB. With the aid of 0.02 mM of TOAB, AgNPs with a size distribution of 15.8 ± 5.3 nm can be readily separated into four portions with very narrow size discrimination, which was verified by SEM.

Overall, though nonspecific interactions with the stationary phase can result in strong interactions or irreversible binding of the analytes, chromatographic methods serve as an attractive alternative in studies related to the separation of AgNPs.

2.1.4 Electrophoresis Methods

A myriad of NPs are presenting stable charges, so electrophoresis methods appear as an attractive strategy for the particle fractionation. NPs can be separated according to their different sizes, shapes, and chemical modifications of the surface. For particles modified with functional groups, the isolation is achieved based on the surface charge due to the ionization/dissociation of chemical groups. Bare particles may acquire surface charges by adsorption of ions from the solution, and are mainly separated by the size [43]. The mainly used electrophoresis methods are gel electrophoresis, isoelectric focusing (IEF), and CE.

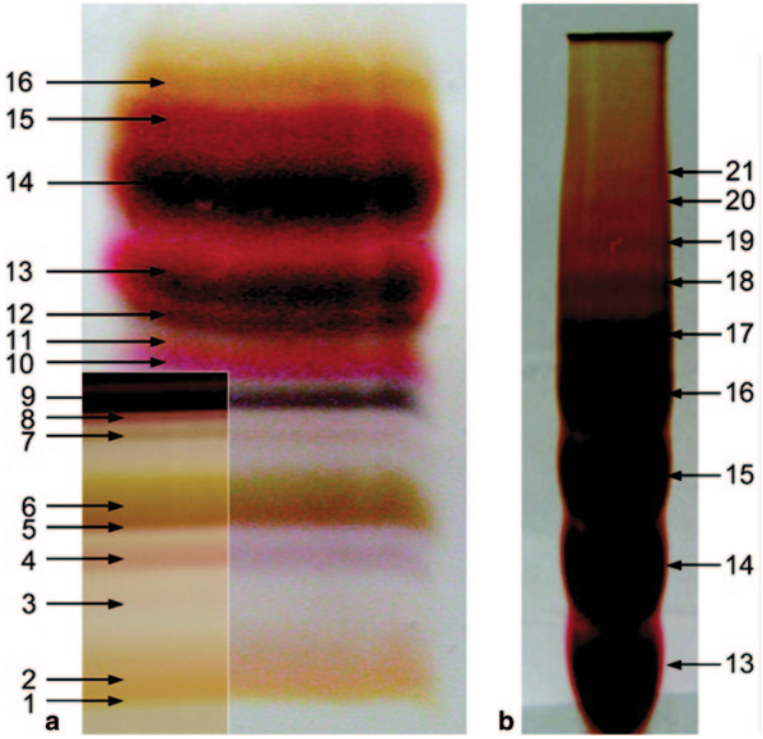

Fig. 2.7 PAGE results for Ag:SG clusters. **a** Bands of discrete Ag:SG clusters. The smallest clusters are at the *bottom* and have the lowest index. *Inset*: finer bands revealed at a higher concentration. **b** Discrete highermass clusters, synthesized with less glutathione. Reprinted with the permission from ref. [45], Copyright 2010 American Chemical Society

Gel electrophoresis is a separation technique primarily based on the different migration behavior of species in the gel medium in an electric field [44], which is widely applied to separating macromolecules such as DNA, RNA, and proteins. And now the separation of NPs is also feasible. The type of gel is one of the key parameters that should be considered. The most commonly used gels are polyacrylamide gel and agarose gel. Polyacrylamide gel electrophoresis (PAGE) was successfully applied to separate 21 diverse glutathione-ligated Ag clusters (Ag:SG) with about 1 nm in diameter [45]. Each Ag:SG cluster can form a band in the PAGE gel, exhibiting different colors, which can be directly discernible by the naked eyes (Fig. 2.7). However, as the pore size of polyacrylamide gel is typically about 3–5 nm and highly heterogeneous, it is not suitable to separate larger NPs. Moreover, the severe shrinkage after polymerization also hinders its large-scale application [46]. As a result, the agarose gel with larger and uniform pore sizes seems to be more applicable for NP discrimination.

Hanauer and coworkers displayed the separation of AgNPs and AuNPs based on their size and shape by agarose gel electrophoresis [47]. Ag nanorods, nanospheres,

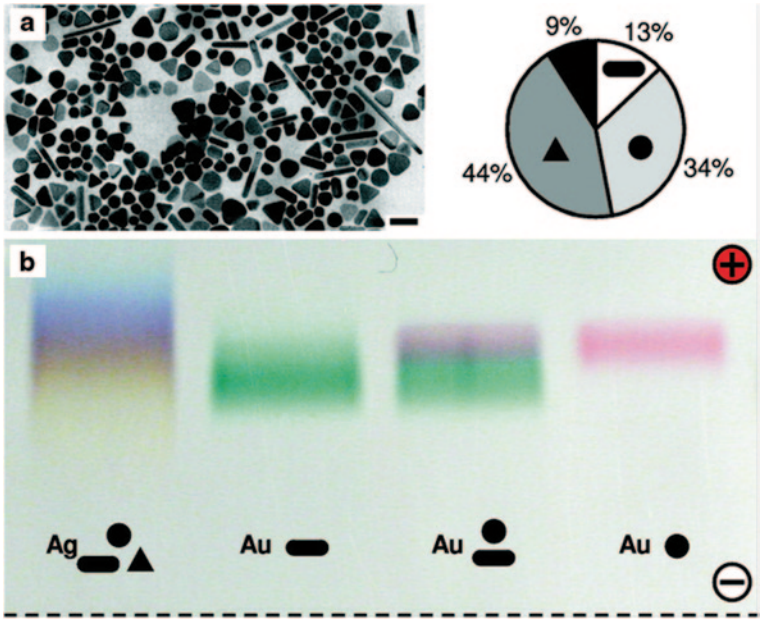

Fig. 2.8 **a** Typical TEM picture of a silver nanoparticle sample (*left*, scale bar 100 nm) and the proportion of spheres, triangles, and rods (*right*). **b** True color photograph of a 0.2% agarose gel run for 30 min at 150 V for the separation of different nanoparticles. Reprinted with the permission from ref. [47], Copyright 2007 American Chemical Society

nanotriangles, together with gold spheres and gold rods can be readily isolated in 0.2% agarose gels in 0.5 TBE (Tris-borate EDTA) buffer (~ pH 9) after modified with SH-PEG-COOH. The separation efficiency can be visually monitored as the gel showed different colors in the silver lanes (Fig. 2.8). Each portion can be collected for further characterization by TEM and local extinction spectroscopy. It was found that the triangles traveled the fastest, and spheres showed a slight tendency to be enriched in the fastest fractions, and rods displayed the lowest mobility. Moreover, nanorods with the highest aspect ratio moved the slowest; for the spherical particles, a clear trend of increasing mobility with increasing size was observed; and the mobility of the triangles showed no clear trend, probably due to the unknown thickness of the flat triangles.

Low melting point agarose gel electrophoresis was also described for enriching SERS-active Ag-multi-nanoparticles [48]. In SERS determination, nanoparticle junctions (hot spots) are required to get a high signal enhancement, so isolating dimer and small clusters of AgNPs from the monomers and large aggregates could contribute to increasing the SERS activity. Ag-multi-NPs assemblies, which gave high SERS intensities, can be readily separated and assembled in one zone by gel electrophoresis after fine controlling surface charges of AgNPs and pore size of agarose gel matrix, indicating the potential applications of gel electrophoresis in selecting superior materials.

IEF is a technique commonly applied to determine the isoelectric point (pI) of proteins and enzymes, and also used to separate different molecules based on differences in their pI [43]. Carboxylic acid groups derivatized Ag and Au colloidal nanoparticles with different sizes were successfully separated by using a miniscale isoelectric focusing unit [49]. The ionization of carboxylic acid groups in the three-dimensional self-assembled monolayers (SAMs) resulted in a strong pH dependent colloidal particle size. The separated bands in the IEF unit were typically 0.04 pH units in all cases and colloidal particles closest in size can be easily separated. The IEF method is fast, cheap, and highly sensitive, which can be used to improve the polydispersity of colloids.

CE is also recognized as a powerful analytical technique for the isolation of various charged ENPs, such as AuNPs, AgNPs, quantum dots, silica, and carbon-based materials. In the case of CE, separation is achieved due to the differential mobilities of the analytes that are injected into hair-thin capillaries filled with an electrolyte in an applied electric field [44]. The migration time is affected by several parameters: size and shape of the NPs, chemical nature and electronic configuration of the NPs, and the ligands or stabilizers added to the medium [43].

Liu's group reported the size and shape dependent separation of different Ag NMs including Ag nanorods [50], Ag nanocubes [51], AgNPs [52] and Au/Ag core/shell nanoparticles [53] by capillary electrophoresis coupled with a diode-array detection (DAD) system. An anionic surfactant, SDS, was added into the running electrolyte to prevent particle coalescence during the separation process, which also contributed to improve the separation performance. By using a mixed buffer of SDS (40 mM) and 3-(cyclohexylamino)propanesulfonic acid (10 mM) at pH 9.7 and an applied voltage of 20 kV, Au/Ag core/shell NPs can be readily separated. The migration time is linearly correlated to the size of the core/shell NPs in the range of 25–90 nm ($R^2 > 0.99$), and the relative standard deviations of these electrophoretic mobilities were $< 0.9\%$ [53]. The reversed-electrode polarity-stacking mode of CE was also developed by the same group for the on-line enhancement of detection and separation of AuNPs and Au/Ag core/shell NPs. Under the optimized conditions, the detection limits of the Au/Ag NPs increased by ca. 140-fold [52], and the on-line DAD detector enabled the simultaneous characterization of NP species. This method is an efficient approach to rapidly monitor reaction mixtures during the fabrication of NPs.

Micellar electrokinetic chromatography (MEKC) appears to be one of the most convenient CE modes for separation of ENPs by size. Recently, Franze and co-worker reported the speciation separation and characterization of AuNPs, AgNPs and their ionic counterparts with MEKC coupled to ICP-MS [38]. The addition of SDS in the mobile phase could change the surface chemistry of NPs, enhance the electrophoretic mobility and thus facilitate the particle separation. Small particles are eluted first due to the smaller surface area and lower charge-to-size ratio, and a good linear relationship ($R^2 > 0.999$) existed between the migration time and particle size. Capillary recoveries were on the order of 72–100%, and the detection limit was in the sub-microgram per liter range coupled with ICP-MS as the detector. The developed method was also capable of detecting real samples such as nutritional supplements and a complex agent penicillamine, showing the potential for the analysis of unknown environmental samples.

Sometimes the separation is challenged by the NP interaction with silanyl groups on the inner wall surface of the silica capillary, which can be resolved by the modification of the capillary or lowering the pH of buffers [44]. The CE technique can be coupled with a myriad of detectors such as UV-vis, ICP-MS, fluorescence spectroscopy and Raman spectroscopy, which can give vast information of the analytes. The fast separation rate, feasibility to analyze many samples at a time, plus the small injection volume made this method the best choice to analyze NPs especially some precious samples.

2.1.5 Density-Gradient Centrifugation

The density-gradient centrifugation method has emerged as an effective tool to sort ENPs according to differences in size and structure. Typically, a density gradient is made in a centrifuge vessel by sequentially layering aqueous solutions with different densities, and then samples are dropped on top of the density gradient and subjected to centrifugation. Particles with similar size and shape have similar sedimentation rates, and would travel down the centrifuge tube to form a certain region in the density gradient after reaching their density equilibria. The commonly used density gradient media are sucrose, glycerol, and ethylene glycol, which are cheap, easily available and have high viscosity and density. Moreover, proper density gradient media also serve as capping agents to hinder particle aggregation during separation [54]. AgNPs synthesized using *Magnolia kobus* plant leaf extracts were successfully separated by density gradient centrifugation with 30, 40, 50, and 60% sucrose solutions as the separation media [55]. The lower density gradient of 30% sucrose could separate the small spheres, triangles, and cubes, whereas most moderate sized spheres, triangles, and pentagons were in the 40% sucrose. A high amount of irregular spheres were located at 50 and 60% sucrose. Each fraction could be easily collected for further TEM characterization. However, most of the gradient centrifugation is performed in aqueous solutions. For NPs that prepared in organic medium, transferring from organic solvents to aqueous solutions may suffer from undesirable particle coagulation.

Sun's group first demonstrated the separation and purification of NPs in organic density gradients. NPs dispersed in organic medium can be directly separated after synthesis and each portion is easily concentrated by evaporating organic solvents after fractionation. Several typical colloidal nanoparticles, including Au, Ag, and CdSe were sorted based on the size and shape [56]. A five-layer step gradient was prepared using 50, 60, 70, 80, and 90% concentration (by volume) cyclohexane solutions of CCl_4 in a centrifuge vessel. After sample loading and centrifugation at 50,000 rpm for 8 min, distinct zones with various colors were formed in the vessel (Fig. 2.9), indicating that different sized AgNPs were successfully isolated. Subsequent TEM images of the fractions demonstrated that particles in the closest zones only had very small size difference (about 2 nm), showing its powerful separation efficiency.

Due to the high surface reactivity, reactions between NPs are very fast, and sometimes down to tens of seconds. Thus, isolation the intermediates of NPs by traditional centrifugation methods in such a short time is not an easy task. Sun's group [57] further reported the use of density gradient ultracentrifuge separation as a pro-

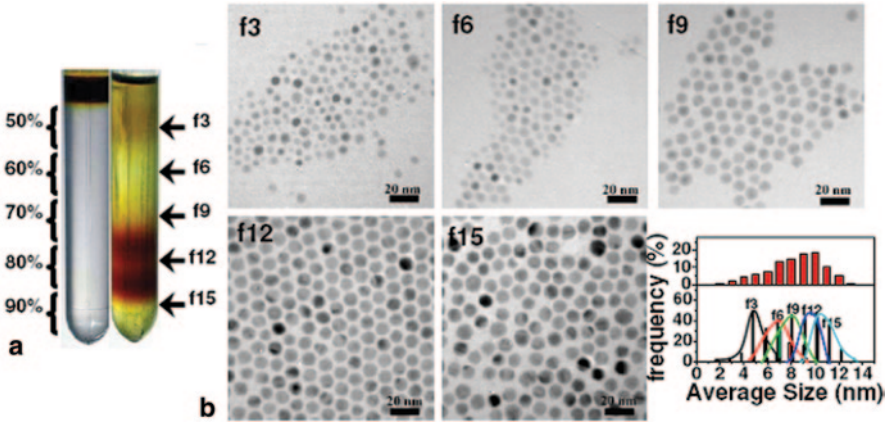

Fig. 2.9 Results demonstrating the separation of Ag nanoparticles (**a**) digital camera images of ultracentrifuge vessels containing Ag nanoparticles before separation and after separation (**b**) TEM images of several Ag fractions. The graph in the *bottom right* corner shows a comparison of the size difference before (*red columns in the upper section*) and after separation (*colored columns in the lower section*). Reprinted with the permission from ref. [56], Copyright 2010 American Chemical Society

cess-analysis microsystem to study the mechanisms of some reactions. For a typical replacement reaction that $AuCl_4^-$ etches triangular Ag nanoplates to form Au, a multilayer density gradient (20 + 30 + 40 + 50 + 60 + 70 %) was made by sequentially layering aqueous solutions with different concentrations of ethylene glycol in a centrifuge vessel. The top layer performed as the buffer to prevent direct reaction, while the second layer introduced with the reactant $HAuCl_4$ acted as the reaction zone. The other higher density zones were used to separate intermediates. After Ag nanoplates loading, larger particles passed through the reaction zone faster, which shortened their duration in the reaction zone, whereas the reaction time for smaller ones prolonged. As a result, the intermediates at different reaction times could be captured to give direct evidences to reveal the reaction mechanism.

2.1.6 Miscellaneous Methods

Except for the above traditional methodologies, a series of novel separation methods are also reported to separate AgNPs from different matrix. Recently, a knotted reactor based solid phase extraction device was developed for the differential analysis of AgNPs and Ag^+ in complex animal tissues [58]. AgNPs, which can be regarded as the precipitates of Ag^0, would be retained on the knotted reactor walls even with the protein coating, while Ag^+ can be selectively adsorbed or detached according to the sample acidity and the volume of the rinse solution. After optimizing the operating conditions, it was found that both AgNPs and Ag^+ could be retained at pH 6 without a rinsing step, whereas Ag^+ would be selectively extracted at pH 10 with a 1000 μL rinse solution, which allows the discrimination of AgNPs and Ag^+ (Fig. 2.10). The proposed method was capable of monitoring the biodistribution and dissolution of

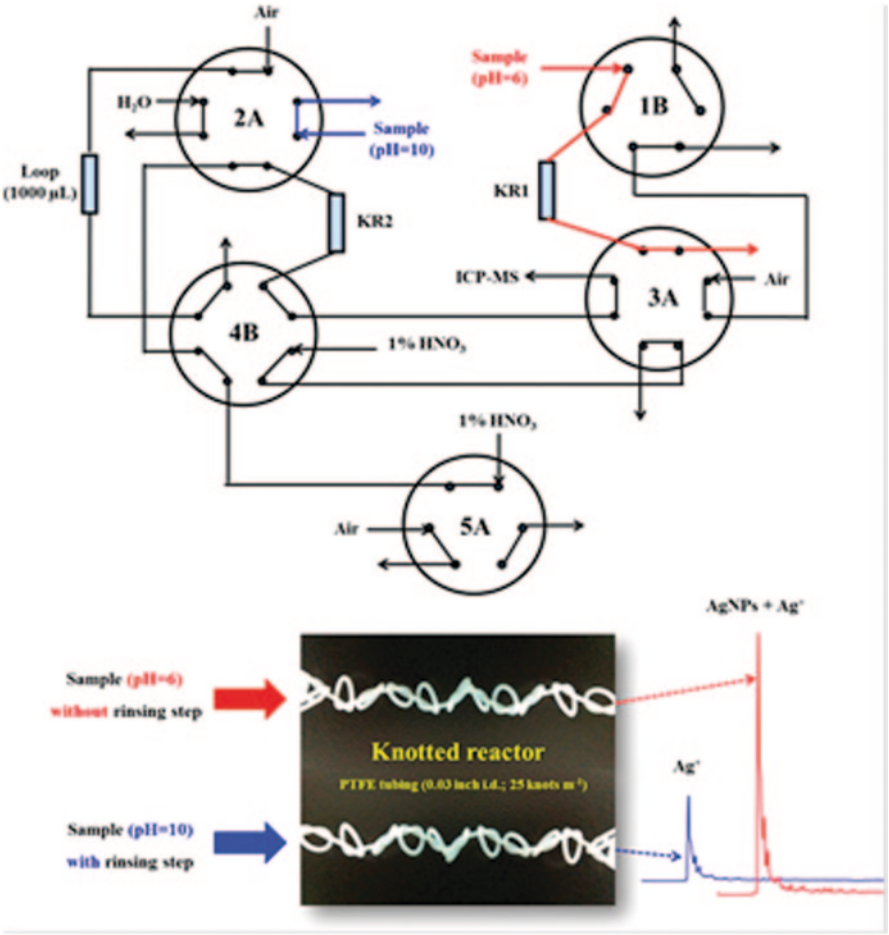

Fig. 2.10 Schematic representation and configuration of the online automatic dual-KR-based differentiation system. When the sample pH was adjusted to 6 and the system run without a rinsing step, the total Ag content, including AgNPs and Ag^+, was retained; when the sample pH was adjusted to 10 and the system run with a 1000-µL rinse solution, the Ag^+ were extracted selectively. The two pretreated components were run through the operating sequence independently but were synchronized with a well-defined time delay. The unmarked *arrow* indicates the outflow of liquid waste. Reprinted with the permission from ref. [58], Copyright 2014 American Chemical Society

AgNPs in rats after 1, 3, and 5 days postadministration. Results revealed that large amounts of AgNPs were deposited in liver and spleen, which were also the main inflammation organs in rats. On the contrary, the Ag^+ -rich targets, such as kidney, lung, and brain, suffered from no significant toxic responses, alerting us to pay more attention to the nanoparticle effects when assessing the AgNP toxicity.

Schuster et al. [59] demonstrated a new method for the extraction of AgNPs by ionic exchange resins. An anionic exchange resin, Amberlite IRN-78 was selected in the study, and the presence of ammonium groups provided them with positive

charges. Thus negatively charged AgNPs, modified by mercaptosuccinic acid (MSA), could be easily captured by the resin because of electrostatic interactions. A solution of 8% (v/v) formic acid in methanol could completely extract the adsorbed AgNPs with gentle shaking at room temperature. The resin can also be recycled by consecutively rinsing with 5% (v/v) hydrochloric acid and 5% (v/v) sodium hydroxide solution. As AgNPs were noncovalently adsorbed onto the ionic exchange resin, particle size and shape was preserved during the separation. Moreover, low concentrations of dissolved organic matter did not disturb the extraction. This proposed method was capable of analyzing real environmental samples, such as natural waters and wastewater from wastewater treatment plants with AgNP concentration at the 80 ng/L level [10]. However, it is challenged by the relatively long extraction time (>40 h).

A rapid size selection method using the pressure tunable solvent properties of CO_2-expanded liquids was developed by Roberts and coworkers [60]. Gaseous CO_2, acting as an anti-solvent, was added to the AgNP solvent hexane to tune the solvent strength. Typically, interaction between the solvent mixture and ligand tails is necessary to sterically stabilize particles of a given size. When changing the pressure of gaseous CO_2 to diminish the solvent strength below the threshold interaction value for a certain particle size, the correspondingly sized AgNPs precipitated. Based on this principle, a polydisperse AgNP solution was readily fractionated into six sections with narrow size distributions by simply changing the CO_2 pressure from 500 to 650 psi. The method eliminated the large quantities of organic solvents that are used in traditional techniques, and is rather environmentally benign, fast, and efficient, which would be a powerful tool for narrowing the size distribution of nanoparticles.

2.2 Characterization and Quantification

2.2.1 Characterization

Since the nanoscale dimensions of AgNPs are beyond the detection ability of traditional optical microscopy, the electron microscopy (EM), which has a much higher resolution, emerges as a more suitable technique for NP characterization. The most preferred ones are TEM and SEM.

In TEM, a high-energy electron beam is transmitted through a very thin layer of the specimen, and non-adsorbed electrons are focused onto an imaging detector, affording a direct image of the target nanoparticle [61]. It provides us not only the information on the particle size and morphology, but also properties including the state of aggregation, dispersion, and sorption. The high-resolution TEM also allows the visualizing atomic layers of crystalline samples, which can be used to identify unknown NPs by counting their characteristic lattice spacing. For TEM, the resolution in state-of-the-art is about 0.07 nm, and it mainly depends on the accelerating voltage for the electron beam and the thickness of the sample [62]. The higher voltage and thinner samples would gain a better theoretical resolution. As a result, the TEM specimen must be thin enough to enable the electron to pass through. The samples are also required to be dry enough, which may cause severe artifacts

in size determination as undesirable particle coagulation or surface alteration may occur during the solvent evaporation process. For complex samples such as food and biological tissues, the sample preparation may be a main task. Commonly, the chemical fixation and staining is needed to preserve the pristine structure of proteins and improve contrast on the micrograph. The subsequent chemical dehydration, drying, and post cutting into thin sections are also time-consuming and strenuous.

The SEM technique uses an electron beam to interact with NP surfaces, and secondary electrons, backscattered electrons or X-ray photons are measured [63]. SEM samples can be analyzed in bulk form, so sample preparation is much easier. Samples can be directly mounted on aluminum or carbon stubs without cutting into thin sections [62]. However, there is a risk that the accumulation of static electric fields at the specimen may occur due to the electron irradiation during imaging, so the sample, at least the surface, must be conductive. Coating the nonconducting sample with a thin layer of gold is generally required, though some surface information may be lost.

The development of new EM techniques like environmental SEM and environmental TEM allows the detection of partially hydrated samples and specimens without the coverage of an electrical conductor. Thus, the imaging artifacts triggered by invasive preparation can be avoided [62]. The EM technique can simultaneously give the elemental composition of NPs if coupled with an energy dispersive devise, e.g., Energy-dispersive X-ray spectroscopy (EDS). Sometimes the EDS method can provide some semiquantitative information and identify the presence of AgNPs in complex samples by elemental analysis.

The EM methods offer the most direct information on the size distribution and shapes of the primary particles. However, as the sample volume that can be analyzed is very small, to gain an accurate and representative result, hundreds of particles have to be counted. And sometimes a certain number of replicates have to be prepared for each specimen. Moreover, since only a very tiny proportion of sample can be observed during analyzing, finding the target particles would be like “looking for a needle in a haystack” for dilute AgNPs [62], which is tedious and time consuming.

Laser light scattering methods, especially the dynamic light-scattering (DLS) technique, are also frequently applied for in situ and real-time NP sizing, and physical characterization of AgNPs. The method is based on the measurement of light scatters of small molecules during Brownian motion in solutions and the correlation of it to the size of particles. The size of NPs measured by DLS (hydrodynamic diameter) may be a little larger than that measured by electron microscopy (core diameter), because a layer of solvent molecules may be included in the hydrodynamic diameter [64]. DLS often serves as the on-line or off-line detector to give the further information of each fraction after AgNPs were separated by FFF or chromatographic systems. However, there are some inherent drawbacks of the DLS technique. Since larger particles scatter more light, the presence of rare but much larger aggregates will skew the effective diameter of AgNPs, giving a large size distribution. Thus, DLS data obtained from polydisperse samples are difficult to interpret. Additionally, it also suffers from rather poor sensitivity for dilute AgNP

solutions. The DLS results are generally given along with the TEM characterization to get a comprehensive description of AgNPs.

Since AgNPs give a high SPR in the UV-vis wavelength range, UV–vis spectroscopy offers the possibility to characterize AgNPs. Due to its cheapness, easy handling, as well as the robustness, UV–vis spectroscopy is becoming one of the most preferred detectors for AgNP characterization. Typically, the maximum absorption wavelength in a UV-vis spectrum is associated with the average particle size, while its full width at half-maximum can give information about the particle homogeneity [65]. Thus, it is frequently used to characterize the stability of AgNPs in complex biological and environmental media. However, UV-vis also faces the problem of low sensitivity. It is not reliable to distinguish between monodisperse samples and slightly aggregated ones because the resulting shift is very subtle. Based on the Bouguer–Lambert–Beer law, UV–vis spectroscopy can quantify the rough concentration of AgNP solutions.

2.2.2 Quantification

As the concentration of AgNPs in environmental matrices is extremely low, techniques for the ultra-trace determination of AgNPs are urgently needed to give a quantitative risk assessment of AgNPs. ICP-AES and ICP-MS allow us to detect trace metals quickly and efficiently, and offer the multi-isotope or multi-element determination, which makes them popular for AgNP quantification. Furthermore, the high ionization efficiency, speed, precision and sensitivity, plus large linear ranges qualify them as the most popular tools for metal detection. ICP-AES and ICP-MS also suffer from some limitations: the presence of some tiny particles may block or clog the sample tips within the spray chamber, and organic ligands associated with AgNPs hinder the fully atomization of the metal in an ICP. Thus, a membrane-filtration or sample-digestion process is always needed before sample loading. The commonly used digestion solvents are concentrated nitric acid and hydrogen peroxide, but this destructive method results in the inadequateness of speciation analysis of metals. Take AgNPs for example, we cannot differentiate NPs from Ag^+, unless a pre-separation procedure is performed before acid digestion.

ICP-AES has some inherent drawbacks: the LODs are superior for light elements, but are not good enough for elements such as As, Se, and Pb [66]. ICP-MS possesses higher selectivity and sensitivity, which is more suitable for ultra-trace detection. ICP-MS can be coupled with a variety of separation techniques, such as FFF, SEC, HDC, HPLC, and CE. The concentration of each portion can be directly determined, avoiding sample losses via the fraction collection or storage process. The element silver exists as two stable isotopes ^{107}Ag and ^{109}Ag, which makes it possible to measure trace Ag with isotope-diluted (ID) ICP-MS. Unlike ICP-MS that detects the absolute intensity of target elements, ID-ICP-MS just measures ratios of two stable isotopes in samples to indirectly quantify the analyte concentration. As long as the isotopic equilibration is achieved, ID-ICP-MS is theoretically capable of compensating for any loss of analytes during sample preparation, suppression of ion

sensitivities by concomitant elements in the sample matrix and instrument drifts, which provides better accuracy and precision [67, 68].

Single particle mass spectrometry (spICP-MS), which was first proposed by Degueldre and colleagues [69, 70], is an efficient method for the discrimination and quantification of AgNPs and Ag(I) species. In the spICP-MS mode, dissolved Ag will generate a stable signal with few pulses, whereas a dilute solution of AgNPs is ablated in the plasma and a burst of ions are produced during vaporization, causing a single pulse greater than the constant dissolved background, whose intensity is proportional to the number of Ag atoms in the particle and frequency is related to the number of AgNPs present in the samples [71, 72]. When analyzing, a direct sample introduction is required and dissolved metal ions and nanoparticles can be readily isolated in a run. Moreover, both the particle size and particle number concentration can be measured simultaneously using spICP-MS. Details of the theory have been outlined in the literatures [69, 70, 73–75]. Usually, the detection limit of spICP-MS is as low as mid ng/L, which is suitable for NP analysis in the environmental and biological samples [76, 77].

Based on these advantages, spICP-MS has been applied for characterization and quantification of AgNPs in different matrices. Recently, Higgins et al. [78] reported the utilization of spICP-MS for the analysis of AgNPs in biological tissues. After digested by TMAH, AgNPs in biological tissues such as ground beef, *Daphnia magna* and soil earthworms can be well liberated, and directly analyzed by spICP-MS. Mass- and number-based recovery of spiked AgNPs was in the range of 83–121 % from all tissues measured. Biological exposure experiments showed the method was also capable of analyzing the bioaccumulation of AgNPs. The *Daphnia magna* nanoparticulate body burden for AgNPs was 59 ± 52 $\mu g/kg_{ww}$ after being exposed to 4.8 μg/L 100 nm AgNPs for 48 h. However, the particle size distribution, which was determined from *Daphnia magna* tissues, showed no obvious shift as compared to the exposure media. Hintelmann et al. [71] validated spICP-MS for AgNP characterization and quantification in the influent and effluent from a wastewater treatment plant and in river water.

The main drawback of spICP-MS is that not all AgNPs are available for spICP-MS analysis. For example, the size detection limits are generally in the range of 20 nm [71, 79], as the signal of smaller nanoparticles can hardly be distinguished from the background metal ions. The accurate size and concentration determination is also challenged by the uncertainty of the nebulization efficiency [80]. Meanwhile, multi-isotope or multi-element detection is missing in the spICP-MS mode, making it impossible to quantify composite nanoparticles [35].

Atomic absorption spectrophotometry (AAS) is a powerful alternative to ICP-MS or ICP-AES for the detection of silver, due to its high sensitivity, selectivity, and accuracy, as well as the relatively low cost. However, AAS also suffers from some drawbacks, e.g., the failure of multi-element analysis and relatively narrow linear range [14].

Each method has its advantages and limitations, and a single method is hard to meet the requirement of quantifying AgNPs in various samples. In most cases, multiple schemes are often carried out to get comprehensive information of the analytes. A brief outline of methods for separation and determination of AgNPs in different matrix is given in Table 2.1.

Table 2.1 Overview of the analysis of AgNPs

Analyte	Matrix	Separation methods	Conditions	Characterization and quantification	Reference
PVP-AgNPs	Aquatic environmental samples	Cloud point extraction	$Na_2S_2O_3$ 10 mM, pH 3.0, TX-114 concentration 0.2% (w/v), 40 ℃ incubated 30 min, centrifuged at 2000 rpm, 5 min	Off-line: TEM, SEM-EDX, UV-vis, ICP-MS	[5]
PVP-AgNPs and Ag^+	Commercial antibacterial products	Cloud point extraction	$Na_2S_2O_3$ 10 mM, pH 3.0, TX-114 concentration 0.2% (w/v), 40 ℃ incubated 30 min, centrifuged at 2000 rpm, 5 min	Off-line: TEM, SEM-EDX, UV-vis, ICP-MS	[7]
Citrate-AgNPs and Ag^+	River water, wastewater samples	Cloud point extraction	40 mL of aqueous sample solution with 1.0 mL of saturated EDTA solution, 400 μL of 1 M sodium acetate, 100 μL 1.25 M acetic acid, and 1 mL of 10% TX-114 (w/w in UPW)	Off-line: UV-vis, ETAAS	[8]
PVP-AgNPs and Ag^+	HepG2 cells	Cloud point extraction	$Na_2S_2O_3$ 20 mM, pH 3.5, TX-114 concentration 0.2% (w/v), 40 ℃ incubated 30 min, centrifuged at 3000 rpm, 5 min	Off-line: TEM-EDX, ICP-MS	[9]
Nanoscale silver particles (n-Ag-Ps)	Wastewater samples	Ionic exchange resin and cloud point extraction	n-Ag-Ps modified with mercaptosuccinic acid, pH 8.0±0.5, 4.5 g of Amberlite IRN-78 nuclear grade ion-exchange resin, sample loading rate: 1.5 mL/min, eluting solvents: 25 mL of 8% (v/v) formic acid in methanol, shaking at 250 rpm for 4−45 h at room temperature	Off-line: ETAAS	[10]

Table 2.1 (continued)

Bare-AgNPs, Citrate-AgNPs, PVP_{10}-AgNPs, PVP_{SA}-AgNPs, MUA-AgNPs, MSA-AgNPs, BSA-AgNPs, Lys-AgNPs, Cys-AgNPs, Starch-AgNPs, AgCl-AgNPs, Ag_2S-AgNPs, Ag_3PO_4-AgNPs	Different kinds of natural organic matter	Cloud point extraction	40 mL of aqueous sample solution with 1.0 mL of saturated EDTA solution, 400 μL of 1.25 M sodium acetate, 100 μL 1 M acetic acid, and 1 mL of 10% TX-114 (w/w in UPW)	Off-line: UV-vis, TEM, ETAAS	[11]
Silver sols	Pure water	Sedimentation field-flow fractionation	Carrier liquid: 0.1% FL-70 solution, injection volume: 50 μL	On-line: UV-vis	[16]
Binary mixture of AgNPs (2–100 nm and 60–150 nm)	Pure water	Sedimentation field-flow fractionation	Carrier liquid: 0.1% FL-70 solution, injection volume: 5–30 μL, flow rate: 0–20 min, increased from 2 to 4 mL/min, 20–50 min 4 mL/min	On-line: UV-vis Off-line: SEM	[17]
Ag, Au, Pd and Pt nanoparticles together	Pure water	Thermal field-flow fractionation	Carrier liquid: tetrahydrofuran and acetonitrile, flow rate: 0.3 mL/min, sample injection: 20 μL	On-line: UV-vis	[18]
PVP-AgNPs	Pure water	Asymmetric flow field-flow fractionation	Carrier liquid: 0.5 mM NH_4HCO_3, pH 7.4, membrane material: PES, cut-off: 10 kDa, spacer height: 350 μm, detector flow rate: 1.0 ml/min, injection flow rate: 0.2 ml/min, focus flow rate: 1.0 ml/min	On-line: UV-vis, ICP-MS, DLS Off-line: TEM	[19]
AgNPs	Pure water	Asymmetric flow field-flow fractionation	Carrier liquid: 0.01% (m/v) SDS solution, pH 8, sample injection volume: 20 μL, membrane material: PES	On-line: UV-vis, ICP-MS Off-line: TEM	[20]
Colloidal Ag dispersions	Pure water	Asymmetric flow field-flow fractionation	Carrier liquid: DI water, membrane material: PVDF and regenerated cellulose	On-line: UV-vis, ICP-MS Off-line: TEM, batch-DLS	[21]

Table 2.1 (continued)

Newly synthesized AgNPs	Synthesized water	Asymmetric flow field-flow fractionation	Channel flow: 1 mL/min; cross flow between 0.4 and 1 mL/min	On-line: UV-vis Off-line: TEM, DLS	[23]
Citrate-AgNPs Pectin-AgNPs Alginate-AgNPs	Aquatic environmental samples	Flow field-flow fractionation	Carrier liquid: 0.02 % FL-70 and 0.02 % NaN_3 in deionized water, pH 9.2–10, sample volume: 20 µL, cross flow rate: 1 mL/min, membrane material: 1 kDa regenerated cellulose membrane	On-line: UV-vis Off-line: TEM, ETAAS	[24]
AgNPs	Cell culture media and cells	Asymmetric flow field-flow fractionation	Carrier liquid: 0.01 % (m/v) SDS solution in ultrapure water, pH 8.0, membrane material: polyether sulfone with cutoff 1 kDa	On-line: UV-vis, ICP-MS Off-line: TEM	[25]
10 nm AgNPs in 2 mM citrate buffer, 20–80 nm AgNPs in 2 mM phosphate buffer, PVP-AgNPs	Tissues of the freshwater oligochaete *Lumbriculus variegatus*	Asymmetric flow field-flow fractionation	Membrane material: 10 kDa regenerated cellulose, channel and cross flow: 1.0 and 0.75 mL/min, injection volume: 50 µL, load time: 15 s, relaxation time: 3.2 min, approximate fractogram time (100 nm elution): 25 min	On-line: UV-vis, ICP-MS Off-line: TEM, DLS	[26]
PVP-AgNPs	Chicken meat	Asymmetric flow field-flow fractionation and single particle ICP-MS	Carrier liquid: 0.5 mM NH_4HCO_3, pH 7.4, membrane material: PES, 10 kDa cut-off, spacer height: 350 µm, detector flow rate: 1.0 ml/min, injection flow rate: 0.2 ml/min, focus flow rate: 1.0 ml/min	Off-line: TEM, ICP-MS	[27]
Uncapped AgNPs (20, 40, and 60 nm)	Surface waters and wastewater samples	Asymmetric flow field-flow fractionation	Carrier liquid: Milli-Q water, membrane material: regenerated cellulose with 10 kDa cut-off, tip flow: 3.5 ml/min, cross flow: 2.5 ml/min, injection flow: 0.2 ml/min, focus flow: 3.3 ml/min, detector flow: 1 ml/min, channel thickness: 350 µm	On-line: UV-vis Off-line: TEM, DLS, ICP-MS	[29]

Table 2.1 (continued)

Silver dispersion (10, 20, and 40 nm) in aqueous buffer containing sodium citrate as stabilizer, MSA-AgNPs	A solution extracted from sport socks, and 10-fold diluted FBS	Reversed-phase high-performance liquid chromatography	Column: Nucleosil 7 μm particle size, C18, 1000 Å pore size, 250 × 4.6 mm, flow rate: 0.5 mL/min, injection volume: 10 μL, mobile phase: 10 mmol/L ammonium acetate, pH 7.0, 10 mmol/L SDS	On-line: HPLC-ICP-MS Off-line: TEM	[35]
Citrate-AgNPs (10, 20, 40, 60, 100 nm), PVP-AgNPs (30 nm), PVA-AgNPs (46.7 nm), GSH protected Ag nanoclusters, Ag_2S NPs (4, 18 nm)	Antibacterial products and environmental waters	High-performance liquid chromatography	Column: Venusil Durashell-NH_2, 5 μm particle size, 500 Å pore size, 250 × 4.6 mm, flow rate: 0.7 mL/min, mobile phase: 0.1% (v/v) FL-70 and 2 mM $Na_2S_2O_3$	On-line: HPLC-ICP-MS Off-line: TEM, UV-vis	[36]
AuNPs and AgNPs	Sewage sludge	Hydrodynamic chromatography	Mobile phase: 0.002 M Na_2HPO_4, 0.2% nonionic surfactant, 0.05% SDS, 0.2% formaldehyde; pH ~ 7.5, injection volume: 20 μL, flow rate: 1.7 mL/min, pressure: 9 MPa	On-line: HDC-ICP-MS Off-line: TEM	[40]
AgNPs dispersed in ethylene glycol	Activated sludge and tap water	Hydrodynamic chromatography	Mobile phase: 0.002 M Na_2HPO_4, 0.2% nonionic surfactant, 0.05% SDS, 0.2% formaldehyde; pH ~ 7.5, injection volume: 20 μL, flow rate: 1.7 mL/min, pressure: 9 MPa	On-line: HDC-ICP-MS Off-line: TEM, DLS	[41]
MUA-AgNPs	Phosphate buffer (20 mM, pH 11)	Counter-current chromatography	Mobile phase: hexane/toluene (1:1, v/v) with 0.02 mM TOAB; injection volume: 5 mL, flow rate: 1 mL/min, oven temperature: 20 °C, rotation of the chromatograph: 700 rpm	On-line: UV-vis Off-line: FT-IR, SEM-EDX	[42]
Silver clusters ligated with glutathione	Pure water	Polyacrylamide gel electrophoresis	30% acrylamide resolving gel and 4% acrylamide stacking gel, eluting buffer: 25 mM THAM and 192 mM glycine	Off-line: STEM, XRD, EDS, NMR, UV-vis	[45]

Table 2.1 (continued)

Ag nano-spheres, triangles, and rods with SH-PEG-COOH modification	Pure water	Agarose gel electrophoresis	0.2% agarose gel in 0.5×TBE (Tris-borate EDTA) buffer (pH~9)	Off-line: TEM UV-vis	[47]
PEG-modified Ag-NPs	Pure water	Agarose gel electrophoresis	1% or 0.75% LMP agarose gel in 0.5×TBE buffer	Off-line: TEM	[48]
4-carboxythiophenol modified Au and Ag colloidal particles	Pure water	Miniscale isoelectric focusing	Electrolyte solutions: 0.1 M ortho-phosphoric acid as anode solution and 0.1 M NaOH as the cathode solution, separation solution: 1.5 ml of glycerol with 1 ml of water, Gradient solutions: (i) high density solution: 3 ml glycerol with 2 ml of the different hydrosols together with 0.2 ml carrier electrolyte, and (ii) low density solution: 3 ml carrier electrolyte, and (ii) low density solution: 3 ml carrier electrolyte. IEF was carried out for 5 h at 400 V and yielded a current of 1.5 A	Off-line: UV-vis	[49]
Ag nanorods and AgNPs with different size	Pure water	Micellar electrokinetic chromatography	Electrolytes: 20 mM SDS and 10 mM Tris-(hydroxymethyl) aminomethane (Tris) (pH 8.5), capillary: uncoated fused-silica capillaries (i.d.: 75 μm; length: 48.5 cm), voltage: 20 kV and 30 kV	On-line: DAD Off-line: SEM	[50]
Ag nano-spheres and Ag nano-cubes	Pure water	Micellar electrokinetic chromatography	Electrolytes: 20 mM SDS and 10 mM Tris-(hydroxymethyl) aminomethane (Tris) (pH 8.5), capillary: uncoated fused-silica capillaries (i.d.: 75 μm, length: 48.5 cm), voltage: 30 kV	On-line: DAD Off-line: SEM	[51]
Au NP and Au/Ag core/shell nanoparticles	Pure water	Micellar electrokinetic chromatography	Electrolytes: 40 mM SDS and 10 mM 3-cyclohexylamino-1-propanesulfonic acid (CAPS) at pH 10.0, capillary: uncoated fused-silica capillaries (i.d.: 75 μm; length: 33.5 cm); voltage: 20 kV, on-line concentration by the reversed electrode polarity stacking mode (REPSM)	On-line: DAD Off-line: SEM	[52]

Table 2.1 (continued)

Au NP and Au/Ag core/shell nanoparticles with different size	Pure water	Micellar electrokinetic chromatography	Electrolytes: 40 mM SDS and 10 mM 3-(cyclohexylamino) propanesulfonic acid at pH 9.7; capillary: uncoated fused silica capillaries (i.d.: 75 μm; length: 50 cm); voltage: 20 kV	On-line: DAD Off-line: SEM	[53]
Citrate-AgNPs (7.2±1.2 and 30.7±3.6 nm), tannic acid-AuNPs (4.8±0.6, 9.1±0.8, 20±1.8, and 48.1±4.2 nm)	A supplement (MesoGold)	Micellar electrokinetic chromatography	Buffer solution: 10 mM N-cyclohexyl-3-aminopropanesulfonic acid (CAPS) and SDS, Voltage: ~29 kV, current: 45 μA, hydrodynamic injection: 50 mbar for 3 s, electrokinetic injection: 20 kV for 8 s, capillary: polyimide-coated fused-silica capillaries (i.d.: 75 μm, length: 70 cm, o.d.: 375 μm)	On-line: ICP-MS	[38]
AgNPs and AuNPs synthesized using Magnolia kobus plant leaf extracts	Pure water	Density gradient centrifugation	Four layer gradient (sucrose solutions with mass fractions of 30, 40, 50, and 60%), centrifuged at 3500 rpm for different time intervals (20, 40, 60, and 90 min)	Off-line: TEM	[55]
Ag, Au and CdSe nanoparticles	Organic solvents	Density gradient centrifugation	Five layer gradient (cyclohexane and tetrachloromethane mixtures with v/v at 50, 60, 70, 80, and 90%), centrifuged at 50,000 rpm, 8 min	Off-line: TEM	[56]
Triangular Ag Nanoplates	Aqueous solutions	Density gradient centrfugation	A multilayer density gradient (20+30+40+50+60+70%) with different concentrations of ethylene glycol, centrifuged at 23 000 rpm for 7 min	Off-line: UV-vis, TEM, EDX	[57]
AgNPs dispersed in pure ethylene glycol	Rat tissues	A knotted reactor-based differentiation scheme	The total Ag content, including AgNPs and Ag^+, was retained at pH 6 without rinsing; Ag^+ was extracted selectively at pH 10 with a 1000 μL rinse solution	On-line: ICP-MS	[58]
Mercaptosuccinic acid (MSA) modified AgNPs	Aquatic environmental samples	Ionic exchange resins	Anionic exchange resins: Amberlite IRN-78, sample loading rate: 1.5 mL/min, elution solution: 8% (v/v) formic acid in methanol, gentle shaking at room temperature	Off-line: IR, SEM-EDX, TEM, GFAAS	[59]

Table 2.1 (continued)

Polydispersed AgNP Solution	Hexane	CO_2 expanded liquid approach	The series of pressurization: 0–500, 550, 600, 625, 650 psi	Off-line: TEM	[60]
AgNPs (20±5, 40±5, 60±5 and 80±7 nm) and Ag^+	Drinking water	Single particle ICP-MS	Measuring mode: single particle detection, dwell time: 5 ms, readings per replicate: 20000, settle time: 3 ms, integration time: 100 s	On-line: Single particle ICP-MS	[71]
AgNPs (20, 60, 100 nm) stabilized in aqueous 2 mM citrate	Wastewater samples and a colloidal Ag consumer product	Single particle ICP-MS	Integration dwell time: 20 ms per reading, readings per replicate: 10450, run time: 4 min, ^{107}Ag monitored	On-line: Single particle ICP-MS	[72]
AgNPs (80 nm in nominal diameter)	2 mM phosphate buffer	Single particle ICP-MS	Time-resolved analysis (TRA) mode, collecting intensities as a function of time, data acquisition rate: 30 s/run, dwell time: 10 ms/event	On-line: Single particle ICP-MS Off-line: TEM, differential centrifugal sedimentation	[76]
AgNPs (60, 100 nm) and AuNPs (100 nm)	Biological tissues	Single particle ICP-MS	Signals averaged for the entire analysis period: 200 s, dwell time: 10 ms, readings per replicate: 20000, total analysis time: 200 s	On-line: Single particle ICP-MS	[78]
AgNPs 40, 60, 80, and 100 nm in nominal diameter)	Algal growth medium (AGM) and AGM supplemented with Suwannee River humic acids	Single particle ICP-MS	Time-resolved analysis (TRA) mode, measurement duration of each run: 30 s, dwell time 10 ms	On-line: Single particle ICP-MS Off-line: DLS, nanoparticle tracking analysis, differential centrifugal sedimentation	[79]
AgNPs (20, 40, 60, and 80 nm in nominal diameter)	Wastewater effluent samples	Single particle ICP-MS	Dwell time: 1, 5, or 10 ms, 10 000 or 40 000 dwells of ^{107}Ag measurements were collected for each dilution	On-line: Single particle ICP-MS	[80]

References

1. Goto K, Taguchi S, Fukue Y, Ohta K, Watanabe H (1977) Spectrophotometric determination of manganese with 1-(2-pyridylazo)-2-naphthol and a nonionic surfactant. Talanta 24 (12):752–753. doi:10.1016/0039-9140(77)80206-3
2. Watanabe H, Tanaka H (1978) Nonionic surfactant as a new solvent for liquid-liquid—extraction of zinc(II) with 1-(2-pyridylazo)-2-naphthol. Talanta 25 (10):585–589. doi:10.1016/0039-9140(78)80151-9
3. Hinze WL, Pramauro E (1993) A critical review of surfactant-mediated phase separations (cloud-point extractions): theory and applications. Crit Rev Anal Chem 24(2):133–177. doi:10.1080/10408349308048821
4. Liu JF, Liu R, Yin YG, Jiang GB (2009) Triton X-114 based cloud point extraction: a thermoreversible approach for separation/concentration and dispersion of nanomaterials in the aqueous phase. Chem Commun (12):1514–1516. doi:10.1039/b821124h
5. Liu JF, Chao JB, Liu R, Tan ZQ, Yin YG, Wu Y, Jiang GB (2009) Cloud point extraction as an advantageous preconcentration approach for analysis of trace silver nanoparticles in environmental waters. Anal Chem 81(15):6496–6502. doi:10.1021/ac900918e
6. Quina FH, Hinze WL (1999) Surfactant-mediated cloud point extractions: an environmentally benign alternative separation approach. Ind Eng Chem Res 38(11):4150–4168. doi:10.1021/ie980389n
7. Chao JB, Liu JF, Yu SJ, Feng YD, Tan ZQ, Liu R (2011) Speciation analysis of silver nanoparticles and silver ions in antibacterial products and environmental waters via cloud point extraction-based separation. Anal Chem 83(17):6875–6882. doi:10.1021/ac201086a
8. Hartmann G, Hutterer C, Schuster M (2013) Ultra-trace determination of silver nanoparticles in water samples using cloud point extraction and ETAAS. J Anal At Spectrom 28(4):567–572. doi:10.1039/c3ja30365a
9. Yu SJ, Chao JB, Sun J, Yin YG, Liu JF, Jiang GB (2013) Quantification of the uptake of silver nanoparticles and ions to HepG2 cells. Environ Sci Technol 47(7):3268–3274. doi:10.1021/es304346p
10. Li L, Hartmann G, Doeblinger M, Schuster M (2013) Quantification of nanoscale silver particles removal and release from municipal wastewater treatment plants in Germany. Environ Sci Technol 47(13):7317–7323. doi:10.1021/es3041658
11. Hartmann G, Baumgartner T, Schuster M (2014) Influence of particle coating and matrix constituents on the cloud point extraction efficiency of silver nanoparticles (Ag-NPs) and application for monitoring the formation of Ag-NPs from Ag^+. Anal Chem 86(1):790–796. doi:10.1021/ac403289d
12. Williams SKR, Runyon JR, Ashames AA (2011) Field-flow fractionation: addressing the nano challenge. Anal Chem 83(3):634–642. doi:10.1021/ac101759z
13. von derKF, Legros S, Larsen EH, Loeschner K, Hofmann T (2011) Separation and characterization of nanoparticles in complex food and environmental samples by field-flow fractionation. Trend Anal Chem 30(3):425–436. doi:10.1016/j.trac.2010.11.012
14. Liu JF, Yu SJ, Yin YG, Chao JB (2012) Methods for separation, identification, characterization and quantification of silver nanoparticles. Trend Anal Chem 33:95–106. doi:10.1016/j.trac.2011.10.010
15. Weinberg H, Galyean A, Leopold M (2011) Evaluating engineered nanoparticles in natural waters. Trend Anal Chem 30(1):72–83. doi:10.1016/j.trac.2010.09.006
16. Oppenheimer LE, Smith GA (1988) Characterization of gold and silver sols by sedimentation field-flow fractionation. Langmuir 4(1):144–147. doi:10.1021/la00079a026
17. Kim ST, Kang DY, Lee SH, Kim WS, Lee JT, Cho HS, Kim SH (2007) Separation and quantitation of silver nanoparticles using sedimentation field-flow Fractionation. J Liq Chromatogr Relat Technol 30(17):2533–2544. doi:10.1080/10826070701540092
18. Shiundu PM, Munguti SM, Williams SKR (2003) Retention behavior of metal particle dispersions in aqueous and nonaqueous carriers in thermal field-flow fractionation. J Chromatogr A 983 (1–2):163–176. doi:10.1016/S0021-9673(02)01694-1

19. Loeschner K, Navratilova J, Legros S, Wagner S, Grombe R, Snell J, von der KF, Larsen EH (2013) Optimization and evaluation of asymmetric flow field-flow fractionation of silver nanoparticles. J Chromatogr A 1272:116–125. doi:10.1016/j.chroma.2012.11.053
20. Bolea E, Jimenez-Lamana J, Laborda F, Castillo JR (2011) Size characterization and quantification of silver nanoparticles by asymmetric flow field-flow fractionation coupled with inductively coupled plasma mass spectrometry. Anal Bioanal Chem 401(9):2723–2732. doi:10.1007/s00216–011-5201-2
21. Hagendorfer H, Kaegi R, Parlinska M, Sinnet B, Ludwig C, Ulrich A (2012) Characterization of silver nanoparticle products using asymmetric flow field flow fractionation with a multidetector approach—a comparison to transmission electron microscopy and batch dynamic light scattering. Anal Chem 84(6):2678–2685. doi:10.1021/ac202641d
22. Mitrano DM, Barber A, Bednar A, Westerhoff P, Higgins CP, Ranville JF (2012) Silver nanoparticle characterization using single particle ICP-MS (SP-ICP-MS) and asymmetrical flow field flow fractionation ICP-MS (AF4-ICP-MS). J Anal At Spectrom 27(7):1131–1142. doi:10.1039/c2ja30021d
23. Cumberland SA, Lead JR (2009) Particle size distributions of silver nanoparticles at environmentally relevant conditions. J Chromatogr A 1216(52):9099–9105. doi:10.1016/j.chroma.2009.07.021
24. Songsilawat K, Shiowatana J, Siripinyanond A (2011) Flow field-flow fractionation with off-line electrothermal atomic absorption spectrometry for size characterization of silver nanoparticles. J Chromatogr A 1218(27):4213–4218. doi:10.1016/j.chroma.2010.12.040
25. Bolea E, Jimenez-Lamana J, Laborda F, Abad-Alvaro I, Blade C, Arola L, Castillo JR (2014) Detection and characterization of silver nanoparticles and dissolved species of silver in culture medium and cells by AsFlFFF-UV-Vis-ICPMS: Application to nanotoxicity tests. Analyst 139(5):914–922. doi:10.1039/c3an01443f
26. Poda AR, Bednar AJ, Kennedy AJ, Harmon A, Hull M, Mitrano DM, Ranville JF, Steevens J (2011) Characterization of silver nanoparticles using flow-field flow fractionation interfaced to inductively coupled plasma mass spectrometry. J Chromatogr A 1218(27):4219–4225. doi:10.1016/j.chroma.2010.12.076
27. Loeschner K, Navratilova J, Kobler C, Molhave K, Wagner S, von der KF, Larsen EH (2013) Detection and characterization of silver nanoparticles in chicken meat by asymmetric flow field flow fractionation with detection by conventional or single particle ICP-MS. Anal Bioanal Chem 405(25):8185–8195. doi:10.1007/s00216-013-7228-z
28. Campbell P, Ma S, Schmalzried T, Amstutz HC (1994) Tissue digestion for wear debris particle isolation. J Biomed Mater Res 28(4):523–526. doi:10.1002/jbm.820280415
29. Hoque ME, Khosravi K, Newman K, Metcalfe CD (2012) Detection and characterization of silver nanoparticles in aqueous matrices using asymmetric-flow field flow fractionation with inductively coupled plasma mass spectrometry. J Chromatogr A 1233:109–115. doi:10.1016/j.chroma.2012.02.011
30. Zattoni A, Casolari S, Rambaldi DC, Reschiglian P (2007) Hollow-fiber flow field-flow fractionation. Curr Anal Chem 3(4):310–323. doi:10.2174/157341107782109608
31. van Bruijnsvoort M, Kok WT, Tijssen R (2001) Hollow-fiber flow field-flow fractionation of synthetic polymers in organic solvents. Anal Chem 73(19):4736–4742. doi:10.1021/ac010144b
32. Lee WJ, Min BR, Moon MH (1999) Improvement in particle separation by hollow fiber flow field-flow fractionation and the potential use in obtaining particle site distribution. Anal Chem 71(16):3446–3452. doi:10.1021/ac981204p
33. Berek D (2010) Size exclusion chromatography—A blessing and a curse of science and technology of synthetic polymers. J Sep Sci 33(3):315–335. doi:10.1002/jssc.200900709
34. Lespes G, Gigault J (2011) Hyphenated analytical techniques for multidimensional characterisation of submicron particles: a review. Anal Chim Acta 692(1–2):26–41. doi:10.1016/j.aca.2011.02.052
35. Soto-Alvaredo J, Montes-Bayon M, Bettmer J (2013) Speciation of silver nanoparticles and silver(I) by reversed-Phase liquid chromatography coupled to ICPMS. Anal Chem 85(3):1316–1321. doi:10.1021/ac302851d

36. Zhou XX, Liu R, Liu JF (2014) Speciation analysis of dissoluble Ag(I) and silver-containing nanoparticles of 1–100 nanometer using liquid chromatography-based separation. Environ Sci Technol 48(24):14516–14524. doi:10.1021/es504088e
37. Fischer CH, Kenndler E (1997) Analysis of colloids.9. Investigation of the electrical double layer of colloidal inorganic nanometer-particles by size-exclusion chromatography. J Chromatogr A 773 (1–2):179–187. doi:10.1016/s0021-9673(97)00203-3
38. Franze B, Engelhard C (2014) Fast separation, characterization, and speciation of gold and silver nanoparticles and their ionic counterparts with micellar electrokinetic chromatography coupled to ICP-MS. Anal Chem 86(12):5713–5720. doi:10.1021/ac403998e
39. McGowan GR, Langhorst MA (1982) Development and application of an integrated, high-speed, computerized hydrodynamic chromatograph. J Colloid Interface Sci 89 (1):94–106. doi:10.1016/0021-9797(82)90124-2
40. Tiede K, Boxall ABA, Tiede D, Tear SP, David H, Lewis J (2009) A robust size-characterisation methodology for studying nanoparticle behaviour in 'real' environmental samples, using hydrodynamic chromatography coupled to ICP-MS. J Anal At Spectrom 24(7):964–972. doi:10.1039/b822409a
41. Tiede K, Boxall ABA, Wang XM, Gore D, Tiede D, Baxter M, David H, Tear SP, Lewis J (2010) Application of hydrodynamic chromatography-ICP-MS to investigate the fate of silver nanoparticles in activated sludge. J Anal At Spectrom 25(7):1149–1154. doi:10.1039/b926029c
42. Shen CW, Yu T (2009) Size-fractionation of silver nanoparticles using ion-pair extraction in a counter-current chromatograph. J Chromatogr A 1216(32):5962–5967. doi:10.1016/j.chroma.2009.06.002
43. Lopez-Lorente AI, Simonet BM, Valcarcel M (2011) Electrophoretic methods for the analysis of nanoparticles. Trends Anal Chem 30(1):58–71. doi:10.1016/j.trac.2010.10.006
44. Surugau N, Urban PL (2009) Electrophoretic methods for separation of nanoparticles. J Sep Sci 32(11):1889–1906. doi:10.1002/jssc.200900071
45. Kumar S, Bolan MD, Bigioni TP (2010) Glutathione-stabilized magic-number silver cluster compounds. J Am Chem Soc 132(38):13141–13143. doi:10.1021/ja105836b
46. Xu XY, Caswell KK, Tucker E, Kabisatpathy S, Brodhacker KL, Scrivens WA (2007) Size and shape separation of gold nanoparticles with preparative gel electrophoresis. J Chromatogr A 1167(1):35–41. doi:10.1016/j.chroma.2007.07.056
47. Hanauer M, Pierrat S, Zins I, Lotz A, Sonnichsen C (2007) Separation of nanoparticles by gel electrophoresis according to size-and shape. Nano Lett 7(9):2881–2885. doi:10.1021/nl071615y
48. Guarrotxena N, Braun G (2012) Ag-nanoparticle fractionation by low melting point agarose gel electrophoresis. J Nanopart Res 14(10). doi:10.1007/s11051–012-1199-4
49. Gole AM, Sathivel C, Lachke A, Sastry M (1999) Size separation of colloidal nanoparticles using a miniscale isoelectric focusing technique. J Chromatogr A 848 (1–2):485–490. doi:10.1016/s0021-9673(99)00408-2
50. Liu FK, Ko FH, Huang PW, Wu CH, Chu TC (2005) Studying the size/shape separation and optical properties of silver nanoparticles by capillary electrophoresis. J Chromatogr A 1062(1):139–145. doi:10.1016/j.chroma.2004.11.010
51. Liu FK, Ko FH (2004) Separation and study of the optical properties of silver nanocubes by capillary electrophoresis. Chem Lett 33(7):902–903. doi:10.1246/cl.2004.902
52. Lin KH, Chu TC, Liu FK (2007) On-line enhancement and separation of nanoparticles using capillary electrophoresis. J Chromatogr A 1161(1–2):314–321. doi:10.1016/j.chroma.2007.05.072
53. Liu FK, Tsai MH, Hsu YC, Chu TC (2006) Analytical separation of Au/Ag core/shell nanoparticles by capillary electrophoresis. J Chromatogr A 1133(1–2):340–346. doi:10.1016/j.chroma.2006.08.033
54. Zhang YC, Shi YF, Liou YH, Sawvel AM, Sun XH, Cai Y, Holden PA, Stucky GD (2010) High performance separation of aerosol sprayed mesoporous TiO_2 sub-microspheres from aggregates via density gradient centrifugation. J Mater Chem 20(20):4162–4167. doi:10.1039/b926183d

55. Lee SH, Salunke BK, Kim BS (2014) Sucrose density gradient centrifugation separation of gold and silver nanoparticles synthesized using Magnolia kobus plant leaf extracts. Biotechnol Biopro Eng 19(1):169–174. doi:10.1007/s12257-013-0561-4
56. Bai L, Ma XJ, Liu JF, Sun XM, Zhao DY, Evans DG (2010) Rapid separation and purification of nanoparticles in organic density gradients. J Am Chem Soc 132(7):2333–2337. doi:10.1021/ja908971d
57. Zhang CL, Luo L, Luo J, Evans DG, Sun XM (2012) A process-analysis microsystem based on density gradient centrifugation and its application in the study of the galvanic replacement mechanism of Ag nanoplates with $HAuCl_4$. Chem Commun 48(58):7241–7243. doi:10.1039/c2cc30457k
58. Su C-K, Liu H-T, Hsia S-C, Sun Y-C (2014) Quantitatively profiling the dissolution and redistribution of silver nanoparticles in living rats using a knotted reactor-based differentiation scheme. Anal Chem 86(16):8267–8274. doi:10.1021/ac501691z
59. Li LXY, Leopold K, Schuster M (2012) Effective and selective extraction of noble metal nanoparticles from environmental water through a noncovalent reversible reaction on an ionic exchange resin. Chem Commun 48(73):9165–9167. doi:10.1039/c2cc34838a
60. McLeod MC, Anand M, Kitchens CL, Roberts CB (2005) Precise and rapid size selection and targeted deposition of nanoparticle populations using CO_2 gas expanded liquids. Nano Lett 5(3):461–465. doi:10.1021/nl047966j
61. Tiede K, Boxall ABA, Tear SP, Lewis J, David H, Hassellov M (2008) Detection and characterization of engineered nanoparticles in food and the environment. Food Addit Contam 25(7):795–821. doi:10.1080/02652030802007553
62. Dudkiewicz A, Tiede K, Loeschner K, Jensen LHS, Jensen E, Wierzbicki R, Boxall ABA, Molhave K (2011) Characterization of nanomaterials in food by electron microscopy. Trends Anal Chem 30(1):28–43. doi:10.1016/j.trac.2010.10.007
63. Simonet BM, Valcarcel M (2009) Monitoring nanoparticles in the environment. Anal Bioanal Chem 393(1):17–21. doi:10.1007/s00216-008-2484-z
64. Fedotov PS, Vanifatova NG, Shkinev VM, Spivakov BY (2011) Fractionation and characterization of nano- and microparticles in liquid media. Anal Bioanal Chem 400(6):1787–1804. doi:10.1007/s00216-011-4704-1
65. Mie G (1908) Articles on the optical characteristics of turbid tubes, especially colloidal metal solutions. Ann Phys 25(3):377–445
66. Mermet JM (2005) Is it still possible, necessary and beneficial to perform research in ICP-atomic emission spectrometry? J Anal At Spectrom 20(1):11–16. doi:10.1039/b4165611j
67. Yang L, Lam JWH, Sturgeon RE, McLaren JW (1998) Decomposition of marine sediments for quantitative recovery of chromium and inductively coupled plasma mass spectrometric analysis. J Anal At Spectrom 13(11):1245–1248. doi:10.1039/a804444i
68. Yang L, Sturgeon RE (2002) On-line determination of silver in sea-water and marine sediment by inductively coupled plasma mass spectrometry. J Anal At Spectrom 17(2):88–93. doi:10.1039/b109409m
69. Degueldre C, Favarger PY, Wold S (2006) Gold colloid analysis by inductively coupled plasma-mass spectrometry in a single particle mode. Anal Chim Acta 555(2):263–268. doi:10.1016/j.aca.2005.09.021
70. Degueldre C, Favarger PY (2003) Colloid analysis by single particle inductively coupled plasma-mass spectroscopy: a feasibility study. Colloids Surf A- Physicochem Eng Asp 217 (1–3):137–142. doi:10.1016/s0927-7757(02)00568-x
71. Laborda F, Jimenez-Lamana J, Bolea E, Castillo JR (2011) Selective identification, characterization and determination of dissolved silver(I) and silver nanoparticles based on single particle detection by inductively coupled plasma mass spectrometry. J Anal At Spectrom 26(7):1362–1371. doi:10.1039/c0ja00098a
72. Mitrano DM, Lesher EK, Bednar A, Monserud J, Higgins CP, Ranville JF (2012) Detecting nanoparticulate silver using single-particle inductively coupled plasma-mass spectrometry. Environ Toxicol Chem 31(1):115–121. doi:10.1002/etc.719
73. Degueldre C, Favarger PY (2004) Thorium colloid analysis by single particle inductively coupled plasma-mass spectrometry. Talanta 62(5):1051–1054. doi:10.1016/j.talanta.2003.10.016

74. Degueldre C, Favarger PY, Bitea C (2004) Zirconia colloid analysis by single particle inductively coupled plasma-mass spectrometry. Anal Chim Acta 518(1–2):137–142. doi:10.1016/j.aca.2004.04.015
75. Degueldre C, Favarger PY, Rosse R, Wold S (2006) Uranium colloid analysis by single particle inductively coupled plasma-mass spectrometry. Talanta 68(3):623–628. doi:10.1016/j.talanta.2005.05.006
76. Pace HE, Rogers NJ, Jarolimek C, Coleman VA, Higgins CP, Ranville JF (2011) Determining transport efficiency for the purpose of counting and sizing nanoparticles via single particle inductively coupled plasma mass spectrometry. Anal Chem 83(24):9361–9369. doi:10.1021/ac201952t
77. von derKF, Ferguson PL, Holden PA, Masion A, Rogers KR, Klaine SJ, Koelmans AA, Horne N, Unrine JM (2012) Analysis of engineered nanomaterials in complex matrices (environment and biota): general considerations and conceptual case studies. Environ Sci Technol 31(1):32–49. doi:10.1002/etc.723
78. Gray EP, Coleman JG, Bednar AJ, Kennedy AJ, Ranville JF, Higgins CP (2013) Extraction and analysis of silver and gold nanoparticles from biological tissues using single particle inductively coupled plasma mass spectrometry. Environ Sci Technol 47(24):14315–14323. doi:10.1021/es403558c
79. Pace HE, Rogers NJ, Jarolimek C, Coleman VA, Gray EP, Higgins CP, Ranville JF (2012) Single particle inductively coupled plasma-mass spectrometry: a performance evaluation and method comparison in the determination of nanoparticle size. Environ Sci Technol 46(22):12272–12280. doi:10.1021/es301787d
80. Tuoriniemi J, Cornelis G, Hassellov M (2012) Size discrimination and detection capabilities of single-particle ICPMS for environmental analysis of silver nanoparticles. Anal Chem 84(9):3965–3972. doi:10.1021/ac203005r

Chapter 3
Source and Pathway of Silver Nanoparticles to the Environment

Yongguang Yin, Sujuan Yu, Xiaoya Yang, Jingfu Liu and Guibin Jiang

Abstract The production and use of silver nanoparticles (AgNPs) in industrial and commercial products increased significantly in recent years. During the production, manufacturing, use and disposal of AgNP containing products, AgNPs would be released into the environment inevitably. Moreover, AgNPs could also be naturally occurred in the environment through biological and chemical reduction processes. In recent years, various chemical and biological pathways, including reduction of Ag^+ by natural organic matters, plants and microorganisms, and generation of AgNPs from macroscale elemental silver objects through dissolution and reduction, were demonstrated for the occurrence of naturally occurred AgNPs. In this chapter, we introduce the occurrences of natural AgNPs in the environments and their possible formation pathways and mechanisms, and discuss the anthropogenic pathways for intentionally and unintentionally produced AgNPs and their release into the environment.

3.1 Introduction

Metallic silver nanoparticles (AgNPs) is not "new" and could be naturally occurred in the environment or anthropogenically produced and then released into the environment. Natural reduction process could mediate the formation of AgNPs from Ag^+ in the natural environment. On the other hand, nanosilver in the form of colloidal silver has also been produced for more than 100 years and has been registered

J. Liu (✉) · Y. Yin · S. Yu · X. Yang · G. Jiang
State Key Laboratory of Environmental Chemistry and Ecotoxicology,
Research Center for Eco-Environmental Sciences, Chinese Academy of Sciences,
P.O. Box 2871, Beijing 100085, China
e-mail: jfliu@rcees.ac.cn

Y. Yin
e-mail: ygyin@rcees.ac.cn

S. Yu
e-mail: sjyu@rcees.ac.cn

G. Jiang
e-mail: gbjiang@rcees.ac.cn

J. Liu, G. Jiang (eds.), *Silver Nanoparticles in the Environment,*
DOI 10.1007/978-3-662-46070-2_3

as a biocidal material in the USA since 1954 [1]. In manufacturing, using, washing, recycling, and disposing of AgNPs and their products, engineered AgNPs could inevitably enter surrounding environments [2].

The occurrence of nanoparticulate silver, including species like Ag^0, AgCl, and Ag_2S, has been widely observed in various environmental compartments. The nanoparticulate silver was confirmed in influent and effluent of wastewater in Boulder, CO, USA by single particle ICP-MS, with the concentration of 200 ng L^{-1} (in influent) and 100 ng L^{-1} (in effluent), respectively [3]. Li et al. measured the concentration of nanoparticulate silver in the field-collected influent samples from nine municipal wastewater treatment plants (WWTPs) in Germany and the concentrations were ranged from 0.06 to 1.50 μg L^{-1} [4]. Owning to the increased production of AgNPs as a potentially new emission source of silver, the atmospheric deposition of silver in Switzerland increased in recent years [5]. The spatial distribution revealed a decrease in the silver concentrations in moss as a function of increasing distance from the AgNP manufacturer. The monthly collected bulk depositions were higher in the area of AgNP production (0.175 ± 0.13 μg m^{-2} day^{-1}) in comparison to rural (0.105 ± 0.08 μg m^{-2} day^{-1}) and urban areas (0.113 ± 0.05 μg m^{-2} day^{-1}) of Eastern Switzerland. Based on a probabilistic material flow analysis from a life cycle perspective of AgNP-containing products, the predicted environmental concentrations (PEC) of AgNPs would significantly increase in various environmental compartments with the increasing use of AgNPs and AgNP-contained products, and the PECs of AgNPs in sewage treatment effluents and surface waters are high enough to pose risks to aquatic organisms [6].

In this chapter, we summarized the natural sources, possible formation pathways, and mechanisms of naturally occurring AgNPs and the anthropogenic production and release of engineered AgNPs into the environment.

3.2 Natural Source of Silver Nanoparticles

Elemental silver could occur naturally as native silver [7–10], or as alloys with gold and other metals (such as electrum) [11,12]. Similar with naturally occurring gold nanoparticles, naturally occurring AgNPs were also observed as "invisible silver" in metal deposits [12–15] and coal mine [16]. In supergene digenite ($Cu_{1.8}S$) from Cu deposits in the Atacama Desert of northern Chile, elemental silver in nano-size was observed by using secondary ion mass spectrometry (SIMS) and high-resolution transmission electron microscope (HRTEM), revealing that samples with high Ag/As ($>\sim 30$) ratios contain nanoparticles of metallic Ag. The TEM images of AgNPs in a selected digenite sample have been shown in Fig. 3.1. Clearly, Fig. 3.1a and b reveal the presence of discrete, submicron sized particles that are disseminated in the digenite matrix, while HRTEM images further show that the nanoparticles are spherical in sizes between 5–10 nm. Indexing of the two-dimensional lattice fringes of the fast Fourier transformation (FFT) of the TEM images reveals a faced-centered cubic structure of elemental AgNPs (inset, Fig 3.1c and d).

In addition, in natural waters, fraction of "dissolved" silver may also partly exist in the form of colloidal and particulate Ag. Besides complexation with macromo-

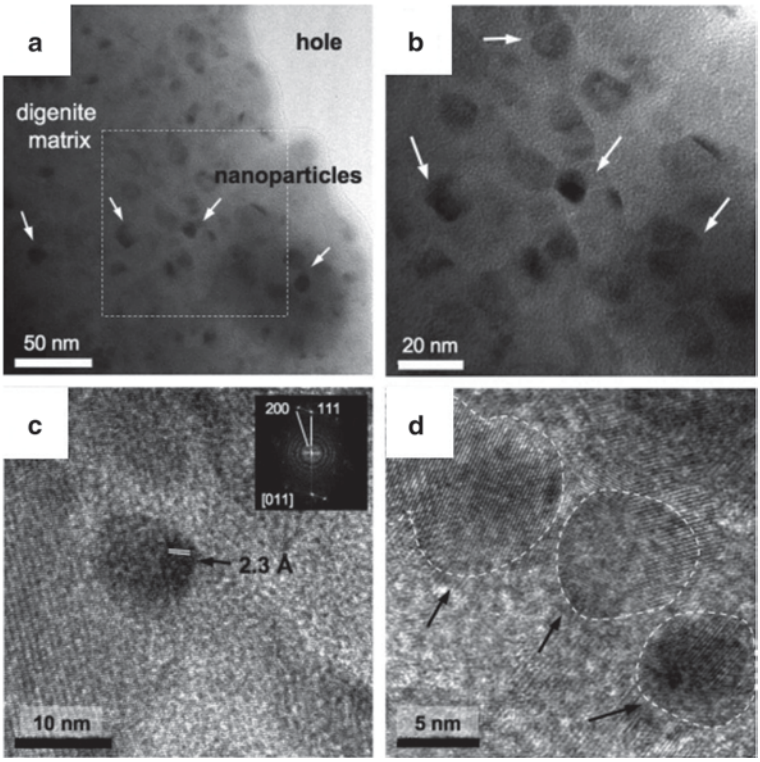

Fig. 3.1 TEM images of AgNPs in digenite sample. TEM images (**a** and **b**) show the presence of discrete, submicron sized particles in the digenite matrix. HRTEM images (**c** and **d**) show that the AgNPs are rounded in shape and range in size between 5–10 nm. Inset in (**c**) is the FFT image of a single nanoparticle, suggesting metallic silver (Ag^0) structure. Reprinted from ref. [14], Copyright 2010 with permission from Elsevier

lecular organic matters and adsorption on iron–manganese oxyhydroxide/sulfide phases [17], it is also proposed that some of the colloidal and particulate silver also exists as elemental AgNPs [18].

In recent years, the formation of AgNPs at environmental relevant conditions has been discovered and these findings imply that not all AgNPs observed in natural waters are of anthropogenic origin [18].

3.2.1 Reduction of Ag^+ by Natural Organic Matters

Natural organic matter (NOM), as heterogeneous mixture of natural macromolecules derived from the debris of organisms, is ubiquitous in water, soil, and sediment. NOM is known to be redox reactive and plays important roles in reduction of many elements, including Fe^{3+}, Hg^{2+}, and I_2 [19]. In recent years, it was found that NOM could also reduce Ag^+ to elemental AgNPs.

In 2009, Sal'nikov et al. [20] observed that Ag^+ could be reduced to AgNPs by peat fulvic acids in aqueous solution under heating. Later, Akaighe et al. [18] systematically studied the reduction of Ag^+ in water by humic acid (HA) from various origins at different temperatures. The formation of AgNPs was controlled by the type and concentration of HA as well as the incubation temperature. Suwannee River HA (SRHA) and three sedimentary HAs could reduce Ag^+ to AgNPs at 22 ℃, while all five soil HAs investigated could not reduce Ag^+ at room temperature within 25 days. Incubation at elevated temperature (90 ℃) significantly accelerated the formation of AgNPs and the reduction was complete within 3 h, as monitored the appearance of the SPR by UV-visible spectrometry. The polydisperse particle size distributions of the formed AgNPs were characterized by TEM, atomic force microscopy (AFM) and dynamic light scattering (DLS). UV-visible spectrometry also indicated that the formed AgNPs are stable in 70 days, owning to the stabilization effect of adsorbed HA on the surface of AgNPs. Similar with HA, fulvic acid (FA) could also reduce Ag^+ to AgNPs [21]. Different sources of FA and HA exhibit distinct reduction abilities, with the following order at 90 ℃ heating: Nordic lake FA > SRHA > Pahokee Peat FA > Suwannee River FA (SRFA).

It has been known for a long time that Fe^{2+} could reduce Ag^+ into elemental Ag [22]. Recently, Adegboyega et al. found that the co-occurrence of Fe^{2+} or Fe^{3+} with NOM could significantly enhance the formation of AgNPs by NOM under heating [23], with the following reaction:

$$NOM_{red} + Fe^{3+} \rightarrow NOM_{ox} + Fe^{2+} \tag{3.1}$$

$$Fe^{2+} + Ag^+ \rightarrow Fe^{3+} + Ag^0 \tag{3.2}$$

Here, Fe^{2+}/Fe^{3+} acted as the electron shuttle [24] to catalyze the transfer of electron from NOM to Ag^+. Considering the widely occurrence of both Fe^{2+}/Fe^{3+} and NOM, this catalysis of Fe^{2+}/Fe^{3+} should have great impacts on the naturally occurring AgNPs in the aquatic environment.

Compared with elevated temperature, solar irradiation is more environmentally relevant for surface water. We found that, similarly with heating, solar irradiation could accelerate the formation of AgNPs from Ag^+ in natural waters including river water and lake water [25]. The formation of AgNPs was validated by combined techniques, including UV-visible spectrometry, HRTEM, selected area electron diffraction (SAED), EDS, and X-ray diffraction (XRD), as showed in Fig. 3.2. UV-visible spectrum results suggest that the formed AgNPs in environmental water are stable at room temperature in the dark, while continuing exposure under sunlight could induce the aggregation and sedimentation of the AgNPs. It was found that after being subjected to dialysis to remove most inorganic ions but retaining dissolved organic matters (DOM), the river water could still reduce Ag^+ to AgNPs, clearly demonstrating that DOM in natural waters plays a major role in the reduction of Ag^+. In addition, compared to untreated water, 80 % hydrated diameter reduction was observed for AgNPs in dialyzed water, suggesting that, in

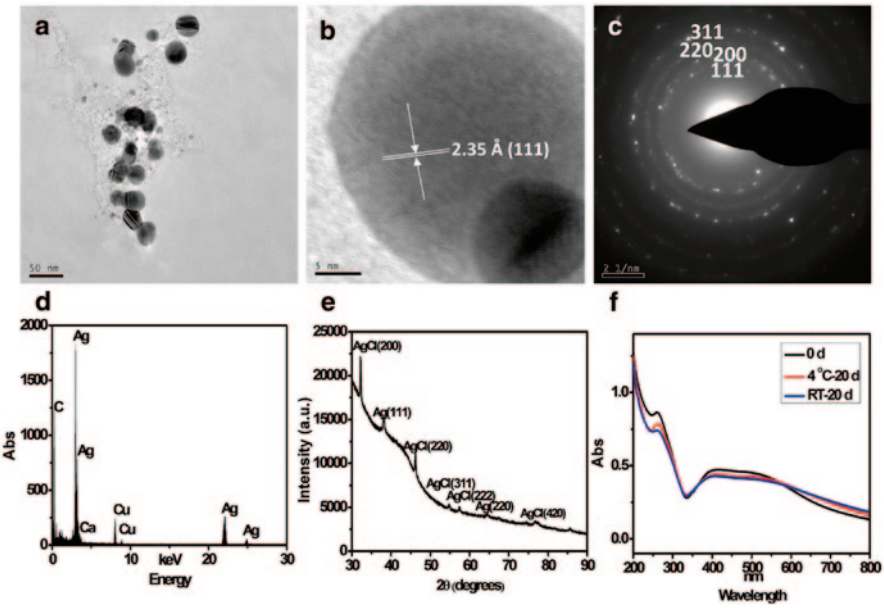

Fig. 3.2 Identification and characterization of AgNPs produced by the reduction of 0.2 mmol L^{-1} $AgClO_4$ in Chaobai River water under sunlight. **a** TEM, **b** HRTEM, **c** SAED, **d** EDS, **e** XRD, and **f** UV-vis spectrum of the formed AgNPs. Note, UV spectrum results suggest the formed AgNPs in environmental water are stable at 4 ℃ and room temperature in the dark. Reprinted with the permission from ref. [25], Copyright 2012 American Chemical Society

this photoreduction process, inorganic ions in environmental water could induce the aggregation of AgNPs.

The kinetics and mechanism of photoreduction of Ag^+ to AgNPs by DOM was investigated under controlled conditions by using HA as a DOM model [25]. The photoreduction of Ag^+ with HA highly depends on the initial concentration of both HA and Ag^+, and the formation of AgNPs fits the pseudo-second-order reaction kinetics. In addition, the formation of AgNPs was found to be strongly dependent on pH for both Aldrich HA and SRHA. No AgNP formation was observed at low pH (pH 4.4 and 5.2 for Aldrich HA and pH 6.2 for SRHA), and the formation rate constant of AgNPs increased significantly with pH values. The pH-dependent reduction indicated that phenol groups in HA played an important role in this process. The photoreduction of Ag^+ to AgNPs was almost completely suppressed when the phenolic group in HA was blocked, demonstrating that the photoreduction should be ascribed to the phenolic group of HA. Purging the solution with N_2 could inhibit the reduction of Ag^+, while purging with O_2 significantly enhanced the formation of AgNPs, indicating the importance of superoxide radical ($O_2^{\cdot-}$) in the reduction. Further, the presence of $O_2^{\cdot-}$ scavenger, superoxide dismutase (SOD, 150 U mL^{-1}), could prevent the formation of AgNPs under natural sunlight, which clearly confirms that $O_2^{\cdot-}$ is the key reductant in DOM-induced photoreduction. The mechanism of photoreduction of Ag^+ to AgNPs by DOM was described by the following reactions:

$$HA_{red} + O_2 + hv \rightarrow HA_{ox} + O_2^{\cdot -} \quad (3.3)$$

$$O_2^{\cdot -} + Ag^+ \rightarrow Ag^0 + O_2 \quad (3.4)$$

$$Ag^0 + O_2^{\cdot -} \rightarrow Ag^{0-} + O_2 \quad (3.5)$$

$$Ag^{0-} + Ag^+ \rightarrow Ag^0 + Ag^0 \quad (3.6)$$

Later, the photoreduction of Ag^+ to AgNPs was further demonstrated by Hou et al. [26]. Besides spherical AgNPs, with further exposure of simulated sunlight, triangular, hexagonal, and rod-like nanostructures were formed from <20 nm AgNPs. It should be noted that it is different from Yin et al.'s result [25] that purging with O_2 did not increase the formation of AgNPs. This difference possibly origins from the different experimental setting (such as source of light). Hou et al. observed that the addition of $NaClO_4$ could inhibit the formation of AgNPs and proposed a mechanism of ligand-to-metal charge transfer in photoactive complexes of Ag^+ and NOM.

Under thermal or light irradiation, NOM from difference sources or with different compositions exhibits different reduction abilities toward Ag^+ [21]. NOM could be in different redox states and with various potentials in different redox environments (such as anaerobic or aerobic conditions). The redox reactivity of NOM has great impacts on the redox transformations of elements occurring in environments. Reduced soil HA could more effectively reduce Ag^+ to AgNPs than untreated or reoxidized HA, as revealed by TEM [27]. AgNP formation occurred within 2 days under redox conditions corresponding to suboxic and oxic systems, while the AgNP formation became fast (in minutes) under reducing conditions (by using reduced HA). In addition, as DOM is a mixture with wide molecular weight (MW) distribution, the exact roles of specific components of DOM in the photoreduction of Ag^+ to AgNPs are still not well understood. In a recent study [28], we found that the difference of MW fractionated natural organic matter (M_f-NOM) on photoreduction of Ag^+ was mainly ascribed to the differential light attenuation of M_f-NOM, rather than the "real" reductive ability. More importantly, compared with low MW fractions, high MW M_f-NOMs showed drastically higher capability in stabilizing the photosynthesized AgNPs against Ca^{2+}-induced aggregation. As shown in Fig. 3.3, Ca^{2+} showed significantly distinguishing effect on the photoreduction of Ag^+ to AgNPs in pristine and M_f-NOM solutions. The change of color and formation of precipitation, as indicators of the aggregation and formation of larger and aggregates of AgNPs in the presence of Ca^{2+}, were more significant for AgNPs in low MW M_f-NOM than that in high MW fractions.

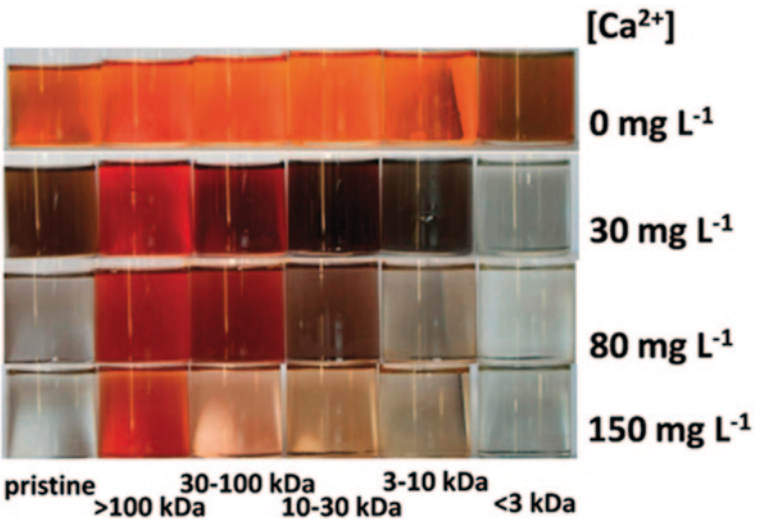

Fig. 3.3 Photography of photoinduced AgNPs solution in the presence of pristine or M_f-NOM and Ca^{2+}. Reaction conditions: 0.2 mmol L^{-1} $AgClO_4$, 5 mg L^{-1} pristine or M_f-NOM, 5 mmol L^{-1} borate buffer (pH 8.0) under simulated sunlight for 29 h. Reprinted with the permission from ref. [28], Copyright 2014 American Chemical Society

3.2.2 Formation from Macroscale Ag Objects Through Dissolution and Reduction

Elemental silver has been widely used for fabrication of jewelry, utensil, coins, as well as electrical contacts and conductors in industry [29]. The oxidation of elemental silver in these macroscale silver objects is inevitable in their use and application when exposure under the atmosphere [30], and the following reduction of Ag^+ could produce new AgNPs. For the first time, Glover et al. [31] tested this hypothesis and demonstrated that macroscale Ag objects including silver wire, sterling silver earring, and silver-plated spoon and fork, when in contact with surfaces, could produce AgNPs with the aid of water. First, a silver wire and a sterling silver earring were exposed to humid air, and a heterogeneous population of AgNPs were observed in the vicinity where each object had contacted the grid. Further, a small droplet of water was placed at the interface between the object (silver-plated spoon and fork) and the substrate, and it was found that during the time of the water-drop evaporation (< 10 min), large numbers of AgNPs were produced (Fig. 3.4). The corresponding EDS spectrum showed that the main component of the nanoparticle is silver, although trace S and Cl also exist. The rapid formation of large numbers of AgNPs was ascribed to the dissolution of more Ag^+ in larger volume of water and then concentration of Ag^+ by evaporation of water. This finding suggested that oxidative dissolution and further reduction is a potential source of natural AgNPs from daily used macroscale Ag objects and the contact of these Ag objects with human skin could form AgNPs. In addition,

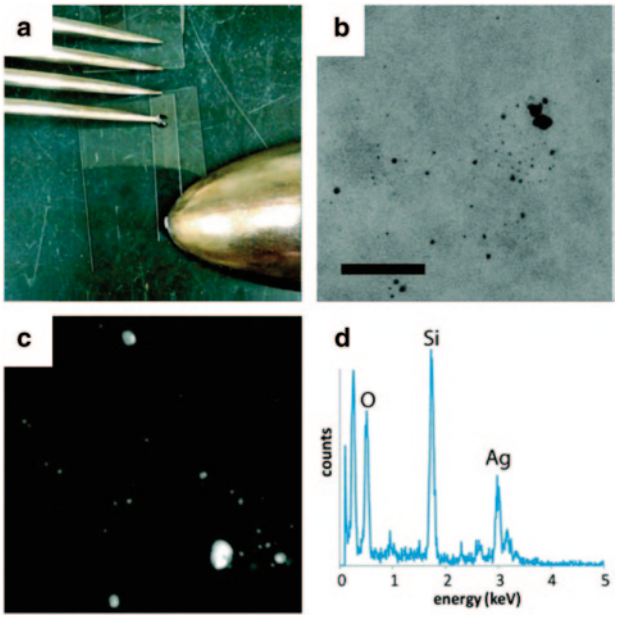

Fig. 3.4 Generation of AgNPs from common elemental silver objects. **a** An optical image of a sterling silver knife and fork in contact with the grid surfaces. **b** A TEM image of particles produced upon introduction and evaporation of a 1 μL droplet of water. **c** A high angle annular dark field (*HAADF*) scanning transmission electron microscopy (*STEM*) image of particles produced upon drying as in panel **b**. **d** EDS spectrum of the generated nanoparticles that confirms their composition is silver. The scale bar shown is 50 nm for both panels **b** and **c**. Reprinted with the permission from ref. [31], Copyright 2011 American Chemical Society

as native elemental silver can occur in natural environments [32], it is reasonable that natural occurring AgNPs could be formed from native silver.

This research also highlighted that AgNPs were not new for human, and the exposure of AgNPs to human began at least since people started using metal silver.

Conventional silver materials such as metallic Ag fiber are also often used in textiles for antibacterial purpose. According to Glover's finding [31], in the washing procedure, the transformation of metallic Ag fibers into AgNPs is also highly possible. In fact, this has been recently proved by Mitrano et al. [33] The commercially available X-Static fabric (tennis socks), containing nylon yarns coated with bulk metallic Ag, could release high amount of total Ag in the washing procedure, which was performed in phosphate-free ECE detergent without optical brightener by washing machine at 40 ℃. The released silver was identified by TEM and EDS as metallic Ag particles of ~20–30 nm in size. This study further confirmed the formation of AgNPs from macroscale Ag objects was a general phenomenon in daily life.

As discussed above, oxidative dissolution of macroscale Ag objects to Ag^+ and further reduction of Ag^+ was proposed as the mechanism of AgNP formation from macroscale Ag objects. While the dissolved O_2 or H_2O_2 play the role of oxidant in this process [31], the reductant accounts for formation AgNPs at room temperature under dark conditions is still unknown and need further study.

3.2.3 Reduction of Ag^+ by Other Chemical Process

Dissolved Fe^{2+} could reduce Ag^+ into elemental silver [22]. Green rusts are mixed Fe^{2+}/Fe^{3+} hydroxides that are found in many suboxic environments. It was shown that, in hydroxysulfate green rust suspensions, the spiked silver acetate ($AgCH_3COO$) could be readily reduced into Ag^0, as probed by X-ray absorption fine structure analysis [34]. Further TEM-EDS analysis revealed that the Ag^0 existed as in submicron-sized particles, as shown in Fig. 3.5. Typically, the Ag^0 particles were multiply twinned and irregular in shape and ranged in size from ~c40 to 100 nm along the longest dimension. The reduction of Ag^+ to AgNPs by Fe^{2+} was later suggested as a green method to prepare AgNP-loaded nanohybrids [35].

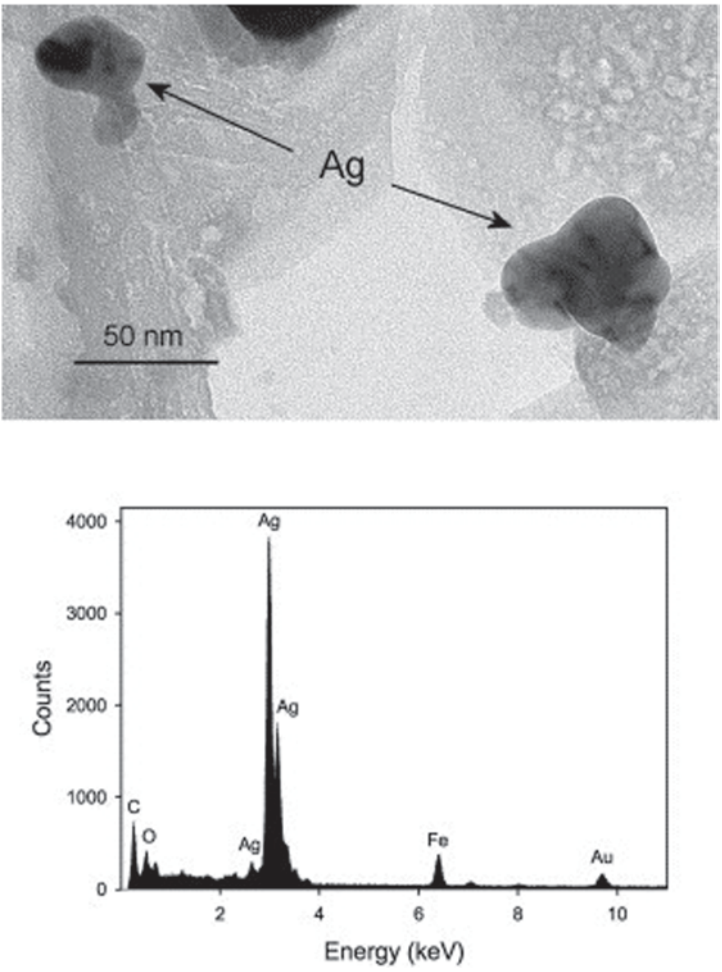

Fig. 3.5 TEM results for Ag^+ amended *green* rust. Bright-field image showing nanosized Ag^0 (*top*). EDS of an Ag particle (*bottom*); C and Au signals are from the TEM grid, and Fe and O signals are from *green* rust. Reprinted from ref. [34], Copyright 2003, with permission from Elsevier

The reduction of Ag^+ to Ag^0 or AgNPs was also observed on surface of granular activated carbon [36], bentonite [37, 38], and silica [39, 40]. For example, by mixing 25 mL of 30 mmol L^{-1} $AgClO_4$ with 10 g Ca-montmorillonite, Ag^+ could be adsorbed in the interlayer space and on the edges of bentonite by cation exchanged, leading to the uniform distribution of Ag^+ on atomic scale. Scanning electron microscopy (SEM) test revealed that further incubation of the mixture induced the reduction of Ag^+ to Ag^0 in nano- or micro size [38]. Under light irradiation (Xe–Hg lamp or visible light), reduction of Ag^+ to AgNPs on colloidal silica was observed and monitored by the appearance of the SPR band at around 410 nm [40]. TEM showed that the size of formed AgNPs were in the range of 10–40 nm. The growth of the nanoparticles was directly related to the time exposed to radiation. The AgNPs could also form without light irradiation under alkali conditions.

3.2.4 Reduction of Ag^+ by Biological Process

3.2.4.1 Reduction by Plant

As early as 1938, it was observed that Ag^+ could be reduced by chloroplast in leave, and it was suggested that ascorbic acid was the substance responsible for the reduction of Ag^+ by the chloroplast [41]. By using electron microscope, it was revealed in 1962 that the Ag^0 located within the chloroplasts, plasmodesmata, or at the surfaces of the cell wall [42]. In 2003, for the first time, Gardea-Torresdey et al. [43] reported the uptake of Ag^+ and formation of AgNPs by living alfalfa plant (*Medicago sativa*). After incubation of alfalfa plant in a silver-rich solid medium for 9 days, X-ray absorption near edge structure (XANES) and extended X-ray absorption fine structure (EXAFS) confirmed the occurrence of Ag^0 in the root and shoot. The TEM images further revealed that in alfalfa plant the formed Ag^0 was spherical nanoparticles (2–20 nm) with the connection of noncrystalline silver atomic wires or clusters as shown in Fig. 3.6. HRTEM showed that the arrangement of Ag atoms in the nanoparticles was very disordered and had many internal defects (twinning, mixed structures, and dislocations), which indicated that the aggregation process could be very fast or not under equilibrium conditions.

Later, the formation of AgNPs from ionic silver precursors has been observed in living *Brassica juncea*, *Festuca rubra*, and *Chlamydomonas reinhardtii*, demonstrating the universality of this reduction process in living plants. In *Brassica juncea*, there was a limit on the amount of AgNP formation (~0.35 wt.% Ag on a dry plant basis), which was proposed to be controlled by the total reducing capacity of the plant for the reduction potential of the ionic silver species [44]. The formed AgNPs were densely around chloroplasts of *Brassica juncea*, which areas were associated with a high content of reducing sugars, and therefore reducing sugars were implicated as the reagents responsible for this reduction [45]. However, another study on the formation of AgNPs in living *Brassica juncea, Festuca rubra,* and *Medicago sativa* showed that the contents of reducing sugars and antioxidant com-

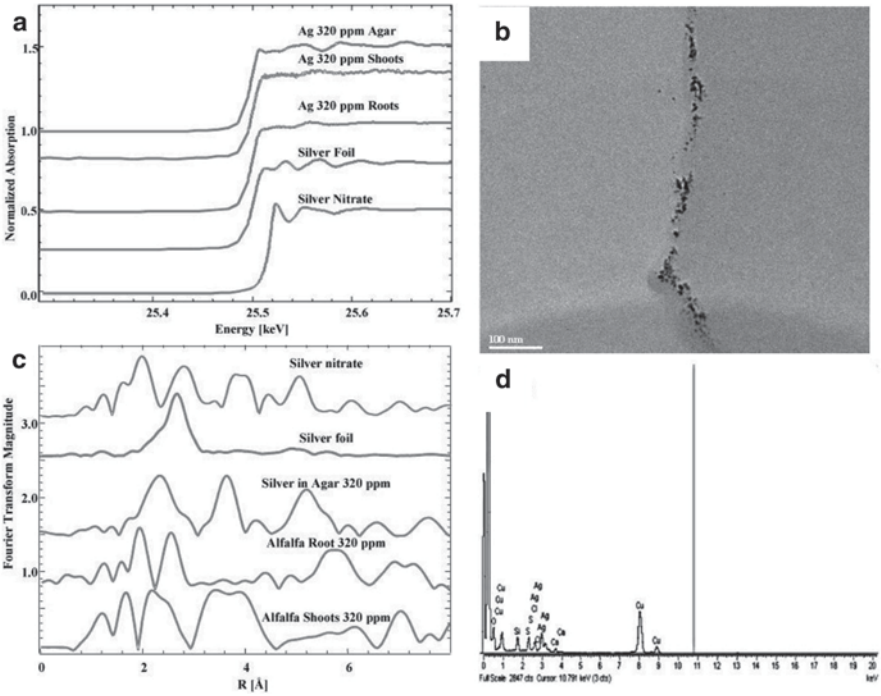

Fig. 3.6 The formation of AgNPs in living alfalfa plants. **a** XANES of the silver alfalfa roots and shoots and Ag model compounds. **b** EXAFS of the silver alfalfa roots and shoots and Ag model compounds. **c** Low-magnification TEM image of the alfalfa shoot showing a unidimensional array of silver nanoparticles. **d** X-ray EDS analysis confirmed that Ag constitutes the nanoparticles. Reprinted with the permission from ref. [43], Copyright 2003 American Chemical Society

pounds were quite different among the species, which suggested that it was unlikely that a single substance was responsible for this process [46]. The biosynthesized AgNPs by *Chlamydomonas reinhardtii* were localized in the peripheral cytoplasm and at one side of flagella root, the site of pathway of adenosine triphosphate transport and its synthesis related enzymes, which provided an evidence for the involvement of oxidoreductive proteins in this reduction process [47]. Alteration in size distribution and decrease of synthesis rate of AgNPs in protein-depleted fractions confirmed the involvement of cellular proteins in AgNP biosynthesis (Table 3.1).

3.2.4.2 Reduction by Microorganism

In 1976, Beveridge et al. found that cell walls of *Bacillus subtilis* could adsorb $AuCl_4^-$ [51], and later demonstrated the Au^0 deposited on cell walls were in the size of ~25 nm [52]. Then, in 1999 Klaus et al. reported the first case of biological synthesis of AgNPs with sizes up to 200 nm by living *Pseudomonas stutzeri* AG259,

Table 3.1 The formation of AgNPs in living plants from ionic silver precursors

Plant species	Ionic silver precursor	Site of AgNPs	Morphology	Size (nm)	Characterization	Reference
Medicago sativa	$AgNO_3$	Shoot and root	Spherical nanoparticles and atomic wires or clusters	2–20	XANES, EXAFS, TEM, EDS	[43]
Brassica juncea and *Medicago sativa*	$AgNO_3$	–	Spherical nanoparticles	~50	TEM, EDS	[48]
Brassica juncea	$AgNO_3$, $Na_3Ag(S_2O_3)_2$, and $Ag(NH_3)_2NO_3$	–	Spherical nanoparticles	4–35 nm for $AgNO_3$, 3–7 nm for $Ag(NH_3)_2NO_3$, and 2–7 nm for $Na_3Ag(S_2O_3)_2$	XANES, TEM	[44]
Brassica juncea	$AgNO_3$ and $[Ag(NH_3)_2]NO_3$	Leaves, stem and roots	Spherical nanoparticles	2–100	XANES, TEM	[45]
Chlamydomonas reinhardtii	$AgNO_3$	Peripheral cytoplasm and at one side of flagella root	Spherical nanoparticles	5–35	TEM, EDS	[47]
Chlamydomonas reinhardtii	$AgNO_3$	On the surface and inside the cells	Spherical nanoparticles	–	Hyperspectral microscopy	[49]
Marine micro algae (*C. calcitrans*, *C. salina*, *I. galbana*, *T. gracilis*)	$AgNO_3$	–	Spherical nanoparticles	–	UV-vis, SEM	[50]
Brassica juncea, *Festuca rubra*, and *Medicago sativa*	$AgNO_3$	Roots, stems, and leaves	Root: in the cortical parenchymal cells, on the cell wall of the xylem vessels and in regions corresponding to the pits; leaf: close to the cell wall and in the cytoplasm and within chloroplasts	–	TEM, EDS	[46]

– not given

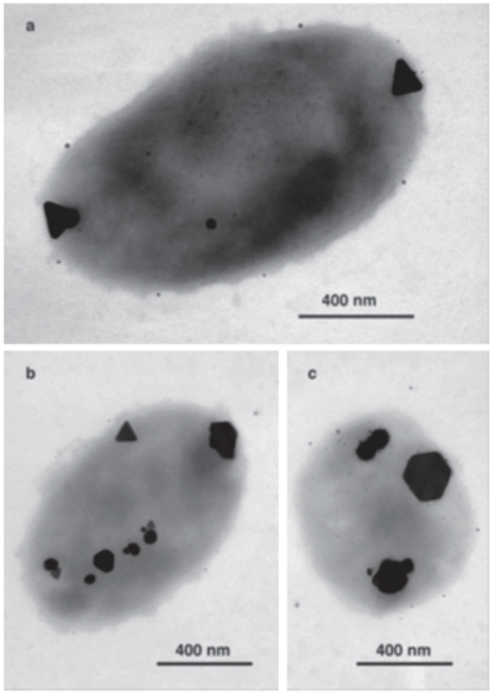

Fig. 3.7 Different morphologies and sizes of AgNPs produced by *P. stutzeri* AG259. **a** Whole cell grown on Ag-containing environment with large, triangular, Ag-containing particles at both poles; an accumulation of smaller Ag-containing particles can be found all over the cell. (**b** and **c**) Triangular, hexagonal, and spherical Ag-containing nanoparticles accumulated at different cellular binding sites. Reprinted with the permission from ref. [53], Copyright 1999 National Academy of Sciences, USA

a bacterial strain isolated from a silver mine [53]. As shown in Fig. 3.7, after incubation with $AgNO_3$, various triangular, hexagonal, and spherical AgNPs were deposited between the cell wall and the plasma membrane. Later the biological synthesis of AgNPs with living bacteria, fungi, and actinomycete (as shown in Table 3.2) became a hotspot and was suggested as a green and environment-friendly approach to synthesize AgNPs. These studies are also helpful for understanding the biomineralization of Ag and formation of naturally occurring AgNPs. For example, in the anaerobic dissolution of silver jarosite minerals ($Ag_6Fe_3(SO_4)_2(OH)_6$) by *Shewanella putrefaciens* CN32, the progressive heterogeneous nucleation of AgNPs within cellular structures and on adjacent mineral grains was observed by environmental SEM and TEM [54].

Mechanism of Biological Reduction

1. Non-enzymatic reduction

Cysteine in protein as reduction agent [55]: After the reduction of Ag^+, the Fourier transform infrared spectroscopy (FTIR) spectroscopy of fungus *T. asperellum* showed that: (1) The intensity of overtone of the amide-II band (~3270 cm^{-1}), the stretching frequency of the O–H band (~3600 cm^{-1}), and the amide-II band, carbonyl and carboxylic C=O stretching bands (~1550, 1640, and 1670 cm^{-1}) decreased, indicating a decrease in the concentration of the peptide linkages in the solution.

Table 3.2 Intracellular and extracellular reduction silver ion to AgNPs by microbes

Species	Localization	Morphology	Size (nm)	Characterization	Reference
Bacteria					
Pseudomonas stutzeri AG259	Intracellular	Triangular, hexagonal, and spherical	–	TEM, EDS	[53]
Bacillus subtilis	–	–	–	UV-vis	[74]
Stenotrophomonas maltophilia	Extracellular	Spherical and cubic	~93	UV-vis, XRD, FESEM	[75]
Escherichia coli, *Bacillus megaterium*, *Acinetobacter* sp. and *Stenotrophomonas maltophilia*	Extracellular	Spherical	15–50	UV-vis, XRD, SEM, TEM, EDS	[76]
Stenotrophomonas	Extracellular	Spherical, triangular, pentagonal, hexagonal, and irregular shaped	40–60	UV-vis, TEM, EDS	[77]
Brevibacterium casei	–	Spherical	10–50	UV-vis, XRD, TEM	[78]
Bacillus licheniformis	–	Spherical	~50	UV-vis, SEM, EDS, XRD	[79]
Staphylococcus aureus	Extracellular	Irregular	160–180	UV-vis, AFM	[80]
Bacillus thuringiensis	–	–	43.52–142.97	UV-vis, SEM, EDS	[81]
Staphylococcus aureus	–	Spherical	–	UV-vis, TEM	[82]
Pseudomonas antarctica, *Pseudomonas proteolytica*, *Pseudomonas meridiana*, *Arthrobacter kerguelensis*, *Arthrobacter gangotriensis*, *Bacillus indicus* and *Bacillus cecembensis*	Extracellular	Spherical	~4.58–~13.35	UV-vis, TEM, AFM	[83]
Lactobacillus casei	–	Spherical	25–100	UV-vis, TEM	[84]
Bacillus cereus	Intracellular	Spherical	4–5	UV-vis, TEM, XRD	[85]
Bacillus megaterium	Extracellular	Spherical to large truncated irregular	80–98.56	UV-vis, AFM	[86]

Table 3.2 (continued)

Species	Localization	Morphology	Size (nm)	Characterization	Reference
Shewanella oneidensis	Extracellular	Spherical	2–11	UV-vis, XRD, TEM, AFM, and EDS	[87]
Klebsiella pneumoniae	Extracellular	Spherical	15–37	UV-vis, XRD, TEM	[88]
Halococcus salifodinae	Intracellular	Spherical	2–20 nm and 20–100 nm in different nutrient solution	TEM	[89]
Bacillus mojavensis	Extracellular	Spherical, hexagonal, polygonal, nanoprisms, and uneven shapes	6–72	UV-vis, XRD, and TEM	[90]
Corynebacterium glutamicum	–	Irregular	5–50	UV-vis, TEM, EDS, XRD	[91]
Fungi					
Fusarium culmorum (MTCC-2090)	–	Spherical	5–25	TEM	[92]
Trichoderma viride	Extracellular	Spherical and rod	5–40	UV-vis, XPS, TEM, EDS	[93]
Aspergillus flavus	Extracellular	Spherical	~8.92	UV-vis, XRD, SEM, TEM	[94]
Humicola sp.	Extracellular	Spherical	5–25	UV-vis, TEM, XRD, XPS	[95]
Aspergillus clavatus	Extracellular	Spherical or hexagonal	10–25	XRD, TEM, AFM	[96]
Septoria apii	–	Spherical	5–30	UV-vis, XRD, AFM	[97]
Phaenerochaete chrysosporium	Extracellular	Spherical	50–200	UV-vis, XRD, SEM, TEM,	[98]
Yeast	Extracellular/ intracellular	Spherical	<20	UV-vis, TEM, EDS, XRD	[99]
Geotricum sp.	Extracellular	Spherical	30–50	UV-vis, AFM, SEM, EDS	[100]

Table 3.2 (continued)

Species	Localization	Morphology	Size (nm)	Characterization	Reference
Trichoderma koningii	–	Spherical	5–20	UV-vis, XRD, AFM	[97]
Epicoccum nigrum	Extracellular	Spherical	1–22	UV-vis, XRD, TEM	[101]
Neurospora crassa	Extrcelllar/ intracellular	Spherical	3–50	SEM, TEM, EDS	[102]
Streptomyces albidoflavus	Extracellular/ intracellular	Spherical	10–40	UV-vis, TEM	[103]
Cladosporium cladosporioides	Extracellular	Spherical	10–100	UV-vis, TEM, XRD	[104]
Neurospora intermedia	Extracellular	Spherical	~19	UV-vis, XRD, SEM, EDS	[105]
Aspergillus fumigatus	Extracellular	Spherical and occasionally triangular	5–25	UV-vis, XRD, TEM	[106]
Fusarium oxysporum	Extracellular	Spherical and occasionally triangular	5–15	UV-vis, TEM	[107]
Fusarium semitectum	Extracellular	Spherical	10–60	UV-vis, TEM, XRD	[108]
Cylindrocladium floridanum	Extracellular	Spherical	7.7–58.3	UV-vis, SEM, EDS, TEM, XRD,	[109]
Aspergillus clavatus	Extracellular	–	–	UV-vis, AFM	[110]
Trichoderma viride	Extracellular	Spherical	2–4 at 40 ℃; 10–40 at 27 ℃; 80–100 at 10 ℃	UV-vis, TEM,	[111]
Aspergillus terreus	Extracellular	Spherical	1–20	UV-vis, TEM, XRD	[112]
Alternaria alternata	Extracellular	Spherical	20–60	UV-vis, SEM, EDS	[113]
Verticillium	Intracellular	Spherical	~25	UV-vis, SEM, TEM, EDS	[59]
Penicillium purpurogenum	Extracellular	Pyramidal, spherical, and ellipsoidal	40–55 at pH 4 and 5; 8–13 at pH 8 and 9	UV-vis, TEM, XRD	[114]

Table 3.2 (continued)

Species	Localization	Morphology	Size (nm)	Characterization	Reference
Cochliobolus lunatus	Extracellular	Spherical	3–21	UV-vis, TEM, SEM, XRD	[115]
Aspergillus oryzae	Extracellular	Spherical	5–50	UV-vis, TEM, EDS, XRD	[116]
Aspergillus tamarii	Extracellular	Spherical	25–50	UV-vis, SEM,	[117]
Puccinia graminis	Extracellular	Spherical	30–120	UV-vis, XRD, SEM, AFM	[118]
Fusarium oxysporum	Extracellular	Spherical	10–20	UV-vis, TEM,	[119]
Eleven different *Fusarium* species	Extracellular	Spherical	2–68	UV-vis, TEM, XRD	[120]
Streptomyces sp.	Extracellular	Spherical	~5	UV-vis, TEM, AFM, XRD	[121]
Cochliobolus lunatus	Extracellular	Spherical	5–100	TEM, AFM, XRD	[122]
Penicillium fellutanum	Extracellular	Spherical	5–25	UV-vis, TEM,	[123]
Actinomyces					
Nocardiopsis sp. MBRC-1	Extracellular	Spherical	30–90	UV-vis, TEM, FESEM, EDX, XRD	[124]
Streptomyces aegyptia	Extracellular	–	–	UV-vis	[125]
Streptomyces parvulus	Extracellular	Spherical	1.66–11.68	TEM	[126]

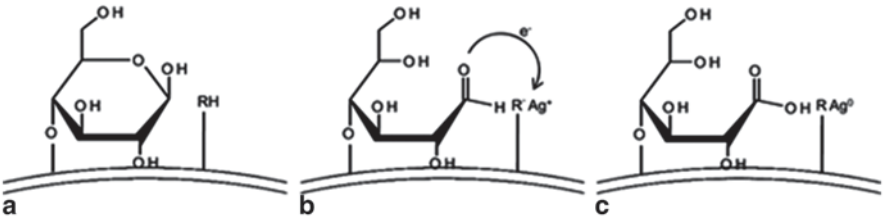

Fig 3.8 Proposed bacterial reduction of Ag^+ to Ag^0 with surface sugar as reduction agent. **a** Bacterial cell with reducing sugars such as glucose and protonated anionic functional groups (–RH). **b** When pH increases, protons dissociate and create negatively charged adsorption sites for Ag^+. The reducing sugars turn into their open-ring structure and are now able to reduce Ag^+. **c** the aldehyde group of the reducing sugar is oxidized to its carboxylic acid, while $Ag^+$is reduced to Ag^0. Reprinted from ref. [56], with kind permission from Springer Science + Business Media

(2) An additional feature at ~970 cm^{-1} (the wagging of trans-ethylenic moiety) appeared after reduction, showing the formation of a C=C double bond. (3) The peak at ~2600 cm^{-1} due to S–H stretching vibrations shifted toward lower wavenumbers. These results combinedly suggested that the protein containing an amino acid with S–H bonds played a key role in this reduction process. It is then suggested that cysteine undergoes dehydrogenation upon reaction with the mild oxidizing agent $AgNO_3$ to produce AgNPs. The β-carbon in cysteine loses one hydrogen radical and one electron in a concerted or two consecutive steps and reduces Ag^+. In this process, the 'CH_2' moiety adjacent to the S–H functional group is lost and then, the α carbon loses one hydrogen to form an α–β C=C bond. The C=C double bond is in conjugation with the lone pair of electrons on the sulfur atom, thereby increasing the acidity of the S–H moiety, which is supported by the redshift of the band due to S–H stretching at ~2600 cm^{-1}.

Sugar as Reduction Agent The FTIR spectroscopy shows that the free aldehyde group in reducing sugars (glucose) could be oxidized into the carboxyl group by Ag^+, suggesting that similar oxidation reaction may also occur in reducing sugars from the hydrolysates of the polysaccharides on the biomass after contact with Ag^+, and polysaccharides from the cell wall plays a leading role in serving as the electron donor for reducing the Ag^+ to Ag^0 [57]. This mechanism could well explain the pH-dependent reduction of Ag^+ by bacteria (as shown in Fig. 3.8) [56]: with the increasing pH, the open of monosaccharide ring leads to the formation of openchain aldehyde, which facilitates the reduction of Ag^+. When Ag^+ is present, the aldehyde group will be oxidized to the corresponding carboxylic acid, and meanwhile, Ag^+ was reduced into Ag^0 and then grows into AgNPs. This assumption was further confirmed later in the reduction of Ag^+ by extracellular polymeric substances from *Escherichia coli* [58].

2. Enzyme-mediated reduction

In 2001, Mukherjee et al. observed the bioreduction of Ag^+ to AgNPs by fungus *Verticillium* located below the cell wall surface, and then suggested that enzymes

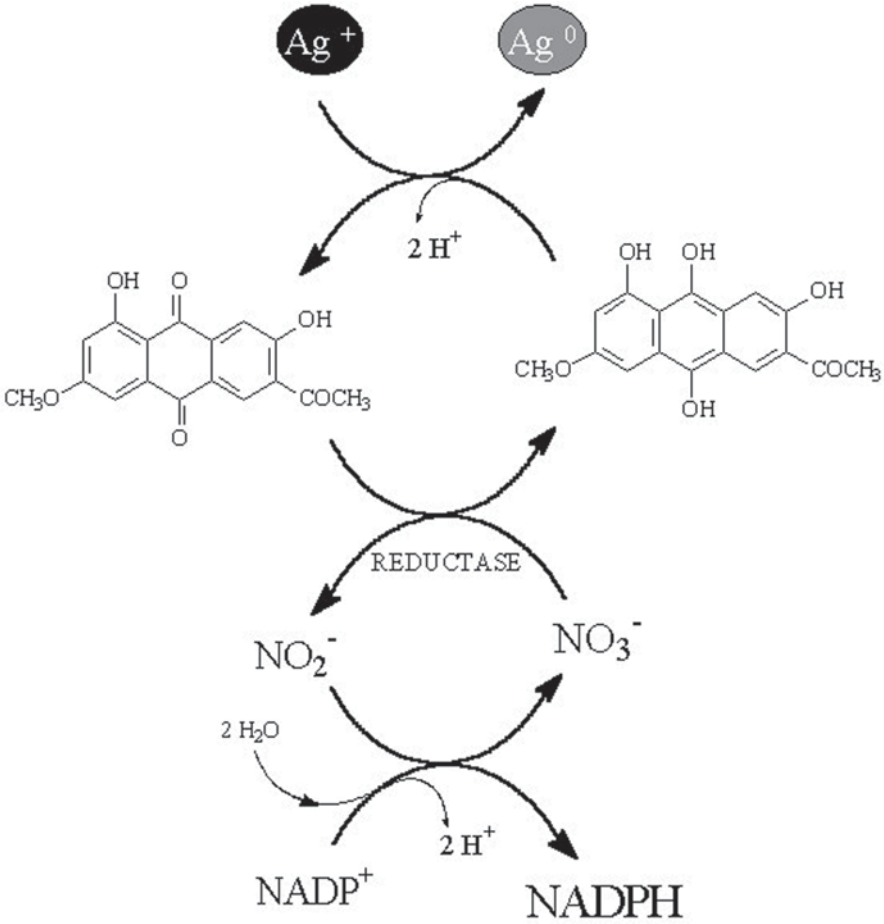

Fig. 3.9 Hypothetical mechanisms of nitrate reductase-mediated AgNPs biosynthesis. Reproduced from ref. [60] by permission of BioMedCentral

present in the cell wall membrane were possibly responsible for the reduction of Ag^+ [59]. Durán et al. detected 2-acetyl-3, 8-dihydroxy-6-methoxy anthraquinone or its isomers and nitrate reductase in extracellular solution of *Fusarium oxysporum* strains, and proposed that the reduction of the Ag^+ occured by a nitrate-dependent reductase and a shuttle quinone extracellular process as shown in Fig. 3.9 [60]. Piperitone, inhibitor of nitroreductase, could partially inhibit the reduction of Ag^+ to metallic AgNPs by *K. pneumoniae* and other different strains of *Enterobacteriaceae*, which further supported the hypotheses of nitroreductase-involved reduction [61]. Ultimately, the in vitro synthesis of AgNPs using nitrate reductase [62] and the nitrate reductase activity-dependent formation of AgNPs [63] clearly demonstrated the crucial role of nitrate reductase in synthesis of AgNPs.

3. Free radical-mediated reduction

Many microorganisms could produce extracellular superoxide [64], and the superoxide could mediate the redox reaction of Fe, Mn, and I, etc [65–68]. It has been demonstrated that superoxide (produced by KO_2 or photo-irradiated solutions containing carbonate, ethanol, and acetone) could reduce Ag^+ to form AgNPs [69]. Thus, it is reasonable that the microorganisms extracellularly produced superoxide could also reduce Ag^+ to AgNPs, although this hypothesis needs to be confirmed by further experiments.

3.2.4.3 Possible Reduction by Animal

Animal proteins such as bovine serum albumin (BSA) [70] and cow milk [71] could reduce Ag^+ into AgNPs, and recent studies also showed that living protozoa *Tetrahymena thermophila* [72] and living human cells (HeLa and HEK293T cell) [73] could convert Ag^+ to AgNPs. These results suggested this reduction process was also highly possible in animal bodies and highlighted the importance of redox transformation of Ag^+ and AgNPs in living animals including humans.

3.3 Anthropogenic Pathway

3.3.1 Intentionally Produced Silver Nanoparticles

Though several natural pathways can result in the formation of AgNPs, this amount is quite low. With the high demand of AgNP related applications, the production and use of AgNPs is steadily increasing year by year. It is estimated that a "best guess" for the production of nano-Ag is 500 t/a worldwide [127], and the number is still growing. The related products include electron devices, solar cells, clothing, personal cares, cosmetics, filtration, and sporting goods. Companies from more than 29 countries in the world are involved in the AgNP production. It was reported that the products of mono nanosilver solution exhibits lasting bactericidal effects and promotes wound healing. AgNP solution is incorporated in a variety of products, such as nanosilver soap, nanosilver antibacterial tableware, nanosilver antibacterial storage box, and nanosilver formaldehyde removal solution. The producers claim that AgNP products will continue to protect against bacteria for up to 24 h after application. With the large spread use of AgNPs, there is no denying that anthropogenic activities play a vital part in the potential Ag pollution.

3.3.2 Unintentionally Produced Silver Nanoparticles

In 1839, Louis–Jacques–Mandé developed a photography technique that utilized a silver-plated sheet of copper, sensitized with iodide vapors to make the silver

react with light, fumed with mercury vapor, and a salt solution to permanently fix the image on the sheet [128]. Because of the photosensitivity of silver halides, especially for silver bromide, silver is still used in photography today. It is reported that in 1978, about 82% of the annual silver emit in the USA was originated from anthropogenic sources, to which the photography industry contributed 42% [128]. Though the use of silver in photography declines with the advent of digital photography, the total amount is still large. After emitted into the environment, there is a risk that exposure silver bromide to light would result in the generation of AgNPs spontaneously. Considering the extensive use of silver bromide in photographic facilities, a large quantity of AgNPs would be unintentional produced. Additionally, silver iodide is widely used for cloud seeding. The involuntary generation of AgNPs in artificial rainmaking process is also anticipated.

3.3.3 Release into the Environment

During the production, manufacturing, use, and disposal of AgNP containing products, AgNPs would enter the environment sooner or later. Gottschalk and Nowack estimated that ranging from 0 to 2% engineered NPs produced would release into the environment from the production procedure [2]. The synthesis process often involves multiple procedures, such as mixing, centrifugation, and filtration to remove impurities and unreacted precursors. The wastewater may be directly discharged into natural systems and powder nanoparticles may escape through open windows to the air. Additionally, other activities, such as sampling for quality control, leaking from broken packaging and accidents during transport could also result in the unintentional release of AgNPs [129]. If AgNPs were produced in closed systems, solvent-free steps were used and all wastes during synthesis and purifying were handled as special wastes, there is no doubt that only negligible emission of AgNPs during production is expected [2].

AgNPs are widely used in our daily life. They are added into disinfectant sprays, incorporated into odor-resistant socks, outdoor paints, antimicrobial plastics and textiles, and simultaneously formed in washing machines. Frequent washing, mechanical abrasion and physicochemical material aging can cause AgNPs to escape to the natural environment. Most AgNPs are supposed to release during their use. The amount and level of silver released depends on the lifetime, usage of the materials, and how AgNPs are embedded into the products. Generally, AgNPs added in liquid products such as sprays and disinfectants are easier to emit to the atmosphere, while AgNPs incorporated in solid matrix such textiles and paints with a strong fixation are supported to release silver slowly [127]. Blaser et al. predicted that biocidal plastics and textiles accounted for up to 15% of the total silver released into water in the European Union in 2010 [130], and most of them will eventually enter the WWTPs. Though it is estimated that more than 90% of AgNPs are removed during wastewater treatment and adsorbed by WWTP biomass [127], the reuse of sewage sludge in certain countries may pose a continued threat to the environment. Untreated sewage sludge is used as agricultural fertilizers, disposed of in solid waste landfills or incinerated in thermal waste treatment plants [131]. As a result,

AgNPs would reenter the terrestrial system, or leach into subsoil and groundwater after applying on field or landfilling. Incinerated silver would mostly end up in slag and fly ashes, or emit to the air directly, causing silver recycling in the environment.

Several studies have reported the release of AgNPs from consumer products under laboratory or field conditions. A typical example is the weathering of AgNPs contained paints which are used for outdoor facades [130]. After exposed to ambient weather conditions for 1 year, as much as 30% of AgNPs were lost and significant amounts of silver were detected in the first few runoff events. The TEM images clearly confirmed the presence of AgNPs with a small particles distribution in selected runoff samples. The released AgNPs are most likely to directly enter the aquatic system with the runoff water. Benn and coworker also investigated the behavior of six types of AgNPs contained socks during washing and the fate of released silver in WWTPs [132]. AgNPs were found to easily release into wastewater during washing and some brands of socks leached almost 100% of silver with a maximum concentration of 650 μg in 500 mL of distilled water. Colloidal and ionic silver were both present in the washing water, and the diameters of particles were mostly in the range of 10–500 nm. Further study demonstrated that most leached silver were adsorbed to biomass or precipitated with chloride or sulfide in WWTPs, implying the potential risks of disposal of sewage sludge as agricultural additives.

Subsequent studies further examined the release of AgNPs from silver nanotextiles during washing simulation [133,134]. Nine fabrics with diverse textures and different silver embedded ways into fibers were selected to investigate the influence of pH, surfactants and oxidizing agents on the release kinetics of silver. Results displayed that both ionic and particulate Ag could release from the textiles, and the mass of silver released varied, e.g., some textile emitted about 45% of total silver during one washing while some only with less than 1%. Higher pH (pH 10) slowed down the dissolution of AgNPs and oxidizing agents such as hydrogen peroxide or peracetic acid (formed by the perborate/tetraacetylethylenediamine system) could significantly enhance the release of Ag. Mechanical stresses also accelerated the dissolution of Ag, and most of silver (at least 50% but mostly > 75%) leached in the washing machine was larger than 450 nm.

Humans are easily exposed to the antibacterial clothing textiles via skin contact. AgNPs are possible to directly release into sweat, which may pose a potential threat as AgNPs are toxic to many mammalian cultured cells. The release of AgNPs from antibacterial fabrics into artificial sweat was also investigated [135]. Five laboratory-prepared fabrics and six commercial fabrics were selected, and then they were incubated in artificial sweat at 37℃ for 24 h to simulate the wearing process. The amounts of silver released varied among different fabrics, ranging from 0 to about 322 mg/kg of fabric weight, mainly depending on the fabric quality, the mass of silver coating and formulations of the artificial sweat.

Silver nanowashing machine, which is advertised to kill majority of the bacteria in the laundry, is also appeared on the market. Farkas et al. found that as much as 11 μg/L silver was released in its effluent and the presence of AgNPs could be identified by a suite of techniques such as sp-ICP-MS, ion selective electrode measurements, filtration and TEM [136]. Additionally, the effluent significantly inhibited the growth of a natural bacterial community. If discharged into the natural water system, it may cause serious negative effects on aquatic organisms. To further

evaluate the leaching and environmental fate of AgNPs from consumer products, AgNP solutions, a silver coated antimicrobial wound dressing and a toy bear with AgNPs contained in its foam stuffing were subjected to a pilot estuarine mesocosm system over a period of 60 days [137]. About 82–99 % of their total silver was released into the water column and then taken up by estuarine biota or adsorbed by sediment, sand, and biofilm. The accumulation of silver in hard clams, grass shrimp, mud snails, cordgrass stalks, and leaves through trophic transfer might trigger important environmental risks as well.

3.4 Summary

Natural occurring or anthropogenic nanoparticulate silver or AgNPs have been observed in various environmental compartments. In recent years, some potential formation pathways of natural occurring AgNPs have been identified, including reduction of Ag^+ by DOM, living organisms and from macroscale Ag objects though dissolution and reduction. Anthropogenic AgNPs could be intentionally or unintentionally produced and then released into the environment in the processes of production, use, recycling, and disposal. After formation or releasing, these natural occurring or anthropogenic AgNPs or nanoparticulate silver could further transport between different environmental compartments and undergo physical and chemical transformation, which are discussed in the following chapter.

References

1. Nowack B, Krug HF, Height M (2011) 120 years of nanosilver history: implications for policy makers. Environ Sci Technol 45(4):1177–1183. doi:10.1021/es103316q
2. Gottschalk F, Nowack B (2011) The release of engineered nanomaterials to the environment. J Environ Monit 13(5):1145–1155. doi:10.1039/c0em00547a
3. Mitrano DM, Lesher EK, Bednar A, Monserud J, Higgins CP, Ranville JF (2012) Detecting nanoparticulate silver using single-particle inductively coupled plasma-mass spectrometry. Environ Toxicol Chem 31 (1):115–121. doi:10.1002/etc.719
4. Li LXY, Hartmann G, Doblinger M, Schuster M (2013) Quantification of nanoscale silver particles removal and release from municipal wastewater treatment plants in Germany. Environ Sci Technol 47(13):7317–7323. doi:10.1021/es3041658
5. Walser T, Schwabe F, Thöni L, De Temmerman L, Hellweg S (2013) Nanosilver emissions to the atmosphere: a new challenge? E3S Web of Conferences 1:14003. doi:http://dx.doi.org/10.1051/e3sconf/20130114003
6. Gottschalk F, Sonderer T, Scholz RW, Nowack B (2009) Modeled environmental concentrations of engineered nanomaterials (TiO_2, ZnO, Ag, CNT, fullerenes) for different regions. Environ Sci Technol 43(24):9216–9222. doi:10.1021/es9015553
7. Greffie C, Bailly L, Milesi J (2002) Supergene alteration of primary ore assemblages from low-sulfidation Au-Ag epithermal deposits at Pongkor, Indonesia, and Nazareno, Peru. Econ Geol Bull Soc 97(3):561–571. doi:10.2113/gsecongeo.97.3.561
8. Warmada IW, Lehmann B, Simandjuntak M (2003) Polymetallic sulfides and sulfosalts of the Pongkor epithermal gold-silver deposit, West Java, Indonesia. Can Mineral 41:185–200. doi:10.2113/gscanmin.41.1.185

9. Leblanc M, Lbouabi M (1988) Native silver mineralization along a rodingite tectonic contact between serpentinite and quartz diorite (Bou-Azzer, Morocco). Econ Geol 83(7):1379–1391. doi:10.2113/gsecongeo.83.7.1379
10. Lu R, Mao JW, Gao JJ, Su HM, Zheng JH (2012) Geological characteristics and occurrence of silver in Xiabao Ag-Pb-Zn deposit, Lengshuikeng ore field, Jiangxi Province, East China. Acta Petrol Sin 28 (1):105–121.
11. Saunders JA, Unger DL, Kamenov GD, Fayek M, Hames WE, Utterback WC (2008) Genesis of middle miocene yellowstone hotspot-related bonanza epithermal Au-Ag deposits, Northern Great Basin, USA. Miner Deposita 43(7):715–734. doi:10.1007/s00126-008-0201-7
12. Deditius AP, Utsunomiya S, Reich M, Kesler SE, Ewing RC, Hough R, Walshe J (2011) Trace metal nanoparticles in pyrite. Ore Geol Rev 42(1):32–46. doi:10.1016/j.oregeorev.2011.03.003
13. Reich M, Palacios C, Barra F, Chryssoulis S (2013) "Invisible" silver in chalcopyrite and bornite from the Mantos Blancos Cu deposit, northern Chile. Eur J Mineral 25(3):453–460. doi:10.1127/0935-1221/2013/0025-2287
14. Reich M, Chryssoulis SL, Deditius A, Palacios C, Zuniga A, Weldt M, Alvear M (2010) "Invisible" silver and gold in supergene digenite (Cu1.8S). Geochim Cosmochim Acta 74(21):6157–6173. doi:10.1016/j.gca.2010.07.026
15. Gomez-Caballero JA, Villasenor-Cabral MG, Santiago-Jacinto P, Ponce-Abad F (2010) Hypogene ba-rich todorokite and associated nanometric native silver in the san miguel tenango mining area, Zacatlan, Puebla, Mexico. Can Mineral 48(5):1237–1253. doi:10.3749/canmin.48.5.1237
16. Qi HW, Hu RZ, Zhang Q (2007) Concentration and distribution of trace elements in lignite from the Shengli coalfield, Inner Mongolia, China: Implications on origin of the associated Wulantuga Germanium Deposit. Int J Coal Geol 71(2–3):129–152. doi:10.1016/j.coal.2006.08.005.
17. Wen LS, Santschi PH, Gill GA, Paternostro CL, Lehman RD (1997) Colloidal and particulate silver in river and estuarine waters of Texas. Environ Sci Technol 31(3):723–731. doi:10.1021/es9603057
18. Akaighe N, MacCuspie RI, Navarro DA, Aga DS, Banerjee S, Sohn M, Sharma VK (2011) Humic acid-induced silver nanoparticle formation under environmentally relevant conditions. Environ Sci Technol 45(9):3895–3901. doi:10.1021/es103946 g
19. Borch T, Kretzschmar R, Kappler A, Van Cappellen P, Ginder-Vogel M, Voegelin A, Campbell K (2010) Biogeochemical redox processes and their impact on contaminant dynamics. Environ Sci Technol 44(1):15–23. doi:10.1021/es9026248
20. Sal'nikov DS, Pogorelova AS, Makarov SV, Vashurina IY (2009) Silver ion reduction with peat fulvic acids. Russ J Appl Chem 82(4):545–548. doi:10.1134/S107042720904003X
21. Adegboyega NF, Sharma VK, Siskova K, Zboril R, Sohn M, Schultz BJ, Banerjee S (2013) Interactions of aqueous Ag^{+} with fulvic acids: mechanisms of silver nanoparticle formation andinvestigation of stability. Environ Sci Technol 47(2):757–764. doi:10.1021/es302305f
22. Mahony JD, Di DM, Shadi TS, Thomas E (1999) A unique sink for silver in sediment. In: the 6th international conference proceedings of transport, fate and effects of silver, Madison, Wisconsin
23. Adegboyega NF, Sharma VK, Siskova KM, Vecerova R, Kolar M, Zboril R, Gardea-Torresdey JL (2014) Enhanced formation of silver nanoparticles in Ag^{+} -NOM-iron(II, III) systems and antibacterial activity studies. Environ Sci Technol 48(6):3228–3235. doi:10.1021/es405641r
24. Jiang J, Kappler A (2008) Kinetics of microbial and chemical reduction of humic substances: implications for electron shuttling. Environ Sci Technol 42(10):3563–3569. doi:10.1021/es7023803
25. Yin YG, Liu JF, Jiang GB (2012) Sunlight-induced reduction of ionic Ag and Au to metallic nanoparticles by dissolved organic matter. ACS Nano 6(9):7910–7919. doi:10.1021/nn302293r
26. Hou WC, Stuart B, Howes R, Zepp RG (2013) Sunlight-driven reduction of silver ions by natural organic matter: formation and transformation of silver nanoparticles. Environ Sci Technol 47(14):7713–7721. doi:10.1021/es400802w

27. Maurer F, Christl I, Hoffmann M, Kretzschmar R (2012) Reduction and reoxidation of humic acid: influence on speciation of cadmium and silver. Environ Sci Technol 46(16):8808–8816. doi:10.1021/es301520s
28. Yin Y, Shen M, Zhou X, Yu S, Chao J, Liu J, Jiang G (2014) Photoreduction and stabilization capability of molecular weight fractionated natural organic matter in transformation of silver ion to metallic nanoparticle. Environ Sci Technol 48(16):9366–9373. doi:10.1021/es502025e.
29. Silver (2014) http://en.wikipedia.org/wiki/Silver. Accessed 21 Oct 2014
30. Graedel TE (1992) Corrosion mechanisms for silver exposed to the atmosphere. J Electrochem Soc 139(7):1963–1970. doi:10.1149/1.2221162.
31. Glover RD, Miller JM, Hutchison JE (2011) Generation of metal nanoparticles from silver and copper objects: nanoparticle dynamics on surfaces and potential sources of nanoparticles in the environment. ACS Nano 5(11):8950–8957. doi:10.1021/nn2031319.
32. Native metal (2014) http://en.wikipedia.org/wiki/Native_metal#Silver. Accessed 21 Oct 2014
33. Mitrano DM, Rimmele E, Wichser A, Erni R, Height M, Nowack B (2014) Presence of nanoparticles in wash water from conventional silver and nano-silver textiles. ACS Nano 8(7):7208–7219. doi:10.1021/nn502228w
34. O'Loughlin EJ, Kelly SD, Kemner KM, Csencsits R, Cook RE (2003) Reduction of Ag(I), Au(III), Cu(II), and Hg(II) by Fe(II)/Fe(III) hydroxysulfate green rust. Chemosphere 53(5):437–446. doi:10.1016/S0045-6535(03)00545-9
35. Ayadi S, Perca C, Legrand L (2013) New one-pot synthesis of Au and Ag nanoparticles using green rust reactive particle as a micro-reactor. Nanoscale Res Lett 8:95. doi:10.1186/1556-276X-8-95
36. Wang TC, Reddy KP, O'Connor C, Fan HJ, Anderson P (1993) Adsorption characteristics of Fe oxide-coated granular activated carbon: implications for silver. Paper presented at the the 1st international conference proceedings of transport, fate and effects of silver, The University of Wisconsin-Madison
37. DL Sedlak AA (1994) Photo-enhanced sorption of silver to bentonite. Paper presented at the 2nd International Conference on the Transport, Fate, and Effects of Silver in the Environment, Madison, WI
38. Konya J, Nagy NM, Foldvari M (2005) The formation and production of nano and micro particles on clays under environmental-like conditions. J Therm Anal Calorim 79(3):537–543. doi:10.1007/s10973-005-0576-y
39. Lawless D, Kapoor S, Kennepohl P, Meisel D, Serpone N (1994) Reduction and aggregation of silver ions at the surface of colloidal silica. J Phys Chem-Us 98(38):9619–9625. doi:10.1021/J100089a042
40. Vinci JC, Bilski P, Kotek R, Chignell C (2010) Controlling the formation of silver nanoparticles on silica by photochemical deposition and other means dagger. Photochem Photobiol 86(4):806–812. doi:10.1111/j.1751-1097.2010.00717.x
41. Weier E (1938) Factors affecting the reduction of silver nitrate by chloroplasts. Am J Bot 25(7):501–507. doi: 10.1149/1.2221162
42. Brown WV, Mollenhauer H, Johnson C (1962) An electron microscope study of silver nitrate reduction in leaf cells. Am J Bot 49(1):57–63. doi:10.2307/2439389
43. Gardea-Torresdey JL, Gomez E, Peralta-Videa JR, Parsons JG, Troiani H, Jose-Yacaman M (2003) Alfalfa sprouts: a natural source for the synthesis of silver nanoparticles. Langmuir 19(4):1357–1361. doi:10.1021/la020835i
44. Haverkamp RG, Marshall AT (2009) The mechanism of metal nanoparticle formation in plants: limits on accumulation. J Nanopart Res 11(6):1453–1463. doi:10.1007/s11051-008-9533-6
45. Beattie IR, Haverkamp RG (2011) Silver and gold nanoparticles in plants: Sites for the reduction to metal. Metallomics 3(6):628–632. doi:10.1039/C1MT00044F
46. Marchiol L, Mattiello A, Poscic F, Giordano C, Musetti R (2014) In vivo synthesis of nanomaterials in plants: location of silver nanoparticles and plant metabolism. Nanoscale Res Lett 9:101. doi:10.1186/1556–276X-9-101
47. Barwal I, Ranjan P, Kateriya S, Yadav SC (2011) Cellular oxido-reductive proteins of *Chlamydomonas reinhardtii* control the biosynthesis of silver nanoparticles. J Nanobiotechnol 9:56. doi:10.1186/1477–3155-9–56

48. Harris AT, Bali R (2008) On the formation and extent of uptake of silver nanoparticles by live plants. J Nanopart Res 10(4):691–695. doi:10.1007/s11051-007-9288-5
49. Leclerc S, Wilkinson KJ (2014) Bioaccumulation of nanosilver by chlamydomonas reinhardtii-nanoparticle or the free Ion? Environ Sci Technol 48 (1):358–364. doi:10.1021/es404037z
50. Merin DD, Prakash S, Bhimba BV (2010) Antibacterial screening of silver nanoparticles synthesized by marine micro algae. Asian Pac J Trop Med 3(10):797–799. doi:10.1016/S1995-7645(10)60191-5
51. Beveridge TJ, Murray RGE (1976) Uptake and retention of metals by cell-walls of *Bacillus subtilis*. J Bacteriol 127(3):1502–1518.
52. Beveridge TJ, Murray RGE (1980) Sites of metal-deposition in the cell-wall of *Bacillus subtilis*. J Bacteriol 141(2):876–887.
53. Klaus T, Joerger R, Olsson E, Granqvist CG (1999) Silver-based crystalline nanoparticles, microbially fabricated. Proc Natl Acad Sci U S A 96(24):13611–13614. doi:10.1073/pnas.96.24.13611
54. Weisener CG, Babechuk MG, Fryer BJ, Maunder C (2008) Microbial dissolution of silver jarosite: examining its trace metal behaviour in reduced environments. Geomicrobiol J 25(7–8):415–424. doi:10.1080/01490450802403073
55. Mukherjee P, Roy M, Mandal BP, Dey GK, Mukherjee PK, Ghatak J, Tyagi AK, Kale SP (2008) Green synthesis of highly stabilized nanocrystalline silver particles by a non-pathogenic and agriculturally important fungus *T. asperellum*. Nanotechnology 19(7):075103. doi:10.1088/0957-4484/19/7/075103
56. Sintubin L, De Windt W, Dick J, Mast J, van der Ha D, Verstraete W, Boon N (2009) Lactic acid bacteria as reducing and capping agent for the fast and efficient production of silver nanoparticles. Appl Microbiol Biotechnol 84(4):741–749. doi:10.1007/s00253-009-2032-6
57. Lin ZY, Zhou CH, Wu JM, Zhou JZ, Wang L (2005) A further insight into the mechanism of Ag^+ biosorption by *Lactobacillus* sp. strain A09. Spectrochim Acta A Mol Biomol Spectrosc 61(6):1195–1200. doi:10.1016/j.saa.2004.06.041
58. Kang FX, Alvarez PJ, Zhu DQ (2014) Microbial extracellular polymeric substances reduce Ag^+ to silver nanoparticles and antagonize bactericidal activity. Environ Sci Technol 48(1):316–322. doi:10.1021/Es403796x
59. Mukherjee P, Ahmad A, Mandal D, Senapati S, Sainkar SR, Khan MI, Parishcha R, Ajaykumar PV, Alam M, Kumar R, Sastry M (2001) Fungus-mediated synthesis of silver nanoparticles and their immobilization in the mycelial matrix: a novel biological approach to nanoparticle synthesis. Nano Lett 1(10):515–519. doi:10.1021/Nl0155274
60. Nelson Durán PDM Oswaldo L Alves Gabriel IH De Souza Elisa Esposito (2005) Mechanistic aspects of biosynthesis of silver nanoparticles by several Fusarium oxysporum strains. J Nanobiotechnol 3:8. doi:10.1186/1477-3155-3-8
61. Shahverdi AR, Minaeian S, Shahverdi HR, Jamalifar H, Nohi AA (2007) Rapid synthesis of silver nanoparticles using culture supernatants of enterobacteria: a novel biological approach. Process Biochem 42(5):919–923. doi:10.1016/j.procbio.2007.02.005
62. Kumar SA, Abyaneh MK, Gosavi SW, Kulkarni SK, Pasricha R, Ahmad A, Khan MI (2007) Nitrate reductase-mediated synthesis of silver nanoparticles from $AgNO_3$. Biotechnol Lett 29(3):439–445. doi:10.1007/s10529-006-9256-7
63. Vaidyanathan R, Gopalram S, Kalishwaralal K, Deepak V, Pandian SRK, Gurunathan S (2010) Enhanced silver nanoparticle synthesis by optimization of nitrate reductase activity. Colloid Surf B Biointerfaces 75(1):335–341. doi:10.1016/j.colsurfb.2009.09.006
64. Diaz JM, Hansel CM, Voelker BM, Mendes CM, Andeer PF, Zhang T (2013) Widespread production of extracellular superoxide by heterotrophic bacteria. Science 340(6137):1223–1226. doi:10.1126/science.1237331
65. Rose AL (2012) The influence of extracellular superoxide on iron redox chemistry and bioavailability to aquatic microorganisms. Front Microbiol 3:124. doi:10.3389/fmicb.2012.00124
66. Learman DR, Voelker BM, Vazquez-Rodriguez AI, Hansel CM (2011) Formation of manganese oxides by bacterially generated superoxide. Nat Geosci 4(2):95–98. doi:10.1038/NGEO1055

67. Hansel CM, Zeiner CA, Santelli CM, Webb SM (2012) Mn(II) oxidation by an ascomycete fungus is linked to superoxide production during asexual reproduction. Proc Natl Acad Sci U S A 109(31):12621–12625. doi:10.1073/pnas.1203885109
68. Li HP, Daniel B, Creeley D, Grandbois R, Zhang SJ, Xu C, Ho YF, Schwehr KA, Kaplan DI, Santschi PH, Hansel CM, Yeager CM (2014) Superoxide production by a manganese-oxidizing bacterium facilitates iodide oxidation. Appl Environ Microbiol 80(9):2693–2699. doi:10.1128/AEM.00400-14
69. Jones AM, Garg S, He D, Pham AN, Waite TD (2011) Superoxide-mediated formation and charging of silver nanoparticles. Environ Sci Technol 45(4):1428–1434. doi:10.1021/es103757c
70. Gautam S, Dubey P, Gupta MN (2013) A facile and green ultrasonic-assisted synthesis of BSA conjugated silver nanoparticles. Colloid Surf B Biointerfaces 102:879–883. doi:10.1016/j.colsurfb.2012.10.007
71. Lee KJ, Park SH, Govarthanan M, Hwang PH, Seo YS, Cho M, Lee WH, Lee JY, Kamala-Kannan S, Oh BT (2013) Synthesis of silver nanoparticles using cow milk and their antifungal activity against phytopathogens. Mater Lett 105:128–131. doi:10.1016/j.matlet.2013.04.076
72. Juganson K, Mortimer M, Kasemets K, Kahru A (2012) Tetrahymena thermophila converts toxic silver ions to less toxic silver nanoparticles. Toxicol Lett 211:S206–S206. doi:10.1016/j.toxlet.2012.03.737
73. El-Said WA, Cho HY, Yea CH, Choi JW (2014) Synthesis of metal nanoparticles inside living human cells based on the intracellular formation process. Adv Mater 26(6):910–918. doi:10.1002/adma.201303699
74. Kannan N, Mukunthan KS, Balaji S (2011) A comparative study of morphology, reactivity and stability of synthesized silver nanoparticles using *Bacillus subtilis* and *Catharanthus roseus* (L.) G. Don. Colloid Surf B Biointerfaces 86(2):378–383. doi:10.1016/j.colsurfb.2011.04.024
75. Oves M, Khan MS, Zaidi A, Ahmed AS, Ahmed F, Ahmad E, Sherwani A, Owais M, Azam A (2013) Antibacterial and cytotoxic efficacy of extracellular silver nanoparticles biofabricated from chromium reducing novel OS4 strain of *Stenotrophomonas maltophilia*. PLoS One 8(3):e59140. doi:10.1371/journal.pone.0059140
76. Zaki S, El Kady MF, Abd-El-Haleem D (2011) Biosynthesis and structural characterization of silver nanoparticles from bacterial isolates. Mater Res Bull 46(10):1571–1576. doi:10.1016/j.materresbull.2011.06.025
77. Malhotra A, Dolma K, Kaur N, Rathore YS, Ashish, Mayilraj S, Choudhury AR (2013) Biosynthesis of gold and silver nanoparticles using a novel marine strain of *Stenotrophomonas*. Bioresour Technol 142:727–731. doi:10.1016/j.biortech.2013.05.109
78. Kalishwaralal K, Deepak V, Pandian SRK, Kottaisamy M, BarathManiKanth S, Kartikeyan B, Gurunathan S (2010) Biosynthesis of silver and gold nanoparticles using *Brevibacterium casei*. Colloid Surf B Biointerfaces 77(2):257–262. doi:10.1016/j.colsurfb.2010.02.007
79. Kalimuthu K, Babu RS, Venkataraman D, Bilal M, Gurunathan S (2008) Biosynthesis of silver nanocrystals by *Bacillus licheniformis*. Colloid Surf B Biointerfaces 65(1):150–153. doi:10.1016/j.colsurfb.2008.02.018
80. Nanda A, Saravanan M (2009) Biosynthesis of silver nanoparticles from *Staphylococcus aureus* and its antimicrobial activity against MRSA and MRSE. Nanomed-Nanotechnol 5(4):452–456. doi:10.1016/j.nano.2009.01.012
81. Banu AN, Balasubramanian C, Moorthi PV (2014) Biosynthesis of silver nanoparticles using *Bacillus thuringiensis* against dengue vector, *Aedes aegypti* (Diptera: Culicidae). Parasitol Res 113(1):311–316. doi:10.1007/s00436-013-3656-0
82. Chaudhari PR, Masurkar SA, Shidore VB, Kamble SP (2012) Effect of biosynthesized silver nanoparticles on *staphylococcus aureus* biofilm quenching and prevention of biofilm formation. Nano-Micro Lett 4(1):34–39. doi:10.3786/nml.v4i1.p34–39
83. Shivaji S, Madhu S, Singh S (2011) Extracellular synthesis of antibacterial silver nanoparticles using psychrophilic bacteria. Process Biochem 46(9):1800–1807. doi:10.1016/j.procbio.2011.06.008

84. Korbekandi H, Iravani S, Abbasi S (2012) Optimization of biological synthesis of silver nanoparticles using *Lactobacillus casei* subsp *casei*. J Chem Technol Biotechnol 87(7):932–937. doi:10.1002/Jctb.3702
85. Babu MMG, Gunasekaran R (2009) Production and structural characterization of crystalline silver nanoparticles from *Bacillus cereus* isolate. Colloid Surf B Biointerfaces 74(1):191–195. doi:10.1016/j.colsurfb.2009.07.016
86. Saravanan M, Vemu AK, Bank SK (2011) Rapid biosynthesis of silver nanoparticles from *Bacillus megaterium* (NCIM 2326) and their antibacterial activity on multi drug resistant clinical pathogens. Colloid Surf B 88(1):325–331. doi:10.1016/j.colsurfb.2011.07.009
87. Suresh AK, Pelletier DA, Wang W, Moon JW, Gu BH, Mortensen NP, Allison DP, Joy DC, Phelps TJ, Doktycz MJ (2010) Silver nanocrystallites: Biofabrication using *shewanella oneidensis*, and an evaluation of their comparative toxicity on gram-negative and gram-positive bacteria. Environ Sci Technol 44(13):5210–5215. doi:10.1021/es903684r
88. Kalpana D, Lee YS (2013) Synthesis and characterization of bactericidal silver nanoparticles using cultural filtrate of simulated microgravity grown *Klebsiella pneumoniae*. Enzyme Microb Technol 52(3):151–156. doi:10.1016/j.enzmictec.2012.12.006
89. Srivastava P, Braganca J, Ramanan SR, Kowshik M (2013) Synthesis of silver nanoparticles using haloarchaeal isolate *Halococcus salifodinae* BK3. Extremophiles 17(5):821–831. doi:10.1007/s00792-013-0563-3
90. Zaki S, Etarahony M, Elkady M, Abd-El-Haleem D (2014) The use of bioflocculant and bioflocculant-producing bacillus mojavensis strain 32A to synthesize silver nanoparticles. J Nanomater:431089. doi:10.1155/2014/431089
91. Sneha K, Sathishkumar M, Mao J, Kwak IS, Yun YS (2010) Corynebacterium glutamicum-mediated crystallization of silver ions through sorption and reduction processes. Chem Eng J 162(3):989–996. doi:10.1016/j.cej.2010.07.006
92. Bawaskar M, Gaikwad S, Ingle A, Rathod D, Gade A, Duran N, Marcato PD, Rai M (2010) A new report on mycosynthesis of silver nanoparticles by *Fusarium culmorum*. Curr Nanosci 6(4):376–380. doi:10.2174/157341310791658919
93. Fayaz AM, Balaji K, Girilal M, Yadav R, Kalaichelvan PT, Venketesan R (2010) Biogenic synthesis of silver nanoparticles and their synergistic effect with antibiotics: a study against gram-positive and gram-negative bacteria. Nanomed-Nanotechnol 6(1):103–109. doi:10.1016/j.nano.2009.04.006
94. Vigneshwaran N, Ashtaputre NM, Varadarajan PV, Nachane RP, Paralikar KM, Balasubramanya RH (2007) Biological synthesis of silver nanoparticles using the fungus *Aspergillus flavus*. Mater Lett 61(6):1413–1418. doi:10.1016/j.matlet.2006.07.042
95. Syed A, Saraswati S, Kundu GC, Ahmad A (2013) Biological synthesis of silver nanoparticles using the fungus *Humicola* sp. and evaluation of their cytoxicity using normal and cancer cell lines. Spectrochim Acta A Mol Biomol Spectrosc 114:144–147. doi:10.1016/j.saa.2013.05.030
96. Verma VC, Kharwar RN, Gange AC (2010) Biosynthesis of antimicrobial silver nanoparticles by the endophytic fungus *Aspergillus clavatus*. Nanomedicine-UK 5(1):33–40. doi:10.2217/Nnm.09.77
97. Huang WD, Yan JJ, Wang Y, Hou CL, Dai TC, Wang ZM (2013) Biosynthesis of Silver Nanoparticles by *Septoria apii* and *Trichoderma koningii*. Chin J Chem 31(4):529–533. doi:10.1002/cjoc.201201138
98. Vigneshwaran N, Kathe AA, Varadarajan PV, Nachane RP, Balasubramanya RH (2006) Biomimetics of silver nanoparticles by white rot fungus, *Phaenerochaete chrysosporium*. Colloid Surf B Biointerfaces 53(1):55–59. doi:10.1016/j.colsurfb.2006.07.014
99. Mourato A, Gadanho M, Lino AR, Tenreiro R (2011) Biosynthesis of crystalline silver and gold nanoparticles by extremophilic yeasts. Bioinorg Chem Appl. 2011:546074 doi:10.1155/2011/546074
100. Jebali A, Ramezani F, Kazemi B (2011) Biosynthesis of silver nanoparticles by *Geotricum* sp. J Clust Sci 22(2):225–232. doi:10.1007/s10876-011-0375-5
101. Qian YQ, Yu HM, He D, Yang H, Wang WT, Wan X, Wang L (2013) Biosynthesis of silver nanoparticles by the endophytic fungus *Epicoccum nigrum* and their activity against pathogenic fungi. Bioprocess Biosyst Eng 36(11):1613–1619. doi:10.1007/s00449-013-0937-z

102. Castro-Longoria E, Vilchis-Nestor AR, Avalos-Borja M (2011) Biosynthesis of silver, gold and bimetallic nanoparticles using the filamentous fungus *Neurospora crassa*. Colloid Surface B Biointerfaces 83(1):42–48. doi:10.1016/j.colsurfb.2010.10.035
103. Prakasham RS, Kumar BS, Kumar YS, Shankar GG (2012) Characterization of silver nanoparticles dynthesized by using marine isolate streptomyces albidoflavus. J Microbiol Biotechnol 22(5):614–621. doi:10.4014/jmb.1107.07013
104. Balaji DS, Basavaraja S, Deshpande R, Mahesh DB, Prabhakar BK, Venkataraman A (2009) Extracellular biosynthesis of functionalized silver nanoparticles by strains of *Cladosporium cladosporioides* fungus. Colloid Surf B Biointerfaces 68(1):88–92. doi:10.1016/j.colsurfb.2008.09.022
105. Hamedi S, Shojaosadati S, Shokrollahzadeh S, Hashemi-Najafabadi S (2014) Extracellular biosynthesis of silver nanoparticles using a novel and non-pathogenic fungus, *Neurospora intermedia*: controlled synthesis and antibacterial activity. World J Microbiol Biotechnol 30(2):693–704. doi:10.1007/s11274-013-1417-y
106. Bfilainsa KC, D'Souza SF (2006) Extracellular biosynthesis of silver nanoparticles using the fungus *Aspergillus fumigatus*. Colloid Surf B Biointerfaces 47(2):160–164. doi:10.1016/j.colsurfb.2005.11.026
107. Ahmad A, Mukherjee P, Senapati S, Mandal D, Khan MI, Kumar R, Sastry M (2003) Extracellular biosynthesis of silver nanoparticles using the fungus *Fusarium oxysporum*. Colloid Surf B Biointerfaces 28(4):313–318. doi:10.1016/S0927-7765(02)00174-1
108. Basavaraja S, Balaji SD, Lagashetty A, Rajasab AH, Venkataraman A (2008) Extracellular biosynthesis of silver nanoparticles using the fungus *Fusarium semitectum*. Mater Res Bull 43(5):1164–1170. doi:10.1016/j.materresbull.2007.06.020
109. Narayanan KB, Park HH, Sakthivel N (2013) Extracellular synthesis of mycogenic silver nanoparticles by Cylind*rocladium floridanum* and its homogeneous catalytic degradation of 4-nitrophenol. Spectrochim Acta A Mol Biomol Spectrosc 116:485–490. doi:10.1016/j.saa.2013.07.066
110. Saravanana M, Nanda A (2010) Extracellular synthesis of silver bionanoparticles from *Aspergillus clavatus* and its antimicrobial activity against MRSA and MRSE. Colloid Surf B Biointerfaces 77(2):214–218. doi:10.1016/j.colsurfb.2010.01.026
111. Fayaz AM, Balaji K, Kalaichelvan PT, Venkatesan R (2009) Fungal based synthesis of silver nanoparticles-An effect of temperature on the size of particles. Colloid Surf B Biointerfaces 74(1):123–126. doi:10.1016/j.colsurfb.2009.07.002
112. Li GQ, He D, Qian YQ, Guan BY, Gao S, Cui Y, Yokoyama K, Wang L (2012) Fungus-mediated green synthesis of silver nanoparticles using *Aspergillus terreus*. Int J Mol Sci 13(1):466–476. doi:10.3390/Ijms13010466
113. Gajbhiye M, Kesharwani J, Ingle A, Gade A, Rai M (2009) Fungus-mediated synthesis of silver nanoparticles and their activity against pathogenic fungi in combination with fluconazole. Nanomedicine-Nanotechnol 5(4):382–386. doi:10.1016/j.nano.2009.06.005
114. Nayak RR, Pradhan N, Behera D, Pradhan KM, Mishra S, Sukla LB, Mishra BK (2011) Green synthesis of silver nanoparticle by *Penicillium purpurogenum* NPMF: the process and optimization. J Nanoparticle Res 13(8):3129–3137. doi:10.1007/s11051-010-0208-08
115. Salunkhe RB, Patil SV, Patil CD, Salunke BK (2011) Larvicidal potential of silver nanoparticles synthesized using fungus *Cochliobolus lunatus* against *Aedes aegypti* (Linnaeus, 1762) and *Anopheles stephensi* Liston (Diptera; Culicidae). Parasitol Res 109(3):823–831. doi:10.1007/s00436-011-2328-1
116. Binupriya AR, Sathishkumar M, Yun SI (2010) Myco-crystallization of silver ions to nanosized particles by live and dead cell filtrates of *Aspergillus oryzae* var. viridis and its bactericidal activity toward *Staphylococcus* aureus KCCM 12256. Ind Eng Chem Res 49(2):852–858. doi:10.1021/Ie9014183
117. Kumar RR, Priyadharsani KP, Thamaraiselvi K (2012) Mycogenic synthesis of silver nanoparticles by the Japanese environmental isolate *Aspergillus tamarii*. J Nanoparticle Res 14(5):860. doi:10.1007/S11051-012-0860-2
118. Kirthi AV, Rahuman AA, Jayaseelan C, Karthik L, Marimuthu S, Santhoshkumar T, Venkatesan J, Kim SK, Kumar G, Kumar SRS, Rao KVB (2012) Novel approach to synthesis silver nanoparticles using plant pathogenic fungi, *Puccinia graminis*. Mater Lett 81:69–72. doi:10.1016/j.matlet.2012.04.103

119. Birla SS, Gaikwad SC, Gade AK, Rai MK (2013) Rapid synthesis of silver nanoparticles from *Fusarium oxysporum* by optimizing physicocultural conditions. Sci World J 2013:796018. doi:10.1155/2013/796018
120. Gaikwad SC, Birla SS, Ingle AP, Gade AK, Marcato PD, Rai M, Duran N (2013) Screening of different *Fusarium* species to select potential species for the synthesis of silver nanoparticles. J Brazil Chem Soc 24(12):1974–1982. doi:10.5935/0103-5053.20130247
121. Karthik L, Kumar G, Kirthi AV, Rahuman AA, Rao KVB (2014) *Streptomyces* sp. LK3 mediated synthesis of silver nanoparticles and its biomedical application. Bioprocess Biosyst Eng 37(2):261–267. doi:10.1007/s00449-013-0994-3
122. Salunkhe RB, Patil SV, Salunke BK, Patil CD, Sonawane AM (2011) Studies on silver accumulation and nanoparticle synthesis by *Cochliobolus lunatus*. Appl Biochem Biotechnol 165(1):221–234. doi:10.1007/s12010-011-9245-8
123. Kathiresan K, Manivannan S, Nabeel MA, Dhivya B (2009) Studies on silver nanoparticles synthesized by a marine fungus, *Penicillium fellutanum* isolated from coastal mangrove sediment. Colloid Surf B Biointerfaces 71(1):133–137. doi:10.1016/j.colsurfb.2009.01.016
124. Manivasagan P, Venkatesan J, Senthilkumar K, Sivakumar K, Kim SK (2013) Biosynthesis, antimicrobial and cytotoxic effect of silver nanoparticles using a novel *Nocardiopsis* sp. MBRC-1. Biomed Res Int 2013:287638. doi:10.1155/2013/287638
125. El-Naggar NE, Abdelwahed NAM, Darwesh OMM (2014) Fabrication of biogenic antimicrobial silver nanoparticles by *Streptomyces aegyptia* NEAE 102 as eco-friendly nanofactory. J Microbiol Biotechnol 24(4):453–464. doi:10.4014/jmb.1310.10095
126. Prakasham RS, Kumar BS, Kumar YS, Kumar KP (2014) Production and characterization of protein encapsulated silver nanoparticles by marine isolate *Streptomyces parvulus* SSNP11. Indian J Microbiol 54(3):329–336. doi:10.1007/s12088-014-0452-1
127. Mueller NC, Nowack B (2008) Exposure modeling of engineered nanoparticles in the environment. Environ Sci Technol 42(12):4447–4453. doi:10.1021/es7029637
128. Agency USEP (2012) U. S. Nanomaterial case study: nanoscale silver in disinfectant spray (Final report). Washington, DC
129. Yu SJ, Yin YG, Liu JF (2013) Silver nanoparticles in the environment. Environ Sci-Process Impacts 15(1):78–92. doi:10.1039/C2EM30595J
130. Kaegi R, Sinnet B, Zuleeg S, Hagendorfer H, Mueller E, Vonbank R, Boller M, Burkhardt M (2010) Release of silver nanoparticles from outdoor facades. Environ Pollut 158(9):2900–2905. doi:10.1016/j.envpol.2010.06.009
131. Blaser SA, Scheringer M, MacLeod M, Hungerbuhler K (2008) Estimation of cumulative aquatic exposure and risk due to silver: Contribution of nano-functionalized plastics and textiles. Sci Total Environ 390(2–3):396–409. doi:10.1016/j.scitotenv.2007.10.010
132. Benn TM, Westerhoff P (2008) Nanoparticle silver released into water from commercially available sock fabrics. Environ Sci Technol 42(11):4133–4139. doi:10.1021/es7032718
133. Geranio L, Heuberger M, Nowack B (2009) The behavior of silver nanotextiles during washing. Environ Sci Technol 43(21):8113–8118. doi: 10.1021/es9018332
134. Lorenz C, Windler L, von Goetz N, Lehmann RP, Schuppler M, Hungerbuhler K, Heuberger M, Nowack B (2012) Characterization of silver release from commercially available functional (nano)textiles. Chemosphere 89(7):817–824. doi:10.1016/j.chemosphere.2012.04.063
135. Kulthong K, Srisung S, Boonpavanitchakul K, Kangwansupamonkon W, Maniratanachote R (2010) Determination of silver nanoparticle release from antibacterial fabrics into artificial sweat. Part Fibre Toxicol 7:8. doi:10.1186/1743-8977-7-8
136. Farkas J, Peter H, Christian P, Urrea JAG, Hassellov M, Tuoriniemi J, Gustafsson S, Olsson E, Hylland K, Thomas KV (2011) Characterization of the effluent from a nanosilver producing washing machine. Environ Int 37(6):1057–1062. doi:10.1016/j.envint.2011.03.006
137. Cleveland D, Long SE, Pennington PL, Cooper E, Fulton MH, Scott GI, Brewer T, Davis J, Petersen EJ, Wood L (2012) Pilot estuarine mesocosm study on the environmental fate of silver nanomaterials leached from consumer products. Sci Total Environ 421:267–272. doi:10.1016/j.scitotenv.2012.01.025

Chapter 4
Fate and Transport of Silver Nanoparticles in the Environment

Yongguang Yin, Sujuan Yu, Mohai Shen, Jingfu Liu and Guibin Jiang

Abstract Anthropogenic and naturally occurring silver nanoparticles (AgNPs), once released or formed in the environment, could transport, distribute, and transform in various environmental environment, which have great impacts on not only their fate but also their uptake and toxicity in the environments. In this chapter, we introduce recent model and experimental studies on the transport and distribution of AgNPs in air, aquatic, and terrestrial systems, and discuss the transformation of AgNPs in the environment including change of coating, aggregation, sedimentation, dissolution and re-reduction, sulfidation and chlorination. These studies highlight that AgNPs are highly dynamic in physical and chemical species in the environment, owning to the distinguished chemical properties of AgNPs from other nanoparticles. Additionally, the knowledge gaps in fate and transport of AgNPs and recommendations for future research are also discussed.

4.1 Introduction

As discussed in the last chapter, intentionally or unintentionally produced anthropogenic silver nanoparticles (AgNPs) could be released into the environment through various pathways. Naturally occurring AgNPs are also present in the environment. These anthropogenic or naturally occurring AgNPs could further transport and distribute in different environmental compartments, depending on the properties of

J. Liu (✉) · Y. Yin · S. Yu · M. Shen · G. Jiang
State Key Laboratory of Environmental Chemistry and Ecotoxicology, Research Center for Eco-Environmental Sciences, Chinese Academy of Sciences, P.O. Box 2871, 100085 Beijing, China
e-mail: jfliu@rcees.ac.cn

Y. Yin
e-mail: ygyin@rcees.ac.cn

S. Yu
e-mail: sjyu@rcees.ac.cn

G. Jiang
e-mail: gbjiang@rcees.ac.cn

J. Liu, G. Jiang (eds.), *Silver Nanoparticles in the Environment,*
DOI 10.1007/978-3-662-46070-2_4

AgNPs themselves and the surrounding environment, while the inevitable physical and chemical transformation of AgNPs could also have great impacts on the fate, transport, bioavailability, and toxicity of AgNPs.

In this chapter, we focus on the transport and distribution of AgNPs in air, aquatic, and terrestrial systems, and the physical and chemical transformation of AgNPs including aggregation, sulfidation, and chlorination.

4.2 Transport and Distribution of AgNPs

Although there are many reports on the aggregation and chemical transformation of AgNPs in the environment, the fate of AgNPs in the environment is still largely unknown. There are still many knowledge gaps on the production, application, releasing, and the physical and chemical transformation of AgNPs in different environmental compartments, which largely limit our understanding on the transport and distribution of AgNPs in the environment [1]. Westerhoff et al. recently suggested describing and modeling the fate of nanoparticles (NPs) by parameterizing the environmental processes of NPs using descriptors like solvent exchange, surface affinity, sorption, sediment retention, self-aggregation, and dissolution kinetics [2]. Although there is still much unknown for these descriptors of AgNPs, several studies have intended to predict the concentration distribution of AgNPs in surface waters, wastewater treatment plant (WWTP) effluents, biosolids, sediments, soils, and air. Gottschalk et al. recently summarized the predicted environmental concentrations (PECs) for AgNPs in different compartments by modeling [3]. The PECs for AgNPs were in the ranges of 0.008 ng L^{-1} [4] ~ 619 ng L^{-1} [5] (surface waters), 0.020 μg L^{-1} [6] ~ 6.54 μg L^{-1} [7] (wastewater treatment plant effluents), 1.6 μg kg^{-1} [6] ~ 6.24 mg kg^{-1} [8] (biosolids), 153-10184 Δng kg^{-1} $year^{-1}$ [8] (sediments), 5.33×10^{-6} μg kg^{-1} [5] ~ 4.091 μg kg^{-1} [8] (soils and soil treated with biosolids), and 0.002 ng m^{-3} [8] ~ 4.4 ng m^{-3} [9] (air), respectively, according to different models and releasing scenarios.

The following briefly introduced the experimental studies on the transport and distribution of AgNPs in air, aquatic, and terrestrial systems.

4.2.1 Air

Although it was shown that the prolonged inhalation exposure to AgNPs could induce adverse health effects [10], the occurrence and transport of AgNPs in air or atmosphere has long been overlooked [11]. The aerosolized AgNPs could be released into the air from the production, use, and disposal of AgNP-containing consumer products, as shown in Fig. 4.1. In the production of AgNPs, both liquid-phase [12] and gas-phase [11] processes could emit aerosolized AgNPs, including spray atomization, liquid-flame spray, thermal evaporation–condensation, chemical vaporization, dry powder dispersion, etc. The AgNP exposure concentrations in air of manufacturing sites could be as high as 0.46 mg/m^3 (for 1 min sampling) [13].

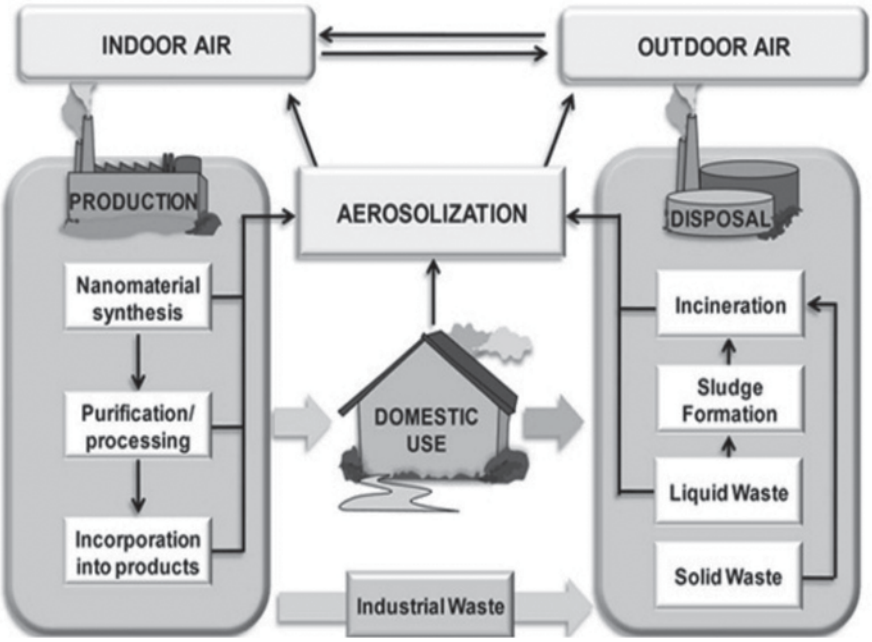

Fig. 4.1 Possible aerosolization routes for AgNPs during the life cycle of consumer products. (Reprinted from ref. [11] with the permission of the Air & Waste Management Association)

The point source emissions of AgNPs in the manufacturing sites could also enhance the concentration of Ag in the atmosphere, and the spatial distribution revealed an increase of the Ag concentrations in moss as a function of decreasing distance from the AgNP manufacturer [14]. Besides production of AgNPs or its products, during the use of commercial products containing AgNPs, it is also estimated that ~14% of AgNP products could potentially release AgNPs into air through spraying, dry powder dispersion, or other unknown pathway [11]. In the use of liquid cleaning products [15] or personal care sprays [16, 17], AgNPs could be emitted into the air intentionally or unintentionally. The release of AgNPs is highly dependent on the sprayed amount [18] and the generated aerosol droplet size distribution [16]. In a study, the emitted Ag in aerosols per spray action from three AgNP products were measured as 0.24–56 ng, and exposure modeling suggested that up to 70 ng of Ag may deposit in the respiratory tract during product use [17]. During and after the spray process, AgNPs grow in size and change morphology, which facilitates the deposition of AgNPs [12, 16]. It was observed that 3 min after spray (1 s), the particle number concentration decreased to ~1/3 of the level achieved directly after spraying [16]. In addition, in the disposal of industrial and consumer waste containing AgNPs, aerosolization and atmospheric emission of AgNPs could happen possibly, especially during municipal or industrial waste incineration and aeration treatment of liquid waste, in which the aerosolized particles may consist of pure AgNPs or inorganic silver salts [11].

4.2.2 Aquatic Systems

4.2.2.1 Natural Water

Lowry et al. spiked polyvinylpyrrolidone (PVP)-AgNPs into water column (16.6 mg/L) of freshwater mesocosms simulating an emergent wetland environment and investigated the fate and transport of AgNPs for 18 months dosing [19]. In the first 8 days, the rapid decreasing of total Ag concentration (to< 1 mg/L) in the water column was observed, demonstrating the rapid aggregation and sedimentation of AgNPs from the water column. The concentration of total Ag in water column after 18 months dosing was further decreased to below the detection limit (<2 μg/L). Accordingly, transport of AgNPs was observed from the water column to the upper layer of surficial sediment (0–1 cm), terrestrial soil, plant biomass, and living fish and insects in the mesocosms. After 18 months dosing, the estimated distribution of mass of Ag in different compartments were water column (<0.05%), terrestrial soil (7%), subaquatic sediment (60%), and plants (0.2%). AgNPs in the subaquatic sediment were mainly transformed to Ag_2S (~55%) and Ag-sulfhydryl compounds (~27%), but ~18% of the original Ag^0 character still remained after aging. Due to the occurrence of Ag in the plant biomass and living fish and insects in the mesocosms, it was suggested that Ag from AgNPs remained bioavailable even after partial sulfidation and when water column total Ag concentrations were low (<2 μg/L). Another study focused on the aggregation and dissolution behavior of gum arabic (GA)-AgNPs and PVP-AgNPs in aquatic microcosms [20, 21]. The results showed that plants-derived dissolved organic matter (DOM) could stabilize PVP-AgNPs as primary particles, but cause GA-AgNPs to be removed from the water column, likely due to dissolution of GA-AgNPs and binding of released Ag^+ on sediment and plant surfaces. Additionally, the presence of plants in the microcosms reduced the concentration of Ag in the water column. These results highlighted the importance of AgNP coating and plant on the fate and transport of AgNPs in natural waters.

4.2.2.2 Wastewater

The fate and transport of AgNPs in wastewater sewer and (WWTPs) has been investigated in recent years. Kaegi et al. [22] spiked Tween-AgNPs (<30 nm) into a 5 km long main trunk sewer and collected 40 wastewater samples after 500, 2400, and 5000 m each according to the expected travel times of AgNPs. Excellent mass recovery of the Ag indicated an efficient transport of AgNPs without substantial losses to the sewer biofilm. The batch incubation of PVP-AgNPs with raw wastewater showed that ~15% AgNPs was sulfidized to Ag_2S after 5 h reaction time. Therefore, AgNPs discharged to the wastewater stream become partially sulfidized in the sewer system and are efficiently transported to the WWTPs. In WWTPs, polyoxyethylene fatty acid ester-AgNPs could adsorb onto wastewater biosolids, both in the sludge and in the effluent, which enhance their transport from wastewa-

ter to sludge [23]. Thus, freely dispersed nanoscale Ag particles were only observed in the effluent during the initial pulse spike. The sulfidation of AgNPs was observed in the nonaerated tank and X-ray absorption spectroscopy (XAS) measurements indicated that most Ag in the sludge and effluent was present as Ag_2S. Recently, another study showed that silver containing nanoparticles could be effectively removed (95%) from the influent by mechanical and biological treatment in typical WWTPs in Germany [24]. These combined results suggested that although in the sewer system AgNPs could be efficiently transported to the WWTPs, AgNPs were finally transferred into sludge as inert Ag_2S.

4.2.3 Terrestrial Systems

4.2.3.1 Soil

AgNPs could be applied deliberately for soil system (i.e., as plant strengthening agent [18]) or released unintentionally through various other pathways to soil (i.e., slag from incinerator [25] and sludge from sewage treatment plant [26, 27]). Considering the complexity of the soil system, our understanding of the transport and distribution of AgNPs in soils is still very limited [28].

Porous medium was usually used to simulate the transport of AgNPs in soils and groundwater aquifers and sand filters. The reported porous medium for AgNP transport included unmodified silica glass beads [29–31], silica glass beads modified with hematite [29], quartz sand [32–34], ferrihydrite-coated sand [33], kaolin-coated sand [33], porous sandstones [35], and ceramics [36]. The deposition or mobility of AgNPs in porous medium is controlled by the following factors: (1) Coating of AgNPs [33]: as compared to the electrostatically stabilized uncoated H_2-AgNPs and citrate (Cit)-AgNPs, the breakthrough of PVP-AgNPs occurred more rapidly in quartz sand. The electrosterically stabilized branched polyethyleneimine (BPEI) coated AgNPs were readily mobile in quartz sand, ferrihydrite-coated sand and kaolin-coated sand. This result highlights the importance of electrostatic coating in stabilization and mobility of AgNPs. (2) Properties of porous medium: The deposition of the H_2-AgNPs, Cit-AgNPs, and PVP-AgNPs followed the order of kaolin-coated sand > ferrihydrite-coated sand > quartz sand [33]. These different porous mediums have distinguishing ζ potential, and thus the interactions of the surface of porous mediums and AgNPs are much different for quartz sand, ferrihydrite-coated sand, and kaolin-coated sand. (3) pH: at fixed ionic strength, retention of PVP-AgNPs by the glass beads increased with pH increased from 4 to 6.5, while further increase in pH to 9 and 11 decreased the retention of PVP-AgNPs [31]. This result is consistent with the variation of ζ potential of AgNPs at different pH. (4) Electrolytes: Both the deposition rate coefficients and attachment efficiencies of PVP-AgNPs increased with the increasing of concentration of $NaNO_3$ from 1 to 300 mmol/L [30]. Similarly, the retention of Cit-AgNPs with 10, 50, and 100 nm diameter increased with increasing ionic strength of $MgSO_4$ in

ceramic disks [36]. The ionic strength-enhanced retention of AgNPs can be ascribed to the following two reasons: First, ionic strength-induced aggregation of AgNPs could increase physical filtration of AgNPs clusters in the porous mediums; second, the ionic strength also decreases the repulsive forces between AgNPs and the surface of the porous mediums [36]. (5) Natural organic matter (NOM) [30]: Suwannee River humic acid (SRHA), representing high molecular weight polymers, decreased the deposition of PVP-AgNPs in glass beads medium, consistent with enhanced electrosteric stabilization by the humic acid (HA). Cysteine, representing low molecular weight multivalent functional groups, could also reduce the deposition of PVP-AgNPs, possibly by enhancing the electric double layer interaction at low ionic strengths. (6) Dissolved oxygen: The mobility of Cit-AgNPs in Ottawa sand increased by 15 % when the dissolved oxygen level was reduced from 8.9 to <0.2 mg/L at pH 4, consisted with the more negative ζ potentials of Cit-AgNPs at low dissolved oxygen levels [32]. (7) Biofilms: Biofilms (multilayer coatings of bacterial cells) are ubiquitous in soils and water–sediment interfaces and play important role in the transport of AgNPs with various coating in soils [37]. The affinity of Cit-AgNPs for porous medium, indicated by attachment efficiency (α), increased in the presence of biofilms (Gram-negative *Pseudomonas aeruginosa* and Gram-positive *Bacillus cereus*), bovine serum albumin (BSA), and alginate, while the attachment of PVP-AgNPs to glass beads was not enhanced by biofilms [37]. The presence of Ca^{2+} significantly hydrophobized biofilm, BSA, and alginate-coated glass beads and further retarded the mobility of Cit-AgNPs, but not PVP-AgNPs. This result was consistent with a later study by using biofilm-coated drinking water sand filters [38]. In another study, significantly reduced retention of PVP-AgNPs at low ionic strength compared to clean sand was observed on *P. aeruginosa*-coated sand, irrespective of biofilm age, probably due to the repulsive electrosteric forces between the PVP coatings and extracellular polymeric substances of the biofilm [39]. In addition, more mature biofilm coating also resulted in earlier breakthrough of PVP-AgNPs compared to younger biofilm coatings, or to the clean sand.

Nature soils were also used to investigate the retention and penetration of AgNPs. The retention, penetration, and remobilization of AgNPs could be influenced by the following factors: (1) Coating of AgNPs [40]: After 1-week incubation of AgNPs with soils, the total Ag content of Cit-AgNPs in pore water was much higher than that of PVP-AgNPs. However, preincubation with sewage sludge negated the difference from the coating. (2) Properties of soils: The nonequilibrium retention (K_r) values of PVP-AgNPs in 16 soils were highly correlated with the soil granulometric clay content, suggesting that negatively charged PVP-AgNPs were adsorbed preferentially at positively charged surface sites of clay-sized minerals [41]. Another study by using 11 natural soils with varying physical and chemical properties also showed fast heteroaggregation between negatively charged AgNPs and positively charged sites on the common soil colloids maghemite or montmorillonite [42]. These two studies suggested that heteroaggregation between AgNPs and clays favorited the deposition of AgNPs in soils. Further, as higher available surfaces for smaller aggregates of soils, the retention of Cit-AgNPs in soil column increased with decreasing aggregate size of soils [43]. In addition, after soil residual chloride was exchanged by nitrate prior to column experiments, the mobility of Cit-AgNPs

was significantly improved in the soil column [43]. (3) Composition of leaching solution: The presence of HA in the leaching solution could significantly increase the penetration of Cit-AgNPs in soil column [43]. The mobility of surfactant-stabilized AgNPs in soil was enhanced with decreasing ionic strength of leaching solution [44, 45]. Comparably, retention of surfactant-stabilized AgNPs was much more significant in the presence of Ca^{2+} than K^{+}, at the same ionic strength and the amount of AgNPs released with a reduction in ionic strength was larger for K^{+} than Ca^{2+} [44]. (4) Flow rate of leaching solution: The retentions of Cit-AgNPs and surfactant-stabilized AgNPs in soil column were reduced by increasing the flow rate of leaching solution [43, 44].

Recently, an intermediate scale field transport study was performed for understanding the transport of AgNPs capped with citrate, Suwannee river natural organic matters (SRNOM), or dodecanethiol [46]. The results showed that due to the heteroaggregation with soil surface, the transport of AgNPs within the vadose zone was very limited and after 1 year in intermediate-scale field lysimeters, >99% of the AgNPs still remained within 5 cm of the original source in the soils. Another study also showed that although movement of PVP-AgNPs from terrestrial soils to water and sediments was observed, most of the added Ag resided in the spiked soils [19]. These results [19, 46], combined with that soil column experiment [42], strongly suggest that the interaction of AgNPs with natural colloids in soils significantly reduces their mobility and hence potential risks from off-site transport [42].

4.2.3.2 Plant

Plants are important components of terrestrial ecosystems and play a critical role in the uptake, bioaccumulation, and subsequent incorporation of AgNPs into terrestrial food web [47, 48]. As shown in Table 4.1, many plant species including editable ones, could uptake and bioaccumulate AgNPs from hydroponic solution. The bioaccumulation of AgNPs could come from two possible sources [47]: the uptake of AgNPs directly, and the uptake of dissolved Ag^{+} from AgNPs. The presence of AgNPs in wheat shoots exposed to Ag^{+} confirmed the uptake of dissolved Ag^{+} from AgNPs, and in situ formation of AgNPs by reduction of Ag^{+} in planta [49]. Another study observed that *Arabidopsis thaliana* exposed to AgNP suspensions bioaccumulated higher silver contents than plants exposed to $AgNO_3$ solutions, indicating the occurrence of direct AgNP uptake by plants [50].

Zucchini shoots exposed to AgNPs could uptake 4.7 times greater Ag than the plants from the corresponding bulk solutions [51]. Similarly, higher uptake of Ag was found for rice when the seeds were treated with smaller AgNPs [52]. However, for *A. thaliana*, smaller AgNPs accumulated more effectively than larger AgNPs at low concentrations (66.84 μg/L), whereas opposite trend was observed at the highest concentration (534.72 μg/L) [50]. In most cases, the exposure was conducted in spiked hydroponic solution. However, the incubation matrix could influence the adsorption and the transformation of spiked AgNPs and then their uptake and bioaccumulation. For example, crop plants *Phaseolus radiatus* and *Sorghum bicolor* could uptake less Ag in soil medium than that in agar, possibly owning to the lower

Table 4.1 The uptake of Ag from AgNPs by terrestrial plants

Plant species	Incubation or exposure matrix	Site for Ag accumulation	Determination and characterization	Ref.
Cucurbita pepo (zucchini)	Hoagland solution	Shoot	ICP-MS	[51]
Arabidopsis thaliana	–	Root and shoot	SEM, TEM	[47]
C. pepo (zucchini)	Hoagland solution	Shoot	ICP-OES	[56]
Bacopa monnieri	Hydroponic solution	Root and stem	AAS	[57]
Haseolus radiatus and *Sorghum bicolor*	Agar and soil media	Root	TEM, EDS	[53]
Lycopersicon esculentum (tomato)	Hoagland solution	Stems, leaves and fruits	ICP-OES	[54]
Poplars and Arabidopsis	Hydroponic solution	Leaves, stems and reproductive organs	ICP-MS	[55]
A. thaliana	1/4 Hoagland media	Root	ICP-MS, confocal microscope, TEM, EDS	[50]
Triticum aestivum L.(wheat)	Sand growth matrix	Shoot	ICP-MS, TEM	[49]
Oryza sativa L.(rice)	Hydroponics solution	Root and leaf	ICP-OES	[52]

bioavailability of AgNPs in soil by greater aggregation in pore water and sorption onto soil particles [53].

For *Phaseolus radiates*, *Sorghum bicolor*, *Oryza sativa* (rice), *Lycopersicon esculentum* (tomato), poplars, and *Arabidopsis*, most of Ag uptake by the plants was trapped in the root [52–55]. However, it was also observed that the concentration of Ag in leaves of *Arabidopsis* was much higher than that in stem [55], indicating the selective transport of Ag in aerial parts of some plant species. It should also be noted that the bioaccumulation of Ag was also detected in the reproductive organs (flower, silique, and floral bud) of *Arabidopsis* and fruits of tomatoes [54, 55], highlighting the importance of management strategies to mitigate the potential risks of AgNP application.

The mechanism of uptake and translocation of AgNPs in plants is still not well understood. Transmission electron microscope (TEM) images revealed that individual and aggregated AgNPs distributed in cell walls of *A. thaliana* root, especially in the pectin-rich/cellulose-poor middle lamella of the wall [50]. The aggregated AgNPs or clumps mainly located at the plasmodesmata. These results indicated that AgNPs passed intercellular space via apoplastic transport.

4.3 Transformation of AgNPs

Once released into the environment, AgNPs would undergo a series of transformation, including change of coating, sorption of inorganic and organic species, and other physical and chemical transformation process. Similar to other engineered NPs, AgNPs will interact with the composition in natural waters, and the aggregation and sedimentation of AgNPs are inevitable [58]. Further, due to the medium redox potential of Ag ($\varphi^{\Theta}(Ag^{+}/Ag^{0}) = 0.80$ V) and the high affinity of Ag^{+} with S^{2-} and Cl^{-}, extensive chemical transformations, including oxidative dissolution, re-reduction, sulfidation, and chlorination, were observed for AgNPs. These transformation processes dictate the transport potential, the environmental fate, and potential toxicological effect of AgNPs.

4.3.1 Change of Coating of AgNPs

To facilitate the dispersion or functionalization of engineered AgNPs, the core of elemental nanoparticulate Ag is often coated with various organic ligands such as PVP, BPEI, polyvinyl alcohol (PVA), polyethylene glycol (PEG), and citrate [59]. Once released into the environment, the coatings of AgNPs could undergo degradation, over-coating (or sorption) and exchange with other environment-occurring organic/inorganic species.

It is reported that PVP and citrate, as the capping agent of AgNPs, could be photodegraded under simulated sunlight [60] or (ultraviolet) UV light [61]. Although there are few reports on the degradation of coating ligands of AgNPs, it is reasonable that various organic ligands of coating could degrade in water, sediment, and soils via various (photo) chemical or biological processes.

Different environment-occurring organic/inorganic species including NOM, polysaccharide, and protein could adsorb on the surface of AgNPs and overcoat or displace the original coating ligands. Although the sorption of NOM and extracellular polymeric substances has great impacts on the aggregation and dispersion of AgNPs in the aquatic environments, there is little report on the sorption behavior and mechanism of NOM and extracellular polymeric substances on the surface of AgNPs [62].

Surface-enhanced Raman spectroscopy showed that the adsorption of humic substances was sensitive to pH, the composition of NOM, and the coating of AgNPs [63]. At pH 7, the interaction of HA with molecular weight (MW) 100–300 kDa with the Cit-AgNP surface mainly takes place through aromatic groups, while the interaction at low pH takes place through carboxylate groups. The adsorption of NOM on AgNP surface at lower pH also induced the conformational change of NOM. The aromatic to aliphatic ratio is higher in HA in comparison to fulvic acid (FA), thus higher affinity of HA for Cit-AgNPs, and of FA for the $NaBH_4$-reduced AgNPs were observed. At neutral pH, only high MW fractions of HA were strongly attached on the surface of Cit-AgNPs, while low MW fractions of FA preferred to adsorb on the surface of $NaBH_4$-reduced AgNPs. Recently, another study by using nuclear magnetic resonance (NMR) and Raman spectroscopy showed that both HA

and FA fractions of NOM were capable of displacing citrate from the surface of AgNPs and suggested that FA interacted with both the ring and polyvinyl domains of PVP and the oxygen atom involved in the PVP–nanoparticle complex [64].

After incubation of AgNPs with exopolysaccharides (EPS), a decrease in absorbance and blue shift (by 5–10 nm) of surface plasmon resonance (SPR) were observed at increasing concentrations of EPS, indicating the adsorption of EPS on AgNPs [65]. The Langmuir model predicts better the adsorption behavior of EPS on AgNPs than Freundlich model, and the adsorption data tend to follow pseudo-second-order kinetics, which suggested that chemisorptions may be the rate limiting step. It was also found that pH and NaCl had great influences on the adsorption of EPS on AgNPs. With the increase of pH from 4 to 9, the adsorbed EPS on AgNPs decreased significantly, which was explained by the decreasing electrostatic interaction between EPS and AgNPs with the increase of pH. When NaCl concentration over 0.1 mol L^{-1}, the adsorption of EPS on AgNPs was drastically decreased, possibly due to less surface area of AgNPs resulting by salt-induced aggregation of AgNPs.

Before or after AgNPs entered the organisms, proteins in biological debris, secretions, and biological fluids adsorbed on the surface of AgNPs to form "protein corona" [66]. The sorption of protein on the surface of AgNPs will influence the dissolution [67], cellular uptake, distribution [68], and subsequent toxicity of AgNPs [67]. The binding of protein to AgNPs could induce the change of conformation and thus enzymatic activity of protein, which possibly induced subsequent biological effects [69–71]. The adsorption of protein is highly dependent on the coating and size of AgNPs, and the protein species. For example, although a number of proteins from *Escherichia coli* were identified to bind specifically to bare or carbonate-coated AgNPs, tryptophanase was observed to have an especially high affinity for AgNPs despite its low abundance in *E. coli* [69]. For BSA, uncoated and surfactant-free AgNPs derived from a laser ablation promoted a maximum protein coating, while it displayed a relatively lower affinity for Cit-AgNPs and PVP-AgNPs [72]. In cell culture media, Cit-AgNPs and PVP-AgNPs (20 or 110 nm diameter) associated a common subset of 11 proteins including albumin, apolipoproteins, keratins, and other serum proteins [73]. In addition, 110 nm Cit-AgNPs and PVP-AgNPs were found to bind the greatest number of proteins, compared to 20 nm Cit-AgNPs and PVP-AgNPs. Also, the protein corona on 20 nm AgNPs consisted of more hydrophobic proteins compared to 110 nm AgNPs.

Besides NOM, extracellular polymeric substances and proteins, thiol-containing small molecules [74–76], uric acid [77], SCN^- [78], dyes [79], pyridinecarboxylic acids [80], perfluorocarboxylic acids [61], As(V) [81], and halide ions [82, 83], could also adsorb on the surface of AgNPs. The sorption of these organic/inorganic species could potentially influence not only the fate and transformation of these organic/inorganic species but also the surface chemistry, aggregation, and dissolution of AgNPs [84].

4.3.2 Dissolution and Re-reduction

Although there are reports about the specific toxicity of Ag^+ compared with AgNPs [85, 86], many recent studies suggested that the acute toxicity of AgNPs mainly

derives from the dissolved Ag^+ [87–90]. Therefore, the dissolution and re-reduction of AgNPs plays crucial roles in not only the fate of AgNPs in the environment but also the toxicity of AgNPs to organisms [91].

Usually, there is an Ag_2O coating on the surface of synthesized AgNPs. Once AgNPs are dispersed in water, the Ag_2O could be dissolved quickly and Ag^+ is released [92]. The releasing of adsorbed Ag^+ on AgNP surface also attributes a rapid initial Ag^+ release in preparation of the AgNP suspension [93]. Besides the above mentioned dissolution process of Ag_2O or adsorbed Ag^+, zero-valent AgNPs could also undergo oxidative dissolution in waters, which depends on both dissolved dioxygen and protons [94]. This oxidative dissolution is influenced by both the properties of AgNPs and other environmental factors: (1) particle size of AgNPs [95–98]: The dissolution of Ag^+ from AgNPs is a heterogeneous oxidation reaction, which suggests that the dissolution is dependent on the surface area and particle size of AgNPs [95]. With the decreasing particle size, the oxidative dissolution of AgNPs and release of Ag^+ increased significantly [95–98], while after surface area renormalization the difference of ion dissolution between different sized AgNPs was quite small, demonstrating the dominant effect of surface area [95]. (2) Coating of AgNPs: Although there are reports that coating has minor effects on dissolution of AgNPs [98], a recent study observed that the initial dissolution of Tween-AgNPs is much faster than Bare-AgNPs and Cit-AgNPs in river water [99]. (3) Oxidant: AgNPs could be oxidized by environment-related oxidants including dissolved oxygen [32, 94, 97], H_2O_2 [94, 100, 101], sodium hypochlorite, and ozone [102]. Removing dissolved oxygen could completely inhibit the oxidative dissolution of AgNPs, indicating the essential role of AgNP surface oxidation initiated by O_2 [94]. In addition, the oxidative dissolution of AgNPs is highly dependent on the concentration of dissolved oxygen, following pseudo-first-order reaction for O_2 [97]. Similarly, the oxidation of AgNPs by H_2O_2 also followed pseudo-first-order reaction for H_2O_2 [100], and the apparent dissolution rate of AgNPs by H_2O_2 is about 100-fold higher than that of O_2 [97]. (4) pH: As the cooperative oxidation process of AgNPs requires both protons and dissolved O_2, the oxidative dissolution of AgNPs increased significantly with decreasing pH [94]. (5) Complexing ligands: The presence of BSA [67], cysteine [84], and NH_4^+ [103, 104], as the complexing ligands of Ag^+, could enhance the oxidative dissolution of AgNPs. As S^{2-} could form insoluble Ag_2S on the surface of AgNPs and inhibit the further oxidation of AgNPs, the oxidative dissolution significantly decreased in the presence of S^{2-} [95, 105]. The influence of Cl^- on oxidative dissolution of AgNPs is more complicated as Cl^- could form numerous soluble and insoluble Ag–Cl species, depending on the Cl/Ag ratio [106]. In the presence of Cl^- at concentration ratio of Cl/Ag = 5, the dissolution of AgNPs decreased significantly, while with further increasing the concentration of Cl^- (with Cl/Ag from 54 to 2675), the dissolution increased, but it was still lower than that of deionized water control (without Cl^-). However, with Cl^- at Cl/Ag = 26750, the dissolution of AgNPs was much higher than that of deionized water control. The Cl/Ag ratio-dependent dissolution kinetics can be well interpreted using the thermodynamically expected speciation of Ag ($AgCl_x^{(x-1)-}$) in the presence of chloride. (6) Temperature: With the increasing of temperature from 4 to 37 °C, the dissolution of AgNPs significantly increased [94]. (7) Light: Light irradiation could accelerate the

surface oxidation of AgNPs [107] and thus enhance the dissolution of AgNPs [60]. However, in the presence NOM, the photoreduction of Ag^+ by NOM could also inhibit the dissolution of AgNPs [60]. (8) Aggregate states: Aggregation of AgNPs could also decrease their oxidative dissolution [109]. The aggregate size and fractal dimension are two important parameters to characterize the dissolution of AgNP aggregates. An aggregate with more open structure would preserve the accessibility of reactive surface sites to oxygen and proton, and therefore is more susceptible to oxidation than condensed aggregates.

As discussed in Chap. 3, the dissolved Ag^+ form AgNPs could be reduced by NOM or other electron donor (i.e., Fe^{2+}) at environmentally relevant conditions. This re-reduction process is not only a possible source of naturally occurring AgNPs but also has great influence on the transformation and fate of engineered AgNPs in the aquatic environment. In previous studies, morphology changes of AgNPs were observed in storage or ecotoxicology exposure process [108, 110–113], especially under sunlight irradiation [110, 114]. For example, as shown in Fig. 4.2, significant morphology changes of monodisperse Cit-, PVP-, and PEG-AgNPs were observed after 21 days incubation in different ecotoxicology exposure media, with formation of "new" smaller and larger AgNPs after the incubation [108].

We proposed that this highly dynamic characteristic of AgNPs is ascribed to the inherent redox instability of silver and the cycle of chemical oxidation of AgNPs

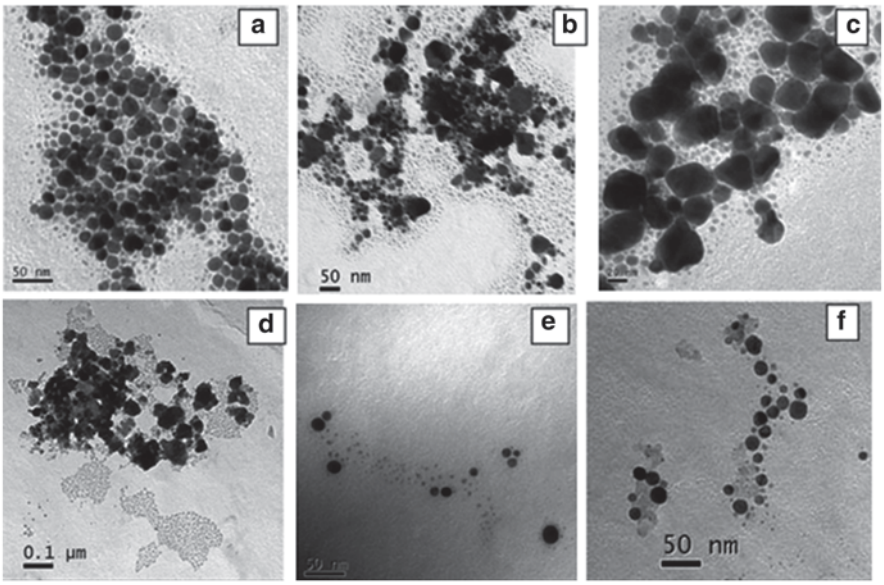

Fig. 4.2 TEM images of AgNPs after 21 days incubation in different media: **a** Cit-AgNPs in CM-10, **b** Cit-AgNPs in NM-10, **c** Cit-AgNPs in SM-10, **d** Cit-AgNPs in NM-1, **e** PVP-AgNPs in CM-1, and **f**. PEG-AgNPs in CM-1. Note: CM-1, a standard OECD media for *Daphnia sp* acute and chronic test; CM-10, a 10-fold dilution of CM-1; NM-1 and NM-10, the chloride was replaced with the same ionic strength nitrate (NM-1 and NM-10); SM-10, the chloride was replaced with the same ionic strength sulfate (SM-10). (Reprinted with the permission from ref. [108], Copyright 2012 American Chemical Society)

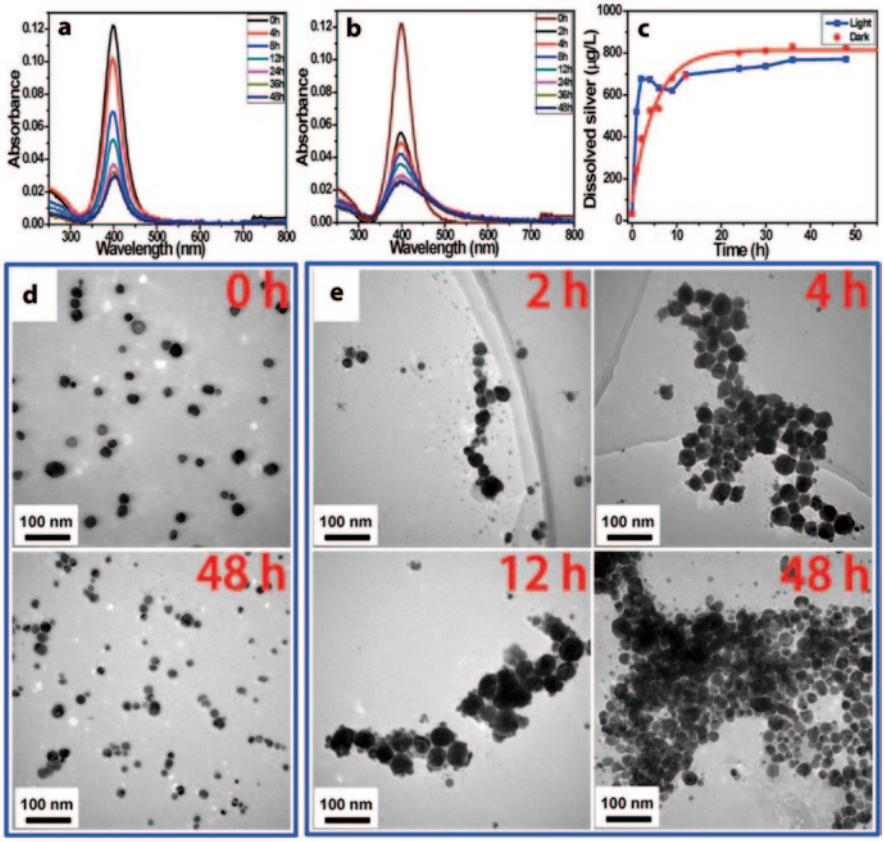

Fig. 4.3 UV-vis absorption spectra, dissolution (ion release) kinetics, TEM images, and EDS analysis of AgNPs in the presence of SRHA. 1.02 mg/L AgNPs, 5 mg C/L SRHA, pH 6.3. **a** UV-vis spectra in the dark, **b** UV-vis spectra in the light, **c** dissolved Ag release curve, **d** TEM images in the dark at time intervals of 24 and 48 h, **e** TEM images in the light at time intervals of 24 and 48 h, and the high resolution TEM and EDS of the new AgNPs. (Reprinted with the permission from ref. [60], Copyright 2014 American Chemical Society)

to release Ag^+ and re-reduction to form AgNPs in aquatic environments [60]. We observed that in the presence of SRHA, the AgNP dissolution was greatly reduced both in the dark and in the light (Fig. 4.3a, 4.3b, 4.3c). Figure 4.3e also showed that there were a great number of small NPs appearing in the solution after 24 h in the light. Higher resolution TEM image and EDS analysis confirmed that these small particles were also nanosilver. After irradiation for 48 h, some AgNPs tended to fuse together, which matched with the λ_{max} red-shifted in the UV-vis spectra results. Based on the above observation, a three-stage pathway for the transformation of AgNPs in aquatic environments was proposed, as shown in Fig. 4.4. In the first stage, light irradiation resulted in the fast oxidation of AgNPs and abundant release of dissolved Ag. The second stage included the re-adsorption of Ag^+ on the AgNP surface and reformation of small particles. Ag ions, diffused away from the parent

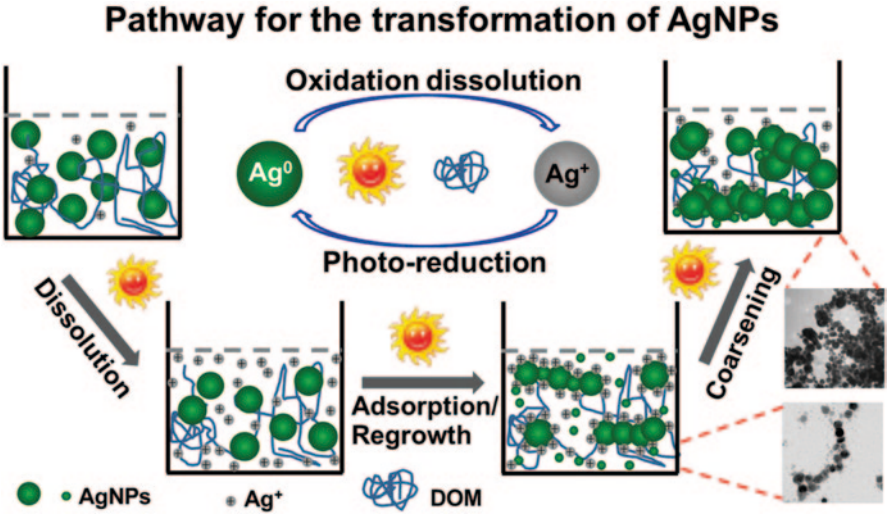

Fig. 4.4 Proposed pathway for the transformation of AgNPs in aquatic environments. (Reprinted with the permission from ref. [60], Copyright 2014 American Chemical Society)

particles, would form new AgNPs around or far away from the parent particles. Meanwhile, reduction of adsorbed Ag^+ on the surface of AgNPs may generate nanobridges to connect nearby particles together, causing particle fusion or self-assembly to form larger structures. In the third stage, many more AgNPs were involved in the cross-linking structures, and small particles also grew on the surface of bigger ones, forming large aggregates and precipitation of Ag nanostructures.

4.3.3 Aggregation and Sedimentation

Homoaggregation is the aggregation between the same particles, while heteroaggregation is the aggregation between particles of different size and properties [115]. Both homoaggregation and heteroaggregation of AgNPs could influence the toxicity of AgNPs [116, 117] potentially by decreasing the dissolution of AgNPs. The aggregation could further induce sedimentation of AgNPs, which also potentially influence the chemical transformation and uptake of AgNPs to benthic organisms.

4.3.3.1 Homoaggregation

Various parameters of AgNPs and water chemistry could have great influence on the homoaggregation of AgNPs, including coating of AgNPs, pH, concentration and type of electrolyte, dissolved oxygen, and DOM. (1) Coating of AgNPs: Hydrodynamic diameter determination revealed that sterically stabilized (PVP) or electrosterically stabilized (BPEI) AgNPs were more stable in $NaNO_3$

solution than uncoated and electrostatically stabilized AgNPs (Cit- and $NaBH_4$-AgNPs), owing to additional steric repulsion [118]. The aggregation kinetics of AgNPs by time-resolved dynamic light scattering further demonstrated that the PVP-AgNPs were significantly more stable than citrate-coated AgNPs in both NaCl and $CaCl_2$ [119]. The role of steric repulsion in stabilization of AgNPs in electrolytes was further evidenced by using Tween 80 [120] and PEG [121] as coatings. (2) pH: Solution pH could significantly influence the charges and ζ potential of electrostatically stabilized AgNPs (Cit-AgNPs and $NaBH_4$-AgNPs) and electrosterically stabilized (BPEI-AgNPs), and thus their aggregation behavior [118]. However, changes in solution pH have no effect on ζ potential and aggregation of the sterically stabilized AgNPs (PVP-AgNPs). In addition, the pH could also influence the ζ potential of naturally occurring organic matter (such as exopolysaccharides and bacterial extracellular proteins) and thus the adsorption of these organic matters on AgNPs [65, 122]. The adsorption of these organic matters could provide additional steric repulsion in stabilization of AgNPs. (3) Concentration and type of electrolyte: In the presence of electrolyte, the charge of AgNPs was screened or neutralized, which accelerated the aggregation of AgNPs [118, 119]. At low concentration range of electrolyte, the increase in electrolyte concentration could elevate the effect of charge screening and hence increase aggregation kinetics (reaction-limited regime) [119]. However, at high electrolyte concentrations, the charge of AgNPs is completely screened and in the so-called diffusion-limited regime, the aggregation kinetics of AgNPs is independent of the electrolyte concentration. Compared with monovalent electrolytes, divalent electrolytes were more efficient in destabilizing AgNPs, as evident by the critical coagulation concentration of electrolytes [118–120]. (4) Dissolved oxygen: in the presence of dissolved oxygen, the aggregation rate of Cit-AgNPs became much faster (3–8 times) than that without dissolved oxygen [123]. In addition, after a linear growth within the initial 4–6 h, the hydrodynamic sizes of AgNPs showed a periodic fluctuation in the presence of dissolved oxygen. As this periodic fluctuation was inhibited by deoxygenation, this phenomenon was ascribed to dissolved oxygen-induced oxidation and dissolution of AgNPs, which could further change the surface energy of AgNPs. (5) DOM and other small organic molecules: The adsorption of DOM could induce additional electrosteric repulsion that elevated the stability of AgNPs suspensions containing low concentrations of mono- or divalent electrolytes [119, 124]. However, at high concentration of Ca^{2+}, enhanced aggregation occurred for PVP-AgNPs and Cit-AgNPs, possibly due to the interparticle bridging by Ca^{2+}-induced aggregation of humic acid [119, 125]. The stability of the AgNPs was also influenced by adsorption of low molecular weight organic molecules. Cysteine, a thiol ligand, could decrease the diameter of PVP-AgNPs, possibly by disaggregation of aggregates in the nanoparticle stock [84]. The influence of aggregation of AgNPs by laundry-relevant surfactants was dependent on the charge and concentration of the co-occurring surfactants [126]. In the presence of anionic sodium dodecylbenzenesulfonate, the negatively charged AgNPs were stable in solution for more than 1 day, while at low concentrations ($\leq$1 mmol/L) of cationic dodecyl trimethylammonium chloride, the neutralization of charge accelerated the agglomeration of AgNPs. However, in the presence high concentration of dodecyl trimethylammonium chloride, further adsorption of the cationic surfactants

made the surface charge of AgNPs positive, which provided repulsive electrostatic forces between AgNPs and prevented AgNPs from agglomeration.

4.3.3.2 Heteroaggregation

The interaction between released AgNPs with natural colloids could result in heteroaggregation in the environment. Compared with homoaggregation, the heteroaggregation of AgNPs should be more general, considering the relatively low concentration of AgNPs and the ubiquity of natural colloids (i.e., clay minerals) in the environment. Although most studies in aggregation of AgNPs focused on the homoaggregation, the heteroaggregation is more relevant for environmental media [62].

A pH-dependent heteroaggregation was observed between Cit-AgNPs and a common natural colloid, montmorillonite [127]. At pH 8, since the face and edge of montmorillonite, and Cit-AgNPs are all negatively charged, the mixing montmorillonite and Ag does not alter the stability of the system. However, at pH 4, the adsorption of negatively charged Cit-AgNPs and the positively charged montmorillonite edges accelerate the heteroaggregation between montmorillonite and Cit-AgNPs and the critical coagulation concentration of the montmorillonite/AgNPs system shifts toward a lower ionic strength compared to either montmorillonite or AgNPs single component system. TEM images demonstrated that most AgNPs were attached to the edges of montmorillonite.

4.3.3.3 Aggregation in Natural Waters

In natural waters, the water chemical composition (DOM, and species and concentration of inorganic ions) and occurrence of natural colloids usually make the aggregation behavior of AgNPs more complicated. The study on the aggregation of AgNPs in natural waters also imply that although a significant fraction of the singly dispersed AgNPs will agglomerate and sediment in the freshwater environments, another fraction of the AgNPs will remain persistent enough in freshwaters to be transported to long distances [128]. In addition, as the agglomerated AgNPs settle down relative slowly (7 days), these could also contribute to the mobility of AgNPs [129].

Generally, owning to the occurrence of natural colloids, the homoaggregation and heteroaggregation of AgNPs occur simultaneously in natural waters. The role of heteroaggregation in aggregation could be evaluated through separation of heteroaggregation from homoaggregation using a simplified Smoluchowski-based aggregation-settling equation applied to data from unfiltered and filtered waters [130]. In presence of natural colloids, the settling fraction of SiO_2-AgNPs and PVP-AgNPs increased and the fraction removed due to the presence of natural colloids varying with water type. Small size of the natural colloids and high DOM content of the water could decrease in aggregation and sedimentation of AgNPs. Therefore, the heteroaggregation of AgNPs with natural colloids should have great impact on the aggregation and sedimentation of AgNPs in natural waters and WWTPs.

In addition, the dispersion of AgNPs also varys significantly with solution chemistry or chemical composition of water [131]. The combination of low electrolyte and high dissolved organic carbon (DOC) concentrations in natural water samples limited the aggregation of AgNPs, while increased ionic strength and lower DOC in natural waters enhanced the aggregation of AgNPs. These results suggest that in complex natural water matrices, DOC and the concentrations of different electrolytes are intricately coupled in controlling the aggregation patterns of AgNPs. Later research further demonstrated the synthesized roles of water chemistry and DOC in agglomeration and disappearance of singly dispersed AgNPs [128].

Similar to simulated waters, surface functionalization (or coating) also have great impacts on the aggregation of AgNPs. Compared to AgNPs with complete citrate capping, AgNPs with partial citrate capping (synthesized in aqueous extract of *Citrus limon*) exhibited significantly more colloidal stability in both lake water and sea water, possibly owning to additional steric hindrance. Similarly, PVP-AgNPs or Tween-AgNPs are more stable against aggregation in river water than Bare-AgNPs or Cit-AgNPs [91, 99].

4.3.3.4 Aggregation-Induced Sedimentation

Both homoaggregation and heteroaggregation could induce the sedimentation of AgNPs in natural water or wastewater treatment processes [129, 130, 132, 133], which result in removal of AgNPs from water and subsequent enrichment of AgNPs in sediment or sludge. The enrichment of AgNPs in sediment or sludge could possibly enhance the sulfidation of AgNPs in anaerobic sulfur-rich environment and the uptake of AgNPs to benthic organisms. Inductively coupled plasma mass spectrometry (ICP-MS) [130] and UV-visible spectrometry [134] were reported to characterize the sedimentation of AgNPs in waters. As the aggregation of AgNPs could also induce the decrease of the SPR intensity of AgNPs [129], UV-visible spectrometry would inevitably overestimate the sedimentation of AgNPs. Comparably, quantification of the sedimentation rate of AgNPs by ICP-MS would be more reliable [130].

4.3.4 Sulfidation

Silver is one of the thiophile elements with a very low solubility product of Ag_2S ($K_{sp}(Ag_2S)$) of 5.92×10^{-51}. Thus, theoretically, after the oxidative dissolution of AgNPs, the resulting Ag^+ tends to bind with S^{2-} to form insoluble Ag_2S. As early as 1984, Lytle et al. observed that silver thiosulfate in photoprocessing discharge could be converted to insoluble Ag_2S and further eliminated by adsorbing on settled sludges in waste treatment process [135]. In 1997, by using XAS, Anderson et al. confirmed that the species of Ag in fixer amended sludge and Ag-trimercapto-s-triazine sludge powder samples was mainly Ag_2S [136]. Later, it was revealed that PVA-AgNPs (average size, 15 ± 9 nm) were also highly reactive with S^{2-} to form Ag_2S precipitates, by using scanning electron microscopy (SEM)

coupled with EDS [137]. These Ag_2S precipitates were not oxidized in aeration conditions for 18 h. These results suggested the importance of Ag_2S as a final transformation product from ionic silver species or elemental AgNPs in the presence of S^{2-}. Then, nanosized Ag_2S (α-Ag_2S) were identified, for the first time, in the final stage sewage sludge materials of a full-scale municipal WWTP using high-resolution transmission electron microscope (HRTEM) combined with EDS [138]. The Ag_2S NPs, with ellipsoidal shape in the size range of 5–20 nm, formed loosely packed aggregates in the sewage sludge samples. As naturally occurring acanthite mineral grains (natural α-Ag_2S) are rare in the sampling areas, the most possible source of nanosized Ag_2S is the in situ sulfidation of AgNPs or soluble Ag species with S^{2-} during wastewater treatment under anaerobic conditions. After that, the sulfidation of AgNPs in the environment and its potential toxic impact is becoming a hotspot, and the sulfidation of AgNPs in simulated lab setting, biological matrix, and in the real environments (WWTPs, wetland, and soil) has been studied.

4.3.4.1 Sulfidation Mechanism and Controlling Factors

In recent years, several pathways were proposed for AgNP sulfidation. Liu et al. proposed two pathways for the oxysulfidation of AgNPs, depending on the concentration of S^{2-} (as shown in Fig. 4.5) [139]:

1. Direct oxysulfidation (particle–fluid reaction) at elevated sulfide concentrations:

$$4Ag + O_2 + 2H_2S \rightarrow 2Ag_2S + 2H_2O \tag{4.1}$$

$$4Ag + O_2 + 2HS^- \rightarrow 2Ag_2S + 2OH^- \tag{4.2}$$

2. Indirect oxysulfidation (oxidative dissolution/precipitation) at low sulfide concentrations:

$$4Ag + O_2 + 4H^+ \rightarrow 4Ag^+ + 2H_2O \tag{4.3}$$

$$2Ag^+ + S^{2-} \rightarrow Ag_2S \tag{4.4}$$

Metal sulfides (MS) can also function as S^{2-} source for this indirect oxysulfidation process [140].

$$2Ag^+ + MS \rightarrow Ag_2S + M^{2+} (M = Cu \text{ or } Zn) \tag{4.5}$$

As MS is more stable than S^{2-}, the metal sulfides mediated sulfidation of AgNPs could occur in oxic environments.

3. Direct sulfidation of AgNPs without oxygen is also proposed as followed [141]:

$$Ag + H_2S \rightarrow Ag_2S + H_2 \tag{4.6}$$

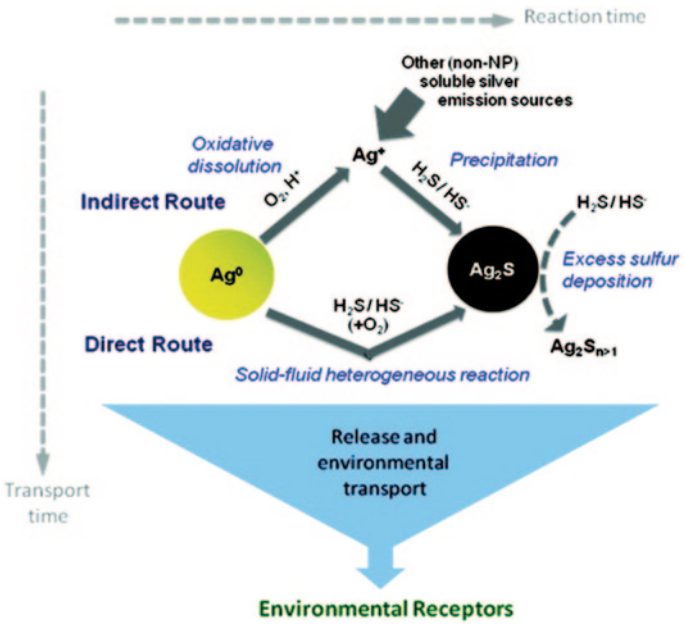

Fig. 4.5 Pathways of AgNPs sulfidation released to the environment. Ag_2S-NPs may be produced by particle–fluid reaction (*direct route*) or by oxidative dissolution to soluble silver followed by sulfide precipitation (*indirect route*). (Reprinted with the permission from ref. [139], Copyright 2011 American Chemical Society)

As the occurrence of H_2S in water is pH-dependent, this direct sulfidation of AgNPs should occur only at pH < 9.6 in anaerobic processes.

Sulfidation of AgNPs was studied in controlled lab setting [105, 139], and it was found that heterogeneous direct oxysulfidation was the main sulfidation pathway at elevated sulfide concentration conditions [139]. The following factors have great impacts on the sulfidation: (1) pH: Decreasing pH from 11.1 to 7.0 significantly improved the sulfidation [139]. (2) Dissolved oxygen: In the presence of 0.1 mmol/L Na_2S at pH 11.1, the sulfidation depends on dissolved oxygen and elimination of oxygen by purging could completely suppress the sulfidation [139]. However, distinguished with experimental simulation, in WWTPs, anaerobic conditions are much favorable than aerobic conditions for sulfidation of AgNPs [22, 23, 142]. This difference may be explained by the following reasons: (1) S^{2-} was consumed under aerobic conditions and thus resulted in slow sulfidation rate [23]. However, the oxidative depletion of S^{2-} was negligible in simulated sulfidation with higher S^{2-} concentration (0.1 mmol/L) [139] rather than that in nonaerated mixed liquor (0.43 mg/L) [23]. (2) Direct sulfidation without oxygen was the main sulfidation pathway in anaerobic environments [141]. (3) Size of AgNPs: Increasing particle size could reduce reaction rates, as this is heterogeneous process that depends on specific surface area. This size-dependent sulfidation has been observed in both simulated experiment (with S^{2-} [139] or metal sulfides [140] as sulfur source) and batch experiment in anaerobic activated sludge [22, 139]. (4) Aggregation states of

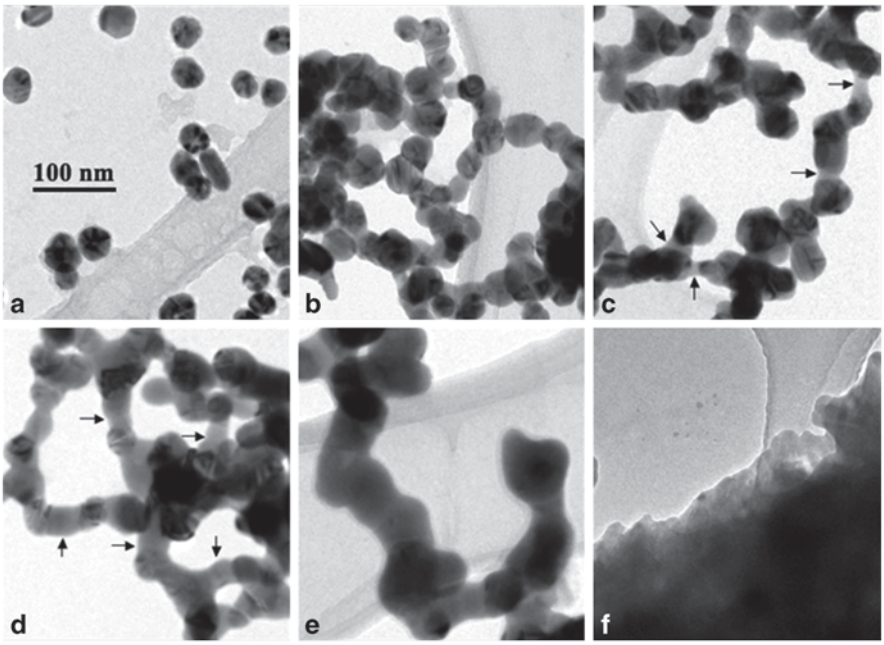

Fig. 4.6 TEM images of the initial and sulfidized synthetic AgNPs: **a** initial; **b** S/Ag = 0.019; **c** S/Ag = 0.055; **d** S/Ag = 0.308; **e** S/Ag = 0.540; and **f** S/Ag = 1.079. Magnification is identical for all six images. (Reprinted with the permission from ref. [105], Copyright 2011 American Chemical Society)

AgNPs: For the same reaction times, larger aggregates have slower sulfidation rates [143]. (5) S/Ag ratio: The increase in S/Ag ratio could enhance the sulfidation of AgNPs [105]. As revealed by TEM (shown in Fig. 4.6), in the sulfidation process, particles strongly aggregated to form chain-like structures. As the sulfidation rate increased, more and more Ag_2S bridges between AgNPs were observed. For high sulfidation ratio (S/Ag = 0.540 and 1.079), the initial sphere of nanoparticle disappeared and an amorphous Ag_2S was evident as the final product.

4.3.4.2 Sulfidation in Various Matrices

Besides study in simulated water, the sulfidation of AgNPs was recently investigated in various matrices, including sewer, WWTP, soil, sediment, and biological samples (as shown in Table 4.2).

Table 4.2 Sulfidation of AgNPs in the environment

	Matrix	Characterization	Ref.
PVA-coated AgNPs (average size, 15 ± 9 nm)	10 μmol/L S^{2-} in 60 mL nitrifying culture	SEM-EDS	[137]
Unidentified Ag source (possible included AgNPs)	Sewage sludge	HRTEM, EDS	[138]
Polyoxyethylene fatty acid ester coated AgNPs	Pilot WWTP fed with municipal wastewater and batch experiments	TEM-HAADF-EDS, XANES	[23]
AgNPs with 5, 30 nm diameter micrometer-sized silver powder	Na_2S solutions (pH 11.1 and 7.0)	XRD, HRTEM	[139]
PVP-AgNPs (39 nm)	1 mmol/L Na_2S, 10 mmol/L $NaNO_3$	XRD, EXAFS, HRTEM	[105]
PVP-AgNPs (10 nm)	aerobic and anaerobic sludge	STEM-HAADF-EDS, XANES	[144]
PVP-AgNPs (5–100 nm), Cit-AgNPs (10 and 100 nm)	Raw wastewater, anaerobic activated sludge	XANES	[22]
Immobilized AgNPs	Full-scale WWTP	AFM, HRTEM, EDS	[142]
PVP-AgNPs (53 nm and 13 nm), Uncoated AgNPs (48 nm)	Soils	XANES	[145]
PVP-AgNPs (10 nm)	Water column and terrestrial soils	EXAFS	[19]
AgNPs with different coating (polyvinyl sulphonate, citrate, mercaptosuccinic acid)	Bench scale anaerobic digesters	XANES	[27]
PVP-AgNPs (52 nm)	Oxic and reduced sludges	EXAFS, XANES	[26]

AFM atomic force microscope, *EXAFS* extended x-ray absorption fine structure, *HAADF* high-angle annular dark-field, *STEM* scanning transmission electron microscopy, *WWTP* wastewater treatment plant, *XANES* X-ray absorption near edge structure, *XRD* X-ray diffraction,

Sulfidation of AgNPs in Sewer and Wastewater Treatment Plant

The sulfidation of AgNPs was investigated in batch experiments to simulate the sulfidation process in urban wastewater systems (main trunk sewer and WWTPs) [22]. PVP-AgNPs (5–100 nm) could be sulfidized with raw wastewater roughly 15% after 5 h reaction time in batch experiments, as revealed by XAS. As higher acid volatile sulfide was observed in the sewer channel (100 mmol/L) than in the batch experiments (3 mmol/L), AgNPs were expected to undergo higher sulfidation in the sewer channel. Then incubation of Cit-AgNPs with different sizes (10 and 100 nm) in anaerobic activated sludge showed a strong size dependence of the

sulfidation kinetics. Both 100 and 10 nm Cit-AgNP firstly showed a rapid sufidation and then a considerably slower sulfidation rate. Comparably, small sized 10 nm AgNPs showed more rapid sufidation than 100 nm AgNPs. After 4 h incubation, only ~5% of the 100 nm AgNPs were sulfidized compared to ~50% of the 10 nm AgNPs. After 24 h, still more than 90% of the Ag was metallic for 100 nm AgNPs, while metallic Ag was less than 5% with 10 nm AgNPs. This size-dependent sulfidation in activated sludge is consistent well with sulfidation of AgNPs by S^{2-} in lab setting [139]. These results indicated that AgNPs discharged to the wastewater stream will become sulfidized to various degrees in the sewer system and will be efficiently transported to the WWTPs, and then the sulfidation of the AgNPs will continue in the WWTPs.

In a field experiment on the fate and transformation of AgNPs in a pilot WWTP, nanosized Ag particles were found to sorb on wastewater biosolids, both in the sludge and in the effluent [23]. TEM-HAADF-EDS revealed that these nanosized Ag particles were always associated with sulfur. Ag K-edge X-ray absorption near edge structure (XANES) spectra confirmed that although some of the AgNPs, spiked to the WWTP influent, reached the effluent in metallic form, most spiked AgNPs were transformed into Ag_2S, both in mixed liquor and effluent samples. Batch incubation experiments were further used to simulate the sulfidation of AgNPs in aerated and nonaerated tanks. In aerated mixed liquor, AgNPs remained dominantly metallic species in 2 h, while the spiked AgNPs (0.5 mg/L) were nearly completely (>90%) transformed to Ag_2S within 2 h in the nonaerated tank, which suggested that enhanced sulfide levels in nonaerated mixed liquor were responsible for the sulfidation of AgNPs. This conclusion was further confirmed by low sulfidation of AgNPs (~60%) at high spiking level (5 mg/L) in nonaerated mixed liquor within 2 h. A similar study also showed that anaerobic conditions were more favorable for sulfidation of PVP-AgNPs than aerobic conditions [144]. In anaerobic digestion, it was found that AgNPs with different coatings (polyvinyl sulphonate, citrate, mercaptosuccinic acid) did not prevent the formation of Ag_2S [27].

Sulfidation of AgNPs in Soil and Sediment

Different AgNPs (15–50 nm, with and without PVP coating) were transformed differently in anaerobic soils, as probed by XAS [145]. After 30 days of incubation, a substantial fraction of PVP-AgNPs (15 nm and 50 nm) were transformed into Ag_2S, Ag_2O, $AgNO_3$, or HA complexed Ag^+, whereas uncoated AgNPs (50 nm) were mostly transformed into the HA complexed Ag^+. This study highly suggests that AgNPs with different coatings may be transformed differently in the environment.

PVP-AgNPs were also spiked to the terrestrial soils, and the Ag speciation in soils was determined after 18 months dosing [19]. The XAS data indicated that in the soil ~47% Ag remained as Ag^0 and other fraction of AgNPs was oxidized to Ag^+ and subsequently sulfidized to Ag_2S (~52%), following an indirect oxysulfidation pathway (oxidative dissolution/precipitation). Comparably, in sediment, ~55 and ~27% Ag was transformed into Ag_2S and Ag-sulfhydryl compounds, respectively.

The relatively low oxidation and sulfidation in the terrestrial environment was possibly ascribed to the drier and more oxic conditions in soils. The low acid volatile sulfide in the terrestrial environment available to the AgNPs possibly accounted for the low sulfidation rate of AgNPs to Ag_2S, compared with laboratory studies using Na_2S as the source of sulfide.

Sulfidation of AgNPs in Cell Culture Media and Biological Sample

The sulfidation of silver nanowires (AgNWs) was observed in cell culture media DCCM-1, but not in DMEM, RPMI-1640 [146]. After incubating AgNWs in DCCM-1 for 1 h at physiological temperature, the formation of small crystals was observed on the surface of the AgNWs. These new small crystals were identified as Ag_2S by SAED, HAADF-STEM, and EDS. Fractions containing small molecule solutes and salts but not the protein component in DCCM-1, possibly accounted for the sulfidation of the AgNWs. However, the exact chemicals accounting for sulfidation of the AgNWs are still not known. Similarly, the sulfidation of AgNPs could also occur in organisms. HRTEM, scanning transmission electron microscope (STEM), and EDS have been employed to elucidate the reactivity of AgNWs inside human alveolar epithelial type 1-like cells [147]. In the first hour of incubation, small particles with 3–9 nm diameter were observed surrounding the ends of the AgNWs, which was confirmed as Ag_2S by STEM-EDS. It was also observed that although the shape of the AgNWs was retained, there was a significant sulfidation at the ends of the wire, indicating greater reactivity at the tip of the AgNWs. With the exposure continuing, the S/Ag peak ratio of particles on AgNW surfaces and the number of Ag_2S particles surrounded the AgNWs increased, indicating a continuous sulfidation. The occurrence of Ag_2S particles on the AgNW surface suggested both oxidative/precipitation (indirect sulfidation) and particle–fluid reaction (direct oxysulfidation) occured in the cell. The formation of Ag_2S, as a "natural trap" for free Ag^+, could possibly decrease the toxicity of silver nanomaterials and Ag^+.

4.3.4.3 Possible Post-transformation of Ag_2S

Ag^+ Dissolution As Ag_2S is the main silver species in activated sludge and the wide application of activated sludge compost, the possible oxidation of S and releasing of Ag^+ in compost application farmland is important to evaluate the fate of Ag_2S and the potential environmental impact of compost application. The study on composting and lime and heat treatment on the transformation of Ag_2S sludge revealed that Ag_2S was stable and persisted in all sludge treatments [26]. In addition, although the reduction of Ag_2S into AgNPs was observed by electron beam irradiation [148] and electrochemical reduction [149] in laboratory settings, the direct reduction of Ag_2S into AgNPs is difficult in nature environments. However, the transformation of Ag_2S under special conditions still cannot be completely ruled out. As S^{2-} in Ag_2S could be possibly oxidized by O_2, H_2O_2, and Fe^{3+} [150–152], the possible

releasing toxic Ag^+ and further transformation of the resulting Ag^+ remains further assessment in activated sludge compost application.

Selenylation As the solubility product of Ag_2Se is much small than that of Ag_2S ($K_{sp}(Ag_2S) = 5.92 \times 10^{-51}$ and $K_{sp}(Ag_2Se) = 3.1 \times 10^{-65}$), the replacement of S^{2-} in Ag_2S by Se^{2-} is thermodynamically favorable with $\Delta G^0_{rxn} = -81.5$ kJ mol^{-1} [153]:

$$Ag_2S + Se^{2-} \rightarrow Ag_2Se + S^{2-}$$

Simulated experiment showed that when incubating pre-sulfidated AgNPs in reduced selenium solutions at equal Se/S molar ratios, the Se/S exchange reaction was complete after 3 days and the final product was Ag_2Se with no detectable Ag_2S [153]. Considering the ultra-low solubility of Ag_2Se, this selenylation process of Ag_2S could further potentially decrease the bioavailability of silver.

4.3.4.4 Environmental Impact of Sulfidation

The sulfidation of AgNPs would have great impacts not only on the fate and transport of AgNPs but also on the bioavailability and toxicity of AgNPs. (1) The ζ potential of sulfidized AgNPs is lower than that for the unsulfidized one, which makes the Ag_2S prone to aggregation and sedimentation [143]. This indicates that the sulfidation of AgNPs will likely influence particle fate and transport by altering colloidal dynamics [139]. (2) Dissolution rates of Ag^+ showed a strong decrease following sulfidation of the AgNPs [105]. At S/Ag ratio as low as 0.019, the dissolved Ag^+ decrease by a factor of about 7. With the increasing S/Ag ratio, the dissolution rate decreases further, even to non-detectable. As the acute toxicity of AgNPs mainly derived from the Ag^+ release, the sulfidation of AgNPs could mitigate the toxicity of AgNPs to organisms including nitrifying bacteria [137], *E. coli* [143, 154], aquatic and terrestrial eukaryotic organisms and aquatic plants [155].

4.3.5 Chlorination

Given the low solubility product of AgCl in water ($K_{sp}(AgCl) = 1.77 \times 10^{-10}$) at room temperature [156], chlorination of Ag^+ could decrease the bioavailability of Ag^+ and thus significantly reduce the toxicity of Ag^+ to mammalian cells [157], which is similar to sulfidation.

Direct chlorination of metal silver has been observed in gas phase by exposure metal silver with Cl_2, as probed by STEM, Auger electron spectroscopy and thermal desorption spectroscopy [158–160].

$$Ag^0 + Cl_2 \rightarrow 2AgCl \tag{4.7}$$

Table 4.3 Chlorination of AgNPs in the environment

	Matrix	Characterization	Ref.
AgNPs powder and AgNPs incorporated into sock	Hypochlorite/detergent solution	XANES	[161]
AgNPs containing T-shirt	Detergent solution containing 8.7 mg/L Cl^-	STEM, EDS	[162]
AgNPs (<20 nm) in fabric sample	Phosphate-free ECE detergent solution	TEM, EDS	[163]
Cit-stabilized AgNPs (40 nm)	Synthetic stomach fluid (0.42 mol/L HCl and 0.40 mol/L glycine, pH 1.5)	TEM, EDS, XRD	[164]
Organically coated AgNPs	Kaolin and 0.01 mol/L NaCl solution	XAS	[165]
PVP-AgNPs	Polyacrylic acid and NaCl solution	XAS, XRD	[105]
Uncoated AgNPs	10 mmol/L NaCl solution	XRD	[118]
Mercaptosuccinic-acid capped AgNPs	Ionic strength 40.3 mmol/L, chloride 30.9 mmol/L, pH 7.4	SEM, TEM, EDS	[166]

At environment-related conditions, AgNPs could be chlorinated directly by hypochlorous or chlorinated by reacting Cl^- with oxidized Ag^+ from AgNPs.

$$2Ag^0 + HOCl \rightarrow AgCl + OH^- + Ag^+ \tag{4.8}$$

$$Ag^+ + Cl^- \rightarrow AgCl \tag{4.9}$$

The chlorination of AgNPs in the environment has been summarized in Table 4.3. In the presence of hypochlorite (HOCl) oxidant and detergent, over 50% of the AgNPs in sock were in situ transformed to AgCl [161]. Exposure of elemental Ag nanopowder with HOCl and detergent also induced the chlorination of AgNPs, further confirming the chlorination of AgNPs by HOCl. Another study also observed that the ultrafiltration only recovered 26% dissolved Ag^+ by oxidation of PVA-AgNPs in the presence of sodium hypochlorite and sodium nitrate, and thus other transformation product was suggested to be AgCl [102]. AgCl nanoparticles and large AgCl particles were observed in the washing solutions for commercially available functional (nano)textiles by STEM and EDS, suggesting AgCl was the most frequently observed chemical form of silver in the washwater [162, 163].

However, direct exposure of elemental Ag nanopowder in 1 mol L^{-1} NaCl evidenced little chemical transformation, which suggests an oxidation step is necessary for the AgNPs to transform into AgCl. The presence of Cl^- and oxidative dissolution of AgNPs could form bridge between AgNPs, which was assumed to be AgCl [120]. The AgCl bridge was further confirmed by SEM, TEM, and EDS [166]. Further increase the concentration of Cl^- would form soluble negatively charged $AgCl_x^{(x-1)-}$ species [166].

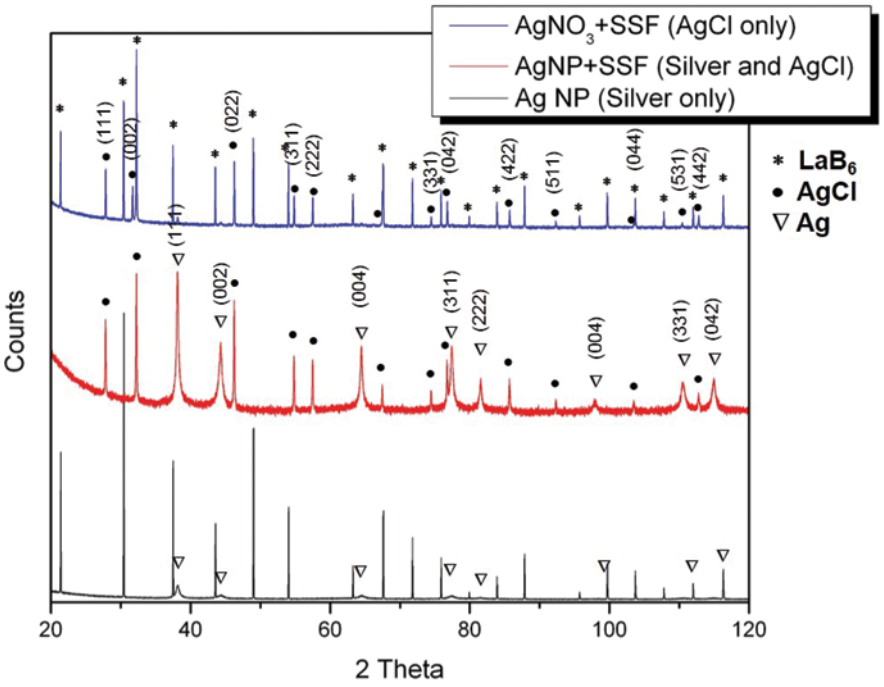

Fig. 4.7 XRD patterns and Rietveld analysis for precipitate resulting from silver nitrate and synthetic human stomach fluid (10 min) (*blue line*); AgNPs (40 nm) exposed to synthetic human stomach fluid for 1 h (*red line*); and untreated AgNPs (40 nm) (*black line*). (Reprinted from ref. [164], Copyright 2012, with permission of Elsevier)

Citrate-stabilized AgNPs, when exposed to synthetic human stomach fluid (containing 0.42 mol/L HCl), could transform into AgCl, evident by TEM, EDS, and XRD [164]. As shown in Fig. 4.7, after exposed to synthetic human stomach fluid for 1 h, significant conversion of AgNPs to AgCl was observed. The extent of conversion to AgCl was influenced by particle size. Over a 1-h period of exposure in synthetic human stomach fluid, smaller AgNPs (1–10 nm) show the highest fractional conversion and the bulk silver particles (>1 μm) are not converted to AgCl.

The further transformation of AgCl in the environment into other silver species is still not well understood. It has been shown that the addition of glutathione dissolves the AgCl precipitates within 45 min by forming Ag–glutathione complexes, which could possibly enhance the bioavailability of silver [153]. Two other transformation pathways of AgCl could also possibly occur in natural environments: (1) Sulfidation: As the $K_{sp}(Ag_2S) << K_{sp}(AgCl)$ in the presence of S^{2-}, further transformation of AgCl into more stable Ag_2S is highly possible. For example, in the washing procedure, AgNPs in textiles could oxidize into Ag^+ and then form AgCl NPs and large AgCl particles, and once discharged into WWTPs, high concentration of S^{2-} could further displace Cl^- and form Ag_2S. This was demonstrated by adding AgCl NPs into anaerobic digester, in which over 90% AgCl was transformed into

Ag_2S [27]. (2) Reduction: It is well known that AgCl is photosensitive and under natural sunlight AgCl could transform into elemental Ag. DNA could accelerate the transformation of AgCl into AgNPs under UV irradiation (360 nm, 150 mW/cm^2) [167]. Similarly, ubiquitous NOM is also possible to accelerate the reduction of AgCl into AgNPs with NOM as reductant and coating agent.

4.4 Summary and Outlook

The anthropogenic or naturally occurred AgNPs could transport, distribute, and transform in different environmental compartments, which significantly impacts their fate and toxicity. Although in recent years many researches focus on the transport and transformation of AgNPs in simulated and natural environments, there still are many open questions to be addressed to enrich our knowledge on the environmental distribution, transport, and transformation of AgNPs: (1) quantitative information on the production, application, and release of AgNPs in industry and commercial products; (2) development of techniques for in situ characterization of ultra-trace Ag for both their concentration and species in the environment; (3) probing important physical and chemical transformation processes of AgNPs, such as the post-transformation of Ag_2S and AgCl and their effects on the transport and toxicity of Ag, as well as the role of different DOM fraction (i.e., molecular weight) on the aggregation, mobility, and transformation of AgNPs; (4) parameterization of the processes of the transport and transformation of AgNPs. In the further study, emerging techniques such as hyperspectral imaging, XAS, and advanced isotope techniques like isotope fractionation ratio characterization and multiple isotope tracers (^{107}Ag and ^{109}Ag) should play important roles in the study on transport and transformation of AgNPs.

References

1. Lowry GV, Hotze EM, Bernhardt ES, Dionysiou DD, Pedersen JA, Wiesner MR, Xing BS (2010) Environmental occurrences, behavior, fate, and ecological effects of nanomaterials: an introduction to the special series. J Environ Qual 39(6):1867–1874. doi:10.2134/jeq2010.0297
2. Westerhoff P, Nowack B (2013) Searching for global descriptors of engineered nanomaterial fate and transport in the environment. Acc Chem Res 46(3):844–853. doi:10.1021/ar300030n
3. Gottschalk F, Sun TY, Nowack B (2013) Environmental concentrations of engineered nanomaterials: review of modeling and analytical studies. Environ Pollut 181:287–300. doi:10.1016/j.envpol.2013.06.003
4. Gottschalk F, Ort C, Scholz RW, Nowack B (2011) Engineered nanomaterials in rivers—exposure scenarios for Switzerland at high spatial and temporal resolution. Environ Pollut 159(12):3439–3445. doi:10.1016/j.envpol.2011.08.023
5. Musee N (2011) Simulated environmental risk estimation of engineered nanomaterials: a case of cosmetics in Johannesburg City. Hum Exp Toxicol 30(9):1181–1195. doi:10.1177/0960327110391387

6. Hendren CO, Badireddy AR, Casman E, Wiesner MR (2013) Modeling nanomaterial fate in wastewater treatment: Monte Carlo simulation of silver nanoparticles (nano-Ag). Sci Total Environ 449:418–425. doi:10.1016/j.scitotenv2013.01.078
7. Tiede K, Westerhoff P, Hansen SF, Fern GJ, Hankin SM, Aitken RJ, Chaudhry Q, Boxall A (2011) Review of the risks posed to drinking water by man-made nanoparticles. Food and Environment Research Agency. Available via http://dwi.defra.gov.uk/research/completed-esearch/reports/dwi70_2_246.pdf. Accessed 15 Oct 2014
8. Gottschalk F, Sonderer T, Scholz RW, Nowack B (2009) Modeled environmental concentrations of engineered nanomaterials (TiO_2, ZnO, Ag, CNT, fullerenes) for different regions. Environ Sci Technol 43(24):9216–9222. doi:10.1021/es9015553
9. Mueller NC, Nowack B (2008) Exposure modeling of engineered nanoparticles in the environment. Environ Sci Technol 42(12):4447–4453. doi:10.1021/es7029637
10. Sung JH, Ji JH, Yoon JU, Kim DS, Song MY, Jeong J, Han BS, Han JH, Chung YH, Kim J, Kim TS, Chang HK, Lee EJ, Lee JH, Yu IJ (2008) Lung function changes in Sprague-Dawley rats after prolonged inhalation exposure to silver nanoparticles. Inhal Toxicol 20(6):567–574. doi:10.1080/08958370701874671
11. Quadros ME, Marr LC (2010) Environmental and human health risks of aerosolized silver nanoparticles. J Air Waste Manage 60(7):770–781. doi:10.3155/1047–3289.60.7.770
12. Park J, Kwak BK, Bae E, Lee J, Kim Y, Choi K, Yi J (2009) Characterization of exposure to silver nanoparticles in a manufacturing facility. J Nanopart Res 11(7):1705–1712. doi:10.1007/s11051-009-9725-8
13. Gangwal S, Brown JS, Wang A, Houck KA, Dix DJ, Kavlock RJ, Hubal EAC (2011) Informing selection of nanomaterial concentrations for toxcast in vitro testing based on occupational exposure potential. Environ Health Persp 119(11):1539–1546. doi:10.1289/ehp.1103750
14. Walser T, Schwabe F, Thöni L, De Temmerman L, Hellweg S (2013) Nanosilver emissions to the atmosphere: a new challenge? E3S Web of Conferences 1:14003
15. Jankowska E, Lukaszewska J (2013) Potential exposure to silver nanoparticles during spraying preparation for air-conditioning cleaning. Med Pr 64(1):57–67. doi:0.13075/mp.5893/2013/0007
16. Hagendorfer H, Lorenz C, Kaegi R, Sinnet B, Gehrig R, Goetz NV, Scheringer M, Ludwig C, Ulrich A (2010) Size-fractionated characterization and quantification of nanoparticle release rates from a consumer spray product containing engineered nanoparticles. J Nanopart Res 12(7):2481–2494. doi:10.1007/s11051-009-9816-6
17. Quadros ME, Marr LC (2011) Silver nanoparticles and total aerosols emitted by nanotechnology-related consumer spray products. Environ Sci Technol 45(24):10713–10719. doi:10.1021/es202770m
18. Lorenz C, Hagendorfer H, von Goetz N, Kaegi R, Gehrig R, Ulrich A, Scheringer M, Hungerbuhler K (2011) Nanosized aerosols from consumer sprays: experimental analysis and exposure modeling for four commercial products. J Nanopart Res 13(8):3377–3391. doi:10.1007/s11051-011-0256-8
19. Lowry GV, Espinasse BP, Badireddy AR, Richardson CJ, Reinsch BC, Bryant LD, Bone AJ, Deonarine A, Chae S, Therezien M, Colman BP, Hsu-Kim H, Bernhardt ES, Matson CW, Wiesner MR (2012) Long-term transformation and fate of manufactured Ag nanoparticles in a simulated large scale freshwater emergent wetland. Environ Sci Technol 46(13):7027–7036. doi:10.1021/es204608d
20. Unrine JM, Colman BP, Bone AJ, Gondikas AP, Matson CW (2012) Biotic and abiotic interactions in aquatic microcosms determine fate and toxicity of Ag nanoparticles. Part 1. Aggregation and dissolution. Environ Sci Technol 46(13):6915–6924. doi:10.1021/es204682q
21 Bone AJ, Colman BP, Gondikas AP, Newton KM, Harrold KH, Cory RM, Unrine JM, Klaine SJ, Matson CW, Di Giulio RT (2012) Biotic and abiotic interactions in aquatic microcosms determine fate and toxicity of Ag nanoparticles. Part 2. Toxicity and Ag speciation. Environ Sci Technol 46(13):6925–6933. doi:10.1021/es204683m
22. Kaegi R, Voegelin A, Ort C, Sinnet B, Thalmann B, Krismer J, Hagendorfer H, Elumelu M, Mueller E (2013) Fate and transformation of silver nanoparticles in urban wastewater systems. Water Res 47(12):3866–3877. doi:10.1016/j.watres.2012.11.060

23. Kaegi R, Voegelin A, Sinnet B, Zuleeg S, Hagendorfer H, Burkhardt M, Siegrist H (2011) Behavior of metallic silver nanoparticles in a pilot wastewater treatment plant. Environ Sci Technol 45(9):3902–3908. doi:10.1021/es1041892
24. Li LXY, Hartmann G, Doblinger M, Schuster M (2013) Quantification of nanoscale silver particles removal and release from municipal wastewater treatment plants in Germany. Environ Sci Technol 47(13):7317–7323. doi: 10.1021/es3041658
25. Holder AL, Vejerano EP, Zhou XZ, Marr LC (2013) Nanomaterial disposal by incineration. Environ Sci-Process Impacts 15(9):1652–1664. doi:10.1039/c3em00224a
26. Ma R, Levard C, Judy JD, Unrine JM, Durenkamp M, Martin B, Jefferson B, Lowry GV (2014) Fate of zinc oxide and silver nanoparticles in a pilot wastewater treatment plant and in processed biosolids. Environ Sci Technol 48(1):104–112. doi:10.1021/es403646x
27. Lombi E, Donner E, Taheri S, Tavakkoli E, Jamting AK, McClure S, Naidu R, Miller BW, Scheckel KG, Vasilev K (2013) Transformation of four silver/silver chloride nanoparticles during anaerobic treatment of wastewater and post-processing of sewage sludge. Environ Pollut 176:193–197. doi:10.1016/j.envpol.2013.01.029
28. Pan B, Xing BS (2012) Applications and implications of manufactured nanoparticles in soils: a review. Eur J Soil Sci 63(4):437–456. doi:10.1111/j.1365-2389.2012.01475.x
29. Lin SH, Cheng YW, Bobcombe Y, Jones KL, Liu J, Wiesner MR (2011) Deposition of silver nanoparticles in geochemically heterogeneous porous media: predicting affinity from surface composition analysis. Environ Sci Technol 45(12):5209–5215. doi:10.1021/es2002327
30. Yang XY, Lin SH, Wiesner MR (2014) Influence of natural organic matter on transport and retention of polymer coated silver nanoparticles in porous media. J Hazard Mater 264:161–168. doi:10.1016/j.jhazmat.2013.11.025
31. Flory J, Kanel SR, Racz L, Impellitteri CA, Silva RG, Goltz MN (2013) Influence of pH on the transport of silver nanoparticles in saturated porous media: laboratory experiments and modeling. J Nanopart Res 15(3):1484. doi:10.1007/s11051–013-1484-x
32. Mittelman AM, Taghavy A, Wang YG, Abriola LM, Pennell KD (2013) Influence of dissolved oxygen on silver nanoparticle mobility and dissolution in water-saturated quartz sand. J Nanopart Res 15(7):UNSP1765. doi:10.1007/s11051-013-1765-4
33. El Badawy AM Hassan AA Scheckel KG Suidan MT Tolaymat TM (2013) Key factors controlling the transport of silver nanoparticles in porous media. Environ Sci Technol 47(9):4039–4045. doi:10.1021/es304580r
34. Tian YA, Gao B, Silvera-Batista C, Ziegler KJ (2010) Transport of engineered nanoparticles in saturated porous media. J Nanopart Res 12(7):2371–2380. doi:10.1007/s11051-010-9912-7
35. Neukum C, Braun A, Azzam R (2014) Transport of stabilized engineered silver (Ag) nanoparticles through porous sandstones. J Contam Hydrol 158:1–13. doi:10.1016/j.jconhyd.2013.12.002
36. Ren DJ, Smith JA (2013) Retention and transport of silver nanoparticles in a ceramic porous medium used for point-of-use water treatment. Environ Sci Technol 47(8):3825–3832. doi:10.1021/es4000752
37. Xiao Y, Wiesner MR (2013) Transport and retention of selected engineered nanoparticles by porous media in the presence of a biofilm. Environ Sci Technol 47(5):2246–2253. doi:10.1021/es304501n
38. Li Z, Hassan AA, Sahle-Demessie E, Sorial GA (2013) Transport of nanoparticles with dispersant through biofilm coated drinking water sand filters. Water Res 47(17):6457–6466. doi:10.1016/j.watres.2013.08.026
39. Mitzel MR, Tufenkji N (2014) Transport of industrial PVP-stabilized silver nanoparticles in saturated quartz sand coated with *Pseudomonas aeruginosa* PAO1 biofilm of variable age. Environ Sci Technol 48(5):2715–2723. doi:10.1021/es404598v
40. Whitley AR, Levard C, Oostveen E, Bertsch PM, Matocha CJ, von der Kammer F, Unrine JM (2013) Behavior of Ag nanoparticles in soil: effects of particle surface coating, aging and sewage sludge amendment. Environ Pollut 182:141–149. DOI:10.1016/j.envpol.2013.06.027
41. Cornelis G, Doolette C, Thomas M, McLaughlin MJ, Kirby JK, Beak DG, Chittleborough D (2012) Retention and dissolution of engineered silver nanoparticles in natural soils. Soil Sci Soc Am J 76(3):891–902. doi:10.2136/sssaj2011.0360

42. Cornelis G, Pang LP, Doolette C, Kirby JK, McLaughlin MJ (2013) Transport of silver nanoparticles in saturated columns of natural soils. Sci Total Environ 463:120–130. doi:10.1016/j.scitotenv.2013.05.089
43. Sagee O, Dror I, Berkowitz B (2012) Transport of silver nanoparticles (AgNPs) in soil. Chemosphere 88(5):670–675. doi:10.1016/j.chemosphere.2012.03.055
44. Liang Y, Bradford SA, Simunek J, Heggen M, Vereecken H, Klumpp E (2013) Retention and remobilization of stabilized silver nanoparticles in an undisturbed loamy sand soil. Environ Sci Technol 47(21):12229–12237. doi:10.1021/es402046u
45. Liang Y, Bradford SA, Simunek J, Vereecken H, Klumpp E (2013) Sensitivity of the transport and retention of stabilized silver nanoparticles to physicochemical factors. Water Res 47(7):2572–2582. doi:10.1016/j.watres.2013.02.025
46. Emerson HP, Hart AE, Baldwin JA, Waterhouse TC, Kitchens CL, Mefford OT, Powell BA (2014) Physical transformations of iron oxide and silver nanoparticles from an intermediate scale field transport study. J Nanopart Res 16(2):2258. doi:10.1007/s11051-014-2258–9
47. Ma XM, Geiser-Lee J, Deng Y, Kolmakov A (2010) Interactions between engineered nanoparticles (ENPs) and plants: phytotoxicity, uptake and accumulation. Sci Total Environ 408(16):3053–3061. doi:10.1016/j.scitotenv.2010.03.031
48. Rico CM, Majumdar S, Duarte-Gardea M, Peralta-Videa JR, Gardea-Torresdey JL (2011) Interaction of nanoparticles with edible plants and their possible implications in the food chain. J Agric Food Chem 59(8):3485–3498. doi:10.1021/jf104517j
49. Dimkpa CO, McLean JE, Martineau N, Britt DW, Haverkamp R, Anderson AJ (2013) Silver nanoparticles disrupt wheat (*Triticum aestivum* L.) growth in a sand matrix. Environ Sci Technol 47(2):1082–1090. doi:10.1021/es302973y
50. Geisler-Lee J, Wang Q, Yao Y, Zhang W, Geisler M, Li KG, Huang Y, Chen YS, Kolmakov A, Ma XM (2013) Phytotoxicity, accumulation and transport of silver nanoparticles by *Arabidopsis thaliana*. Nanotoxicology 7(3):323–337. doi:10.3109/17435390.2012.658094
51. Stampoulis D, Sinha SK, White JC (2009) Assay-dependent phytotoxicity of nanoparticles to plants. Environ Sci Technol 43 (24):9473–9479. doi:10.1021/es901695c
52. Thuesombat P, Hannongbua S, Akasit S, Chadchawan S (2014) Effect of silver nanoparticles on rice (*Oryza sativa* L. cv. KDML 105) seed germination and seedling growth. Ecotoxicol Environ Saf 104:302–309. doi:10.1016/j.ecoenv.2014.03.022
53. Lee WM, Kwak JI, An YJ (2012) Effect of silver nanoparticles in crop plants *Phaseolus radiatus* and *Sorghum bicolor*: media effect on phytotoxicity. Chemosphere 86(5):491–499. doi:10.1016/j.chemosphere.2011.10.013
54. Song U, Jun H, Waldman B, Roh J, Kim Y, Yi J, Lee EJ (2013) Functional analyses of nanoparticle toxicity: a comparative study of the effects of TiO_2 and Ag on tomatoes (*Lycopersicon esculentum*). Ecotoxicol Environ Saf 93:60–67. doi:10.1016/j.ecoenv.2013.03.033
55. Wang J, Koo Y, Alexander A, Yang Y, Westerhof S, Zhang QB, Schnoor JL, Colvin VL, Braam J, Alvarez PJJ (2013) Phytostimulation of Poplars and Arabidopsis exposed to silver nanoparticles and Ag^+ at sublethal concentrations. Environ Sci Technol 47(10):5442–5449. doi:10.1021/es4004334
56. Hawthorne J, Musante C, Sinha SK, White JC (2012) Accumulation and phytotoxicity of engineered nanoparticles to *Cucurbita Pepo*. Int J Phytoremediation 14(4):429–442. doi:10.1080/15226514.2011.620903
57. Krishnaraj C, Jagan EG, Ramachandran R, Abirami SM, Mohan N, Kalaichelvan PT (2012) Effect of biologically synthesized silver nanoparticles on *Bacopa monnieri* (Linn.) Wettst. plant growth metabolism. Process Biochem 47(4):651–658. doi:10.1016/j.procbio.2012.01.006
58. Petosa AR, Jaisi DP, Quevedo IR, Elimelech M, Tufenkji N (2010) Aggregation and deposition of engineered nanomaterials in aquatic environments: role of physicochemical interactions. Environ Sci Technol 44(17):6532–6549. doi:10.1021/es100598h
59. Levard C, Hotze EM, Lowry GV, Brown GE (2012) Environmental transformations of silver nanoparticles: impact on stability and toxicity. Environ Sci Technol 46(13):6900–6914. doi:10.1021/es2037405

60. Yu SJ, Yin YG, Chao JB, Shen MH, Liu JF (2014) Highly dynamic PVP-coated silver nanoparticles in aquatic environments: chemical and morphology change induced by oxidation of Ag^0 and reduction of Ag^+. Environ Sci Technol 48(1):403–411. doi:10.1021/es404334a
61. Li Y, Niu JF, Shang EX, Crittenden J (2014) Photochemical transformation and photoinduced toxicity reduction of silver nanoparticles in the presence of perfluorocarboxylic acids under UV irradiation. Environ Sci Technol 48(9):4946–4953. doi:10.1021/es500596a
62. Philippe A, Schaumann GE (2014) Interactions of dissolved organic matter with natural and engineered inorganic colloids: a review. Environ Sci Technol 48(16):8946–8962. doi:10.1021/es502342r
63. Sanchez-Cortes S, Francioso O, Ciavatta C, Garcia-Ramos JV, Gessa C (1998) pH-dependent adsorption of fractionated peat humic substances on different silver colloids studied by surface-enhanced Raman spectroscopy. J Colloid Interface Sci 198(2):308–318. doi:10.1006/jcis.1997.5293
64. Lau BLT, Hockaday WC, Ikuma K, Furman O, Decho AW (2013) A preliminary assessment of the interactions between the capping agents of silver nanoparticles and environmental organics. Colloid Surf A 435:22–27. doi:10.1016/j.colsurfa.2012.11.065
65. Khan SS, Mukherjee A, Chandrasekaran N (2011) Impact of exopolysaccharides on the stability of silver nanoparticles in water. Water Res 45(16):5184–5190. doi:10.1016/j.watres.2011.07.024
66. Gebauer JS, Malissek M, Simon S, Knauer SK, Maskos M, Stauber RH, Peukert W, Treuel L (2012) Impact of the nanoparticle-protein corona on colloidal stability and protein structure. Langmuir 28(25):9673–9679. doi:10.1021/La301104a
67. Ostermeyer AK, Mumuper CK, Semprini L, Radniecki T (2013) Influence of bovine serum albumin and alginate on silver nanoparticle dissolution and toxicity to *Nitrosomonas europaea*. Environ Sci Technol 47(24):14403–14410. doi:10.1021/es4033106
68. Shang L, Dorlich RM, Trouillet V, Bruns M, Nienhaus GU (2012) Ultrasmall fluorescent silver nanoclusters: protein adsorption and its effects on cellular responses. Nano Res 5(8):531–542. doi:10.1007/s12274-012-0238-x
69. Wigginton NS, De Titta A, Piccapietra F, Dobias J, Nesatty VJ, Suter MJF, Bernier-Latmani R (2010) Binding of silver nanoparticles to bacterial proteins depends on surface modifications and inhibits enzymatic activity. Environ Sci Technol 44(6):2163–2168. doi:10.1021/Es903187s
70. Ravindran A, Singh A, Raichur AM, Chandrasekaran N, Mukherjee A (2010) Studies on interaction of colloidal Ag nanoparticles with bovine serum albumin (BSA). Colloid Surf B 76(1):32–37. doi:10.1016/j.colsurfb.2009.10.005
71. Voicescu M, Ionescu S, Angelescu DG (2012) Spectroscopic and coarse-grained simulation studies of the BSA and HSA protein adsorption on silver nanoparticles. J Nanopart Res 14(10):1174. doi:10.1007/s11051-012-1174-0
72. Podila R, Chen R, Ke PC, Brown JM, Rao AM (2012) Effects of surface functional groups on the formation of nanoparticle-protein corona. Appl Phys Lett 101(26):263701. doi:10.1063/1.4772509
73. Shannahan JH, Lai XY, Ke PC, Podila R, Brown JM, Witzmann FA (2013) Silver nanoparticle protein corona composition in cell culture media. PLoS One 8(9):e74001. doi:10.1371/journal.pone.0074001
74. Gan W, Xu BL, Dai HL (2011) Activation of thiols at a silver nanoparticle surface. Angew Chem Int Ed Engl 50(29):6622–6625. doi:10.1002/anie.201101430
75. Huang GG, Han XX, Hossain MK, Kitahama Y, Ozaki Y (2010) A study of glutathione molecules adsorbed on silver surfaces under different chemical environments by surface-enhanced Raman scattering in combination with the heat-induced sensing method. Appl Spectrosc 64(10):1100–1108. doi: 10.1366/000370210792973523
76. Jing CY, Fang Y (2007) Experimental (SERS) and theoretical (DFT) studies on the adsorption behaviors of L-cysteine on gold/silver nanoparticles. Chem Phys 332(1):27–32. doi:10.1016/j.chemphys.2006.11.019

77. Bonifacio A, Dalla Marta S, Spizzo R, Cervo S, Steffan A, Colombatti A, Sergo V (2014) Surface-enhanced Raman spectroscopy of blood plasma and serum using Ag and Au nanoparticles: a systematic study. Anal Bioanal Chem 406(9–10):2355–2365. doi:10.1007/s00216-014-7622-1
78. Wang CY, Liu CY, Wang M, Shen T (1999) Spectroscopic studies of thiocyanate in silver hydrosol and the influence of halide ions. Spectrochimca Acta A 55(5):991–998. doi:10.1016/S1386-1425(98)00240-6
79. Lee PC, Meisel D (1982) Adsorption and surface-enhanced Raman of dyes on silver and gold sols. J Phys Chem-Us 86(17):3391–3395. doi:10.1021/j100214a025
80. Barthelmes J, Plieth W (1995) Sers investigations on the adsorption of pyridine carboxylic-acids on silver—influence of pH and supporting electrolyte. Electrochimca Acta 40(15):2487–2490. doi:10.1016/0013-4686(95)00103-L
81. Du JJ, Cui JL, Jing CY (2014) Rapid in situ identification of arsenic species using a portable Fe_3O_4@Ag SERS sensor. Chem Commun 50(3):347–349. doi:10.1039/c3cc46920d
82. Garrell RL, Shaw KD, Krimm S (1983) Surface enhanced Raman-spectroscopy of halide-ions on colloidal silver—morphology and coverage dependence. Surf Sci 124(2–3):613–624. doi:10.1016/0039-6028(83)90815-4
83. Bell SEJ, Sirimuthu NMS (2005) Surface-enhanced Raman spectroscopy as a probe of competitive binding by anions to citrate-reduced silver colloids. J Phys Chem A 109(33):7405–7410. doi:10.1021/jp052184f
84. Gondikas AP, Morris A, Reinsch BC, Marinakos SM, Lowry GV, Hsu-Kim H (2012) Cysteine-induced modifications of zero-valent silver nanomaterials: implications for particle surface chemistry, aggregation, dissolution, and silver speciation. Environ Sci Technol 46(13):7037–7045. doi:10.1021/es3001757
85. Kim KJ, Sung WS, Moon SK, Choi JS, Kim JG, Lee DG (2008) Antifungal effect of silver nanoparticles on dermatophytes. J Microbiol Biotechnol 18(8):1482–1484
86. Yang Y, Gajaraj S, Wall JD, Hu ZQ (2013) A comparison of nanosilver and silver ion effects on bioreactor landfill operations and methanogenic population dynamics. Water Res 47(10):3422–3430. doi:10.1016/j.watres.2013.03.040
87. Visnapuu M, Joost U, Juganson K, Kunnis-Beres K, Kahru A, Kisand V, Ivask A (2013) Dissolution of silver nanowires and nanospheres dictates their toxicity to *Escherichia coli*. Biomed Res Int 2013:819252–819260. doi:10.1155/2013/819252
88. Kennedy AJ, Hull MS, Bednar AJ, Goss JD, Gunter JC, Bouldin JL, Vikesland PJ, Steevens JA (2010) Fractionating nanosilver: importance for determining toxicity to aquatic test organisms. Environ Sci Technol 44(24):9571–9577. doi:10.1021/es1025382
89. Xiu ZM, Zhang QB, Puppala HL, Colvin VL, Alvarez PJJ (2012) Negligible particle-specific antibacterial activity of silver nanoparticles. Nano Lett 12(8):4271–4275. doi:10.1021/nl301934w
90. Newton KM, Puppala HL, Kitchens CL, Colvin VL, Klaine SJ (2013) Silver nanoparticle toxicity to *Daphnia magna* is a function of dissolved silver concentration. Environ Toxicol Chem 32(10):2356–2364. doi:10.1002/etc.2300
91. Angel BM, Batley GE, Jarolimek CV, Rogers NJ (2013) The impact of size on the fate and toxicity of nanoparticulate silver in aquatic systems. Chemosphere 93(2):359–365. doi:10.1016/j.chemosphere.2013.04.096
92. Sotiriou GA, Meyer A, Knijnenburg JTN, Panke S, Pratsinis SE (2012) Quantifying the origin of released Ag^+ ions from nanosilver. Langmuir 28(45):15929–15936. doi:10.1021/la303370d
93. Dobias J, Bernier-Latmani R (2013) Silver release from silver nanoparticles in natural waters. Environ Sci Technol 47(9):4140–4146. doi:10.1021/es304023p
94. Liu JY, Hurt RH (2010) Ion release kinetics and particle persistence in aqueous nano-silver colloids. Environ Sci Technol 44(6):2169–2175. doi:10.1021/es9035557
95. Liu JY, Sonshine DA, Shervani S, Hurt RH (2010) Controlled release of biologically active silver from nanosilver surfaces. ACS Nano 4(11):6903–6913. doi:10.1021/nn102272n
96. Zhang W, Yao Y, Sullivan N, Chen YS (2011) Modeling the primary size effects of citrate-coated silver nanoparticles on their ion release kinetics. Environ Sci Technol 45(10):4422–4428. doi:10.1021/es104205a

97. Ho CM, Wong CK, Yau SKW, Lok CN, Che CM (2011) Oxidative dissolution of silver nanoparticles by dioxygen: a kinetic and mechanistic study. Chem-Asian J 6(9):2506–2511. doi:10.1002/asia.201100034
98. Ma R, Levard C, Marinakos SM, Cheng YW, Liu J, Michel FM, Brown GE, Lowry GV (2012) Size-controlled dissolution of organic-coated silver nanoparticles. Environ Sci Technol 46(2):752–759. doi:10.1021/es201686j
99. Li X, Lenhart JJ (2012) Aggregation and dissolution of silver nanoparticles in natural surface water. Environ Sci Technol 46(10):5378–5386. doi:10.1021/es204531y
100. Ho CM, Yau SKW, Lok CN, So MH, Che CM (2010) Oxidative dissolution of silver nanoparticles by biologically relevant oxidants: a kinetic and mechanistic study. Chem-Asian J 5(2):285–293. doi:10.1002/asia.200900387
101. He D, Garg S, Waite TD (2012) H_2O_2-mediated oxidation of zero-valent silver and resultant interactions among silver nanoparticles, silver ions, and reactive oxygen species. Langmuir 28(27):10266–10275. doi:10.1021/la300929g
102. Yuan ZH, Chen YB, Li TT, Yu CP (2013) Reaction of silver nanoparticles in the disinfection process. Chemosphere 93(4):619–625. doi:10.1016/j.chemosphere.2013.06.010
103. Maurer-Jones MA, Mousavi MPS, Chen LD, Buhlmann P, Haynes CL (2013) Characterization of silver ion dissolution from silver nanoparticles using fluorous-phase ion-selective electrodes and assessment of resultant toxicity to *Shewanella oneidensis*. Chem Sci 4(6):2564–2572. doi:10.1039/c3sc50320h
104. Mumper CK, Ostermeyer AK, Semprini L, Radniecki TS (2013) Influence of ammonia on silver nanoparticle dissolution and toxicity to *Nitrosomonas europaea*. Chemosphere 93(10):2493–2498. doi:10.1016/j.chemosphere.2013.08.098
105. Levard C, Reinsch BC, Michel FM, Oumahi C, Lowry GV, Brown GE (2011) Sulfidation processes of PVP-coated silver nanoparticles in aqueous solution: impact on dissolution rate. Environ Sci Technol 45(12):5260–5266. doi:10.1021/es2007758
106. Levard C, Mitra S, Yang T, Jew AD, Badireddy AR, Lowry GV, Brown GE (2013) Effect of chloride on the dissolution rate of silver nanoparticles and toxicity to *E. coli*. Environ Sci Technol 47(11):5738–5745. doi:10.1021/es400396f
107. Grillet N, Manchon D, Cottancin E, Bertorelle F, Bonnet C, Broyer M, Lerme J, Pellarin M (2013) Photo-oxidation of individual silver nanoparticles: a real-time tracking of optical and morphological changes. J Phys Chem C 117(5):2274–2282. doi:10.1021/jp311502h
108. Tejamaya M, Romer I, Merrifield RC, Lead JR (2012) Stability of citrate, PVP, and PEG coated silver nanoparticles in ecotoxicology media. Environ Sci Technol 46(13):7011–7017. doi:10.1021/es2038596
109. He D, Bligh MW, Waite TD (2013) Effects of aggregate structure on the dissolution kinetics of citrate-stabilized silver nanoparticles. Environ Sci Technol 47(16):9148–9156. doi:10.1021/es400391a
110. Cheng YW, Yin LY, Lin SH, Wiesner M, Bernhardt E, Liu J (2011) Toxicity reduction of polymer-stabilized silver nanoparticles by sunlight. J Phys Chem C 115(11):4425–4432. doi:10.1021/jp109789j
111. Glover RD, Miller JM, Hutchison JE (2011) Generation of metal nanoparticles from silver and copper objects: nanoparticle dynamics on surfaces and potential sources of nanoparticles in the environment. ACS Nano 5(11):8950–8957. doi:10.1021/nn2031319
112. Shi JP, Ma CY, Xu B, Zhang HW, Yu CP (2012) Effect of light on toxicity of nanosilver to *Tetrahymena pyriformis*. Environ Toxicol Chem 31(7):1630–1638. doi:10.1002/etc.1864
113. Pettibone JM, Gigault J, Hackley VA (2013) Discriminating the states of matter in metallic nanoparticle transformations: what are we missing? ACS Nano 7(3):2491–2499. doi:10.1021/nn3058517
114. Shi JP, Xu B, Sun X, Ma CY, Yu CP, Zhang HW (2013) Light induced toxicity reduction of silver nanoparticles to *Tetrahymena Pyriformis*: effect of particle size. Aquat Toxicol 132:53–60. doi:10.1016/j.aquatox.2013.02.001
115. Yu WL, Borkovec M (2002) Distinguishing heteroaggregation from homoaggregation in mixed binary particle suspensions by multiangle static and dynamic light scattering. J Phys Chem B 106(51):13106–13110. doi:10.1021/jp021792h

116. Park JW, Oh JH, Kim WK, Lee SK (2014) Toxicity of citrate-coated silver nanoparticles differs according to method of suspension preparation. B Environ Contam Tox 93(1):53–59. doi:10.1007/s00128-014-1296-4
117. Huynh KA, McCaffery JM, Chen KL (2014) Heteroaggregation reduces antimicrobial activity of silver nanoparticles: evidence for nanoparticle–cell proximity effects. Environ Sci Technol Lett 1(9):361–366. doi:10.1021/ez5002177
118. El Badawy AM Luxton TP Silva RG Scheckel KG Suidan MT Tolaymat TM (2010) Impact of environmental conditions (pH, ionic strength, and electrolyte type) on the surface charge and aggregation of silver nanoparticles suspensions. Environ Sci Technol 44(4):1260–1266. doi:10.1021/es902240k
119. Huynh KA, Chen KL (2011) Aggregation kinetics of citrate and polyvinylpyrrolidone coated silver nanoparticles in monovalent and divalent electrolyte solutions. Environ Sci Technol 45(13):5564–5571. doi:10.1021/es200157h
120. Li X, Lenhart JJ, Walker HW (2012) Aggregation kinetics and dissolution of coated silver nanoparticles. Langmuir 28(2):1095–1104. doi:10.1021/la202328n
121. Zook JM, Halter MD, Cleveland D, Long SE (2012) Disentangling the effects of polymer coatings on silver nanoparticle agglomeration, dissolution, and toxicity to determine mechanisms of nanotoxicity. J Nanopart Res 14(10):1165. doi: 10.1007/S11051-012-1165-1
122. Khan SS, Srivatsan P, Vaishnavi N, Mukherjee A, Chandrasekaran N (2011) Interaction of silver nanoparticles (SNPs) with bacterial extracellular proteins (ECPs) and its adsorption isotherms and kinetics. J Hazard Mater 192(1):299–306. doi: 10.1016/j.jhazmat.2011.05.024
123. Zhang W, Yao Y, Li KG, Huang Y, Chen YS (2011) Influence of dissolved oxygen on aggregation kinetics of citrate-coated silver nanoparticles. Environ Pollut 159(12):3757–3762 doi:10.1016/j.envpol.2011.07.013
124. Baalousha M, Nur Y, Romer I, Tejamaya M, Lead JR (2013) Effect of monovalent and divalent cations, anions and fulvic acid on aggregation of citrate-coated silver nanoparticles. Sci Total Environ 454:119–131. doi:10.1016/j.scitotenv.2013.02.093
125. Akaighe N, Depner SW, Banerjee S, Sharma VK, Sohn M (2012) The effects of monovalent and divalent cations on the stability of silver nanoparticles formed from direct reduction of silver ions by Suwannee river humic acid/natural organic matter. Sci Total Environ 441:277–289. doi:10.1016/j.scitotenv.2012.09.055
126. Skoglund S, Lowe TA, Hedberg J, Blomberg E, Wallinder IO, Wold S, Lundin M (2013) Effect of laundry surfactants on surface charge and colloidal stability of silver nanoparticles. Langmuir 29(28):8882–8891. doi:10.1021/la4012873
127. Zhou DX, Abdel-Fattah AI, Keller AA (2012) Clay particles destabilize engineered nanoparticles in aqueous environments. Environ Sci Technol 46(14):7520–7526. doi:10.1021/es3004427
128. Chinnapongse SL, MacCuspie RI, Hackley VA (2011) Persistence of singly dispersed silver nanoparticles in natural freshwaters, synthetic seawater, and simulated estuarine waters. Sci Total Environ 409(12):2443–2450. doi:10.1016/j.scitotenv.2011.03.020
129. Piccapietra F, Sigg L, Behra R (2012) Colloidal stability of carbonate-coated silver nanoparticles in synthetic and natural freshwater. Environ Sci Technol 46(2):818–825. doi:10.1021/Es202843h
130. Quik JTK, Velzeboer I, Wouterse M, Koelmans AA, van de Meent D (2014) Heteroaggregation and sedimentation rates for nanomaterials in natural waters. Water Res 48:269–279. doi:10.1016/j.watres.2013.09.036
131. Gao J, Youn S, Hovsepyan A, Llaneza VL, Wang Y, Bitton G, Bonzongo JCJ (2009) Dispersion and toxicity of selected manufactured nanomaterials in natural river water samples: effects of water chemical composition. Environ Sci Technol 43(9):3322–3328. doi:10.1021/es803315v
132. Kiser MA, Ryu H, Jang HY, Hristovski K, Westerhoff P (2010) Biosorption of nanoparticles to heterotrophic wastewater biomass. Water Res 44(14):4105–4114. doi:10.1016/j.watres.2010.05.036
133. Sun Q, Li Y, Tang T, Yuan ZH, Yu CP (2013) Removal of silver nanoparticles by coagulation processes. J Hazard Mater 261:414–420. doi:10.1016/j.jhazmat.2013.07.066

134. Stebounova LV, Guio E, Grassian VH (2011) Silver nanoparticles in simulated biological media: a study of aggregation, sedimentation, and dissolution. J Nanopart Res 13(1):233–244. doi:10.1007/s11051-010-0022-3
135. Lytle PE (1984) Fate and speciation of silver in publicly owned treatment works. Environ Toxicol Chem 3(1):21–30. doi:10.1002/etc.5620030104
136. Anderson PR, O'Conner C, Bunker G (1997) X-ray absorption spectroscopy study of model silver compounds. Paper presented at the the 5th international conference proceedings of transport, fate and effects of silver in the environment, Hamilton, Ontario, Canada
137. Choi O, Cleuenger TE, Deng BL, Surampalli RY, Ross L, Hu ZQ (2009) Role of sulfide and ligand strength in controlling nanosilver toxicity. Water Res 43(7):1879–1886. doi:10.1016/j.watres.2009.01.029
138. Kim B, Park CS, Murayama M, Hochella MF (2010) Discovery and characterization of silver sulfide nanoparticles in final sewage sludge products. Environ Sci Technol 44(19):7509–7514. doi:10.1021/es101565j
139. Liu JY, Pennell KG, Hurt RH (2011) Kinetics and mechanisms of nanosilver oxysulfidation. Environ Sci Technol 45(17):7345–7353. doi: 10.1021/es201539s
140. Thalmann B, Voegelin A, Sinnet B, Morgenroth E, Kaegi R (2014) Sulfidation kinetics of silver nanoparticles reacted with metal sulfides. Environ Sci Technol 48(9):4885–4892. doi:10.1021/es5003378
141. Liu ZH, Zhou Y, Maszenan AM, Ng WJ, Liu Y (2013) pH-dependent transformation of Ag nanoparticles in anaerobic processes. Environ Sci Technol 47(22):12630–12631. doi:10.1021/es404514 g
142. Kent R, Oser J, Vikesland PJ (2014) Controlled evaluation of silver nanoparticle sulfidation in a full-scale wastewater treatment plant. Environ Sci Technol 48(15):8564–8572. doi:10.1021/es404989t
143. Reinsch BC, Levard C, Li Z, Ma R, Wise A, Gregory KB, Brown GE, Lowry GV (2012) Sulfidation of silver nanoparticles decreases *Escherichia coli* growth inhibition. Environ Sci Technol 46(13):6992–7000. doi:10.1021/es203732x
144. Doolette CL, McLaughlin MJ, Kirby JK, Batstone DJ, Harris HH, Ge HQ, Cornelis G (2013) Transformation of PVP coated silver nanoparticles in a simulated wastewater treatment process and the effect on microbial communities. Chem Cent J 7:46. doi:10.1186/1752-153X-7-46
145. VandeVoort AR, Tappero R, Arai Y (2014) Residence time effects on phase transformation of nanosilver in reduced soils. Environ Sci Pollut R 21(13):7828–7837. doi:10.1007/s11356-014-2743-9
146. Chen S, Theodorou IG, Goode AE, Gow A, Schwander S, Zhang JF, Chung KF, Tetley TD, Shaffer MS, Ryan MP, Porter AE (2013) High-resolution analytical electron microscopy reveals cell culture media-induced changes to the chemistry of silver nanowires. Environ Sci Technol 47(23):13813–13821. doi:10.1021/es403264d
147. Chen S, Goode AE, Sweeney S, Theodorou IG, Thorley AJ, Ruenraroengsak P, Chang Y, Gow A, Schwander S, Skepper J, Zhang JF, Shaffer MS, Chung KF, Tetley TD, Ryan MP, Porter AE (2013) Sulfidation of silver nanowires inside human alveolar epithelial cells: a potential detoxification mechanism. Nanoscale 5(20):9839–9847. doi:10.1039/c3nr03205a
148. Motte L, Urban J (2005) Silver clusters on silver sulfide nanocrystals: synthesis and behavior after electron beam irradiation. J Phys Chem B 109(46):21499–21501. doi:10.1021/jp0542322
149. Bourret GR, Lennox RB (2011) Electrochemical synthesis of Ag(0)/Ag_2S heterojunctions templated on pre-formed Ag_2S nanowires. Nanoscale 3(4):1838–1844. doi:10.1039/c0nr00886a
150. Di Toro DM, Mahony JD, Carbonaro RF, DeMarco T, Morrissey JC, Pablo RJ, Page JJ, Shadi TS (1997) The oxidation of silver sulfide and other heavy metal sulfides in sediments. Paper presented at the the 5th international conference proceedings of transport, fate and effects of silver in the environment, Hamilton, Ontario, Canada

151. Manolopoulos H, Adams NWH, Kramer JR (1996) Oxidation of silver-bearing iron sulfides: a preliminary study. Paper presented at the the 4th international conference proceedings of transport, fate and effects of silver in the environment, Madison, Wisconsin
152. Dale AL, Lowry GV, Casman EA (2013) Modeling nanosilver transformations in freshwater sediments. Environ Sci Technol 47(22):12920–12928. doi:10.1021/es402341t
153. Liu JY, Wang ZY, Liu FD, Kane AB, Hurt RH (2012) Chemical transformations of nanosilver in biological environments. ACS Nano 6(11):9887–9899. doi:10.1021/nn303449n
154. Li ZQ, Reinsch BC, Ma R, Gregory KB, Lowry GV (2010) Sulfidation eliminates bactericidal effects of silver nanoparticles to *Escherichia coli*. Abstr Pap Am Chem S 240
155. Levard C, Hotze EM, Colman BP, Dale AL, Truong L, Yang XY, Bone AJ, Brown GE, Tanguay RL, Di Giulio RT, Bernhardt ES, Meyer JN, Wiesner MR, Lowry GV (2013) Sulfidation of silver nanoparticles: natural antidote to their toxicity. Environ Sci Technol 47(23):13440–13448. doi:10.1021/es403527n
156. Gherrou A, Kerdjoudj H, Molinari R, Drioli E (2002) Removal of silver and copper ions from acidic thiourea solutions with a supported liquid membrane containing D2EHPA as carrier. Sep Purif Technol 28(3):235–244. doi:10.1016/S1383-5866(02)00080-1
157. Zhang SK, Du C, Wang ZZ, Han XG, Zhang K, Liu LH (2013) Reduced cytotoxicity of silver ions to mammalian cells at high concentration due to the formation of silver chloride. Toxicol in Vitro 27(2):739–744. doi:10.1016/j.tiv.2012.12.003
158. Andryushechkin BV, Eltsov KN, Shevlyuga VM (1999) Atomic structure of silver chloride formed on Ag(111) surface upon low temperature chlorination. Surf Sci 433:109–113. doi:10.1016/S0039-6028(99)00058-8
159. Andryushechkin BV, Eltsov KN, Shevlyuga VM, Yurov VY (1999) Direct STM observation of surface modification and growth of AgCl islands on Ag(111) upon chlorination at room temperature. Surf Sci 431(1–3):96–108. doi:10.1016/s0039-6028(99)00429-x
160. Andryushechkin BV, Eltsov KN, Shevlyuga VM, Tarducci C, Cortigiani B, Bardi U, Atrei A (1999) Epitaxial growth of AgCl layers on the Ag(100) surface. Surf Sci 421(1–2):27–32. doi:10.1016/S0039-6028(98)00801-2
161. Impellitteri CA, Tolaymat TM, Scheckel KG (2009) The speciation of silver nanoparticles in antimicrobial fabric before and after exposure to a hypochlorite/detergent solution. J Environ Qual 38(4):1528–1530. doi:10.2134/jeq2008.0390
162. Lorenz C, Windler L, von Goetz N, Lehmann RP, Schuppler M, Hungerbuhler K, Heuberger M, Nowack B (2012) Characterization of silver release from commercially available functional (nano)textiles. Chemosphere 89(7):817–824. doi:10.1016/j.chemosphere.2012.04.063
163. Mitrano DM, Rimmele E, Wichser A, Erni R, Height M, Nowack B (2014) Presence of nanoparticles in wash water from conventional silver and nano-silver textiles. ACS Nano 8(7):7208–7219. doi:10.1021/nn502228w
164. Rogers KR, Bradham K, Tolaymat T, Thomas DJ, Hartmann T, Ma LZ, Williams A (2012) Alterations in physical state of silver nanoparticles exposed to synthetic human stomach fluid. Sci Total Environ 420:334–339. doi:10.1016/j.scitotenv.2012.01.044
165. Scheckel KG, Luxton TP, El Badawy AM, Impellitteri CA, Tolaymat TM (2010) Synchrotron speciation of silver and zinc oxide nanoparticles aged in a kaolin suspension. Environ Sci Technol 44(4):1307–1312. doi:10.1021/es9032265
166. Chambers BA, Afrooz ARMN, Bae S, Aich N, Katz L, Saleh NB, Kirisits MJ (2014) Effects of chloride and ionic strength on physical morphology, dissolution, and bacterial toxicity of silver nanoparticles. Environ Sci Technol 48(1):761–769. doi:10.1021/es403969x
167. Wang G, Nishio T, Sato M, Ishikawa A, Nambara K, Nagakawa K, Matsuo Y, Niikura K, Ijiro K (2011) Inspiration from chemical photography: accelerated photoconversion of AgCl to functional silver nanoparticles mediated by DNA. Chem Commun 47(33):9426–9428. doi:10.1039/c1cc13385c

Chapter 5
Toxicological Effects and Mechanisms of Silver Nanoparticles

Qunfang Zhou, Wei Liu, Yanmin Long, Cheng Sun and Guibin Jiang

Abstract Silver compounds have been used for centuries in health care products as an antiseptic. Currently, the use of silver nanoparticles (AgNPs) in consumer products is increasing. There are emerging concerns on the possible contribution of AgNPs to environmental and human toxicity. In this chapter, we summarize the toxicological effects of AgNPs, and discuss the toxicological mechanisms and potential influencing factors. The specific risk assessment for AgNPs is not feasible as information on possible long term effects at environmental relevant doses are lacking.

Silver and silver products have been known for thousands of years because of their prestige and effect in hygiene. With the rapid development of nanotechnology, silver-based nanomaterials are increasingly used in a wide range of applications nowadays. It can be expected that the exposure of silver is inevitable due to its release in ion or particle forms from versatile usages of silver nanoparticles (AgNPs). The activity that makes them desirable as an antimicrobial agent could also pose a threat to the microbial communities in the environment as well as some other nontarget living species. Although the current exposure level of AgNPs may not be extremely hazardous to humans or environmental organisms, it may result in low internal exposure. Accordingly, concerns about their negative biological effects on environmental species and human health are arising.

During the past decade, abundant studies have been carried out on the evaluation of environmental toxicity and potential human health hazards for various AgNPs materials. The diverse toxic phenotypes in environmental and human health

Q. Zhou (✉) · Y. Long · C. Sun · G. Jiang
State Key Laboratory of Environmental Chemistry and Ecotoxicology,
Research Center for Eco-Environmental Sciences, Chinese Academy of Sciences,
P.O. Box 2871, 100085 Beijing, China
e-mail: zhouqf@rcees.ac.cn

W. Liu
Institute of Chemical Safety, Chinese Academy of Inspection and Quarantine,
100123 Beijing, China

G. Jiang
e-mail: gbjiang@rcees.ac.cn

J. Liu, G. Jiang (eds.), *Silver Nanoparticles in the Environment,*
DOI 10.1007/978-3-662-46070-2_5

including general toxicity, cytotoxicity, immune responses and allergies, dermal toxicity, genotoxicities, reproductive and developmental toxicity, were described in multiple experimental models by simulative tests in vitro and in vivo. Lots of efforts have been contributed to clarify the molecular mechanisms of AgNPs induced toxicities. The high attention mainly focused on the following questions: what kind of toxicity can AgNPs cause; how does AgNPs regulate its toxicities in organisms; what can affect AgNPs' biological effects. To address these questions, toxicological effects and mechanisms of AgNPs were reviewed in this chapter. The toxicological effects induced by AgNPs in various models were summarized firstly. The discussion was subsequently carried out on the mechanism of AgNPs focusing on reactive oxygen species (ROS) involved or silver ion release dependent effects. The factors which may influence AgNPs' toxicity were summarized in the end. Despite of the abundant toxicological data available, current knowledge on the hazards of AgNPs is still too limited to draw general conclusions.

5.1 Toxicological Effects in Various Models

It is widely reported that AgNPs may cause toxicological effects in various models including microbial toxicity, genotoxicity and cellular toxicity, toxicities in aquatic organisms, terrestrial species and mammals, and potential hazards to human health.

5.1.1 Microbial Toxicity

AgNPs, as a broad-spectrum antimicrobial agent, are currently the most widely commercialized nanomaterial [1, 2] to control bacterial growth in dental work, catheters, and burn wounds. As shown in the study [3, 4], 10 nm AgNPs damaged the cell membrane of *Escherichia coli* and declined the membrane potential. This anti-bacteria pattern is similar to silver ions. AgNPs possess antimicrobial activity in a wide range, they can inhibit many Gram-positive and -negative bacteria such as *Escherichia coli, Pseudomonas aeruginosa, Salmonella, Vibrio, Clostridium, Enterococcus, Streptococcus, Lester bacteria,* and so on [5–8]. While, it is reported that the effect of glutathione (GSH) coated AgNPs on the Gram negative bacteria *E. coli* was more intense than Gram positive bacteria *Staphylococcus aureus* , as the Gram negative bacteria could be associated with the penetration of the colloid into the cytoplasm, with the subsequent local interaction of silver with the cell components, causing damages to the cells (Fig. 5.1), but for the Gram positive bacteria, antimicrobial effect is limited since the thick peptidoglycan layer of the cell wall prevents the penetration of the AgNPs inside the cytoplasm [6]. Besides, AgNPs have good inhibition effect on drug resistant bacteria such as *methicillin-resistant S. aureus* [9–11], showing the bactericidal effects are not affected by drug-resistant mechanisms. Nanosilver also has significant inhibitory activity on yeast, fungi such as *Aspergillus, Candida,* by suppressing the mycelial growth and spore germination

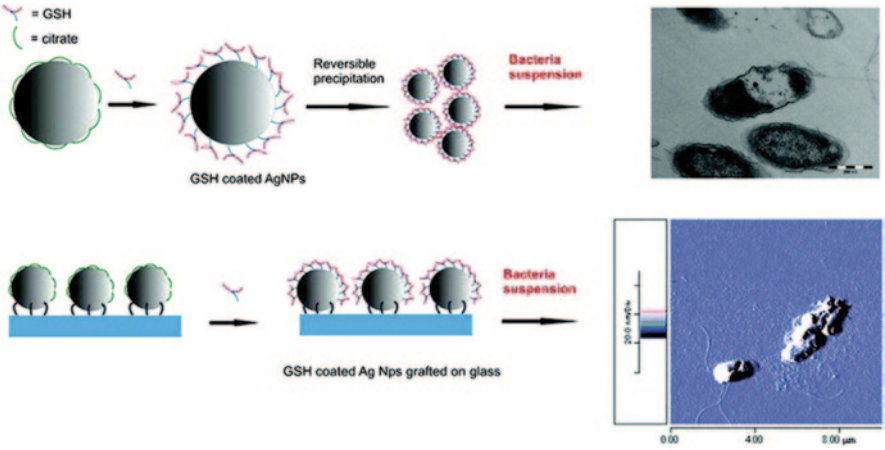

Fig. 5.1 The antimicrobial effects of glutathione (*GSH*) capped AgNPs. The dispersed GSH capped AgNPs is much more active than GSH AgNPs grafted on glass to *E. coli* due to the limitation of the translational freedom of nanoparticles (*NPs*). (Reprinted with the permission from ref. [6], Copyright 2012 American Chemical Society)

[12]. Moreover, AgNPs were shown to reduce the amount of the hepatitis B virus (HBV) covalent ring DNA [13], and inhibit RNA synthesis of intracellular HBV. At the same time, nanosilver combined with human immunodeficiency virus (HIV) I glycoprotein gp120, and competitive inhibition of the binding of gp120 and CD4+T cells, thereby inhibiting HIV infection in T cells [14, 15]. Researches on antibacterial effects of AgNPs were summarized in Table 5.1.

The antibacterial properties of nanosilver are in negative correlation with its particle size, the smaller the AgNPs are, due to the larger surface area, the easier it is for AgNPs to destroy the microbial membrane and enter into the cells [21]. Free radical generation of AgNPs may be responsible for the antimicrobial effects. As Kim et al. reported, the inhibitory effect of AgNPs was abolished by the addition of the antioxidant N-acetyl-L-cysteine (NAC) [5]. It is well known that silver ion (Ag^+) and Ag-based compounds are highly toxic to microorganisms, however, Ag^+ has only limited usefulness as an antimicrobial agent for some limitations such as no continuous release of Ag^+. These kinds of limitations can be overcome by AgNPs. Compared with Ag^+, the ability of AgNPs to reach bacteria proximity and a high surface/mass ratio can produce a high concentration of Ag^+ in cell surroundings, causing high microbicidal effects for a longer time [22]. However, in a research using nontuberculous mycobacteria (NTM) as a model, it is found that although the nanosilver has significant inhibitory effects on NTM, this bacteria can generate variants resistant to silver, and this variant has also resistance to the common antibiotics [23].

The debates on the mechanism of antimicrobial effect of Ag^+ and AgNPs are still open. To date, multiple possibilities have been proposed: (i) Ag^+ interactions with cysteine in critical regions of proteins and other cell constituents; (ii) causing K^+

Table 5.1 Summary for the antibacterial effects of silver nanoparticles (AgNPs)

	Tested bacteria	Doses	Effects	Ref.
Uncoated AgNPs (13.5 ± 2.6 nm)	Yeast, *Escherichia coli,* and *Staphylococcus aureus*	6.6–13.2 nM	Effective inhibited bacterial growth in *yeast* and *E. coli*, no significant effects in *S. aureus*	[5]
Glutathione coated AgNPs	Gram-negative and Gram-positive bacterial strains: *E. coli* and *S. aureus*	0.35 μg/cm^2 grafted on glass	Silver interacted with the cell components. *E. coli* is more intense to AgNPs than *S. aureus*	[6]
8 nm AgNPs embeded in diameter 40 nm, length 10 μm nanofiber	*E. coli* and *S. aureus*	13–1718 ng/mL	The embedded AgNPs exhibited excellent antibacterial performance against Gram-negative and Gram-positive microbials	[8]
Cationic antimicrobials coated AgNPs (63.5 ± 38.8 nm)	*E. faecalis*, *E. coli*, *Pseudomonas aeruginosa*and *S. aureus*	15 and 30 mg/L	AgNPs was observed in both kind of microbials, particles in *S. aureus* 70%, in *E. coli.*40%	[16]
AgNPs coated with amorphous carbon (35.4 ± 5.1 nm)	*E. coli*	2.04 ± 0.07 mg/L	AgNPs were 20 × less toxic to *E. coli* than Ag^+, their toxicity increased 2.3-fold after exposure to air for 0.5 h	[17]
AgNPs (20 nm, 40 nm, and 100 nm)	*Thalassiosira pseudonana* and *Synechococcus sp.*	0.05–20 μM	There is a shared effect of AgNPs and released silver responsible for the toxicity in both organisms and the toxic effects resulted from a mixture of parameters including aggregated state, size of the AgNPs, stability of the preparation, and speciation of the released silver	[18]
Cubic, wiry, triangular, and spherical silver nanostructures	*E. coli, Bacillus subtilis,* and *S. aureus*	3–30 μg	Both physicochemical properties of AgNPs and the type of bacteria have significant influence on the antibacterial activity of AgNPs. Cubic, wiry, and triangular structures showed the most antibacterial activities against *E. coli* and *B. subtilis* after spherical silver. Triangular, spherical, wiry, and cubic structures had the most antibacterial activity against *S. aureus*	[19]
Citrate coated AgNPs, small and large PVP-coated AgNPs, and gum arabic coated AgNPs with diameters range from 5 to 75 nm	*Caenorhabditis elegans*	0.9–463 mg/L	Both dissolved silver and coating influenced AgNPs toxicity. There was a linear correlation between AgNPs toxicity and dissolved silver, but no correlation between size and toxicity. Oxidative dissolution was key to the toxicity of most AgNPs	[20]

PVP polyvinylpyrolidone

loss from the membrane, with disruption of cellular transport systems; (iii) causing damage in respiration; (iv) perturbation of cellular growth; and (v) interaction with DNA [24]. AgNPs antimicrobial effect may arise from direct physical processes caused by nano-objects, like disruption of cell membrane and penetration of nanoparticles (NPs) into the cytoplasm, DNA binding, or interaction with bacterial ribosome [25].

5.1.2 Cellular Uptake and Cytotoxicity

Internalized AgNPs was observed in various cell types, such as human mesenchymal stem cells (hMSC), primary T-cells, primary monocytes, and astrocytes [26–28]. Using transmission electron microscope (TEM) and laser scanning confocal microscopy, AgNPs can be observed to pass through the cell membrane and enter into the cytoplasm. Studies showed that single or clustered AgNPs were attached to the cell membrane and were internalized into cells, and distributed throughout the cytoplasm, but they were not observed in the nucleus. Large endosomes and lysosomes with AgNPs were also observed [29]. It was found that AgNPs were internalized via endocytotic pathways [26]. The study of cellular phagocytosis of nanosilver using TEM and ICP-MS [30] showed that silver nitrate ($AgNO_3$) and nanosilver with three different sizes (5, 20, 50 nm) could enter the cells. 20 nm and 50 nm AgNPs could be found in the cytoplasm using TEM. Quantitative analysis showed that levels of Ag^+ and 5 nm AgNPs in cells were much higher than those of 20 nm and 50 nm AgNPs. Toxicity of AgNPs is correlated with their uptake by cells, the more are AgNPs internalized, the greater is their toxicity. The uptake can be controlled by the surface chemistry of the NPs. For example, the PEGylation coating reduced cellular uptake of AgNPs and exhibited lower cytotoxicity, while the mercaptoundecanoic acid (MUA) coating enhanced the cytoxicity of AgNPs [31].

A review by Johnston et al. [32] pointed out that silver particulate exposure could cause inflammatory, oxidative, genotoxic, and cytotoxic consequences in mammalian cells. The biological effect of AgNPs to cells showed dose- and size-dependent. AgNPs were cytotoxic to macrophages and were able to elicit an inflammatory response which was indicated by the expression of the inflammatory cytokines IL-6, IL-10, and TNF-α [33]. In the human lung cells A549 and human hepatic HepG2 cells which were treated with AgNPs, the level of malondialdehyde (MDA), 8-heterogeneous prostaglandin F2 α (8-epi-PGF2 α), 8- hydroxy-2′-deoxyguanosine (8-oxo-dG) and oxidative stress factors were significantly raised, heat shock protein A1A (HSPA1A), and heme oxygenase-1 (HO-1) levels also showed dose related upregulation [34]. These results showed that nanosilver could cause oxidative damage and heat shock proteins (HSPs) interference in human cells. The cell cycle arrest was also found in cancer cells exposed to NLS-AgNPs by the generation of ROS [35]. In undifferentiated PC12 cells, citrate-coated AgNPs (6 nm) impaired DNA synthesis [36]. PVP-coated AgNPs with 70 nm diameter induced the formation of DNA double strand breaks (DSB), chromosomal aberrations, and sister chromatid exchanges (CHO9, K1, V79B cell lines) at 5 μg/mL [37]. The 50 nm AgNPs

induced DNA damage to hMSC cells after 1, 3, and 24 h exposure at 0.1 μg/mL by comet assay and chromosomal aberration test [38], showing the genotoxic effect of AgNPs. Using cerebellum granule cell (CGCs) primary culture, AgNPs was found to attenuate the cellular viability through apoptosis coupled to oxidative stress, showing the potential neurotoxicity of this kind of nanomaterial [39]. Several adverse effects were often reported in view of cytotoxicity of AgNPs, which included chromosome instability, mitotic arrest, and significant alterations in cell morphology. The toxicity was mediated by intracellular calcium. Different responses were found between normal and cancerous cells upon AgNPs stimulation, which underline the importance of relevant cellular models for biological studies [40].

5.1.3 Aquatic Organisms

Since the released nanoparticles ultimately enter water ecosystems, the maximum toxic effects could be magnified in aquatic ecosystems. Many studies investigated the aquatic toxicity of nanosilver particles due to its large application. Various aquatic organisms such as algal species, cladoceran species, and freshwater fish species are used for this purpose. The toxicities including acute and chronic biological effects have been addressed to clarify the potential toxicity profile of this artificial nanomaterial for the risk assessment of its versatile application.

Pelagic invertebrates including *Daphnia magna*, *Ceriodaphnia dubia*, *Thamnocephalus platyurus* etc. are popular models in aquatic toxicity evaluation. Based on the review by Fabrega et al. [41], nanoparticle capping, ionic strength, and the presence of organic matter in the test media are important parameters for AgNPs toxicity to invertebrates. Studies on the adverse effects of AgNPs on two aquatic crustaceans, *D. magna* and *T. platyurus* showed that nanosilver were highly toxic to both crustaceans. The pattern of the toxic response of both crustacean species to silver compounds was almost similar in artificial freshwater and in natural waters. The adult mortality was more sensitive than the reproduction [42]. The toxicity study of oxide-coated AgNPs (44.5 nm) showed 48 h LC50 values were 40 μg/L for *D. pulex* adults and 67 μg/L for *C. dubia* neonates [43]. As for citrate coated AgNPs, the 48 h EC50 values varied from 1.1–11 μg/L [44–46]. PVP-coated AgNPs were found to cause the toxicity with the 48 h LC50 up to 97 μg/L [46]. Comparative toxicity assessment of nanosilver on three Daphia species in acute, chronic, and multi-generation experiments showed the effects of nanosilver vary within one genus and change with exposure duration. Long-term studies considering different aquatic species are needed to better understand the possible effects of nanosilver on aquatic ecosystem [47]. Proteomic evaluation of citrate-coated AgNPs toxicity in *D. magna* showed AgNPs increased carbonyl levels besides the increased protein thiol content which was similar to silver ion. Lower acute toxicity of AgNPs was observed and the toxicity of silver nanoparticle and ion follow somewhat different biologic pathways, potentially leading to different interactions with natural compounds or pollutants in the aquatic environment [48].

A few studies were conducted to test the effects of AgNPs on algae species, and the algal growth and photosynthesis were discussed. Freshwater green algae *P. subcapitata* is one of the algal species recommended in the ISO standard and OECD guideline tests for algal growth inhibition. It is commonly used in AgNPs toxicity evaluation. The 96 h EC50 of this algae was tested to be 190 μg/L for metaloxide coated AgNPs [43], and the toxicity could be influenced by water chemistry and the presence of organic matter, thus EC50 (96 h) ranged from 4.6 μg/L in algal culture medium to 192 μg/L in a wetland water sample [49]. Some other studies showed EC50 values around 20 μg/L for two different sizes of AgNPs [46], which indicated AgNPs was very toxic toward this algae species. Some other green algae such as *Chlamydomonas reinhardtii* confirmed the toxicity level of AgNPs. Carbonate-coated AgNPs caused the toxicity with EC50 values ranging from 355 to 92 μg/L based on *C. reinhardtii* tests, and the toxicity observed couldn't be explained by Ag^+ in AgNPs dispersions. Nanoparticles could react with algae and deliver the toxic Ag^+, thus showing the different toxicity profile from what induced by comparable levels of Ag^+ alone [3].

Fish, as the typical dominant species in the aquatic system is widely used for the toxicological studies. Many studies have evaluated the aquatic toxicity of nanosilver based on various fish models. The acute toxicity, fish behavior, and embryo development are often considered as useful toxicity endpoints. Bilberg et al. [50] studied in vivo toxicity of AgNPs and silver ions in zebrafish (*Danio rerio*). The results showed that AgNPs were lethal to zebrafish and could alter fish behavior revealed by increased rate of operculum movement and surface respiration, showing respiratory toxicity due to nanosilver exposure-related stress. Fish embryo and larval are sensitive aquatic experimental models for the developmental toxicities of aquatic pollutants. Ahamed et al. [51] summarized the effects on embryo development in a wide array of species including zebrafish (*Danio rerio*), Japanese medaka (*Oryzias latipes*), and Fathead minnow (*Pimephales promelas*). Increased incidences of abnormalities and malformations in embryos, hatching delay, and increased mortality as well as reproductive failure were observed upon nanosilver exposure. The study on the effects of AgNPs on fathead minnow (*P. promelas*) embryos indicated that AgNPs entered into the embryos and induced a concentration-dependent increase in larval abnormalities, mostly edema [52]. AgNPs were observed in zebrafish eggs using single particle real-time observation technology. As shown in Fig. 5.2, AgNPs could enter or exit eggshell freely through chorion pore canals (CPCs), and moved in embryonic fluid as Brown diffusion. The movement rate of AgNPs in embryonic fluid was much lower than it was in water outside the eggshell. It is about 3×10^{-9} cm^2/s, which is 1/26 of the rate in water. The slow diffusion caused aggregation of particles in the eggs. The AgNPs which aggregated in egg yolk could lead to abnormal development of juvenile. The malformation effective concentration was about 0.19 nM [53]. When using Japanese Medaka as the experimental model, AgNPs were found to lead to significant development stunt and multiple malformations in the development of the embryos. There were various malformations including eyes, head, heart, and finfold development such as eyes developmental asymmetry, anophthalmia, decreased optic cup pigmentation, exophthalmia, finfold abnormality,

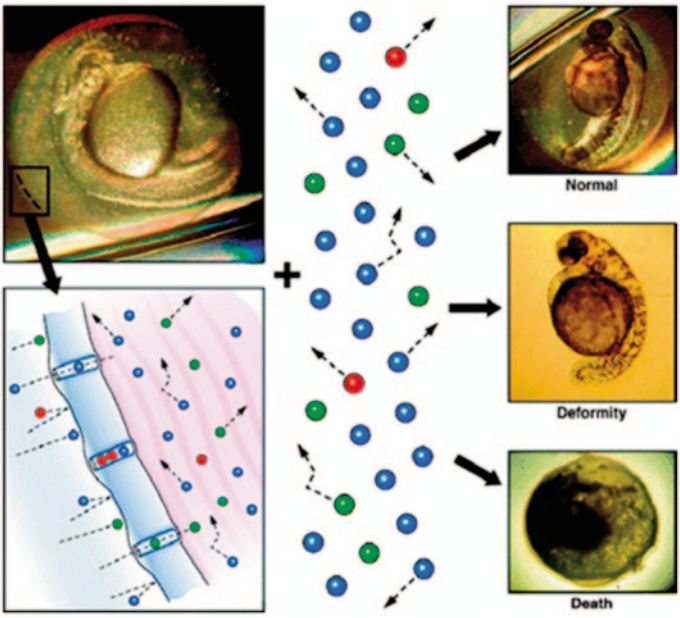

Fig. 5.2 AgNPs enter into or out eggshells through CPCs and do the Brown movement in the egg yolk. Nanosilver in eggs induces malformation or death of the embryo. (Reprinted with the permission from ref. [53], Copyright 2007 American Chemical Society)

anal swelling, pericardial edema, and reduced head [54]. Sometimes, people would argue that the effects of nanoparticles often resort to the use of unrealistically high concentrations, which can change the properties of the particles and reveal little about their behavior at commonly used levels. Scientists did find that "surprisingly low" concentrations of nanosilver led to gill failure and death in salmon [55]. Aquatic species are a particular concern because nanosilver has been detected in wastewater from sewage treatment plants.

The aquatic toxicity of nanosilver can be affected by various factors. Sharma [56] reviewed the stability and toxicity of AgNPs in aquatic environment, which pointed out the stability of AgNPs influences their toxicity in the aquatic environment, and solution parameters are largely responsible for the stability of AgNPs in biological and natural environments. Surface coating is also an important influencing factor in view of AgNPs induced toxicity in aquatic environment. There is a layer of Ag^+ outside the new-synthesized AgNPs. After a long time of storage, the ratio of surface Ag^+ increases, so does the toxicity of AgNPs. While with a layer of dissolved organic carbon (DOC) modification, the toxicity of AgNPs was significantly decreased, and no significant change was found with the increase of storage time [57]. It means the organic carbon compounds will change toxicity of nanosilver in aquatic environment. Study on the effect of salinity on nanosilver' toxicity showed that LC50 of the colloidal AgNPs for rainbow trout fry in 12 pg/mL salinity

was almost 20 and 2 folds higher than 0.4 and 6 pg/mL salinities, respectively. It indicated that the release of AgNPs into fresh water ecosystems can lead to more biological, physical, and chemical irrecoverable impacts in comparison with saline water ecosystems [58]. In addition, aggregation and dispersion of AgNPs in exposure media were also discussed for aquatic toxicity tests [59].

5.1.4 Terrestrial species

Some parts of silver may be released from AgNP application and deposited in the terrestrial systems including soils and sewage sludge. Those particles can be absorbed on the soil matrix and directly contact with the soil organisms, thus causing unexpected toxicities. In this scenario, the exposure routes may include water route, nutrition absorption, and body surface contact. Plants could be directly affected by polluted soil. Yin et al. [60] showed that gummi arabicum-coated AgNPs and $AgNO_3$ at 40 mg/L inhibited growth of *Lolium multiflorum*, and morphological damage was induced by AgNPs. Some terrestrial animals such as earthworms and nematodes are ideal models for the evaluation of AgNPs toxicity in soils as they have highly permeable skin. Shoults-Wilson et al. [61] studied the growth and reproductive toxicity in earthworm *Eisenia fetida* exposed to a range of concentrations of $AgNO_3$ and two polyvinylpyrolidone (PVP) coated AgNPs with different particle size distributions in naturally occurring sandy loam and a standardized artificial soil. The results showed that significant reproductive toxicity was observed in organisms exposed to AgNPs concentrations approximately eight times higher than those at which the effects from ionic Ag were observed. Thus the study concluded that the Ag ions were possibly responsible for the effects on growth and development caused by AgNPs exposure, and soil type was a more important determinant of Ag accumulation from AgNPs than particle size. The research on the effects of silver nanoparticle surface coating on bioaccumulation and reproductive toxicity in *E. fetida* showed the significant decreased reproduction in earthworms exposed to $AgNO_3$ (94.21 mg/kg) as well as earthworms exposed to AgNPs with either oleic acid (727.6 mg/kg) or PVP coatings (773.3 mg/kg). Earthworms accumulated Ag in a concentration-dependent manner from all Ag sources. No differences were observed in Ag accumulation or toxicity between earthworms exposed to AgNPs with either coating [62]. Gene expression patterns revealed that oxidative stress was induced by both PVP-AgNPs and $AgNO_3$ in *E. fetida*, showing oxidation occurred after or during particle or silver ion uptake in earthworms [63]. Due to AgNPs' excellent microbial toxicity, some soil microorganisms are highly sensitive to AgNPs exposure. A commercial available spray containing AgNPs clearly reduced soil microbial biomass after 4-month incubation at the dose of 3.2 μg Ag per g dry soil [64]. Unicellular eukaryotes and other microfauna in soil appear to be much less sensitive to AgNPs than bacteria, and more sensitive to ionic than to nanoparticular silver [65].

5.1.5 Mammals

In view of the toxicity of nanosilver, the studies based on rodent experimental models are valuable for the risk assessment on the potential hazards caused by the application of commercial AgNPs-based products. As the exposure to nanoparticles includes inhalation, dermal contact, ingestion, various exposure routes have been explored using some rodents like mice and rats in preceding studies. Uptake, distribution, and organ toxicities are widely discussed.

Oral administration of nanosilver caused increased Ag level in the peripheral blood [66]. Silver content in blood of rats treated with silver nitrate was significantly higher than that of AgNPs treated groups, showed that the ionic silver more easily entered into the blood circulation system through the digestive system than AgNPs. After 28 days administration, Ag could be detected in numbers of important organs such as liver, spleen, lung, brain, and heart. In most tissues, the content of silver in silver nitrate treated group was higher than that in nanosilver treated groups. The silver content in blood of rats could be cleared in a week after the last administration. However, the silver remove in tissues needs much longer time. In most tissues, silver was detectable in 84 days after the last administration. And the clearance of silver is faster in the nanosilver treated groups than that in the silver nitrate group. In brain and testis, AgNPs could be a long-term accumulation. AgNPs injected in rats can be translocated from the blood to all the main organs and Ag level in tissues was significantly higher in rats treated with 20 nm AgNPs when compared with 200 nm AgNPs [67]. A single intravenous dose of nanosivler also caused accumulation of Ag in all examined rabbit organs including liver, kidney, spleen, lung, brain, testis, and thymus up to 28 days [68].

Translocation of AgNPs through systemic circulation may lead to multiple adverse effects of AgNPs in animals, wherein, hematological toxicity, immunotoxicity, hepatoxicity, renal toxicity, neurotoxicity, and reproductive toxicity are mostly concerned and widely discussed. In a study, when mice were treated with nanosilver through oral administration for 28 days, AgNPs enter the blood circulation system through the digestive tract, resulting in decrease of blood mononuclear cells and phenotype change of lymphocyte. The T cell percentage of $CD4^+/CD8^+$ and the ratio of $CD4^+/CD8^+$ increased, while the percentage of natural killer (NK/NKT) cells decreased [69]. Nanosilver not only inhibited lymphocyte activity, but also reduced the proliferation of lymphocytes. It induced the monocyte respiratory burst and significant increase of macrophages and granulocyte. These results showed that nanosilver exposure affected the peripheral white blood cells and might lead to changes of immune responses to exogenous biology. Nanosilver could significantly cause reduction of the hemoglobin content in blood cells of mice. On the embryonic period of red cell precursors, RNA transcription was significantly inhibited by AgNPs, resulting in the down regulation of hemoglobin level in red blood cells and fetal anemia, and the anemia could induce embryonic development retardation [70]. Hepatotoxicity study of AgNPs in Sprague-Dawley rats demonstrated that AgNPs exposure increased the activities of liver enzymes (ALT, AST, ALP) and AgNPs induced hepatotoxic effects against tissue cells are particle size-dependent.

In vivo study by lateral tail vein injection in rats showed AgNPs exposure affected inflammatory mediator expression, indicated by increase of interleukin-8 (IL-8)/macrophage inflammatory protein 2, IL-1R1 and tumor necrosis factor-α in liver tissue [71]. Intraperitoneally injected AgNPs induced obvious histopathological alterations in rat kidney and liver such as swollen epithelium with cytoplasmic vacuolization, thickening of the basement membrane, destruction of some mitochondrial cristae, destructed cristae of some mitochondria, endosomes, and larger lysosomes filled with AgNPs in the Kupffer cells [72]. The reproductive/developmental toxicity screening test showed that repeated dose of citrate-capped AgNPs did not affect mating, fertility, implantation, delivery, and foetus in rats [73]. AgNPs were also found to be able to induce inflammation in microvessel vascular endothelial cells and affect the integrity of blood brain barrier [74]. Neurotoxicity indicated by impaired hippocampus function was thus observed in rats treated by AgNPs through nasal administration [75]. Neurobehavioral study showed the functional injury of central nervous system (CNS) by decreasing their locomotor activities in Sprague-Dawley rats with intravenous injection of AgNPs [76]. These findings provided solid evidences on the potential biological effects of AgNPs, which needs to be concerned during their application.

5.1.6 Potential Hazards to Human Health

Human beings have been exposed to airborne particles throughout their evolutionary stages. The rapidly developing field of nanotechnology is providing new sources of such exposures through inhalation, ingestion, dermal, injection, and the combination, which has caused special concerns considering its potential hazards to human health. In order to assess consumer exposure to nanomaterials, we need to identify the consumer products containing nanomaterials in the first step. The subsequent investigation on the actual existence of nanomaterials is required for those products which claim to be nanomaterials-based. Next, the important characteristics of the nanomaterials such as chemical entity, shape, size, and concentration have to be analyzed carefully in those products, and nanomaterial release during use needs to be assessed [77].

AgNPs are highly relevant for human exposure due to their use in food contact materials, dietary supplements, and antibacterial wound treatments. Debates of their effects on human health are continuing. The most distinct adverse effect observed in clinic cases is the accumulation of silver or silver sulfide particles in the skin after chronic intake of silver products like colloidal silver (solution contains AgNPs and silver ions). These particles in the skin darken with exposure to sunlight, resulting in a permanent blue–gray discoloration of the skin, known as argyria [78]. Both localized and generalized argyria can occur as a result of topical use of silver-containing solution and the ingestion of such substances, respectively. Although nanosilver-based dressing and surgical sutures have received approval for clinical application, and good control of wound infection is achieved, their dermal toxicity is still a topic of concern. A condition related to argyria, corneal agyrosis was also reported due

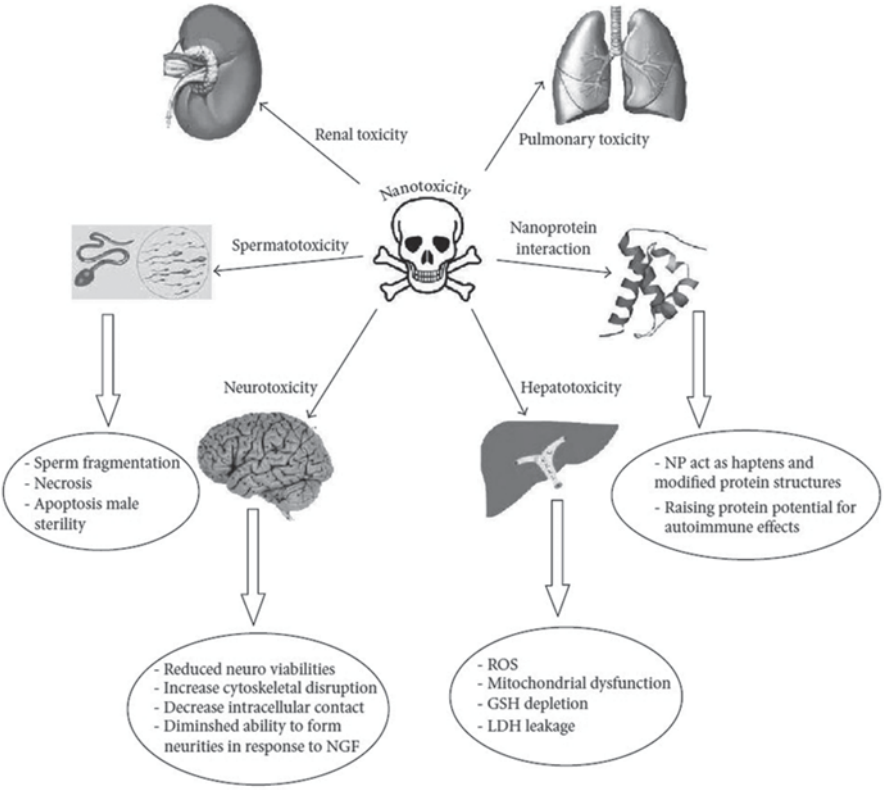

Fig. 5.3 Summary of the potential toxicities of nanoparticles. (Reprinted with the permission from ref. [80], Copyright 2009A. El-Ansary and S. Al-Daihan)

to the deposition of silver granules in the deep stroma and Descemet's membrane following the use of topical silver nitrate [78]. Ingestion of colloidal silver could induce neurological problems, kidney damage, stomach upset, headaches, fatigue, and skin irritation [79]. In the review by EI-Ansary and Al-Daihan [80], the most important recorded toxic effects of therapeutically used nanoparticles were summarized (Fig. 5.3), which can well elucidate the potential effects of AgNPs on human health. Overall, the hazards of nanosilver to human being are poorly understood and there are many unsolved questions that need to be imperatively answered before the direct application of nanosilver on a large scale.

5.2 Toxicological Mechanisms

AgNPs, as one of the most commonly used nanomaterials, have strong antibacterial properties. In view of the mechanisms for AgNPs inhibit microbial growth, it can be summarized in three aspects: release of soluble Ag(I) species followed by disruption

of adenosine triphosphate (ATP) production and DNA replication upon uptake; AgNPs caused direct damage to cell membranes and generation of ROS mediated by both AgNPs and Ag (I) [81–84]. The unexpected toxicities may be caused by AgNPs in the similar way under certain circumstances, which has raised ecological and human health concerns. In view of toxicological mechanisms for AgNPs, the debate is being continued on the concepts of reactive radicals and release of silver ion. The key points for addressing these arguments are to figure out how ROS play roles in AgNPs mediated toxicity, and whether AgNPs mediated toxicity is mechanistically unique to nanoparticluate silver, or if it is a result of the release of silver ions.

5.2.1 ROS Dependent Pathway

ROS are generated intrinsically or extrinsically within the cell and they play a key role as a messenger in normal cell signal transduction and cell cycling. The reactive radicals including superoxide anion, hydroxyl radial, hydrogen peroxide, singlet oxygen, and hypochlorous acid constitute a pool of oxidative species. These reactive molecules are formed by a number of different mechanisms and can be detected by various techniques. Nonspecific oxidative damage to the nontarget organisms is one of the greatest concerns in the application of nanomaterials. Figure 5.4 depicted prooxidant pathway of NP-induced toxicity [85]. NP-elicited ROS is at the center stage for majority of the ensuing adverse outcomes. Accumulation of reactive oxygen species induces and regulates the induction of apoptosis, which is characterized by the reduction in mitochondrial membrane potential, release of cytochrome C from mitochondria, phosphatidylserine externalization, DNA and nuclear fragmentation, and the activation of metacaspases. Given its chemical reactivity, oxidative stress can amount to DNA damage, lipid peroxidation, and activation of signaling networks associated with loss of cell growth, fibrosis, EMT, and carcinogenesis. Phagocytes including neutrophils and macrophages generate massive ROS upon incomplete phagocytosis of NP through the nicotinamide adenine dinucloetide phosphate (NADPH)-oxidase enzyme system whereas NP-induced ROS triggers an inflammatory cascade of chemokine and cytokine expression via activation of cell signaling pathways such as MAPK, NF-κB, Akt, and RTK. The common methods for the evaluation are based on oxidative stress and direct ROS generation intra- and extracellularly.

It is widely reported that the toxicity of AgNPs is related with oxidative stress, which in turn may trigger proinflammatory responses. Both extracellular and intracellular ROS generation can be caused by AgNPs [86]. The release of ROS during the electron transport of mitochondrial aerobic respiration is the major source of the reactive species. Contact between cells and nanoparticles can also induce ROS release, leading to an imbalance toward the pro-oxidative state. Hydroxyl radicals are considered as an important component of cell death. AgNP generated hydroxyl radicals played a significant role in mitochondrial dysfunctional apoptosis in *Candida albicans* cells, causing antifungal effects [87]. AgNPs agglomerated in the cytoplasm and nuclei of treated hepatoma cells can produce size-dependent toxicity

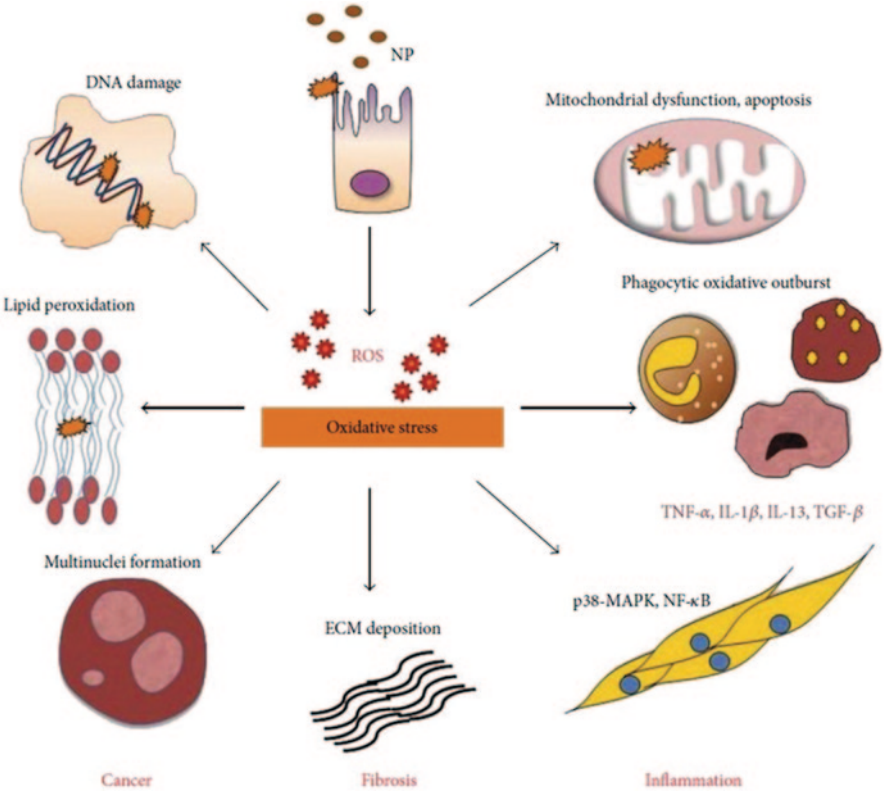

Fig. 5.4 Various NPs exhibit oxidative stress dependent toxicities. (Reprinted with the permission from ref. [85], Copyright 2013 Amruta Manke et al.)

through the induction of intracellular oxidative stress. A more than 10-fold increase of ROS levels in cells exposed to 15 nm AgNPs is likely to be mediated [12]. Silver ion mediated perturbation of the bacterial respiratory chain has raised the possibility of ROS generation. Silver-ion-mediated ROS-generation affected bactericidal activity. The major form of ROS generated was the superoxide-radical; H_2O_2 was not induced [88]. In nanosilver-resistant HCT116 cells, nanosilver-induced apoptosis was associated with the generation of ROS and JNK activation, and inhibition of either ROS or JNK attenuated nanosilver-induced apoptosis [89].

Alterations in expression levels or activities of the key protein components in oxidative defense system are commonly used to evaluate cellular oxidative stress caused by nanomaterials. When the cells (HT-1080, A431) were challenged with 1/2 IC50 concentration of AgNPs, decreased GSH and superoxide dismutase (SOD) activity, as well as increased lipid peroxidation showed clear signs of oxidative stress [90]. In human lung epithelia (A549) cells, AgNPs was found to induce oxidative stress in dose and time-dependent manner indicated by depletion of GSH and induction of ROS, lipid peroxidation (LPO), SOD, and catalase [91]. AgNPs can induce oxidative stress in higher plants as well. People found that a dose-dependent

increase in levels of reactive oxygen species, SOD and peroxidase activity, and the antioxidant glutathione content in *Spirodela polyrhiza* treated with 6-nm AgNPs, while silver ion did not change the reactive oxygen species level or antioxidant enzymes activity at the relevant level to AgNPs released [92].

The mechanism for AgNPs induced toxicity through the generation of reactive radicals can be confirmed by the usage of antioxidative agents during the exposure. Both vitamin C (Vit C) and NAC could completely reverse the generation of ROS upon AgNPs [93]. When antioxidants such as NAC were used, the toxicity of AgNPs could be efficiently blocked or prevented. Pretreatment of the A549 cells with NAC decreased the effects of AgNPs on the reduced cell viability, change in the matrix metalloproteinase (MMP), and proportion of cells in the sub-G1population, showing AgNPs induced in vitro toxicities are mediated via ROS-dependent pathway [94]. Another antioxidant, Vit C was also reported to be able to reverse AgNPs caused cellular and molecular alterations including cytotoxicity, apoptosis, cell cycle status, and several critical regulators in chronic myeloid leukemia cells [95], showing that oxidative stress plays key roles in AgNPs induced cellular toxicities.

5.2.2 ROS Independent Pathway

Although enhanced generation of ROS leading to oxidative stress is assumed to be responsible for the toxicity of nanomaterials in most cases, non-oxidative stress-related mechanisms have also been recently reported [96, 97]. Pretreatment of the A549 cells with NAC had no effect on the AgNP-mediated S phase arrest or down-regulation of the cell cycle associated proliferating cell nuclear antigen (PCNA) protein, showing in vitro toxic effects of AgNPs on A549 cells are mediated via ROS-independent pathway in view of cell cycle arrest [94]. Noncytotoxic level of AgNP didn't induce cellular ROS generation in HepG2 cells, but displayed hormesis effect through p38 activation. NAC pretreatment didn't inhibit phorsphorylation of p38, indicating this hormesis effect of AgNPs at nontoxic level was independent of ROS [98].

5.2.3 Release of Silver Ions

Silver is well known for its antimicrobial activity, and the Ag^+ ion is generally recognized as a bioactive species. Silver ions block bacterial growth by inhibiting the essential enzymatic functions of the microorganism via interaction with the thiol group of L-cysteine. Dissolution of AgNPs releases antimicrobial Ag^+ ions, which may compromise cell functionality and stop the spread of germs [99]. Regarding the toxicological effects of AgNPs, release of silver ion from the AgNPs is often considered as the main mechanism as well.

Lots of studies have compared the toxicological profiles of silver ions and AgNPs to clarify the relationship between particle-specific effects and silver ion

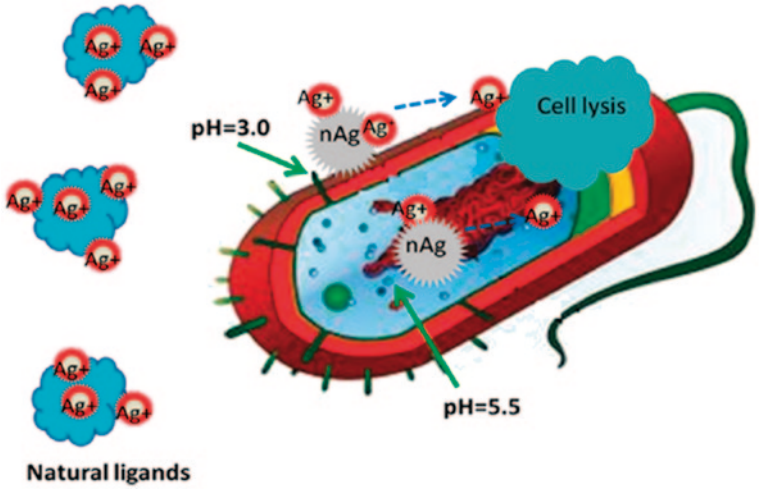

Fig. 5.5 Schematic of AgNPs, Ag^+, and cell interactions. (Reprinted with the permission from ref. [99], Copyright 2012 American Chemical Society)

induced activities. Most of tones emphasized the importance of silver ion release in AgNPs induced biological toxicities, especially for antibacterial effects. The research group at Rice University reported regardless of the parameters (e.g., shape, size, surface coating, etc.) of the AgNPs, their toxicity to the bacteria only depended on the concentration of the silver ions released under aerobic conditions [99]. As shown in Fig. 5.5, AgNPs may serve as a vehicle to deliver Ag^+ more effectively (being less susceptible to binding and reduced bioavailability by common natural ligands) to the bacteria cytoplasm and membrane, whose proton motive force would decrease the local pH (as low as pH 3.0) and enhance Ag^+ release. The antibacterial activity could be controlled by modulating the release of silver ions from AgNPs through controlling the oxygen availability and the parameters of the AgNPs [99]. It is believed that ions, not particles make silver toxic to bacteria. Cao et al. [100] proposed the interaction of dissolved silver ion with cell wall and cytoplasmic proteins, resulting in the impaired function or inactivation. Silver ions from the environment or originated from the sustained dissolution of AgNPs disrupted respiration, established proton motive force [101] as an effect of interactions with thiol groups of enzymes and other proteins, and inhibited enzymes acting in the phosphrous, sulphur, and nitrogen cycles of the bacteria [68].

Many researches provided support for the predominant role of silver ion in the explanation of AgNPs induced effects in cell models as well. It was reported that a linear correlation between AgNPs toxicity and dissolved silver was found when the toxicities of AgNPs to Caenorhabditis elegans were tested. A critical role for dissolved silver complexed with thiols in the toxicity of all tested AgNPs was highlighted using three independent and complementary approaches to investigate the mechanisms of toxicity of differentially coated and sized AgNPs. Although some

AgNPs also act via oxidative stress, which is commonly believed to be an effect specific to nanoparticulate silver, in no case was the toxicity of AgNPs greater than would be predicted by complete dissolution of the same mass of silver as silver ions [20]. The investigation on the degree of silver ion fraction from AgNPs suspensions contributing to the toxicity of AgNPs in A549 lung cells showed that the toxicity from silver ion plays the dominant role and AgNPs did not add measurable additional toxicity to AgNP suspension when the initial level of silver ion was higher than 5.5 % [102]. The type of cell death induced by silver ions and silver nanoparticle coated with PVP were dependent on the dose and the exposure time, with silver ion being the most toxic in human monocytic cell line [103]. The intracellular silver release rather than differences in cellular uptake or intracellular localization is a likely explanation for the observed differences in AgNP induced cytotoxicity [104]. As NAC is both a silver ion chelator and an antioxidant to scavenge ROS, the fact that only NAC but not Vit C could protect the acute myeloid leukemia (AML) cells from losses of MMP, DNA damage, and apoptosis thoroughly indicated release of silver ions played critical roles in the AgNPs-induced cytotoxic effect against AML cells [93].

5.2.4 Particle Specific Effect of AgNPs

The high surface area of metal-based NPs increases the potential that metal ions are released from these NPs [105], the arguments to which degree the toxicity of NPs results from released metal ions and how much toxicity is related to the NPs per se is continued. A series of toxicological investigations of NPs imply that, e.g., size, shape, chemical composition, surface charge, solubility, their ability to bind and affect biological sites as well as their metabolism and excretion influence the toxicity of NPs [106, 107]. These gave the evidences on the particle related effects.

When considering the toxicity of AgNPs, the most elusive question has been whether AgNPs exert direct particle specific effects beyond the known antimicrobial activity of the released silver ions. Cao et al. [108] stated the adhesion of AgNPs embedded in titanium to the bacteria surface correlated with the surface ζ potential of nanoparticles, which may alter the membrane properties, thus causing reduced proliferation of the bacteria. Identification of a number of proteins from *E. coli* showed that some protein fragments were characteristics of strong binding to AgNPs, but not of association with silver ions [22]. A study of Choi and Hu [109] pointed out DNA damage was correlated with the fraction of AgNPs less than 5 nm in nitrifying organisms, and this was more toxic than any other forms of silver including silver ion and AgCl colloids due to easier (active) transport through the cell membrane of uncharged AgNPs than of charged silver ions. Other authors reported that the measured silver ion content of the AgNP suspension could not fully explain the observed toxicity of the AgNP suspension and that both silver ions and AgNPs contribute to the toxicity [3, 110]. At low silver ion fractions (less than 2.6 %), AgNP suspensions are more toxic than their supernatant [102], showing the particle

specific effect of AgNPs does exist. Some comparative studies also gave distinct findings in the biological effects caused by silver ions and AgNPs. Based on metal-responsive metallothionein 1b (MT1b) mRNA expression, oxidative stress-related glutathione peroxidase 1 (GPx1) and catalase expression, people found AgNP cytotoxicity is primarily the result of oxidative stress and is independent of the toxicity of Ag^+ ions [12]. In the study of "hormesis" effects caused by AgNPs in HepG2, the treatment of HepG2 cells with silver ion at the same dose levels induced distinct biological effects, suggesting that different intrinsic properties exist for AgNPs and Ag^+ [98]. In the study of neurodevelopment using PC12 cell line, the greater inhibition of protein synthesis at lower concentrations of citrate-coated AgNPs and a loss of effect at higher concentrations, totally distinct from the monotonic dose-effect relationship for silver ions, which indicates that this AgNPs induced disruption in protein synthesis is through a mechanism unrelated to freely dissolved silver ions [36]. All these findings indicated that AgNP effect is not simply due to the release of silver ion into the surrounding environment and that particle-specific effect does contribute to the toxicity of AgNPs.

5.3 Potential Influencing Factors

It is well accepted that materials on nanoscale are provided with many fascinating properties which are mostly decided by the morphological and structural factors, such as size, core composition, and surface coating. Unexceptionally, the toxicity of AgNPs is also considered to be defined by these factors. As discussed in the sections of 5.1 and 5.2, the chemistry of Ag ion release and/or ROS production mainly gave rise to the toxicity of AgNPs to the organisms. Accordingly, the influencing factors were dictating the toxicity through adjusting the related chemical process and the related cases are discussed in the terms of the factors within this section.

5.3.1 Particle Size and Shape

The extremely small size is the unique property possessed by the nanoparticles, but it is also the origin for the toxicity of nanoparticles. As for AgNPs, the small size means four points: (1) inclining to enter into organisms; (2) a large number of surface atoms available for diverse reactions; (3) more released Ag ion from the nanoparticles; and (4) more ROS production on the surface, which eventually result in corresponding toxicity [96, 109, 111]. Thus, the toxicity generally increases along with the decreasing size of AgNPs, which has already been confirmed by the results of the related work [30, 88, 112].

Chen et al. [113] studied the disturbance of cellular energy metabolism and RNA polymerase activity by AgNPs with different sizes and shapes. Compared with 40-nm nanospheres and 45-nm nanoplates, the nanospheres with the sizes of 20 and

25 nm were more capable of altering cellular energy metabolism at the doses of 2 and 4 μg/mL, thus it was speculated that the smaller-sized AgNPs were more prone to enter into cells and efficiently disturbed the normal machinery [113]. Meanwhile, they also found that spherically-shaped AgNPs with smaller size showed a more obvious inhibition on the globin expression in erythroid cells than the larger ones, for the smaller-sized AgNPs can release more Ag^+ which inactivated the RNA polymerase through binding with them [114]. The smaller-sized AgNPs of 15 nm also can produce more ROS in the concentration range of 0–75 μg/mL and further induced obvious damage of mitochondrial membrane structure, leading to a mitochondria-driving apoptosis of cells. As a consequence, after 24 h of exposure, the viability of cells exposed with 15 and 30 nm AgNPs exhibited significant decrease along with the dose increasing from 10 to 75 μg/mL. This result suggested the toxicity was mediated through an oxidative stress [115]. This size-dependent toxicity of AgNPs also occurred on the alga and bacteria [99, 116]. Besides, the shape is another dominant factor for dictating the unique of nanoparticles. In shape-controlled synthesis of AgNPs (e.g., sphere, wire, star, pillar, and plate), the strategy was mainly focused on gaining a preferential growth of specific lattice faces during reaction by adjusting the conditions (e.g., reaction temperature, time, coordinate ligand, and the precursor form) [117]. Subsequently, some typical crystal defects inevitably existed on the surface of nanoparticles with diverse shapes, thereby giving rise to toxicities through specific surface reactions such as oxidation and dissolution.

According to the theoretical result, the Ag atoms on the <111> facets of nanoparticles are most active and favorably bind with oxygen to accelerate release of ROS and Ag ion. In this view, the AgNPs with high density of <111> facets would induce more obvious toxicity to the organisms, e.g., bacteria [81]. For example, due to containing more <111> facets, truncated triangular nanoplates exhibited a greater antibacterial activity than the AgNPs with the spherical and rod shapes [118]. It has also reported that the silver nanoplate with high-level tacking faults and point defects had a considerable toxicity because of the increased generation of the super oxide. In this term, the corresponding uptake and toxicity of the silver nanoplate were significantly inhibited by saturating the crystal defects with the high-affinitive ligand of cysteine molecules (Fig. 5.6) [119].

5.3.2 Surface Coating

The stable nanoparticles including AgNPs composed of two parts of core and surface coating. The surface coating molecule plays an important role in saturating the dangling bonds of the surface atom on one side, on the other side the structures of charge or long chain nanoparticles keep each nanoparticle in a certain distance and in a stable state [120]. Accordingly, the surface coating is also very important in regulating the toxicity of AgNPs. The importance will be discussed in the terms of surface charge and aggregation state in this part.

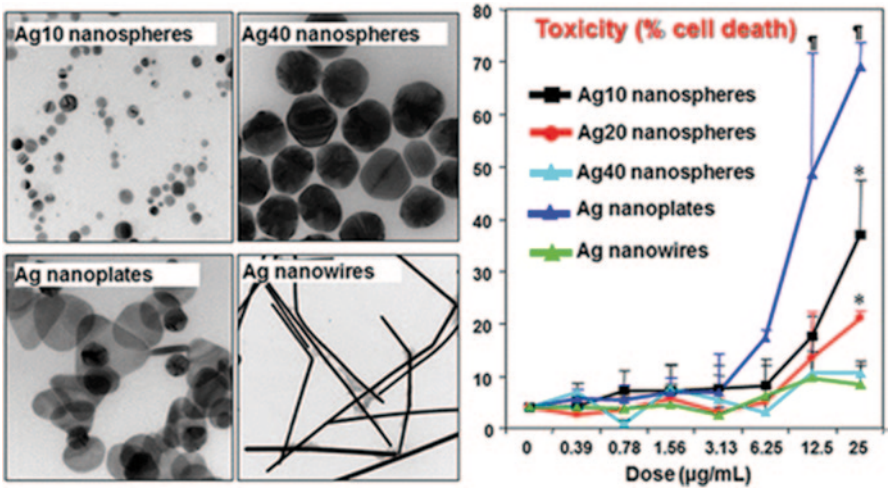

Fig. 5.6 Transmission electron microscope (TEM) characterizations of the AgNPs and the corresponding curve for cell death as indicated. (Reprinted with the permission from ref. [119], Copyright 2012 American Chemical Society)

Comparison on the toxicity from four AgNPs with respective ζ potential of −38, −22, −10, and +40 mV concludes that the negatively charged AgNPs (citrate-AgNPs) have a barrier with the cell membrane rising from the electrostatic repelling that limits the cell-particle interactions and reduces the toxicity. In contrast, the repulsion force on the positively charged AgNPs (BPEI-AgNPs) turns into attraction force, which allows for a stronger interactions, causing a greater damage to the membrane of bacillus species Gram-positive bacteria [121]. Three biocompatible peptides with diverse surface charge were functionalized with the AgNPs, and the charge-independent transport and dependent toxicity in early developing zebrafish were witnessed using dark-field optical microscopy and spectroscopy. It was discovered that the more negatively charged AgNPs (Ag-CALNNE NPs$^{-4\zeta}$) showed greater toxicity, while the more positively charged AgNPs (Ag-CALNNK NPs$^{+\zeta}$) less toxic (Fig. 5.7) [122].

As mentioned, the surface coating shows a great importance in maintaining stability of nanoparticles, which also determines the following chemistry and related toxicity. Many surfactants and polymers including SDS, PVP, poly(lactic-co-glycolic acid) PLGA, and hydroxyl modified ionic liquids or cationic surfactants, have been used to modify AgNPs to obtain stable nanoparticles. With the decrease in the stability of AgNPs, the aggregation tends to form, which leads to a decreased toxicity [123, 124].

5.3.3 Compositions and Others

Environmental conditions including pH, ionic strength, and coordination ligand can influence the charge state, the stability and the compositions of the core.

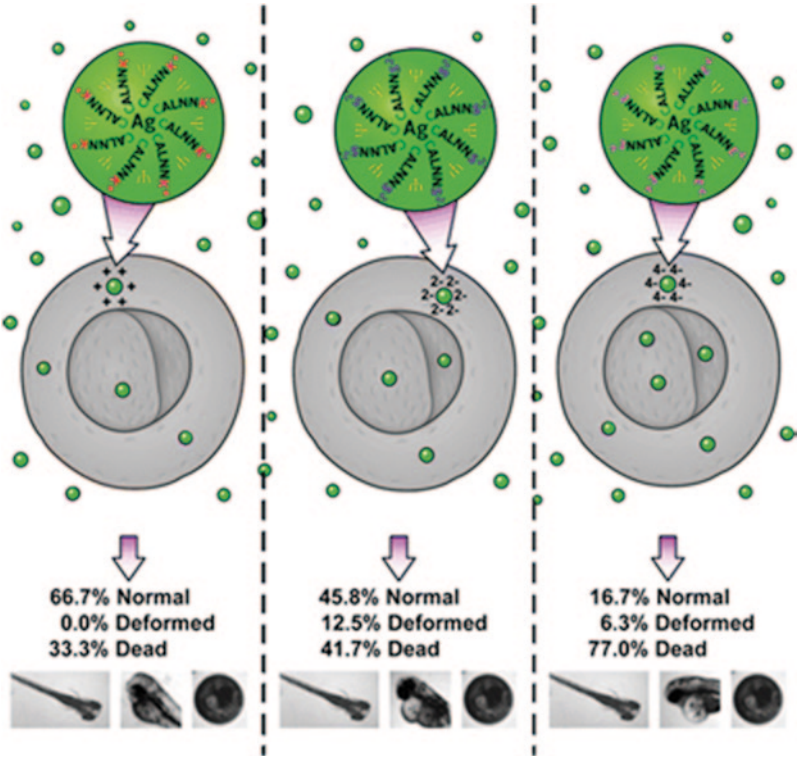

Fig. 5.7 The scheme illustrating the effect of surface charge on the toxicity of nanosilver to zebra embryos. (Reprinted with the permission from ref. [122], Copyright 2013 American Chemical Society)

High ionic strength and pH close to the isoelectric point can screen the repulsion interactions between nanoparticles and lead to the aggregation and even precipitation of nanoparticles in the media [125]. pH value also strongly influences the vital chemical reaction of ion release and ROS production where both are closely related to AgNPs toxicity [126, 127]. When the Ag-affinitive compound or ion (cysteine, Na_2S, Cl^-) existing in the media, the original toxicity eliminates by decreasing the bioavailable toxic species. In the case of coexistence with Na_2S or NaCl, Ag atoms on the surface of AgNPs will gradually transform into the extremely stable compound of Ag_2S ($K_{sp} = 1.6 \times 10^{-49}$) or AgCl ($K_{sp} = 1.8 \times 10^{-10}$), thus accounting for a negligible toxicity in the terms of decreasing ion dissolution rate and surface charge [128, 129]. As for the ligands containing case, for example, cysteine or humic acid either bind with the surface Ag atom or coordinate the ion form of Ag to detoxify the active species of AgNPs (Fig. 5.8) [130], accordingly alleviating the original biological toxicity [126, 131]. The related specific studies are discussed in Chap. 6. An interesting phenomenon was observed that the Ag ion could be transformed into nanoscaled Ag under illumina-

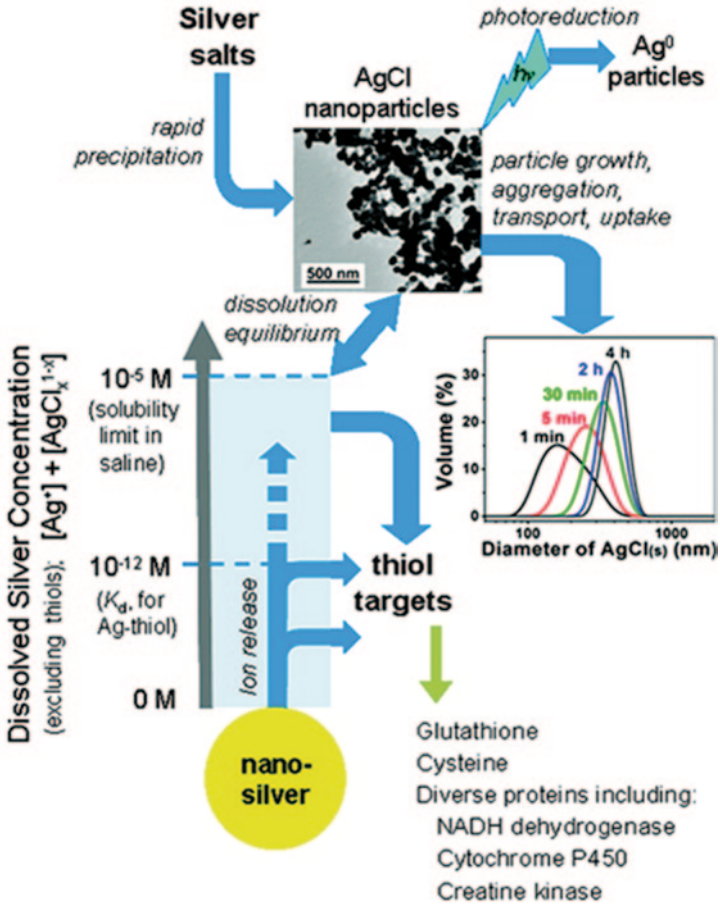

Fig. 5.8 Chemical transformation for nanosilver under different environmental conditions. (Adapted with the permission from ref. [130], Copyright 2010 American Chemical Society)

tion of visible light together with the presence of the natural organic matter, like humic acid [132, 133].

The inter-transformation of Ag between the form of ion and nanoparticle leads an intricate role in the related toxicity and needs more attention, because the balance is in charge of the toxic species and final biological effects.

5.4 Perspectives

The environmental exposure to silver originates from many anthropogenic sources including a wide range of technical application in dustry, medical applications, water disinfection, and consumer products. AgNPs represent a new source of

bioavailable silver for environmental exposure that delivers silver to organisms via multiple ways, causing potential environmental, and human health problems. Current available toxicologcial data on AgNPs has given some information on its potential harzards to ecosystem including atmospheric, terrestrial, and aquatic systems. However, no information can be found on long-term (low) exposure to silver or silver containing products in the general population. Additionally, as an effective antimicrobial agents in medical care and consumer products, AgNPs could cause the occurrence of cross-resistance in microorganisms and also result in the deviation of bacterial population balance for the normal condition, which may pose the sequential hazardous threaten. Considering direct as well as indirect effects occurring via the distribution of AgNPs into the environment, the implications of the widespread use of AgNPs for the environment and human health remains unclear.

References

1. Tang B, Li J, Hou X, Afrin T, Sun L, Wang X (2013) Colorful and antibacterial silk fiber from anisotropic silver nanoparticles. Ind Eng Chem Res 52(12):4556–4563. doi:10.1021/ie3033872
2. Lombi E, Donner E, Scheckel KG, Sekine R, Lorenz C, Von Goetz N, Nowack B (2014) Silver speciation and release in commercial antimicrobial textiles as influenced by washing. Chemosphere 111:352–358. doi:10.1016/j.chemosphere.2014.03.116
3. Navarro E, Piccapietra F, Wagner B, Marconi F, Kaegi R, Odzak N, Sigg L, Behra R (2008) Toxicity of silver nanoparticles to *Chlamydomonas reinhardtii*. Environ Sci Technol 42(23):8959–8964. doi:10.1021/es801785m
4. Ruden S, Hilpert K, Berditsch M, Wadhwani P, Ulrich AS (2009) Synergistic interaction between silver nanoparticles and membrane-permeabilizing antimicrobial peptides. Antimicrob Agents Chemother 53(8):3538–3540. doi:10.1128/aac.01106-08
5. Kim JS, Kuk E, Yu KN, Kim JH, Park SJ, Lee HJ, Kim SH, Park YK, Park YH, Hwang CY, Kim YK, Lee YS, Jeong DH, Cho MH (2014) Antimicrobial effects of silver nanoparticles (vol 1, pp 95, 2007). Nanomed-Nanotechnol Biol Med 10(5):1119–1119. doi:10.1016/j.nano.2014.04.007
6. Taglietti A, Fernandez YAD, Amato E, Cucca L, Dacarro G, Grisoli P, Necchi V, Pallavicini P, Pasotti L, Patrini M (2012) Antibacterial activity of glutathione-coated silver nanoparticles against Gram positive and Gram negative bacteria. Langmuir 28(21):8140–8148. doi:10.1021/la3003838
7. Li WR, Xie XB, Shi QS, Duan SS, Ouyang YS, Chen YB (2011) Antibacterial effect of silver nanoparticles on *Staphylococcus aureus*. Biometals 24(1):135–141. doi:10.1007/s10534-010-9381-6
8. Song J, Kang H, Lee C, Hwang SH, Jang J (2012) Aqueous synthesis of silver nanoparticle embedded cationic polymer nanofibers and their antibacterial activity. ACS Appl Mater Interfaces 4(1):460–465. doi:10.1021/am201563t
9. Panacek A, Kvitek L, Prucek R, Kolar M, Vecerova R, Pizurova N, Sharma VK, Nevecna Tj, Zboril R (2006) Silver colloid nanoparticles: synthesis, characterization, and their antibacterial activity. J Phys Chem B 110(33):16248–16253. doi:10.1021/jp063826h
10. Shahverdi AR, Fakhimi A, Shahverdi HR, Minaian S (2007) Synthesis and effect of silver nanoparticles on the antibacterial activity of different antibiotics against Staphylococcus aureus and Escherichia coli. Nanomed-Nanotechnol Biol Med 3(2):168–171. doi:10.1016/j.nano.2007.02.001

11. Kim JS, Kuk E, Yu KN, Kim JH, Park SJ, Lee HJ, Kim SH, Park YK, Park YH, Hwang CY, Kim YK, Lee YS, Jeong DH, Cho MH (2007) Antimicrobial effects of silver nanoparticles. Nanomed-Nanotechnol Biol Med 3(1):95–101. doi:10.1016/j.nano.2006.12.001
12. Kim SW, Kim KS, Lamsal K, Kim Y-J, Kim SB, Jung M, Sim SJ, Kim HS, Chang SJ, Kim JK, Lee YS (2009) An in vitro study of the antifungal effect of silver nanoparticles on oak wilt pathogen Raffaelea sp. J Microbiol Biotechnol 19(8):760–764. doi:10.4014/jmb.0812.649
13. Lu L, Sun RWY, Chen R, Hui CK, Ho CM, Luk JM, Lau GKK, Che CM (2008) Silver nanoparticles inhibit hepatitis B virus replication. Antivir Ther 13(2):253–262
14. Sun RWY, Chen R, Chung NPY, Ho CM, Lin CLS, Che CM (2005) Silver nanoparticles fabricated in Hepes buffer exhibit cytoprotective activities toward HIV-1 infected cells. Chem Commun (40):5059–5061. doi:10.1039/b510984a
15. Lara HH, Ayala-Nunez NV, Ixtepan-Turrent L, Rodriguez-Padilla C (2010) Mode of antiviral action of silver nanoparticles against HIV-1. J Nanobiotechnol 8(1). doi:10.1186/1477-3155-8-1
16. Hoppens MA, Sylvester CB, Qureshi AT, Scherr T, Czaps DR, Duran RS, Savage PB, Hayes D (2014) Ceragenin mediated selectivity of antimicrobial silver nanoparticles. ACS Appl Mater Interfaces 6(16):13900–13908. doi:10.1021/am504640f
17. Xiu ZM, Ma J, Alvarez PJJ (2011) Differential effect of common ligands and molecular oxygen on antimicrobial activity of silver nanoparticles versus silver ions. Environ Sci Technol 45(20):9003–9008. doi:10.1021/es201918f
18. Burchardt AD, Carvalho RN, Valente A, Nativo P, Gilliland D, Garcia CP, Passarella R, Pedroni V, Rossi F, Lettieri T (2012) Effects of silver nanoparticles in diatom thalassiosira pseudonana and cyanobacterium synechococcus sp. Environ Sci Technol 46(20):11336–11344. doi:10.1021/es300989e
19. Ashkarran AA, Ghavami M, Aghaverdi H, Stroeve P, Mahmoudi M (2012) Bacterial effects and protein corona evaluations: crucial ignored factors in the prediction of bio-efficacy of various forms of silver nanoparticles. Chem Res Toxicol 25(6):1231–1242. doi:10.1021/tx300083s
20. Yang X, Gondikas AP, Marinakos SM, Auffan M, Liu J, Hsu-Kim H, Meyer JN (2012) Mechanism of silver nanoparticle toxicity is dependent on dissolved silver and surface coating in Caenorhabditis elegans. Environ Sci Technol 46(2):1119–1127. doi:10.1021/es202417t
21. Pal S, Tak YK, Song JM (2007) Does the antibacterial activity of silver nanoparticles depend on the shape of the nanoparticle? A study of the gram-negative bacterium Escherichia coli. Appl Environ Microb 73(6):1712–1720. doi:10.1128/aem.02218-06
22. Wigginton NS, De Titta A, Piccapietra F, Dobias J, Nesatty VJ, Suter MJF, Bernier-Latmani R (2010) Binding of silver nanoparticles to bacterial proteins depends on surface modifications and inhibits enzymatic activity. Environ Sci Technol 44(6):2163–2168. doi:10.1021/es903187s
23. Larimer C, Islam MS, Ojha A, Nettleship I (2014) Mutation of environmental mycobacteria to resist silver nanoparticles also confers resistance to a common antibiotic. Biometals 27(4):695–702. doi:10.1007/s10534-014-9761-4
24. Chamakura K, Perez-Ballestero R, Luo Z, Bashir S, Liu J (2011) Comparison of bactericidal activities of silver nanoparticles with common chemical disinfectants. Colloid Surf B 84(1):88–96. doi:10.1016/j.colsurfb.2010.12.020
25. Yamanaka M, Hara K, Kudo J (2005) Bactericidal actions of a silver ion solution on Escherichia coli, studied by energy-filtering transmission electron microscopy and proteomic analysis. Appl Environ Microb 71(11):7589–7593. doi:10.1128/aem.71.11.7589-7593.2005
26. Greulich C, Diendorf J, Simon T, Eggeler G, Epple M, Koeller M (2011) Uptake and intracellular distribution of silver nanoparticles in human mesenchymal stem cells. Acta Biomater 7(1):347–354. doi:10.1016/j.actbio.2010.08.003
27. Greulich C, Diendorf J, Gessmann J, Simon T, Habijan T, Eggeler G, Schildhauer TA, Epple M, Koeller M (2011) Cell type-specific responses of peripheral blood mononuclear cells to silver nanoparticles. Acta Biomater 7(9):3505–3514. doi:10.1016/j.actbio.2011.05.030
28. Luther EM, Koehler Y, Diendorf J, Epple M, Dringen R (2011) Accumulation of silver nanoparticles by cultured primary brain astrocytes. Nanotechnology 22(37). doi:10.1088/0957-4484/22/37/375101

29. Peng H, Zhang X, Wei Y, Liu W, Li S, Yu G, Fu X, Cao T, Deng X (2012) Cytotoxicity of silver nanoparticles in human embryonic stem cell-derived fibroblasts and an L-929 cell line. J Nanomater. doi:10.1155/2012/160145
30. Liu W, Wu Y, Wang C, Li HC, Wang T, Liao CY, Cui L, Zhou QF, Yan B, Jiang GB (2010) Impact of silver nanoparticles on human cells: effect of particle size. Nanotoxicology 4(3):319–330. doi:10.3109/17435390.2010.483745
31. Caballero-Diaz E, Pfeiffer C, Kastl L, Rivera-Gil P, Simonet B, Valcarcel M, Jimenez-Lamana J, Laborda F, Parak WJ (2013) The toxicity of silver nanoparticles depends on their uptake by cells and thus on their surface chemistry. Part Part Syst Charact 30(12):1079–1085. doi:10.1002/ppsc.201300215
32. Johnston HJ, Hutchison G, Christensen FM, Peters S, Hankin S, Stone V (2010) A review of the in vivo and in vitro toxicity of silver and gold particulates: particle attributes and biological mechanisms responsible for the observed toxicity. Crit Rev Toxicol 40(4):328–346. doi:10.3109/10408440903453074
33. Martinez-Gutierrez F, Thi EP, Silverman JM, de Oliveira CC, Svensson SL, Hoek AV, Morales Sanchez E, Reiner NE, Gaynor EC, Pryzdial ELG, Conway EM, Orrantia E, Ruiz F, Av-Gay Y, Bach H (2012) Antibacterial activity, inflammatory response, coagulation and cytotoxicity effects of silver nanoparticles. Nanomed-Nanotechnol Biol Med 8(3):328–336. doi:10.1016/j.nano.2011.06.014
34. Xin L, Wang J, Wu Y, Guo S, Tong J (2014) Increased oxidative stress and activated heat shock proteins in human cell lines by silver nanoparticles. Hum Exp Toxicol doi:10.1177/0960327114538988
35. Austin LA, Kang B, Yen C-W, El-Sayed MA (2011) Nuclear targeted silver nanospheres perturb the cancer cell cycle differently than those of nanogold. Bioconjugate Chem 22(11):2324–2331. doi:10.1021/bc200386m
36. Powers CM, Badireddy AR, Ryde IT, Seidler FJ, Slotkin TA (2011) Silver nanoparticles compromise neurodevelopment in PC12 cells: critical contributions of silver ion, particle size, coating, and composition. Environ Health Perspect 119(1):37–44. doi:10.1289/ehp.1002337
37. Ahlberg S, Antonopulos A, Diendorf J, Dringen R, Epple M, Flock R, Goedecke W, Graf C, Haberl N, Helmlinger J, Herzog F, Heuer F, Hirn S, Johannes C, Kittler S, Koller M, Korn K, Kreyling WG, Krombach F, Lademann J, Loza K, Luther EM, Malissek M, Meinke MC, Nordmeyer D, Pailliart A, Raabe J, Rancan F, Rothen-Rutishauser B, Ruhl E, Schleh C, Seibel A, Sengstock C, Treuel L, Vogt A, Weber K, Zellner R (2014) PVP-coated, negatively charged silver nanoparticles: a multi-center study of their physicochemical characteristics, cell culture and in vivo experiments. Beilstein J Nanotech 5:1944–1965. doi:10.3762/bjnano.5.205
38. Hackenberg S, Scherzed A, Kessler M, Hummel S, Technau A, Froelich K, Ginzkey C, Koehler C, Hagen R, Kleinsasser N (2011) Silver nanoparticles: evaluation of DNA damage, toxicity and functional impairment in human mesenchymal stem cells. Toxicol Lett 201(1):27–33. doi:10.1016/j.toxlet.2010.12.001
39. Yin N, Liu Q, Liu J, He B, Cui L, Li Z, Yun Z, Qu G, Liu S, Zhou Q, Jiang G (2013) Silver nanoparticle exposure attenuates the viability of rat cerebellum granule cells through apoptosis coupled to oxidative stress. Small 9(9–10):1831–1841. doi:10.1002/smll.201202732
40. Reidy B, Haase A, Luch A, Dawson KA, Lynch I (2013) Mechanisms of silver nanoparticle release, transformation and toxicity: a critical review of current knowledge and recommendations for future studies and applications. Materials 6(6):2295–2350. doi:10.3390/ma6062295
41. Fabrega J, Luoma SN, Tyler CR, Galloway TS, Lead JR (2011) Silver nanoparticles: behaviour and effects in the aquatic environment. Environ Int 37 (2):517–531. doi:10.1016/j.envint.2010.10.012
42. Blinova I, Niskanen J, Kajankari P, Kanarbik L, Kaekinen A, Tenhu H, Penttinen OP, Kahru A (2013) Toxicity of two types of silver nanoparticles to aquatic crustaceans Daphnia magna and Thamnocephalus platyurus (pp 3456). Environ Sci Pollut Res 20(6):4293–4293. doi:10.1007/s11356-013-1734-6

43. Griffitt RJ, Luo J, Gao J, Bonzongo J-C, Barber DS (2008) Effects of particle composition and species on toxicity of metallic nanomaterials in aquatic organisms. Environ Toxicol Chem 27(9):1972–1978. doi:10.1897/08-002.1
44. von Nickisch-Rosenegk M, Teschke T, Bier FF (2012) Construction of an artificial cell membrane anchor using DARC as a fitting for artificial extracellular functionalities of eukaryotic cells. J Nanobiotechnol 10. doi:10.1186/1477-3155-10-1
45. Allen HJ, Impellitteri CA, Macke DA, Heckman JL, Poynton HC, Lazorchak JM, Govindaswamy S, Roose DL, Nadagouda MN (2010) Effects from filtration, capping agents, and presence/absence of food on the toxicity of silver nanoparticles to Daphnia magna. Environ Toxicol Chem 29(12):2742–2750. doi:10.1002/etc.329
46. Kennedy AJ, Hull MS, Bednar AJ, Goss JD, Gunter JC, Bouldin JL, Vikesland PJ, Steevens JA (2010) Fractionating nanosilver: importance for determining toxicity to aquatic test organisms. Environ Sci Technol 44(24):9571–9577. doi:10.1021/es1025382
47. Voelker C, Boedicker C, Daubenthaler J, Oetken M, Oehlmann J (2013) Comparative toxicity assessment of nanosilver on three daphnia species in acute, chronic and multi-generation experiments. PloS One 8(10). doi:10.1371/journal.pone.0075026
48. Rainville L-C, Carolan D, Varela AC, Doyle H, Sheehan D (2014) Proteomic evaluation of citrate-coated silver nanoparticles toxicity in Daphnia magna. Analyst 139(7):1678–1686. doi:10.1039/c3an02160b
49. McLaughlin J, Bonzongo J-CJ (2012) Effects of natural water chemistry on nanosilver behavior and toxicity to Ceriodaphnia dubia and Pseudokirchneriella subcapitata. Environ Toxicol Chem 31(1):168–175. doi:10.1002/etc.720
50. Bilberg K, Hovgaard MB, Besenbacher F, Baatrup E (2012) In vivo toxicity of silver nanoparticles and silver ions in zebrafish (Danio rerio). J Toxicol 2012:293784–293784. doi:10.1155/2012/293784
51. Ahamed M, AlSalhi MS, Siddiqui MKJ (2010) Silver nanoparticle applications and human health. Clin Chim Acta 411(23–24):1841–1848. doi:10.1016/j.cca.2010.08.016
52. Laban G, Nies LF, Turco RF, Bickham JW, Sepulveda MS (2010) The effects of silver nanoparticles on fathead minnow (Pimephales promelas) embryos. Ecotoxicology 19(1):185–195. doi:10.1007/s10646-009-0404-4
53. Lee KJ, Nallathamby PD, Browning LM, Osgood CJ, Xu XHN (2007) In vivo imaging of transport and biocompatibility of single silver nanoparticles in early development of zebrafish embryos. ACS Nano 1(2):133–143. doi:10.1021/nn700048y
54. Wu Y, Zhou Q, Li H, Liu W, Wang T, Jiang G (2010) Effects of silver nanoparticles on the development and histopathology biomarkers of Japanese medaka (Oryzias latipes) using the partial-life test. Aquat Toxicol 100(2):160–167. doi:10.1016/j.aquatox.2009.11.014
55. Weaver E (2012) Nanosivler toxic to fish at "surprising low" levels. Environmental Building News. http://www2.buildinggreencom/article/nanosilver-toxic-fish-surprisingly-low-levels. Accessed Oct. 2012
56. Sharma VK (2013) Stability and toxicity of silver nanoparticles in aquatic environment: a review. In: Shamim N, Sharma VK (eds) Sustainable nanotechnology and the environment: advances and achievements. vol 1124. ACS Symposium Series, American Chemical Society, Washington, DC, pp 165–179
57. Kennedy AJ, Chappell MA, Bednar AJ, Ryan AC, Laird JG, Stanley JK, Steevens JA (2012) Impact of organic carbon on the stability and toxicity of fresh and stored silver nanoparticles. Environ Sci Technol 46(19):10772–10780. doi:10.1021/es302322y
58. Kalbassi MR, Salari-joo H, Johari A (2011) Toxicity of silver nanoparticles in aquatic ecosystems: salinity as the main cause in reducing toxicity. Iranian J Toxicol 5(12):436–443
59. Roemer I, White TA, Baalousha M, Chipman K, Viant MR, Lead JR (2011) Aggregation and dispersion of silver nanoparticles in exposure media for aquatic toxicity tests. J Chromatogr A 1218(27):4226–4233. doi:10.1016/j.chroma.2011.03.034
60. Yin L, Cheng Y, Espinasse B, Colman BP, Auffan M, Wiesner M, Rose J, Liu J, Bernhardt ES (2011) More than the ions: the effects of silver nanoparticles on Lolium multiflorum. Environ Sci Technol 45(6):2360–2367. doi:10.1021/es103995x

61. Shoults-Wilson WA, Reinsch BC, Tsyusko OV, Bertsch PM, Lowry GV, Unrine JM (2011) Role of particle size and soil type in toxicity of silver nanoparticles to earthworms. Soil Sci Soc Am J 75(2):365–377. doi:10.2136/sssaj2010.0127nps
62. Shoults-Wilson WA, Reinsch BC, Tsyusko OV, Bertsch PM, Lowry GV, Unrine JM (2011) Effect of silver nanoparticle surface coating on bioaccumulation and reproductive toxicity in earthworms (Eisenia fetida). Nanotoxicology 5(3):432–444. doi:10.3109/17435390.2010.537382
63. Tsyusko OV, Hardas SS, Shoults-Wilson WA, Starnes CP, Joice G, Butterfield DA, Unrine JM (2012) Short-term molecular-level effects of silver nanoparticle exposure on the earthworm, Eisenia fetida. Environ Pollut 171:249–255. doi:10.1016/j.envpol.2012.08.003
64. Hansch M, Emmerling C (2010) Effects of silver nanoparticles on the microbiota and enzyme activity in soil. J Plant Nutr Soil Sci 173(4):554–558. doi:10.1002/jpln.200900358
65. SCENIHR (Scientific committee on emerging and newly identified health risks), Nanosilver: safety, health and environmental effects and role in antimicrobial resistance. European Union, 2013, ISSN: 1831-4783, DOI:10.2772/76851
66. van der Zande M, Vandebriel RJ, Van Doren E, Kramer E, Rivera ZH, Serrano-Rojero CS, Gremmer ER, Mast J, Peters RJB, Hollman PCH, Hendriksen PJM, Marvin HJP, Peijnenburg AACM, Bouwmeester H (2012) Distribution, elimination, and toxicity of silver nanoparticles and silver ions in rats after 28-day oral exposure. ACS Nano 6(8):7427–7442. doi:10.1021/nn302649p
67. Dziendzikowska K, Gromadzka-Ostrowska J, Lankoff A, Oczkowski M, Krawczynska A, Chwastowska J, Sadowska-Bratek M, Chajduk E, Wojewodzka M, Dusinska M, Kruszewski M (2012) Time-dependent biodistribution and excretion of silver nanoparticles in male Wistar rats. J Appl Toxicol 32(11):920–928. doi:10.1002/jat.2758
68. Lee YJ, Kim J, Oh J, Bae S, Lee S, Hong IS, Kim SH (2012) Ion-release kinetics and ecotoxicity effects of silver nanoparticles. Environ Toxicol Chem 31(1):155–159. doi:10.1002/etc.717
69. Malaczewska J (2014) Effect of 28-day oral administration of silver nanocolloid on the peripheral blood leukocytes in mice. Pol J Vet Sci 17(2):263–273. doi:10.2478/pjvs-2014-0037
70. Wang Z, Liu SJ, Ma J, Qu GB, Wang X, Yu SJ, He J, Liu JF, Xia T, Jiang GB (2013) Silver nanoparticles induced RNA polymerase-silver binding and RNA transcription inhibition in Erythroid Progenitor cells. ACS Nano 7(5):4171–4186. doi:10.1021/nn400594s
71. Gaiser BK, Hirn S, Kermanizadeh A, Kanase N, Fytianos K, Wenk A, Haberl N, Brunelli A, Kreyling WG, Stone V (2013) Effects of silver nanoparticles on the liver and hepatocytes in vitro. Toxicol Sci 131(2):537–547. doi:10.1093/toxsci/kfs306
72. Sarhan OMM, Hussein RM (2014) Effects of intraperitoneally injected silver nanoparticles on histological structures and blood parameters in the albino rat. Int J Nanomed 9:1505–1517. doi:10.2147/ijn.s56729
73. Hong JS, Kim S, Lee SH, Jo E, Lee B, Yoon J, Eom IC, Kim HM, Kim P, Choi K, Lee MY, Seo YR, Kim Y, Lee Y, Choi J, Park K (2014) Combined repeated-dose toxicity study of silver nanoparticles with the reproduction/developmental toxicity screening test. Nanotoxicology 8(4):349–362. doi:10.3109/17435390.2013.780108
74. Trickler WJ, Lantz SM, Murdock RC, Schrand AM, Robinson BL, Newport GD, Schlager JJ, Oldenburg SJ, Paule MG, Slikker W, Jr, Hussain SM, Ali SF (2010) Silver nanoparticle induced blood-brain barrier inflammation and increased permeability in primary rat brain microvessel endothelial cells. Toxicol Sci 118(1):160–170. doi:10.1093/toxsci/kfq244
75. Liu Y, Guan W, Ren G, Yang Z (2012) The possible mechanism of silver nanoparticle impact on hippocampal synaptic plasticity and spatial cognition in rats. Toxicol Lett 209(3):227–231. doi:10.1016/j.toxlet.2012.01.001
76. Zhang Y, Ferguson SA, Watanabe F, Jones Y, Xu Y, Biris AS, Hussain S, Ali SF (2013) Silver nanoparticles decrease body weight and locomotor activity in adult male rats. Small 9(9–10):1715–1720. doi:10.1002/smll.201201548
77. Wijnhoven S, Dekkers S, Hagens W, De Jong W (2009) Exposure to nanomaterials in consumer products. RIVM letter report 340370001/2009
78. Geyer O, Rothkoff L, Lazar M (1989) clearing of corneal argyrosis by yag laser. Brit J Ophthalmol 73(12):1009–1010. doi:10.1136/bjo.73.12.1009

79. White JML, Powell AM, Brady K, Russell-Jones R (2003) Severe generalized argyria secondary to ingestion of colloidal silver protein. Clin Exp Dermatol 28(3):254–256. doi:10.1046/j.1365–2230.2003.01214.x
80. El-Ansary A, Al-Daihan S (2009) On the toxicity of therapeutically used nanoparticles: an overview. J Toxicol 2009:754810–754810. doi:10.1155/2009/754810
81. Morones JR, Elechiguerra JL, Camacho A, Holt K, Kouri JB, Ramirez JT, Yacaman MJ (2005) The bactericidal effect of silver nanoparticles. Nanotechnology 16(10):2346–2353. doi:10.1088/0957-4484/16/10/059
82. Hwang ET, Lee JH, Chae YJ, Kim YS, Kim BC, Sang BI, Gu MB (2008) Analysis of the toxic mode of action of silver nanoparticles using stress-specific bioluminescent bacteria. Small 4(6):746–750. doi:10.1002/smll.200700954
83. Smetana AB, Klabunde KJ, Marchin GR, Sorensen CM (2008) Biocidal activity of nanocrystalline silver powders and particles. Langmuir 24(14):7457–7464. doi:10.1021/la800091y
84. Kohn T, Nelson KL (2007) Sunlight-mediated inactivation of MS2 coliphage via exogenous singlet oxygen produced by sensitizers in natural waters. Environ Sci Technol 41(1):192–197. doi:10.1021/es061716i
85. Manke A, Wang L, Rojanasakul Y (2013) Mechanisms of nanoparticle-induced oxidative stress and toxicity. Biomed Res Int 2013:942916–942916. doi:10.1155/2013/942916
86. He D, Jones AM, Garg S, Pham AN, Waite TD (2011) Silver nanoparticle-reactive oxygen species interactions: application of a charging-discharging model. J Phys Chem C 115(13):5461–5468. doi:10.1021/jp111275a
87. Hwang I-s, Lee J, Hwang JH, Kim K-J, Lee DG (2012) Silver nanoparticles induce apoptotic cell death in Candida albicans through the increase of hydroxyl radicals. Febs J 279(7):1327–1338. doi:10.1111/j.1742-4658.2012.08527.x
88. Park MVDZ, Neigh AM, Vermeulen JP, de la Fonteyne LJJ, Verharen HW, Briede JJ, van Loveren H, de Jong WH (2011) The effect of particle size on the cytotoxicity, inflammation, developmental toxicity and genotoxicity of silver nanoparticles. Biomaterials 32(36):9810–9817. doi:10.1016/j.biomaterials.2011.08.085
89. Hsin YH, Chena CF, Huang S, Shih TS, Lai PS, Chueh PJ (2008) The apoptotic effect of nanosilver is mediated by a ROS- and JNK-dependent mechanism involving the mitochondrial pathway in NIH3T3 cells. Toxicol Lett 179(3):130–139. doi:10.1016/j.toxlet.2008.04.015
90. Arora S, Jain J, Rajwade JM, Paknikar KM (2008) Cellular responses induced by silver nanoparticles: in vitro studies. Toxicol Lett 179(2):93–100. doi:10.1016/j.toxlet.2008.04.009
91. Suliman YA, Ali D, Alarifi S, Harrath AH, Mansour L, Alwasel SH (2013) Evaluation of cytotoxic, oxidative stress, proinflammatory and genotoxic effect of silver nanoparticles in human lung epithelial cells. Environ Toxicol. doi:10.1002/tox.21880
92. Yang X, Jiang C, Hsu-Kim H, Badireddy AR, Dykstra M, Wiesner M, Hinton DE, Meyer JN (2014) Silver nanoparticle behavior, uptake, and toxicity in caenorhabditis elegans: effects of natural organic matter. Environ Sci Technol 48(6):3486–3495. doi:10.1021/es404444n
93. Guo D, Zhu L, Huang Z, Zhou H, Ge Y, Ma W, Wu J, Zhang X, Zhou X, Zhang Y, Zhao Y, Gu N (2013) Anti-leukemia activity of PVP-coated silver nanoparticles via generation of reactive oxygen species and release of silver ions. Biomaterials 34(32):7884–7894. doi:10.1016/j.biomaterials.2013.07.015
94. Chairuangkitti P, Lawanprasert S, Roytrakul S, Aueviriyavit S, Phummiratch D, Kulthong K, Chanvorachote P, Maniratanachote R (2013) Silver nanoparticles induce toxicity in A549 cells via ROS-dependent and ROS-independent pathways. Toxicol In Vitro 27(1):330–338. doi:10.1016/j.tiv.2012.08.021
95. Guo D, Zhao Y, Zhang Y, Wang Q, Huang Z, Ding Q, Guo Z, Zhou X, Zhu L, Gu N (2014) The cellular uptake and cytotoxic effect of silver nanoparticles on chronic myeloid leukemia cells. J Biomed Nanotechnol 10(4):669–678. doi:10.1166/jbn.2014.1625
96. Nel A, Xia T, Madler L, Li N (2006) Toxic potential of materials at the nanolevel. Science 311(5761):622–627. doi:10.1126/science.1114397
97. Petersen EJ, Nelson BC (2010) Mechanisms and measurements of nanomaterial-induced oxidative damage to DNA. Anal Bioanal Chem 398(2):613–650. doi:10.1007/s00216-010-3881-7

98. Jiao ZH, Li M, Feng YX, Shi JC, Zhang J, Shao B (2014) Hormesis effects of silver nanoparticles at non-cytotoxic doses to human Hepatoma cells. PloS One 9(7). doi:10.1371/journal.pone.0102564
99. Xiu ZM, Zhang QB, Puppala HL, Colvin VL, Alvarez PJJ (2012) Negligible particle-specific antibacterial activity of silver nanoparticles. Nano Lett 12(8):4271–4275. doi:10.1021/nl301934w
100. Cao H, Liu X (2010) Silver nanoparticles-modified films versus biomedical device-associated infections. Wiley Interdiscip Rev-Nanomed Nanobiotechnol 2(6):670–684. doi:10.1002/wnan.113
101. Sedlak RH, Hnilova M, Grosh C, Fong H, Baneyx F, Schwartz D, Sarikaya M, Tamerler C, Traxler B (2012) Engineered Escherichia coli silver-binding periplasmic protein that promotes silver tolerance. Appl Environ Microbiol 78(7):2289–2296. doi:10.1128/aem.06823-11
102. Beer C, Foldbjerg R, Hayashi Y, Sutherland DS, Autrup H (2012) Toxicity of silver nanoparticles-Nanoparticle or silver ion? Toxicol Lett 208(3):286–292. doi:10.1016/j.toxlet.2011.11.002
103. Foldbjerg R, Olesen P, Hougaard M, Dang DA, Hoffmann HJ, Autrup H (2009) PVP-coated silver nanoparticles and silver ions induce reactive oxygen species, apoptosis and necrosis in THP-1 monocytes. Toxicol Lett 190(2):156–162. doi:10.1016/j.toxlet.2009.07.009
104. Gliga AR, Skoglund S, Wallinder IO, Fadeel B, Karlsson HL (2014) Size-dependent cytotoxicity of silver nanoparticles in human lung cells: the role of cellular uptake, agglomeration and Ag release. Part Fibre Toxicol 11. doi:10.1186/1743-8977-11-11
105. Mudunkotuwa IA, Grassian VH (2011) The devil is in the details (or the surface): impact of surface structure and surface energetics on understanding the behavior of nanomaterials in the environment. J Environ Monit 13(5):1135–1144. doi:10.1039/c1em00002k
106. Castranova V (2011) Overview of current toxicological knowledge of engineered nanoparticles. J Occup Environ Med 53(6):S14–S17. doi:10.1097/JOM.0b013e31821b1e5a
107. Schrand AM, Rahman MF, Hussain SM, Schlager JJ, Smith DA, Ali SF (2010) Metal-based nanoparticles and their toxicity assessment. Wiley Interdiscip Rev-Nanomed Nanobiotechnol 2(5):544–568. doi:10.1002/wnan.103
108. Cao H, Liu X, Meng F, Chu PK (2011) Biological actions of silver nanoparticles embedded in titanium controlled by micro-galvanic effects. Biomaterials 32(3):693–705. doi:10.1016/j.biomaterials.2010.09.066
109. Choi O, Hu Z (2008) Size dependent and reactive oxygen species related nanosilver toxicity to nitrifying bacteria. Environ Sci Technol 42(12):4583–4588. doi:10.1021/es703238h
110. Kawata K, Osawa M, Okabe S (2009) In vitro toxicity of silver nanoparticles at noncytotoxic doses to HepG2 human hepatoma cells. Environ Sci Technol 43(15):6046–6051. doi:10.1021/es900754q
111. Ma R, Levard C, Marinakos SM, Cheng Y, Liu J, Michel FM, Brown GE Jr, Lowry GV (2012) Size-controlled dissolution of organic-coated silver nanoparticles. Environ Sci Technol 46(2):752–759. doi:10.1021/es201686j
112. Lim DH, Jang J, Kim S, Kang T, Lee K, Choi IH (2012) The effects of sub-lethal concentrations of silver nanoparticles on inflammatory and stress genes in human macrophages using cDNA microarray analysis. Biomaterials 33(18):4690–4699. doi:10.1016/j.biomaterials.2012.03.006
113. Chen Y, Wang Z, Xu M, Wang X, Liu R, Liu Q, Zhang Z, Xia T, Zhao J, Jiang G, Xu Y, Liu S (2014) Nanosilver incurs an adaptive shunt of energy metabolism mode to glycolysis in tumor and nontumor cells. ACS Nano 8(6):5813–5825. doi:10.1021/nn500719m
114. Wang J, Koo Y, Alexander A, Yang Y, Westerhof S, Zhang Q, Schnoor JL, Colvin VL, Braam J, Alvarez PJJ (2013) Phytostimulation of poplars and arabidopsis exposed to silver nanoparticles and Ag^+ at sublethal concentrations. Environ Sci Technol 47(10):5442–5449. doi:10.1021/es4004334

115. Carlson C, Hussain SM, Schrand AM, Braydich-Stolle LK, Hess KL, Jones RL, Schlager JJ (2008) Unique cellular interaction of silver nanoparticles: size-dependent generation of reactive oxygen species. J Phys Chem B 112(43):13608–13619. doi:10.1021/jp712087m
116. Zhao CM, Wang WX (2012) Size-dependent uptake of silver nanoparticles in Daphnia magna. Environ Sci Technol 46(20):11345–11351. doi:10.1021/es3014375
117. Wiley B, Sun Y, Xia Y (2007) Synthesis of silver nanostructures with controlled shapes and properties. Acc Chem Res 40(10):1067–1076. doi:10.1021/ar7000974
118. Pal S, Tak YK, Joardar J, Kim W, Lee JE, Han MS, Song JM (2009) Nanocrystalline silver supported on activated carbon matrix from hydrosol: antibacterial mechanism under prolonged incubation conditions. J Nanosci Nanotechno 9(3):2092–2103. doi:10.1166/jnn.2009.427
119. George S, Lin S, Jo Z, Thomas CR, Li L, Mecklenburg M, Meng H, Wang X, Zhang H, Xia T, Hohman JN, Lin S, Zink JI, Weiss PS, Nel AE (2012) Surface defects on plate-shaped silver nanoparticles contribute to its hazard potential in a fish gill cell line and zebrafish embryos. ACS Nano 6(5):3745–3759. doi:10.1021/nn204671v
120. Levard C, Hotze EM, Lowry GV, Brown GE Jr (2012) Environmental transformations of silver nanoparticles: impact on stability and toxicity. Environ Sci Technol 46(13):6900–6914. doi:10.1021/es2037405
121. El Badawy AM, Silva RG, Morris B, Scheckel KG, Suidan MT, Tolaymat TM (2011) Surface charge-dependent toxicity of silver nanoparticles. Environ Sci Technol 45(1):283–287. doi:10.1021/es1034188
122. Lee KJ, Browning LM, Nallathamby PD, Xu X-HN (2013) Study of charge-dependent transport and toxicity of peptide-functionalized silver nanoparticles using zebrafish embryos and single nanoparticle plasmonic spectroscopy. Chem Res Toxicol 26(6):904–917. doi:10.1021/tx400087d
123. Kvitek L, Panacek A, Soukupova J, Kolar M, Vecerova R, Prucek R, Holecova M, Zboril R (2008) Effect of surfactants and polymers on stability and antibacterial activity of silver nanoparticles (NPs). J Phys Chem C 112(15):5825–5834. doi:10.1021/jp711616v
124. Teeguarden JG, Hinderliter PM, Orr G, Thrall BD, Pounds JG (2007) Particokinetics in vitro: dosimetry considerations for in vitro nanoparticle toxicity assessments. Toxicol Sci 95(2):300–312. doi:10.1093/toxsci/kfl165
125. El Badawy AM, Luxton TP, Silva RG, Scheckel KG, Suidan MT, Tolaymat TM (2010) Impact of environmental conditions (pH, ionic strength, and electrolyte type) on the surface charge and aggregation of silver nanoparticles suspensions. Environ Sci Technol 44(4):1260–1266. doi:10.1021/es902240k
126. Liu J, Hurt RH (2010) Ion release kinetics and particle persistence in aqueous nano-silver colloids. Environ Sci Technol 44(6):2169–2175. doi:10.1021/es9035557
127. He W, Zhou YT, Wamer WG, Boudreau MD, Yin JJ (2012) Mechanisms of the pH dependent generation of hydroxyl radicals and oxygen induced by Ag nanoparticles. Biomaterials 33(30):7547–7555. doi:10.1016/j.biomaterials.2012.06.076
128. Levard C, Reinsch BC, Michel FM, Oumahi C, Lowry GV, Brown GE Jr (2011) Sulfidation processes of pvp-coated silver nanoparticles in aqueous solution: impact on dissolution rate. Environ Sci Technol 45(12):5260–5266. doi:10.1021/es2007758
129. Liu J, Pennell KG, Hurt RH (2011) Kinetics and mechanisms of nanosilver oxysulfidation. Environ Sci Technol 45(17):7345–7353. doi:10.1021/es201539s
130. Liu JY, Sonshine DA, Shervani S, Hurt RH (2010) Controlled release of biologically active silver from nanosilver surfaces. ACS Nano 4(11):6903–6913. doi:10.1021/nn102272n
131. Arnaout CL, Gunsch CK (2012) Impacts of silver nanoparticle coating on the nitrification potential of nitrosomonas Europaea. Environ Sci Technol 46(10):5387–5395. doi:10.1021/es204540z
132. Yin Y, Liu J, Jiang G (2012) Sunlight-induced reduction of ionic ag and au to metallic nanoparticles by dissolved organic matter. ACS Nano 6(9):7910–7919. doi:10.1021/nn302293r
133. Akaighe N, MacCuspie RI, Navarro DA, Aga DS, Banerjee S, Sohn M, Sharma VK (2011) Humic acid-induced silver nanoparticle formation under environmentally relevant conditions. Environ Sci Technol 45(9):3895–3901. doi:10.1021/es103946g

Chapter 6
Environmental Bioeffects and Safety Assessment of Silver Nanoparticles

Sujuan Yu, Lingxiangyu Li, Qunfang Zhou, Jingfu Liu and Guibin Jiang

Abstract The large production and expanding application of silver nanoparticles (AgNPs) in consumer market would inevitably bring additional sources of AgNPs in the natural environment, and the long-term and incremental exposure to both biota and human is also expected, which prompts scientists to consider more comprehensively the impacts of AgNPs on ecosystem health and safety in light of their toxicity as shown in Chap. 5. As the number of literature focused on the ecological effects of AgNPs gradually increase, it is possible to describe preliminarily the current knowledge of environmental bioeffects and safety assessment of AgNPs. In this chapter, we try to summarize and discuss the works that has been done so far to follow the environmental bioeffects and risk assessment of AgNPs.

6.1 Environmental Bioeffects

6.1.1 Bioavailability and Uptake

There are extensive evidences that the environmental bioeffects of nanoparticles (NPs) are strongly dependent on their bioavailability in the environment [1, 2]. In general, given the high reactivity of silver nanoparticles (AgNPs) in natural environments, organisms as we above-mentioned in Chap. 5 could be exposed to various forms of silver, including free silver ions, dissolved organic and inorganic silver

J. Liu (✉) · S. Yu · L. Li · Q. Zhou · G. Jiang
State Key Laboratory of Environmental Chemistry and Ecotoxicology, Research Center for Eco-Environmental Sciences, Chinese Academy of Sciences,
P.O. Box 2871, 100085 Beijing, China
e-mail: jfliu@rcees.ac.cn

S. Yu
e-mail: sjyu@rcees.ac.cn

Q. Zhou
e-mail: zhouqf@rcees.ac.cn

G. Jiang
e-mail: gbjiang@rcees.ac.cn

J. Liu, G. Jiang (eds.), *Silver Nanoparticles in the Environment,*
DOI 10.1007/978-3-662-46070-2_6

complexes, and discrete single and/or aggregated and/or agglomerated AgNPs, which could show observed differences in their bioavailability to the organisms [3, 4]. Normally, compared to AgNPs and dissolved organic and inorganic silver complexes, free silver ions are more available for organisms.

The intrinsic properties of AgNPs such as structure, size, shape, surface coating, and composition, would largely affect their uptake and bioaccumulation to organisms. George et al. [5] investigated and compared the bioavailability of nanosized Ag spheres, plates, and wires in Holtfreter's medium, finding that the bioavailability of Ag is significantly lower for Ag-nanoplate relative to Ag-nanosphere. Size dependent uptake of AgNPs in *Daphnia magna* was also reported [6]. Commercial AgNPs with three nominal sizes (20, 50, 100 nm) and two surface coatings (citrate and tannic acid) were used in the study to investigate the size effect on the influx rate in a model organism, *D. magna*. For both types of surface coatings and different AgNP concentrations, the uptake rates always followed the sequence of 20 > 50 > 100 nm (Fig. 6.1), suggesting that the size of AgNPs played a key role in the bioavailability of AgNPs. After AgNPs enter the natural environment, their properties would be gradually altered, which would in turn lead to the changes in their bioavailability to organisms [7]. A previous work investigated the effect of different coatings on the silver ions release from AgNPs in natural water under artificial light condition, and found that bare- and citrate-coated AgNPs aggregated quickly in natural waters, while sterically dispersed AgNPs coated with Tween 80 were stable for a longer time and released silver ions much quicker, which indicated a higher bioavailability and toxicity toward aquatic organisms [8].

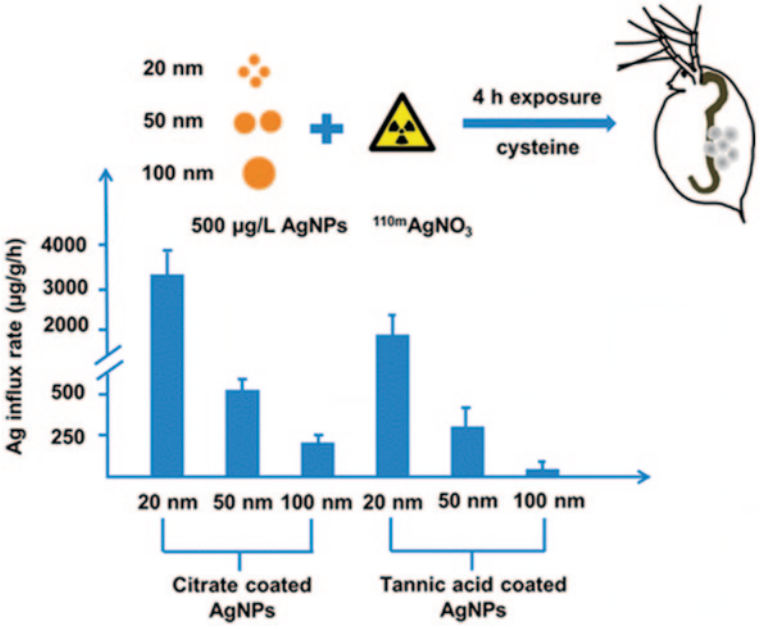

Fig. 6.1 Size-dependent uptake of silver nanoparticles in *Daphnia magna*. (Reprinted with the permission from ref. [6], Copyright 2012 American Chemical Society)

In addition, previous studies also reported that various factors like the pH, ionic strength/composition, and natural organic matter (NOM) could affect the silver speciation in the environment (Fig. 6.2), which in turn altered the bioavailability and uptake of AgNPs [1, 9, 10]. In particular, NOM has been reported to have the ability to mitigate the toxicity of AgNPs to biofilm due to the marked reduction in their bioavailability [11]. Another study also reported that the toxicity of AgNPs to *Ceriodaphnia dubia* decreased greatly in the presence of NOM, probably because the DOC coating inhibited silver ion release or made AgNPs less available for *C. dubia* [12]. Wang and coworker [13] investigated the effects of salinity on the bioavailability of citrate-coated AgNPs in the presence or absence of a nonionic surfactant (Tween 20) to marine medaka (*Oryzias melastigma*), and limited bioavailability of citrated-coated AgNPs was observed at high salinity (e.g., 30 psu). Additionally, they also found that well dispersion is of great importance for the bioavailability of AgNPs in a highly ionic environment. Clearly, the bioavailability of AgNPs is strongly dependent on environmental conditions.

Bioavailability has been reported to be one of the most important factors controlling uptake and bioaccumulation of metal-containing nanoparticles in the organisms. The uptake efficiency is dependent on bioavailability of AgNPs [14]. Without bioavailability, the dose dependent ecotoxicological effects of AgNPs could not be fully evaluated. Wang [13] found that the calculated uptake rate constant of citrate-coated AgNPs in marine medaka (*O. melastigma*) was 2.1 L/kg/d at a salinity of 15 psu, while no uptake was determined at salinity of 30 psu due to the limited bioavailability of AgNPs under this condition. Moreover, Aerle et al. [15] found that toxicity in exposed zebrafish embryos (*Danio rerio*) caused by AgNPs is principally associated with bioavailable silver ions in the water.

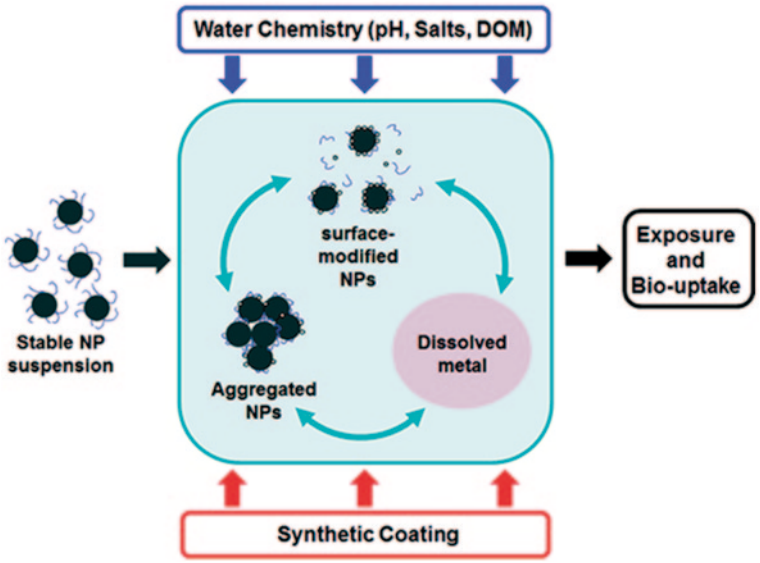

Fig. 6.2 Forms and bioavailability of silver in the environment. (Reprinted with the permission from ref. [1], Copyright 2012 American Chemical Society)

Till date, many works focused on variation of bioavailability and toxicity of AgNPs resulted from chemical transformations have been reported [9, 16, 17]. Among the various transformations, sulfidation of AgNPs has recently attracted much attention, since Kim et al. discovered the presence of Ag_2S-NPs in sewage sludge due to the AgNP transformation during wastewater treatment processes [18]. AgNPs easily react with inorganic sulfide to transform into Ag_2S, and the degree of sulfidation is closely related with the HS^-/Ag ratio, the polydispersity, and aggregation state of AgNPs [17]. The sulfidation has also been proved to be one of the best ways to control the silver ion release of AgNPs, which would in turn lead to great reduction in *Escherichia coli* growth inhibition [19]. Generally, the higher the Ag_2S:Ag^0 ratio was in the sulfidized AgNPs, the less growth inhibition of *E. coli* was observed (Fig. 6.3). Moreover, Levard and coworkers [16] reported the sulfidation could significantly reduce toxicity of AgNPs to four different types of eukaryotic organisms, including zebrafish, killifish, nematode worm, and least

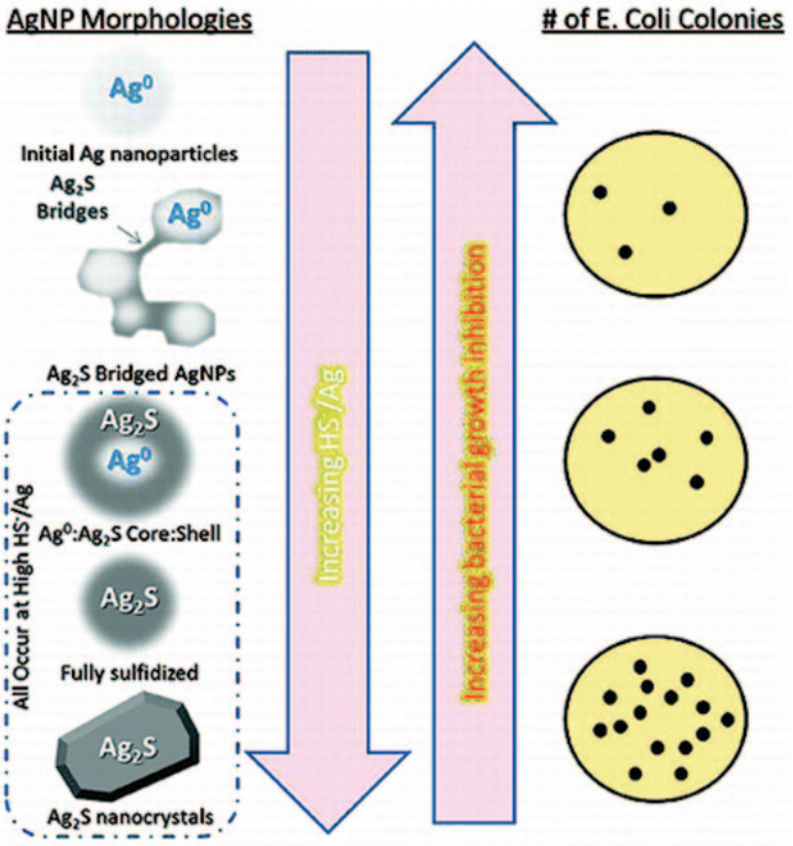

Fig. 6.3 Sulfidation of silver nanoparticles decreases *Escherichia coli* growth inhibition. (Reprinted with the permission from ref. [19], Copyright 2012 American Chemical Society)

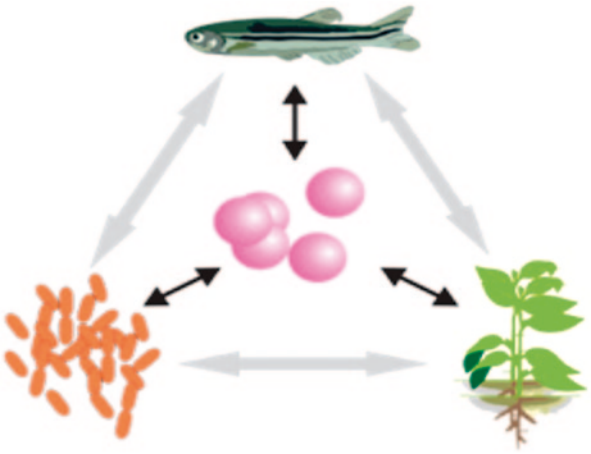

Fig. 6.4 Ecotoxicological effects of silver nanoparticles (*AgNPs*) in the natural environment. (Reprinted with the permission from ref. [2], Copyright 2013 American Chemical Society)

duckweed. The toxicity decrease was significant for killifish and duckweed, even for a very low degree of sulfidation (about 2 mol % S). This was attributed to the lower solubility of Ag_2S compared to AgNPs, which resulted in a dramatic decrease in Ag^+release. In addition to sulfidation, chloridation has also been proved to play an important role in mitigating the toxicity of AgNPs [9]. In the presence of chloride with Cl/Ag ratios $\leq$2675, AgCl particles can be directly formed and precipitated on the surface of AgNPs, which slowed down the oxidation and dissolution rate of AgNPs. The decreased amount of soluble Ag resulted in much lower growth inhibition toward *E. coli*. In total, the bioavailability of AgNPs could decrease greatly in the presence of sulfide or chloride in the aquatic environment [9, 20].

6.1.2 Ecotoxicological Effects

Over the past decade, AgNPs have been extremely popular in biological and medical fields due to their antimicrobial activity toward a broad spectrum of microorganisms. It is obvious that most, if not all, of the usage would create wastes, increase potential for their widespread release into the water body, and hence raise concerns on the ecotoxicological effects of AgNPs. Accordingly, much work on the ecotoxicological effects of AgNPs has been investigated using a suite of in vitro and in vivo tests. Hence, we would summarize the current body of literature focused on the ecotoxicological effects of AgNPs.

As Fig. 6.4 cited from Maurer-Jones et al. [2] points out, for the various components of the food web, namely bacteria, plants, and multicellular aquatic and terrestrial organisms, most literature concentrated on these organisms. In general, bacteria, acting as the components of the base of food web, play a very important role in the natural environment. Till date, there has been a large number of literature on effects of AgNPs on bacteria [9, 21]. Fabrega et al. [22] investigated the impact

of humic acid on the toxicity of AgNPs to *Pseudomonas fluorescens* over a 24 h exposure at pH 6–9, which demonstrated that humic acid could mitigate toxicity of AgNPs to the bacterial at pH 9, while the toxicological response could not be explained by the dose of dissolved silver. Normally, the toxicological effect is strongly dependent on the concentration of AgNPs or released silver ions; bacterial (bacterioplankton) production could be significantly inhibited once the concentration of AgNPs is higher than 1 mg/L [23]. However, in treatments with low concentrations of AgNPs (10 and 20 μg Ag/L) after 48 h, the production of bacterial community did not alter much but with a reduction of alkaline phosphatase. In light of this finding, the authors declared that AgNP concentrations in the ng/L range in natural aquatic environments are unlikely to negatively impact aquatic biogeochemical cycles [23].

The effect of AgNPs of different sizes (5, 10, and 25 nm) and coatings (poly ethylene glycol and carbon) on the plants like poplars (*populus deltoides nigra*) and *Arabidopsis thaliana* were investigated at a wide range of concentrations (0.01–100 mg/L) by Wang et al. [24]. They demonstrated that all forms of silver used in their study were phytotoxic to these plants once AgNPs was above a specific concentration. More importantly, a stimulatory effect was found on root elongation, fresh weight, and evapotranspiration of both plants even at a narrow range of sublethal concentrations of AgNPs. Dimkpa et al. also reported that AgNPs affect the growth and metabolism of wheat in a sand growth matrix, and obvious reduction in the length of shoots and roots of wheat was observed in a dose-dependent manner (Fig. 6.5) [25]. Moreover, transmission electron microscopy (TEM) images clearly showed that AgNPs were present in both the shoots and roots of the exposed wheat, implying the uptake and transport of AgNPs in the sand. The possible accumulation of AgNPs in food crops may pose a potential threat to the humans. AgNPs could also trigger the alteration in gene expression in *A. thaliana*. *A. thaliana* exposed to 5 mg/L polyvinylpyrrolidone (PVP)-coated AgNPs (20 nm) showed upregulation

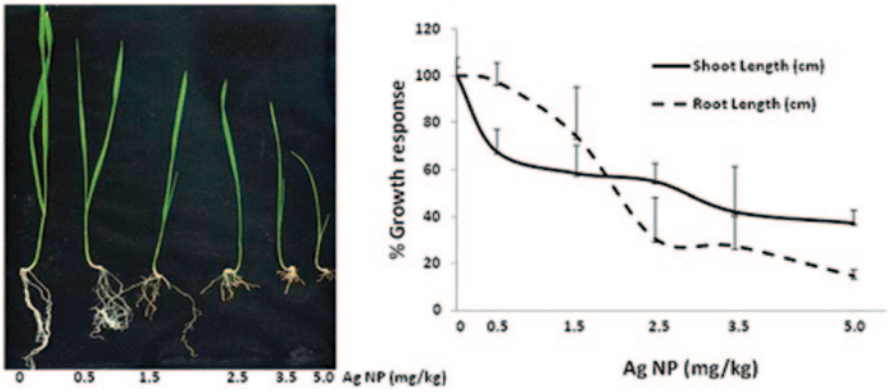

Fig. 6.5 Dose-dependent growth response of wheat to challenge with AgNPs for 14 days in a sand matrix. (Reprinted with the permission from ref. [25], Copyright 2013 American Chemical Society)

of 286 genes and downregulation of 81 genes compared to nonexposed plants [26]. Further study revealed that upregulated genes were primarily related to the response to metals and oxidative stress, while downregulated genes were more related to response to pathogens and hormonal stimuli. In another study conducted by Patlolla et al. [27], broad bean plant seedlings were exposed to AgNPs (60 nm) in a range of 12.5–100 mg/L, and the frequency of chromosomal aberrations and micronuclei induction increased in a AgNP dose-dependent manner. Together, all these works suggest that AgNPs could greatly impact plant development. Additionally, AgNPs have the potential to impact the eukaryotic organism development. More than 50% of *Drosophila melanogaster* exposed to 20 mg/L AgNPs were unable to leave their pupae, and they could not even finish their development cycle under this condition (Fig. 6.6) [28]. Another study also reported that AgNPs could induce heat shock stress, oxidative stress, DNA damage, and apoptosis in *D. melanogaster* [29], implying that more careful assessments of AgNP risks are warranted.

In addition to the bacteria and plants, AgNPs also have been found to be toxic to multicellular aquatic and terrestrial organisms. Medaka and zebrafish, two of the most frequently used fish models, have been used to study ecotoxicological effects of AgNPs in the aquatic environment. Kwok et al. [30] reported that gum arabic-coated AgNPs showed the highest toxicity to Japanese medaka (*Oryzias latipes*), while PVP-coated and citrate-coated AgNPs exhibited similar and lower toxicity. Bar-Ilan et al. [31] found that silver ions, released from AgNPs, could surely exert significant toxicity to zebrafish embryos. The alteration of zebrafish developments and larval behaviors caused by AgNPs was also reported [32]. Moreover, it is likely that AgNPs would affect the organisms along with food chains, though information on this topic is sorely lacking right now.

Although it is very important to begin with classical biological models like medaka and zebrafish, there has been some work focused on the impact of AgNPs on another susceptible fish to fully understand the ecotoxicological effects. Recently, Jang and coworkers [33] investigated the toxicokinetics of total silver in common

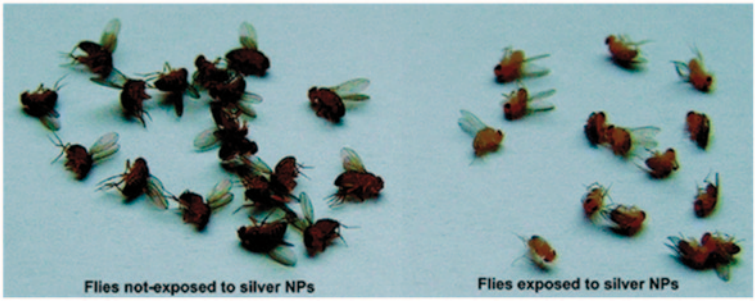

Fig. 6.6 Comparison of body pigmentation and body proportion of flies hatched on culture medium without AgNPs (on the *left*) and with AgNPs at a concentration of 20 mg/L of silver (on the *right*). (Reprinted with the permission from ref. [28], Copyright 2011 American Chemical Society)

carp (*Cayprinus carpio*). After carp was exposed to AgNPs at 0.62 mg/L for 7 days and followed by a 2 week depuration period, they found that liver contained the highest concentration of silver (5.61 mg/kg), and its concentration still kept a high-level (4.22 mg/kg) even after depuration for 14 days. Thus, the function of liver would be affected by this level of silver.

Earthworm is one of the classical models to investigate the effect of AgNPs in soil on the terrestrial organisms, since it comprises a critical component of the ecosystem. Till date, a handful of experiments have been conducted on earthworm response to AgNPs in soils. Heckmann et al. [34] investigated the effect of high dose of AgNPs (1000 mg/kg) on the earthworms, and 100% reproductive failure was observed, which was also reported by Shoults-Wilson et al. [35]. In another study, after the earthworm *Eisenia fetida* was exposed to AgNPs (10 and 80 nm) for 14 days, the activities of acid phosphatase and Na^+, K^+-ATPase were inhibited significantly in a dose-dependent manner, and the toxicity of 10 nm AgNPs was higher than the larger ones [36].

Taken all together, these findings demonstrate that AgNPs could impose toxicological effects on organisms in the environment, which should raise much more concerns in the future.

6.1.3 Combined Toxicity with Various Environmental Pollutants

Normally, organisms are exposed to more than one kind of pollutants in the natural environment, such as organic pollutants like persistent organic pollutants (POPs) and antibiotics, and inorganic pollutants like metal ions and other NPs. The coexistence of AgNPs and other environmental pollutants would mutually impact their fate, transport, and transformation, and further lead to changes in their toxicity to organisms. In this regard, some studies have raised the question about the possible interaction between AgNPs and other pollutants in the environment and about the mutual influence on their combined toxicity. However, understandings of the environmental fate and in situ toxicity of AgNPs with various other environmental pollutants on biota and ecosystems is sorely lacking right now. Ghosh and coworkers [37] investigated synergistic action of cinnamaldehyde with AgNPs against spore-forming bacteria, and found that the antibacterial activity of AgNPs was greatly enhanced in the presence of cinnamaldehyde. In addition to that, combination of AgNPs and antibiotic like amoxicillin could exhibit a greater bactericidal efficiency on *E. coli* cells compared to AgNPs or amoxicillin alone [38], as also reported in another study conducted by Hwang et al. [39]. Torre-Roche et al. [40] demonstrated that exposure of *Cucurbita pepo* (zucchini) and *Glycine max* (soybean) to AgNPs led to a significant reduction in the uptake of p,p'-Dichlorodiphenyldichloroethylene (p'-DDE). In the presence of 500 mg/L bulk of Ag or AgNPs, DDE uptake by *C. pepo* can be suppressed by 21−29%. The interaction of AgNPs with cocontaminants was greatly influenced by the Ag particle size (bulk vs NP) and plant species. Ultravoilet (UV)-induced toxicity reduction of citrate-AgNPs in the presence of perfluorocarboxylic acids was also reported recently [41]. Perfluorocarboxylic

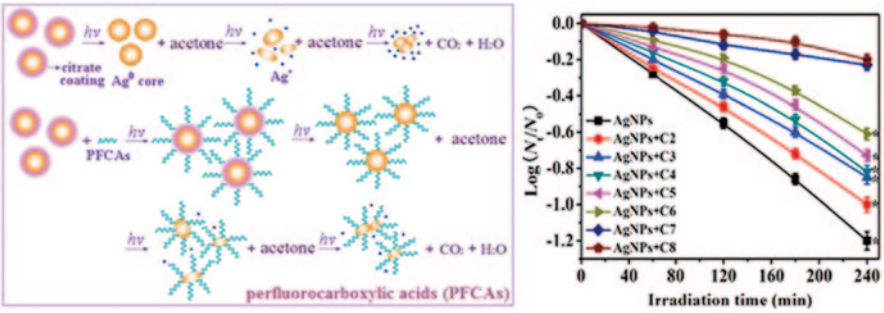

Fig. 6.7 Kinetics of *E. Coli* inactivation by AgNPs with or without perfluorinated carboxylic acids (*PFCAs*) under ultravoilet (UV) irradiation. (Reprinted with the permission from ref. [41], Copyright 2014 American Chemical Society)

acids with carbon chain length C2–C8 adsorbed on the surface of AgNPs would suppress Ag^+dissolution, enhance the AgNP stability, and decline the reactive oxygen species (ROS) production. UV-induced toxicity of AgNPs toward *E. coli* cells was decreased largely as well, and longer chain length of perfluorocarboxylic acids resulted in less toxicity (Fig. 6.7), which was probably due to the lower Ag^+dissolution. These studies highlight that when assessing the risks posed by AgNPs, both their inherent toxicity and their possible interactions with various organic or inorganic pollutions should be considered.

In total, these existing findings on the synergistic effects of AgNPs and other various environmental pollutants have already pointed out the scientific chances in the future. In particular, although the enhanced toxicity of combined AgNPs and other environmental pollutants has been found, the potential mechanism of the enhancement is still not clear.

6.2 Exposure and Risk Assessment

AgNPs have been one of the highest developed nanomaterials around the world, and it is estimated that about 500 t/a AgNPs were produced worldwide [42]. Moreover, as surveyed on October 2013, among the 1628 consumer products that containing nanomaterials, 383 were clamed to contain AgNPs [43], and the number is still growing. The rapid production and application of AgNPs have led to increased exposure and substantial release of AgNPs into the natural system. Once reached the environment, there are a variety of ways that AgNPs transported to water bodies, plants, and environmental organisms, which would ultimately get recycled back to humans. Commonly, the primary human exposure of AgNPs would occur via ingestion (food and water), inhalation (AgNP powders and dusts), and skin contact (various consumer products). And among the myriad of products containing AgNPs, humans are exposed mostly to three major categories that are food, consumer products, and medical products [44].

AgNPs are commonly added in water filters for household use to kill bacteria in drinking water; however, the inevitable release of AgNPs in water would result in the direct ingestion of AgNPs in everyone's life. Moreover, as it was reported, nanotechnologies are being involved throughout all stages of food production chain. In order to prolong the shelf life of food, AgNPs are used as additives and directly included into food. In the processing process, AgNPs are also reported to be incorporated into food preparation equipments. To decrease food decay and prevent bacterial growth during conservation, AgNPs containing packaging materials and food storage devices are frequently used. In general, the exposure risks largely depend on the ways that AgNPs were incorporated into the products. For example, for AgNPs that are bound in the packaging materials or coated on the surface of food storage devices or bags, though the direct contact may result in the release of AgNPs, the amount is relatively small, and a low exposure is expected. However, for AgNPs that are included as additives in food, they may be eaten directly and the consumer exposure may be high [44].

AgNPs are incorporated into a myriad of consumer products in our everyday life, such as nanosilver toothpastes, towels, soaps, cosmetics, antiodor sprays, disinfectants, functional textiles, socks, washing machines, and so on. Undoubtedly, the frequent contact with these products would increase the dermal exposure to AgNPs. Kulthong et al. [45] examined the release of AgNPs from nanosilver treated fabrics in artificial sweat to mimic the behavior of Ag nanotextiles during wearing. They found that silver was released from different textiles to varying degrees, ranging from 0 mg/kg to about 322 mg/kg of fabric weight. The amount of silver released was dependent on the quantity of silver coating, the fabric quality, and the artificial sweat formulations. This study indicated that sweat might promote the transfer of AgNPs from treated fabrics to the skin surface to enhance the dermal exposure during wearing. Moreover, the daily use of nanosilver toothpastes, towels, soaps, cosmetics would also result in the chronic exposure to AgNPs. Nanosilver spray, which is used to kill bacteria in the air, is also an important source for human exposure. Quadros and Marr [46] determined and characterized the emissions of airborne particles from consumer spray products containing AgNPs, and further assessed the potential for inhalation exposure to silver during product use. Surprisingly, they found that the normal use of silver-containing spray products carried the potential for inhalation of silver-containing aerosols, and up to 70 ng of silver might deposit in the respiratory tract during product use. The direct use of spray can also result in Ag deposition on skins or on surfaces of the walls, tables, floors, and other household products. For children (e.g., toddlers), touching these surfaces, handling sprayed products and then mouthing their hands, or mouthing of objects (e.g., toys) that have been sprayed with AgNPs are also possible routes for oral exposures [47].

Silver is well known for its excellent antimicrobial properties for decades, and AgNPs have long been used in medical areas. Nanosilver dressings and band-aid are widely applied to avoid infections after surgeries; however, there is a risk that AgNPs released would enter the body directly through broken skins. AgNPs are also used as additives in bone cements, coatings of implants for joint replacement, and intramedullary nails for bone fractures. The implant of AgNPs can also lead to the slow release of Ag, which may pose a potential exposure to human bodies.

Though a large variety of products containing AgNPs are appeared on the market, only little information about the products is available. In most cases, the manufactures only declare that their products possess superior antibacterial ability in the presence of AgNPs; however, information on the concentration, size, shape of AgNPs is missing. To estimate the risk of exposure, more information of the products is needed such as the types of incorporation, the concentration and forms of AgNPs, the size, surface coatings, and the dispersion state [44].

Frequent washing, abrasion, and disposal can lead to AgNPs release into the environment [48]. In spite of the role of wastewater treatment plant in removal of AgNPs from waste streams, tens or hundreds ng/L level of nanosized silver was still determined in the effluent of wastewater treatment plants. Accordingly, the concentration of AgNPs in the aquatic environment was predicted to reach ng/L level [49]. Since AgNPs are being widely used all over the world, the amounts of AgNPs and their transformation products in aquatic environments are expected to gradually increase over time. Recently, Comfort et al. [50] evaluated the cell response to long-term exposure of low-dose AgNPs, and found that chronic exposure of HaCaT cells to AgNPs in the ng/L range could activate sustained stress and signaling responses. However, up to now, there is no direct evidence that AgNPs at ng/L levels in the aquatic environment could harm organisms. Thus, scientists should raise more concerns about the potential risks of low levels of AgNPs in aquatic systems.

As previous studies reported, majority of AgNPs in water stream will be removed in wastewater treatment processes, causing a large amount of nanosized silver accumulated in the sludge. However, sewage sludge is used as fertilizers to modify the soils in some countries, which would inevitably impose risks of AgNPs on the bacteria, plants, and animals in terrestrial systems.

In natural system, AgNPs would undergo different pathways during transport, and the related environmental risks may be gradually mitigated by modification, aggregation, or complexing. The potential hazards are largely dependent on the species of silver; however, studies on the transformation of AgNPs in the natural system are still limited. Thus, in order to accurately assess the risks of AgNP exposure, much more information about the transformation of AgNPs and factors affecting the silver species and toxicity in the environment is also needed.

References

1. Gondikas AP, Morris A, Reinsch BC, Marinakos SM, Lowry GV, Hsu-Kim H (2012) Cysteine-induced modifications of zero-valent silver nanomaterials: implications for particle surface chemistry, aggregation, dissolution, and silver speciation. Environ Sci Technol 46(13):7037–7045. doi:10.1021/es3001757
2. Maurer-Jones MA, Gunsolus IL, Murphy CJ, Haynes CL (2013) Toxicity of engineered nanoparticles in the environment. Anal Chem 85(6):3036–3049. doi:10.1021/ac303636s
3. Fabrega J, Luoma SN, Tyler CR, Galloway TS, Lead JR (2011) Silver nanoparticles: behaviour and effects in the aquatic environment. Environ Int 37(2):517–531. doi:10.1016/j.envint.2010.10.012
4. Lubick N (2008) Nanosilver toxicity: ions, nanoparticles-or both? Environ Sci Technol 42(23):8617–8617. doi:10.1021/es8026314

5. George S, Lin SJ, Jo ZX, Thomas CR, Li LJ, Mecklenburg M, Meng H, Wang X, Zhang HY, Xia T, Hohman JN, Lin S, Zink JI, Weiss PS, Nel AE (2012) Surface defects on plate-shaped silver nanoparticles contribute to its hazard potential in a fish gill cell line and zebrafish embryos. ACS Nano 6 (5):3745–3759. doi:10.1021/nn204671v
6. Zhao CM, Wang WX (2012) Size-dependent uptake of silver nanoparticles in Daphnia magna. Environ Sci Technol 46(20):11345–11351. doi:10.1021/es3014375
7. Cunningham S, Brennan-Fournet ME, Ledwith D, Byrnes L, Joshi L (2013) Effect of nanoparticle stabilization and physicochemical properties on exposure outcome: acute toxicity of silver nanoparticle preparations in zebrafish (Danio rerio). Environ Sci Technol 47(8):3883–3892. doi:10.1021/es303695f
8. Li X, Lenhart JJ (2012) Aggregation and dissolution of silver nanoparticles in natural surface water. Environ Sci Technol 46(10):5378–5386. doi:10.1021/es204531y
9. Levard C, Mitra S, Yang T, Jew AD, Badireddy AR, Lowry GV, Brown GE Jr (2013) Effect of chloride on the dissolution rate of silver nanoparticles and toxicity to *E. coli*. Environ Sci Technol 47(11):5738–5745. doi:10.1021/es400396f
10. Yang XY, Jiang CJ, Hsu-Kim H, Badireddy AR, Dykstra M, Wiesner M, Hinton DE, Meyer JN (2014) Silver nanoparticle behavior, uptake, and toxicity in Caenorhabditis elegans: effects of natural organic matter. Environ Sci Technol 48(6):3486–3495. doi:10.1021/es404444n
11. Wirth SM, Lowry GV, Tilton RD (2012) Natural organic matter alters biofilm tolerance to silver nanoparticles and dissolved silver. Environ Sci Technol 46(22):12687–12696. doi:10.1021/es301521p
12. Kennedy AJ, Chappell MA, Bednar AJ, Ryan AC, Laird JG, Stanley JK, Steevens JA (2012) Impact of organic carbon on the stability and toxicity of fresh and stored silver nanoparticles. Environ Sci Technol 46(19):10772–10780. doi:10.1021/es302322y
13. Wang J, Wang WX (2014) Salinity influences on the uptake of silver nanoparticles and silver nitrate by marine medaka (Oryzias melastigma). Environ Toxicol Chem 33(3):632–640. doi:10.1002/etc.2471
14. Yang X, Gondikas AP, Marinakos SM, Auffan M, Liu J, Hsu-Kim H, Meyer JN (2012) Mechanism of silver nanoparticle toxicity is dependent on dissolved silver and surface coating in Caenorhabditis elegans. Environ Sci Technol 46(2):1119–1127. doi:10.1021/es202417t
15. van Aerle R Lange A Moorhouse A Paszkiewicz K Ball K Johnston BD de-Bastos E Booth T Tyler CR Santos EM (2013) Molecular mechanisms of toxicity of silver nanoparticles in zebrafish embryos. Environ Sci Technol 47(14):8005–8014. doi:10.1021/es401758d
16. Levard C, Hotze EM, Colman BP, Dale AL, Truong L, Yang XY, Bone AJ, Brown GE, Tanguay RL, Di Giulio RT, Bernhardt ES, Meyer JN, Wiesner MR, Lowry GV (2013) Sulfidation of silver nanoparticles: natural antidote to their toxicity. Environ Sci Technol 47(23):13440–13448. doi:10.1021/es403527n
17. Levard C, Reinsch BC, Michel FM, Oumahi C, Lowry GV, Brown GE (2011) Sulfidation processes of PVP-coated silver nanoparticles in aqueous solution: impact on dissolution rate. Environ Sci Technol 45(12):5260–5266. doi:10.1021/es2007758
18. Kim B, Park CS, Murayama M, Hochella MF (2010) Discovery and characterization of silver sulfide nanoparticles in final sewage sludge products. Environ Sci Technol 44(19):7509–7514. doi:10.1021/es101565j
19. Reinsch BC, Levard C, Li Z, Ma R, Wise A, Gregory KB, Brown GE Jr, Lowry GV (2012) Sulfidation of silver nanoparticles decreases *Escherichia coli* growth inhibition. Environ Sci Technol 46(13):6992–7000. doi:10.1021/es203732x
20. Thalmann B, Voegelin A, Sinnet B, Morgenroth E, Kaegi R (2014) Sulfidation kinetics of silver nanoparticles reacted with metal sulfides. Environ Sci Technol 48(9):4885–4892. doi:10.1021/es5003378
21. Xiu Z, Zhang Q, Puppala HL, Colvin VL, Alvarez PJJ (2012) Negligible particle-specific antibacterial activity of silver nanoparticles. Nano lett 12(8):4271–4275. doi:10.1021/nl301934w
22. Fabrega J, Fawcett SR, Renshaw JC, Lead JR (2009) Silver nanoparticle impact on bacterial growth: effect of pH, concentration, and organic matter. Environ Sci Technol 43(19):7285–7290. doi:10.1021/es803259g

23. Das P, Xenopoulos MA, Williams CJ, Hoque ME, Metcalfe CD (2012) Effects of silver nanoparticles on bacterial activity in natural waters. Environ Toxicol Chem 31(1):122–130. doi:10.1002/etc.716
24. Wang J, Koo Y, Alexander A, Yang Y, Westerhof S, Zhang QB, Schnoor JL, Colvin VL, Braam J, Alvarez PJJ (2013) Phytostimulation of poplars and arabidopsis exposed to silver nanoparticles and Ag^+ at sublethal concentrations. Environ Sci Technol 47(10):5442–5449. doi:10.1021/es4004334
25. Dimkpa CO, McLean JE, Martineau N, Britt DW, Haverkamp R, Anderson AJ (2013) Silver nanoparticles disrupt wheat (*Triticum aestivum* L.) growth in a sand matrix. Environ Sci Technol 47(2):1082–1090. doi:10.1021/es302973y
26. Kaveh R, Li YS, Ranjbar S, Tehrani R, Brueck CL, Van Aken B (2013) Changes in Arabidopsis thaliana gene expression in response to silver nanoparticles and silver ions. Environ Sci Technol 47(18):10637–10644. doi:10.1021/es402209w
27. Patlolla AK, Berry A, May L, Tchounwou PB (2012) Genotoxicity of silver nanoparticles in Vicia faba: a pilot study on the environmental monitoring of nanoparticles. Int J Env Res Public Health 9(5):1649–1662. doi:10.3390/ijerph9051649
28. Panacek A, Prucek R, Safarova D, Dittrich M, Richtrova J, Benickova K, Zboril R, Kvitek L (2011) Acute and chronic toxicity effects of silver nanoparticles (NPs) on *Drosophila melanogaster*. Environ Sci Technol 45(11):4974–4979. doi:10.1021/es104216b
29. Ahamed M, Posgai R, Gorey TJ, Nielsen M, Hussain SM, Rowe JJ (2010) Silver nanoparticles induced heat shock protein 70, oxidative stress and apoptosis in *Drosophila melanogaster*. Toxicol Appl Pharmcol 242(3):263–269. doi:10.1016/j.taap.2009.10.016
30. Kwok KWH, Auffan M, Badireddy AR, Nelson CM, Wiesner MR, Chilkoti A, Liu J, Marinakos SM, Hinton DE (2012) Uptake of silver nanoparticles and toxicity to early life stages of Japanese medaka (*Oryzias latipes*): effect of coating materials. Aquat Toxicol 120:59–66. doi:10.1016/j.aquatox.2012.04.012
31. Bar-Ilan O, Albrecht RM, Fako VE, Furgeson DY (2009) Toxicity assessments of multisized gold and silver nanoparticles in zebrafish embryos. Small 5 (16):1897–1910. doi:10.1002/smll.200801716
32. Powers CM, Slotkin TA, Seidler FJ, Badireddy AR, Padilla S (2011) Silver nanoparticles alter zebrafish development and larval behavior: distinct roles for particle size, coating and composition. Neurotoxicol Teratol 33(6):708–714. doi:10.1016/j.ntt.2011.02.002
33. Jang M, Kim W, Lee S, Henry TB, Park J (2014) Uptake, tissue distribution, and depuration of total silver in common carp (Cyprinus carpio) after aqueous exposure to silver nanoparticles. Environ Sci Technol 48(19):11568–11574. doi:10.1021/es5022813
34. Heckmann LH, Hovgaard MB, Sutherland DS, Autrup H, Besenbacher F, Scott-Fordsmand JJ (2011) Limit-test toxicity screening of selected inorganic nanoparticles to the earthworm *Eisenia fetida*. Ecotoxicology 20(1):226–233. doi:10.1007/s10646-010-0574-0
35. Shoults-Wilson WA, Reinsch BC, Tsyusko OV, Bertsch PM, Lowry GV, Unrine JM (2011) Role of particle size and soil type in toxicity of silver nanoparticles to earthworms. Soil Sci Soc Am J 75(2):365–377. doi:10.2136/sssaj2010.0127nps
36. Hu C, Li M, Wang W, Cui Y, Chen J, Yang L (2012) Ecotoxicity of silver nanoparticles on earthworm Eisenia fetida: responses of the antioxidant system, acid phosphatase and ATPase. Toxicol Environ Chem 94(4):732–741. doi:10.1080/02772248.2012.668020
37. Ghosh IN, Patil SD, Sharma TK, Srivastava SK, Pathania R, Navani NK (2013) Synergistic action of cinnamaldehyde with silver nanoparticles against spore-forming bacteria: a case for judicious use of silver nanoparticles for antibacterial applications. Int J Nanomed 8:4721–4731. doi:10.2147/ijn.s49649
38. Li P, Li J, Wu CZ, Wu QS (2005) Synergistic antibacterial effects of beta-lactam antibiotic combined with silver nanoparticles. Nanotechnology 16(9):1912–1917. doi:10.1088/0957-4484/16/9/082
39. Hwang IS, Hwang JH, Choi H, Kim KJ, Lee DG (2012) Synergistic effects between silver nanoparticles and antibiotics and the mechanisms involved. J Med Microbiol 61(12):1719–1726. doi:10.1099/jmm.0.047100-0

40. De La Torre-Roche R Hawthorne J Musante C Xing BS Newman LA Ma XM White JC (2013) Impact of Ag nanoparticle exposure on p,p'-DDE bioaccumulation by *Cucurbita pepo* (zucchini) and *Glycine max* (soybean). Environ Sci Technol 47(2):718–725. doi:10.1021/es3041829
41. Li Y, Niu JF, Shang EX, Crittenden J (2014) Photochemical transformation and photoinduced toxicity reduction of silver nanoparticles in the presence of perfluorocarboxylic acids under UV irradiation. Environ Sci Technol 48(9):4946–4953. doi:10.1021/es500596a
42. Mueller NC, Nowack B (2008) Exposure modeling of engineered nanoparticles in the environment. Environ Sci Technol 42(12):4447–4453. doi:10.1021/es7029637
43. http://www.nanotechproject.org/cpi/about/analysis/. Accessed 10 Dec 2014
44. Wijnhoven SWP, Peijnenburg W, Herberts CA, Hagens WI, Oomen AG, Heugens EHW, Roszek B, Bisschops J, Gosens I, Van de Meent D, Dekkers S, De Jong WH, Van Zijverden M, Sips A, Geertsma RE (2009) Nano-silver—a review of available data and knowledge gaps in human and environmental risk assessment. Nanotoxicology 3(2):109–138. doi:10.1080/17435390902725914
45. Kulthong K, Srisung S, Boonpavanitchakul K, Kangwansupamonkon W, Maniratanachote R (2010) Determination of silver nanoparticle release from antibacterial fabrics into artificial sweat. Part Fibre Toxicol 7. doi:10.1186/1743-8977-7-8
46. Quadros ME, Marr LC (2011) Silver nanoparticles and total aerosols emitted by nanotechnology-related consumer spray products. Environ Sci Technol 45 (24):10713–10719. doi:10.1021/es202770m
47. EPA US (2012) Nanomaterial case study: nanoscale silver in disinfectant spray (Final report). US Environmental Protection Agency, Washington, DC:EPA/600/R-610/081F
48. Hedberg J, Skoglund S, Karlsson ME, Wold S, Wallinder IO, Hedberg Y (2014) Sequential studies of silver released from silver nanoparticles in aqueous media simulating sweat, laundry detergent solutions and surface water. Environ Sci Technol 48(13):7314–7322. doi:10.1021/es500234y
49. Gottschalk F, Sonderer T, Scholz RW, Nowack B (2009) Modeled environmental concentrations of engineered nanomaterials (TiO_2, ZnO, Ag, CNT, fullerenes) for different regions. Environ Sci Technol 43(24):9216–9222. doi:10.1021/es9015553
50. Comfort KK, Braydich-Stolle LK, Maurer EI, Hussain SM (2014) Less is more: Long-term in vitro exposure to low levels of silver nanoparticles provides new insights for nanomaterial evaluation. ACS Nano 8(4):3260–3271. doi:10.1021/nn5009116